Universidad de La Laguna
Oficina de Sede Electrónica
Entrada
Nº registro: 2020/46124
Nº reg. oficina: OF002/2020/45309
Fecha: 07/07/2020 15:26:22

UNIVERSIDAD Ð LA LAGUNA
Departamento de Astrofísica

Universidad de La Laguna

Unveiling the outskirts of galaxies using deep imaging

A dissertation submitted by
Nushkia Chamba
in partial fulfilment of the requirements for the degree of
Doctor of Philosophy in Astrophysics
at the Universidad de La Laguna

INSTITUTO Ð ASTROFÍSICA Ð CANARIAS
San Cristóbal de La Laguna, Tenerife
June 2020

Este documento incorpora firma electrónica, y es copia auténtica de un documento electrónico archivado por la ULL según la Ley 39/2015.
Su autenticidad puede ser contrastada en la siguiente dirección https://sede.ull.es/validacion/

Identificador del documento: 2622200 Código de verificación: mbm0ekWs

Firmado por:	ROSHAN NUSHKIA CHAMBA *UNIVERSIDAD DE LA LAGUNA*	Fecha: 07/07/2020 13:28:26
	IGNACIO TRUJILLO CABRERA *UNIVERSIDAD DE LA LAGUNA*	07/07/2020 13:58:21
	Johan Hendrik Knapen Koelstra *UNIVERSIDAD DE LA LAGUNA*	07/07/2020 15:23:08
	María de las Maravillas Aguiar Aguilar *UNIVERSIDAD DE LA LAGUNA*	08/07/2020 15:55:11

Universidad de La Laguna
Oficina de Sede Electrónica
Entrada
Nº registro: 2020/46124
Nº reg. oficina: OF002/2020/45309
Fecha: 07/07/2020 15:26:22

Examination date: July XXth, 2020
Thesis supervisors: Prof. Johan H. Knapen & Dr. Ignacio Cabrera Trujillo
SUNDIAL secondment supervisor: Dr. Michael H. F. Wilkinson

© Nushkia Chamba 2020

Este documento incorpora firma electrónica, y es copia auténtica de un documento electrónico archivado por la ULL según la Ley 39/2015.
Su autenticidad puede ser contrastada en la siguiente dirección https://sede.ull.es/validacion/

Identificador del documento: 2622200 Código de verificación: mbm0ekWs

Firmado por:	ROSHAN NUSHKIA CHAMBA *UNIVERSIDAD DE LA LAGUNA*	Fecha: 07/07/2020 13:28:26
	IGNACIO TRUJILLO CABRERA *UNIVERSIDAD DE LA LAGUNA*	07/07/2020 13:58:21
	Johan Hendrik Knapen Koelstra *UNIVERSIDAD DE LA LAGUNA*	07/07/2020 15:23:08
	María de las Maravillas Aguiar Aguilar *UNIVERSIDAD DE LA LAGUNA*	08/07/2020 15:55:11

Universidad de La Laguna
Oficina de Sede Electrónica
Entrada
Nº registro: 2020/46124
Nº reg. oficina: OF002/2020/45309
Fecha: 07/07/2020 15:26:22

To my late grandmother Neyney,
Mum, Dad, Nat, Nyo,
Aunty Fazlyn & Uncle Delano
for all your love and support.

And in memory of my colleague Rebeca Galera Rosillo
– I know nothing of planetary nebulae
but this thesis is yours as much as it is mine.

Este documento incorpora firma electrónica, y es copia auténtica de un documento electrónico archivado por la ULL según la Ley 39/2015.
Su autenticidad puede ser contrastada en la siguiente dirección https://sede.ull.es/validacion/

Identificador del documento: 2622200 Código de verificación: mbm0ekWs

Firmado por:	ROSHAN NUSHKIA CHAMBA *UNIVERSIDAD DE LA LAGUNA*	Fecha: 07/07/2020 13:28:26
	IGNACIO TRUJILLO CABRERA *UNIVERSIDAD DE LA LAGUNA*	07/07/2020 13:58:21
	Johan Hendrik Knapen Koelstra *UNIVERSIDAD DE LA LAGUNA*	07/07/2020 15:23:08
	María de las Maravillas Aguiar Aguilar *UNIVERSIDAD DE LA LAGUNA*	08/07/2020 15:55:11

Universidad de La Laguna
Oficina de Sede Electrónica
Entrada
Nº registro: 2020/46124
Nº reg. oficina: OF002/2020/45309
Fecha: 07/07/2020 15:26:22

Este documento incorpora firma electrónica, y es copia auténtica de un documento electrónico archivado por la ULL según la Ley 39/2015.
Su autenticidad puede ser contrastada en la siguiente dirección https://sede.ull.es/validacion/

Identificador del documento: 2622200 Código de verificación: mbm0ekWs

Firmado por:	ROSHAN NUSHKIA CHAMBA *UNIVERSIDAD DE LA LAGUNA*	Fecha: 07/07/2020 13:28:26
	IGNACIO TRUJILLO CABRERA *UNIVERSIDAD DE LA LAGUNA*	07/07/2020 13:58:21
	Johan Hendrik Knapen Koelstra *UNIVERSIDAD DE LA LAGUNA*	07/07/2020 15:23:08
	María de las Maravillas Aguiar Aguilar *UNIVERSIDAD DE LA LAGUNA*	08/07/2020 15:55:11

Universidad de La Laguna
Oficina de Sede Electrónica
Entrada
Nº registro: 2020/46124
Nº reg. oficina: OF002/2020/45309
Fecha: 07/07/2020 15:26:22

Abstract

The traditional measurement of the size of galaxies, the effective radius, is a relic of the epoch when shallow imaging was unable to capture the full extension of astronomical sources. However, current deep imaging surveys have revolutionised our view of galaxies and the characteristics of their faint outskirts, allowing us to regard critically our own conventions. From this perspective, it is time to move from a size definition based on the light concentration of galaxies, the effective radius, to a definition that intuitively captures the concept of the size of galaxies, such as its edge or boundary. In this dissertation, a physically motivated definition for the size of a galaxy based on the gas density threshold value for star formation in galaxies is studied. Remarkably, the new size definition not only captures what the human visual system identifies as the edge of a galaxy, but also dramatically decreases the scatter in the stellar mass–size relation by more than a factor of two. Compared to other size measures, the new parameter is unique in that it also unifies galaxies spanning five orders of magnitude in stellar mass on a single mass–size relationship. To place this discovery in the context of galaxy formation and evolution, its application is discussed on the understanding of the origin of discs and the nature of ultra-diffuse galaxies.

Resumen

La forma habitual de medir el tamaño de las galaxias, el radio efectivo, es el resultado de una época cuando las imágenes astronómicas eran poco profundas y, por tanto, incapaces de capturar la extensión completa de las fuentes astronómicas. Esta situación ha cambiado drásticamente en la actualidad con la llegada de cartografiados muy profundos. Estas nuevas imágenes nos han permitido estudiar las características de las galaxias en sus regiones externas y débiles, permitiéndonos explorar críticamente nuestras convenciones sobre el tamaño de estos objetos. Por este motivo, ha llegado el momento de sustituir una definición de tamaño basado en la concentración de la luz, el radio efectivo, por una definición que capture el concepto intuitivo de tamaño de las galaxias, como su borde o frontera. En este trabajo, proponemos una nueva definición de tamaño de las galaxias basada en la posición del umbral de la densidad de gas necesario para formar estrellas. Esta es una definición de tamaño con motivación física. Es importante resaltar que esta nueva definición de tamaño no sólo captura lo que la visión humana identifica como borde de la galaxia, sino que además reduce de forma drástica la dispersión de la relación masa-tamaño en un factor mayor que dos. Comparada con otras definiciones de tamaño, la nueva forma de medir la extensión de las galaxias es única, en el sentido que unifica en una única relación masa-tamaño, galaxias que difieren hasta cinco ordenes de magnitud en masa. Para poner nuestros resultados en el contexto de la formación y evolución de galaxias, exploramos como cambia nuestro entendimiento del origen de las galaxias discos y la naturaleza de las galaxias ultra-difusas.

Este documento incorpora firma electrónica, y es copia auténtica de un documento electrónico archivado por la ULL según la Ley 39/2015.
Su autenticidad puede ser contrastada en la siguiente dirección https://sede.ull.es/validacion/

Identificador del documento: 2622200 Código de verificación: mbm0ekWs

Firmado por:	ROSHAN NUSHKIA CHAMBA *UNIVERSIDAD DE LA LAGUNA*	Fecha: 07/07/2020 13:28:26
	IGNACIO TRUJILLO CABRERA *UNIVERSIDAD DE LA LAGUNA*	07/07/2020 13:58:21
	Johan Hendrik Knapen Koelstra *UNIVERSIDAD DE LA LAGUNA*	07/07/2020 15:23:08
	María de las Maravillas Aguiar Aguilar *UNIVERSIDAD DE LA LAGUNA*	08/07/2020 15:55:11

Universidad de La Laguna
Oficina de Sede Electrónica
Entrada
Nº registro: 2020/46124
Nº reg. oficina: OF002/2020/45309
Fecha: 07/07/2020 15:26:22

Este documento incorpora firma electrónica, y es copia auténtica de un documento electrónico archivado por la ULL según la Ley 39/2015.
Su autenticidad puede ser contrastada en la siguiente dirección https://sede.ull.es/validacion/

Identificador del documento: 2622200 Código de verificación: mbm0ekWs

Firmado por:	ROSHAN NUSHKIA CHAMBA *UNIVERSIDAD DE LA LAGUNA*	Fecha: 07/07/2020 13:28:26
	IGNACIO TRUJILLO CABRERA *UNIVERSIDAD DE LA LAGUNA*	07/07/2020 13:58:21
	Johan Hendrik Knapen Koelstra *UNIVERSIDAD DE LA LAGUNA*	07/07/2020 15:23:08
	María de las Maravillas Aguiar Aguilar *UNIVERSIDAD DE LA LAGUNA*	08/07/2020 15:55:11

Universidad de La Laguna
Oficina de Sede Electrónica
Entrada
Nº registro: 2020/46124
Nº reg. oficina: OF002/2020/45309
Fecha: 07/07/2020 15:26:22

Contents

1 Introduction **1**
1.1 From the Big Bang to the formation and evolution of galaxies . . . 1
1.2 ΛCDM predictions and the low surface brightness Universe . . . 5
1.3 Pioneering discoveries . . . 7
1.3.1 Stellar haloes . . . 8
1.3.2 Truncations . . . 9
1.3.3 Low surface brightness galaxies . . . 11
1.4 Deep imaging: a frontier for galaxy evolution studies . . . 14
1.4.1 From deep photographic sky surveys to CCD imaging . . . 14
1.4.2 State-of-the-art surveys . . . 17
1.4.3 Going beyond 31 mag/arsec^2: unveiling galactic stellar haloes . . . 20
1.4.4 The structure of the outer disc . . . 23
1.4.5 Ultra-diffuse galaxies . . . 25
1.4.6 Summary and highlights . . . 29
1.5 The size–stellar mass relation . . . 30
1.5.1 Motivation for studies on galaxy formation and evolution . . . 30
1.5.2 Historical perspectives on the concept of galaxy size . . . 31
1.5.3 A tale of two citations . . . 37
1.6 Thesis scope and overview . . . 38

2 A physically motivated definition for the size of galaxies **41**
2.1 Introduction . . . 41
2.2 Towards a physically motivated definition for the size of galaxies . . . 44
2.3 Imaging Data: the IAC Stripe82 Legacy Project . . . 45
2.4 Target selection . . . 45
2.5 Methodology . . . 46
2.5.1 Removal of scattered light from point sources and masking . . . 47
2.5.2 The effect of inclination . . . 47
2.5.3 Stellar mass density profiles . . . 48
2.5.4 Estimating the structural parameters of galaxies . . . 50
2.6 Results . . . 51
2.6.1 The properties of the R_1–mass relation . . . 51
2.6.2 The intrinsic scatter of the R_1–mass relation . . . 55
2.7 Discussion . . . 59
2.7.1 R_1 compared to other popular size definitions . . . 59

Este documento incorpora firma electrónica, y es copia auténtica de un documento electrónico archivado por la ULL según la Ley 39/2015.
Su autenticidad puede ser contrastada en la siguiente dirección https://sede.ull.es/validacion/

Identificador del documento: 2622200 Código de verificación: mbm0ekWs

Firmado por:	ROSHAN NUSHKIA CHAMBA *UNIVERSIDAD DE LA LAGUNA*	Fecha: 07/07/2020 13:28:26
	IGNACIO TRUJILLO CABRERA *UNIVERSIDAD DE LA LAGUNA*	07/07/2020 13:58:21
	Johan Hendrik Knapen Koelstra *UNIVERSIDAD DE LA LAGUNA*	07/07/2020 15:23:08
	María de las Maravillas Aguiar Aguilar *UNIVERSIDAD DE LA LAGUNA*	08/07/2020 15:55:11

Universidad de La Laguna
Oficina de Sede Electrónica
Entrada
Nº registro: 2020/46124
Nº reg. oficina: OF002/2020/45309
Fecha: 07/07/2020 15:26:22

2.7.2 The slope of the stellar mass–size relation . . . 63
2.7.3 The tilt of the stellar mass–size relation at 10^{11} $M_\odot$ . . . 63
2.8 Conclusions . . . 65

3 Are ultra-diffuse galaxies Milky Way-sized? 66
3.1 Introduction . . . 66
3.2 Data and sample selection . . . 67
3.3 Methodology . . . 68
3.4 Results . . . 69
3.5 Discussion . . . 72
3.6 Conclusions . . . 74

4 The edges of galaxies: from dwarfs to giants 75
4.1 Introduction . . . 75
4.2 Defining the edge of a galaxy . . . 76
4.3 Data and sample selection . . . 80
4.4 Methodology . . . 81
4.5 Results . . . 82
4.6 Analysis . . . 90
4.7 Summary and future improvements . . . 93

5 Conclusions and future work 95
5.1 Summary of results . . . 95
5.1.1 A physically motivated definition for the size of galaxies . . . 95
5.1.2 The nature of ultra-diffuse galaxies . . . 96
5.1.3 Revealing the edges of galaxies with deep imaging . . . 96
5.2 Future research questions . . . 96

Bibliography 99

A Appendix: The sizes of galaxies 113
A.1 Erratum (Trujillo et al., MNRAS, 495, 3777–3779, 2020) . . . 113
A.2 Is 1 $M_\odot/\mathrm{pc}^2$ a good proxy for the location of the gas density threshold? . . . 118
A.3 Other potential size indicators . . . 119
A.4 The limits of the new size definition . . . 120
A.5 Stellar mass determination . . . 121
A.6 Comparing the R_1–stellar mass and HI size–mass relations . . . 121

B Appendix: Ultra-diffuse galaxies 124
B.1 Table of measurements . . . 124
B.2 Comparison with an isophotal size indicator: The Holmberg radius . . . 124
B.3 Other stellar mass density proxies to measure the size of dwarfs and UDGs . . . 124

Acknowledgements 129

Este documento incorpora firma electrónica, y es copia auténtica de un documento electrónico archivado por la ULL según la Ley 39/2015.
Su autenticidad puede ser contrastada en la siguiente dirección https://sede.ull.es/validacion/

Identificador del documento: 2622200 Código de verificación: mbm0ekWs

Firmado por:	ROSHAN NUSHKIA CHAMBA *UNIVERSIDAD DE LA LAGUNA*	Fecha: 07/07/2020 13:28:26
	IGNACIO TRUJILLO CABRERA *UNIVERSIDAD DE LA LAGUNA*	07/07/2020 13:58:21
	Johan Hendrik Knapen Koelstra *UNIVERSIDAD DE LA LAGUNA*	07/07/2020 15:23:08
	María de las Maravillas Aguiar Aguilar *UNIVERSIDAD DE LA LAGUNA*	08/07/2020 15:55:11

Universidad de La Laguna
Oficina de Sede Electrónica
Entrada
Nº registro: 2020/46124
Nº reg. oficina: OF002/2020/45309
Fecha: 07/07/2020 15:26:22

1

Introduction

Imaging surveys in the low surface brightness regime are the frontier in the study of galaxy formation and evolution. They have unveiled faint structures in the outskirts of galaxies and a growing number of previously invisible low surface brightness galaxies, both of which provide important tests for the Λ Cold Dark Matter (ΛCDM) cosmological paradigm. In this Chapter, I provide a brief introduction to these topics, discuss why they are important within the currently favoured ΛCDM framework and motivate the research I have undertaken during my thesis.

1.1 From the Big Bang to the formation and evolution of galaxies

One of the most fundamental discoveries in cosmology, both theoretically and observationally, is the expansion of the Universe. After Einstein (1916) published his theory of General Relativity, Friedmann (1922) derived expanding solutions to the field equations. A few years later, Lemaître (1927) independently arrived at the same expanding solutions and provided observational support to his findings, i.e. that the recession velocity of galaxies linearly correlates with their distances. This phenomenon was also identified by Hubble (1929) around the same period (Lemaître 1931; Hubble & Humason 1931). Both, the theory of gravitation which predicted an expanding Universe and the subsequent discovery of the expansion led to the Hot Big Bang model. According to this model, our Universe began as a compressed, much denser and hotter state than what we experience today.

Several years later, Gamow (1948) followed by Alpher et al. (1948) demonstrated that the Hot Big Bang model is capable of producing known chemical elements such as helium and hydrogen, during a process called primordial nucleosynthesis. Alpher & Herman (1948) argued that if our Universe did begin from a hot state, then the expansion of the Universe would cool the early radiation emitted from this dense body towards the microwave wavelengths. Such a relic radiation should thus be observable in the present form of the Universe. This is the Cosmic Microwave Background (CMB) radiation which was accidentally discovered in the 1960s (Penzias & Wilson 1965; Dicke et al. 1965) and was shown to be a perfect black body, i.e. a homogeneous and uniform source of light at a fixed temperature of 2.7 K. Therefore, a natural question is how structures emerged from such isotropic conditions?

As it turns out, the CMB is not as uniform as it seemed when it was first discovered.

Este documento incorpora firma electrónica, y es copia auténtica de un documento electrónico archivado por la ULL según la Ley 39/2015.
Su autenticidad puede ser contrastada en la siguiente dirección https://sede.ull.es/validacion/

Identificador del documento: 2622200 Código de verificación: mbm0ekWs

Firmado por:	ROSHAN NUSHKIA CHAMBA *UNIVERSIDAD DE LA LAGUNA*	Fecha: 07/07/2020 13:28:26
	IGNACIO TRUJILLO CABRERA *UNIVERSIDAD DE LA LAGUNA*	07/07/2020 13:58:21
	Johan Hendrik Knapen Koelstra *UNIVERSIDAD DE LA LAGUNA*	07/07/2020 15:23:08
	María de las Maravillas Aguiar Aguilar *UNIVERSIDAD DE LA LAGUNA*	08/07/2020 15:55:11

Universidad de La Laguna
Oficina de Sede Electrónica
Entrada
Nº registro: 2020/46124
Nº reg. oficina: OF002/2020/45309
Fecha: 07/07/2020 15:26:22

This was realised when the Cosmic Background Explorer (COBE) discovered anisotropies in the CMB (Smoot et al. 1992). These anisotropies encode information on the decoupling of the photon from matter when the Universe was only 380,000 years old. In fact, the CMB can be considered the light which 'escaped' the primordial plasma of the early Universe as a consequence of recombination, i.e. the formation of the first atoms. However, the expansion of the Universe alone cannot account for the amplitude of the observed perturbations in the CMB. To this end, Guth (1981) hypothesised that the Universe underwent a period of rapid exponential expansion shortly after the Big Bang called inflation. Hawking (1982), among others (Guth & Pi 1982; Starobinsky 1982; Bardeen et al. 1983) then proposed that the amplitude of the anisotropies in the CMB can be recovered by quantum fluctuations in the scalar field which drives inflation.

Indeed, the structures of the Universe we observe today stem from the low amplitude density perturbations in the CMB, combined with the effect of gravity. This growth of structures after the CMB can be described using the concept of Jeans gravitational instability (Jeans 1902). According to this idea, the small density perturbations began to collapse and grow when gravity overcame the radiation pressure which supported them. This occurred in regions where the mass was greater than the characteristic Jeans mass. Interestingly, the first investigations on the issue of gravitational instability in an expanding Universe was performed by Lifshitz (1946) within the framework of General Relativity and later by Bonnor (1957) who used Newtonian gravity. As these studies were performed even before the CMB was discovered, the theory of gravitational instability was not placed within the full cosmological context for galaxy formation until the pioneering work by Silk (1968), Peebles (1969) and Zel'Dovich (1970), to list a few.

Such studies in the 1970s opened a debate on how structures formed and consisted of two major schools of thought: 1) the *top-down* approach where galaxies formed from the fragmentation and collapse of large perturbations and 2) the *bottom-up* models where galaxies formed via the hierarchical assembly of small perturbations. The top-down approach dissolved because it significantly over-estimated the amplitudes of the observed primordial fluctuations, while the bottom-up approach, although with very different requirements, persisted into the currently favoured standard cosmological model for structure formation, the Λ Cold Dark Matter (ΛCDM) model (Blumenthal et al. 1984; Navarro et al. 1996; Peebles & Ratra 2003). As its name suggests, dark matter and dark energy (represented by the cosmological constant Λ) are two main ingredients of this model.

In fact, without dark matter, i.e. matter that does not emit any light and is thus invisible to us, the initial density fluctuations in the CMB would have been unable to collapse and form the large scale structures that we observe today such as clusters and galaxies like our Milky Way. The existence of dark matter was first pointed out by Zwicky (1937) upon his analysis of the Coma cluster. However, the idea that all galaxies are embedded in dark matter haloes was more firmly supported many decades later when it became a requirement to explain the flat rotation curves of spiral galaxies at large radii (Roberts 1976; Rubin et al. 1978), among other findings (e.g. Einasto et al. 1974; Ostriker et al. 1974). Until now, the precise nature of dark matter is unknown. However, if dark matter is treated as collisionless particles in galaxy formation models, then White & Rees (1978) has shown that galaxies can form in two stages: dark matter haloes formed via hierarchical clustering, followed by the cooling and condensation of gas in dark matter potential wells (hierarchical assembly) which formed the stellar material in a galaxy. In such a model, spiral galaxies which are characterised by a rotationally supported disc (Eggen et al. 1962; Fall & Efstathiou 1980; Mo et al. 1998), could be associated to peaks in

Este documento incorpora firma electrónica, y es copia auténtica de un documento electrónico archivado por la ULL según la Ley 39/2015.
Su autenticidad puede ser contrastada en la siguiente dirección https://sede.ull.es/validacion/

Identificador del documento: 2622200 Código de verificación: mbm0ekWs

Firmado por:	ROSHAN NUSHKIA CHAMBA *UNIVERSIDAD DE LA LAGUNA*	Fecha: 07/07/2020 13:28:26
	IGNACIO TRUJILLO CABRERA *UNIVERSIDAD DE LA LAGUNA*	07/07/2020 13:58:21
	Johan Hendrik Knapen Koelstra *UNIVERSIDAD DE LA LAGUNA*	07/07/2020 15:23:08
	María de las Maravillas Aguiar Aguilar *UNIVERSIDAD DE LA LAGUNA*	08/07/2020 15:55:11

Universidad de La Laguna
Oficina de Sede Electrónica
Entrada
Nº registro: 2020/46124
Nº reg. oficina: OF002/2020/45309
Fecha: 07/07/2020 15:26:22

the dark matter density field. While the more massive elliptical galaxies, mainly ellipsoidal in shape and supported by random stellar motions, could be linked to the highest of these peaks (Blumenthal et al. 1984). Additionally, mergers between galaxies were shown to be more likely if they had a dark matter halo (Efstathiou & Silk 1983), which further reinforced the importance of earlier studies showing how galaxies interact and cause tidal distortions in their outskirts (e.g. Toomre & Toomre 1972). Predictions from such interactions in modern ΛCDM simulations will be discussed in the next section.

The second ingredient in the standard ΛCDM model is dark energy, represented by the cosmological constant Λ which is associated to this energy. Until the early 1990s, Λ was set to be zero in Einstein's equations of General Relativity which is the simplest inflationary universe model, i.e. a flat cosmology. However, this dramatically changed when two independent research teams studied distant type Ia supernovae and discovered that the expansion of the Universe is accelerating (Riess et al. 1998; Perlmutter et al. 1999). These simultaneous studies showed that Λ is non-zero and positive. Although the exact nature of dark energy is also unknown, it is possible to ascertain how much of dark energy must exist in the Universe because of how this energy affects the expansion of the Universe (parameterised by Λ). Therefore, based on current direct and indirect observations of the baryonic and non-baryonic components of the Universe, respectively, the cosmological parameters to describe the Universe have been well constrained: the matter density is $\Omega_m = 0.3153 \pm 0.0073$, $\sim 16\%$ of which corresponds to ordinary baryonic matter (protons, neutrons and electrons[1]) and $\sim 84\%$ make up the non-baryonic dark matter and the dark energy density is $\Omega_\Lambda = 0.6847 \pm 0.0073$, in a flat Universe with $\Omega_{\rm tot} = 1$ and age 13.797 Gyr (Planck Collaboration et al. 2018).

Despite the fact that the precise nature of dark matter and dark energy is unknown, and other open issues remain on structure at small scales (one of which I will discuss later) as well as how cosmological accretion, feedback processes and environmental effects interplay in the formation of galaxies (see also Mo et al. (2010) and Somerville & Davé (2015)), the standard ΛCDM model has been very successful in reproducing the large scale structure of the Universe (Fig. 1.1). In other words, it is capable of providing a self-consistent picture on the evolution of structures into their present form through cosmic time. In the context of galaxy formation and evolution relevant for this thesis, there are currently three major morphological types of galaxies in the nearby Universe: elliptical, spiral (dubbed early- and late-type galaxies, respectively by Hubble (1926)) and dwarf galaxies. As mentioned above, elliptical galaxies are ellipsoidal in shape, are supported by random stellar motions and largely evolved via merging and accretion. Spiral galaxies, on the other hand, are supported by the angular momentum in their discs and usually exhibit a spiral arm structure which hosts ongoing star formation. Compared to the more massive ellipticals and spirals, the dwarfs are the smallest galaxies as well as the most abundant type of galaxy. The dwarf galaxies are also the most diverse in terms of their appearance, from dwarf ellipticals/spheroidals, dwarf spirals to dwarf irregulars. All these morphological types may be studied at different wavelengths, from the radio to x-rays, including in their gaseous components. While an in-depth description of the different processes that shape the morphology of galaxies is beyond the scope of this thesis, some of the major characteristics of these galaxies and modern ideas on their formation relevant for the research undertaken here will be presented later in this Chapter.

[1] A slight abuse of terminology here because electrons are not baryons in the Standard Model of Particle Physics.

Este documento incorpora firma electrónica, y es copia auténtica de un documento electrónico archivado por la ULL según la Ley 39/2015.
Su autenticidad puede ser contrastada en la siguiente dirección https://sede.ull.es/validacion/

Identificador del documento: 2622200 Código de verificación: mbm0ekWs

Firmado por:	ROSHAN NUSHKIA CHAMBA *UNIVERSIDAD DE LA LAGUNA*	Fecha: 07/07/2020 13:28:26
	IGNACIO TRUJILLO CABRERA *UNIVERSIDAD DE LA LAGUNA*	07/07/2020 13:58:21
	Johan Hendrik Knapen Koelstra *UNIVERSIDAD DE LA LAGUNA*	07/07/2020 15:23:08
	María de las Maravillas Aguiar Aguilar *UNIVERSIDAD DE LA LAGUNA*	08/07/2020 15:55:11

Universidad de La Laguna
Oficina de Sede Electrónica
Entrada
Nº registro: 2020/46124
Nº reg. oficina: OF002/2020/45309
Fecha: 07/07/2020 15:26:22

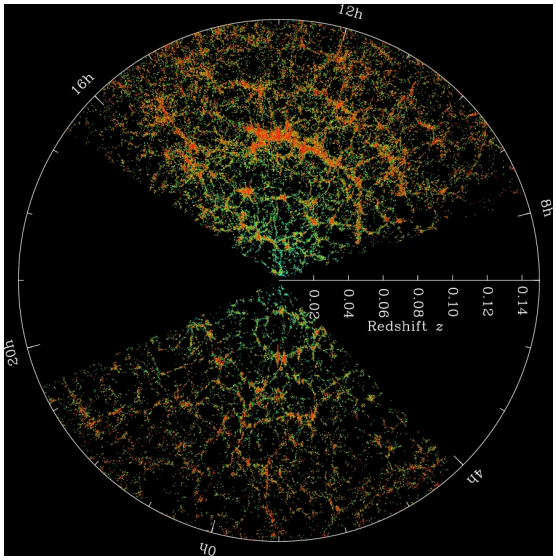

Figure 1.1: A map of the Universe from a modern survey telescope on the ground (the Sloan Digital Sky Survey (SDSS), see Sect. 1.4.2). The reference point in the centre is our Sun at the present time (redshift zero). Each dot is a galaxy; the colour is the global $(g-r)$ colour of that galaxy. The map consists of galaxies observed over one-third of the sky, up to a redshift of 0.15 which corresponds to when the Universe was about 12 Gyrs old. *Credit: M. Blanton and SDSS.*

From now onwards, I focus only on the main topic of this thesis, i.e. the low surface brightness Universe, within the ΛCDM framework described in this Section. In Sect. 1.2, I briefly discuss the predictions of state-of-the-art ΛCDM hydrodynamical simulations of galaxies in the low surface brightness regime. This includes faint structures such as stellar haloes, the intracluster light, low surface brightness galaxies and how they can provide important information on the assembly history of galaxies. I then highlight key discoveries in the observed low surface brightness Universe that are considered the foundation of current research in this field in Sect. 1.3, followed by an overview of the use of the deepest imaging to study galaxy formation and evolution in this context in Sect. 1.4. In particular, key investigations on the study of stellar haloes and faint dwarf galaxies are discussed in detail to motivate the research undertaken in Chapters 2–4 of this thesis. Sect. 1.5 then further motivates the work undertaken in those Chapters from a historical perspective. Finally, a summary and overview of this thesis is presented in Sect. 1.6.

Este documento incorpora firma electrónica, y es copia auténtica de un documento electrónico archivado por la ULL según la Ley 39/2015.
Su autenticidad puede ser contrastada en la siguiente dirección https://sede.ull.es/validacion/

Identificador del documento: 2622200 Código de verificación: mbm0ekWs

Firmado por:	ROSHAN NUSHKIA CHAMBA *UNIVERSIDAD DE LA LAGUNA*	Fecha: 07/07/2020 13:28:26
	IGNACIO TRUJILLO CABRERA *UNIVERSIDAD DE LA LAGUNA*	07/07/2020 13:58:21
	Johan Hendrik Knapen Koelstra *UNIVERSIDAD DE LA LAGUNA*	07/07/2020 15:23:08
	María de las Maravillas Aguiar Aguilar *UNIVERSIDAD DE LA LAGUNA*	08/07/2020 15:55:11

Universidad de La Laguna
Oficina de Sede Electrónica
Entrada
Nº registro: 2020/46124
Nº reg. oficina: OF002/2020/45309
Fecha: 07/07/2020 15:26:22

1.2 ΛCDM predictions and the low surface brightness Universe

A prediction of the hierarchical galaxy formation scenario in the ΛCDM paradigm introduced above is that all galaxies have experienced mergers (e.g. Purcell et al. 2007; Cooper et al. 2010). Merging events occur during the assembly and growth of a galaxy, with neighbouring low-mass systems and less frequently with other massive galaxies. The remnants of these past interactions are manifested in a faint, filamentary network of extended structures in the surroundings of the host galaxy. These include faint tidal streams, shells and tails in the galaxy outskirts.[2] Individually, the chemical, structural and kinematical properties of these tidal structures can be used to trace the progenitors or participants of the interaction like globular clusters or dwarf satellites (e.g. Belokurov et al. 2006; Martell & Grebel 2010) and ultimately the shape of the dark matter halo (Bland-Hawthorn & Gerhard 2016). Collectively, tidal features combine to form the stellar halo. As an illustration, snapshots of simulated Milky Way mass haloes from Cooper et al. (2010) are shown in Fig. 1.2. The figure shows that the majority of sub-structure in the stellar halo is of extremely low surface brightness ($\mu > 28$–30 mag/arcsec^2). If observational surveys reach such faint surface brightness limits, then simulations predict that 50% of galaxies should have at least one tidal stream (Bullock & Johnston 2005; Johnston et al. 2008). However, a more recent study has shown that this expectation is highly sensitive to the surface brightness limit used, showing that between two and three times more streams are detectable with a surface brightness cut of 33 mag/arcsec^2 than with 29 mag/arcsec^2 (Mancillas et al. 2019). In terms of stellar mass, recent simulations also show that for Milky Way-like galaxies, the stellar halo contributes between 1–2% of stellar mass to the galaxy and is dominated by old, metal-poor accreted or ex-situ stars (Cooper et al. 2013; Pillepich et al. 2015). This can be seen in the right panels of Fig. 1.2, where only stars stripped by satellite galaxies are shown. Although the contribution of these faint structures in stellar mass is very low for Milky Way-like galaxies, this may not be the case for more massive galactic systems, belonging to other morphological types or located within more dense environments such as in clusters. Therefore, mapping the stellar halo for larger samples of galaxies can lead to a more complete picture on the accretion history of galactic systems.

Cosmological simulations in the ΛCDM theory also show a diffuse distribution of stellar light in the outskirts of galaxy clusters (e.g. Rudick et al. 2011; Contini et al. 2014; Pillepich et al. 2018a; Henden et al. 2019). This is called the intra-cluster light and, although faint ($\mu > 26$ mag/arcsec^2), makes up about 10–30% of the light emitted from clusters (e.g. Krick & Bernstein 2007; Mihos et al. 2017; Montes & Trujillo 2018; Jiménez-Teja et al. 2018). In principle, the intra-cluster light is defined using stars that are bound to the cluster potential, but not to any particular galaxy within the cluster (see the recent review by Montes 2019). It originates from the assembly of clusters via the accretion of galaxies or small galactic groups, and extends out to several hundred kiloparsecs from the central cluster galaxy (Fig. 1.3). Studying the intra-cluster light is thus important because it reflects the efficiency of cluster assembly as well as the underlying dark matter distribution of the cluster (Montes & Trujillo 2019; Alonso Asensio et al. 2020).

[2] Although the nature of these sub-structures may be related to specific types of merging events (i.e. major or minor mergers. See e.g. Duc et al. (2015)), no such distinction will be made in this thesis and they will be collectively referred to as tidal features or structures.

Este documento incorpora firma electrónica, y es copia auténtica de un documento electrónico archivado por la ULL según la Ley 39/2015.
Su autenticidad puede ser contrastada en la siguiente dirección https://sede.ull.es/validacion/

Identificador del documento: 2622200 Código de verificación: mbm0ekWs

Firmado por:	ROSHAN NUSHKIA CHAMBA *UNIVERSIDAD DE LA LAGUNA*	Fecha: 07/07/2020 13:28:26
	IGNACIO TRUJILLO CABRERA *UNIVERSIDAD DE LA LAGUNA*	07/07/2020 13:58:21
	Johan Hendrik Knapen Koelstra *UNIVERSIDAD DE LA LAGUNA*	07/07/2020 15:23:08
	María de las Maravillas Aguiar Aguilar *UNIVERSIDAD DE LA LAGUNA*	08/07/2020 15:55:11

Universidad de La Laguna
Oficina de Sede Electrónica
Entrada
Nº registro: 2020/46124
Nº reg. oficina: OF002/2020/45309
Fecha: 07/07/2020 15:26:22

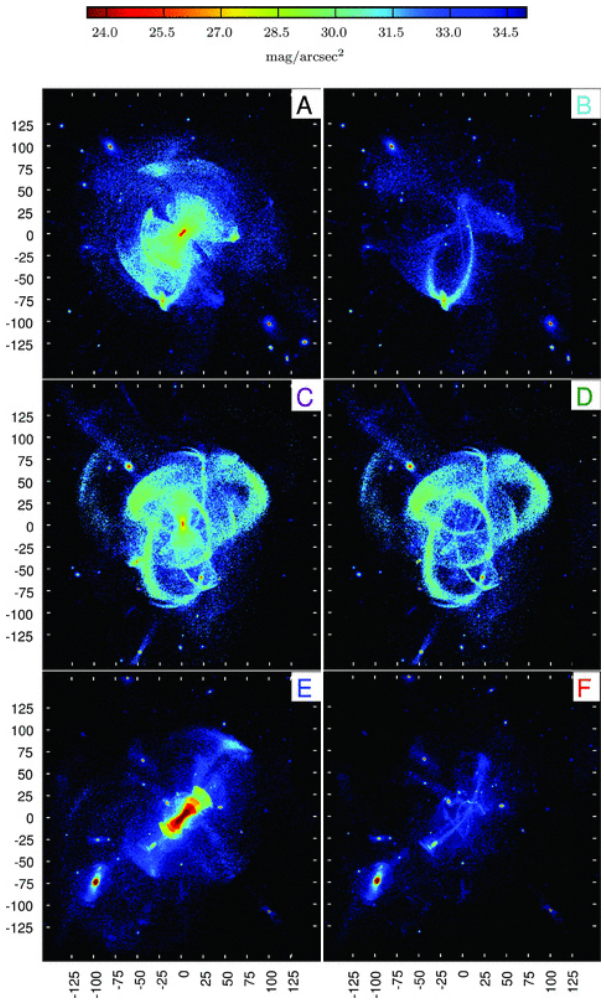

Figure 1.2: Milky Way stellar mass haloes at $z = 0$ in the Aquarius simulation. *Left panels:* Simulated V-band surface brightness maps, shown to a limiting depth of 35 mag/arcsec^2. X and Y axes are in kpc. *Right panels:* The same maps but showing only the stars stripped from satellites. *Adapted from Cooper et al. (2010).*

Este documento incorpora firma electrónica, y es copia auténtica de un documento electrónico archivado por la ULL según la Ley 39/2015.
Su autenticidad puede ser contrastada en la siguiente dirección https://sede.ull.es/validacion/

Identificador del documento: 2622200 Código de verificación: mbm0ekWs

Firmado por:	ROSHAN NUSHKIA CHAMBA *UNIVERSIDAD DE LA LAGUNA*	Fecha: 07/07/2020 13:28:26
	IGNACIO TRUJILLO CABRERA *UNIVERSIDAD DE LA LAGUNA*	07/07/2020 13:58:21
	Johan Hendrik Knapen Koelstra *UNIVERSIDAD DE LA LAGUNA*	07/07/2020 15:23:08
	María de las Maravillas Aguiar Aguilar *UNIVERSIDAD DE LA LAGUNA*	08/07/2020 15:55:11

Universidad de La Laguna
Oficina de Sede Electrónica
Entrada
Nº registro: 2020/46124
Nº reg. oficina: OF002/2020/45309
Fecha: 07/07/2020 15:26:22

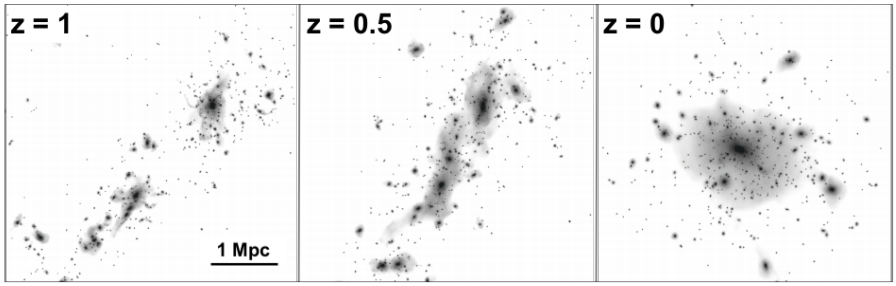

Figure 1.3: Formation of intra-cluster light during the assembly of a $10^{15} M_{\odot}$ galaxy cluster from $z = 1$ (left) to the present day (right). *Adapted from Rudick et al. (2011).*

In addition to stellar haloes and the intra-cluster light, another prediction of dark matter only ΛCDM models is the existence of hundreds of satellite galaxies around the Milky Way and in the Local Group. These are sub-haloes that are within the virial radius of the host halo, but are not disrupted via merging. Observationally, however, there is a deficit of more than an order of magnitude in the satellite galaxy population in these systems, the so-called 'missing satellite problem' (Klypin et al. 1999; Moore et al. 1999). Where are these sub-haloes? Bullock et al. (2001) demonstrated that low-mass satellite haloes can form significant populations of stars only if they accreted a substantial fraction of their gas before the epoch of reionization, otherwise the sub-haloes would remain dark and invisible. Later discoveries of the first ultra-faint dwarf galaxies, i.e. galaxies with central surface brightness $\mu(0) > 27$ mag/arcsec^2, in the Local Group (e.g. Willman et al. 2005; Zucker et al. 2006) showed that the observed nearby satellite population is incomplete and many more low surface brightness galaxies are likely hidden. Studies addressing the missing satellite problem have since evolved along these avenues: simulations accounting for baryonic affects such as star formation and feedback in galaxy formation (e.g. Okamoto et al. 2010; Sawala et al. 2016), observations of the satellite population in galaxies beyond the Local Group (e.g. Geha et al. 2017; Tanaka et al. 2018) and those accounting for survey selection effects, questioning whether a missing satellite problem exists (Kim et al. 2018; Read & Erkal 2019). Studies on low surface brightness satellites certainly offer a new front to re-examine star formation on small galactic scales and expand current knowledge on the faint end of galaxy luminosity functions.

1.3 Pioneering discoveries

In general, the modelled shapes, sizes and properties of the low surface brightness structures discussed in the previous section, namely, stellar haloes, intra-cluster light and ultra-faint galaxies are dependent on the cosmological parameters of galaxy formation models. What do these faint structures look like in the real Universe? In this section, I highlight key discoveries in the low surface brightness Universe that are considered the foundation of current research in this field.

Este documento incorpora firma electrónica, y es copia auténtica de un documento electrónico archivado por la ULL según la Ley 39/2015.
Su autenticidad puede ser contrastada en la siguiente dirección https://sede.ull.es/validacion/

Identificador del documento: 2622200 Código de verificación: mbm0ekWs

Firmado por:	ROSHAN NUSHKIA CHAMBA *UNIVERSIDAD DE LA LAGUNA*	Fecha: 07/07/2020 13:28:26
	IGNACIO TRUJILLO CABRERA *UNIVERSIDAD DE LA LAGUNA*	07/07/2020 13:58:21
	Johan Hendrik Knapen Koelstra *UNIVERSIDAD DE LA LAGUNA*	07/07/2020 15:23:08
	María de las Maravillas Aguiar Aguilar *UNIVERSIDAD DE LA LAGUNA*	08/07/2020 15:55:11

Universidad de La Laguna
Oficina de Sede Electrónica
Entrada
Nº registro: 2020/46124
Nº reg. oficina: OF002/2020/45309
Fecha: 07/07/2020 15:26:22

1.3.1 Stellar haloes

In 1969, two simultaneous, completely independent research programmes produced the first pictures of an enormous 'corona' or halo around Messier 87 (M87 or NGC 4486), one of the most massive elliptical galaxies in the Virgo Cluster. de Vaucouleurs (1969) observed M87 by repeated photoelectric scanning with the 36-inch McDonald Observatory telescope and Arp & Bertola (1969) exposed IIIa-J photographic plates (specifically designed using emulsions sensitive towards faint signals against the sky background) with the 48-inch Palomar Schmidt telescope. These authors found that M87's halo spanned over one degree on the sky or about 0.3 Mpc (see Fig. 1.4):

> *'A faint outer corona surrounding the main body of M87...has been traced out to a* ***minimum*** *diameter in excess of one degree at a brightness level of 1 per cent of the night sky,* $\mu_B \sim 27.3\, mag/arcsec^2$*.'*
>
> —Gerard de Vaucouleurs (1969)

In other words, the halo is about one hundred times fainter than the night sky ($\mu_{sky} \sim 22\,\mathrm{mag/arcsec^2}$). This is in fact the traditional definition of low surface brightness light, i.e. astronomical light that is at a brightness level of 1% of μ_{sky}.

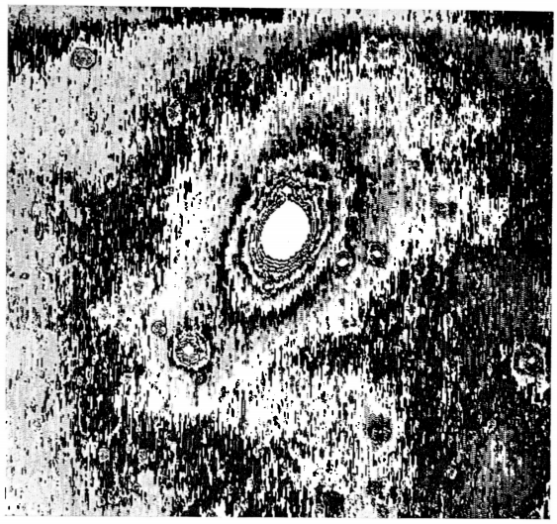

Figure 1.4: First deep image of a stellar halo around a galaxy. This is the 'isodensitracing' of the IIIa-J plate centred on M87, exposed using the 48-inch Palomar Schmidt telescope in 1969. Each successive change of symbol (space-dot-dash) corresponds to an optical density variation of 0.01. The outermost isophote encloses a diameter of $\sim 1°$. *Credit: Arp & Bertola (1969).*

Este documento incorpora firma electrónica, y es copia auténtica de un documento electrónico archivado por la ULL según la Ley 39/2015.
Su autenticidad puede ser contrastada en la siguiente dirección https://sede.ull.es/validacion/

Identificador del documento: 2622200 Código de verificación: mbm0ekWs

Firmado por:	ROSHAN NUSHKIA CHAMBA *UNIVERSIDAD DE LA LAGUNA*	Fecha: 07/07/2020 13:28:26
	IGNACIO TRUJILLO CABRERA *UNIVERSIDAD DE LA LAGUNA*	07/07/2020 13:58:21
	Johan Hendrik Knapen Koelstra *UNIVERSIDAD DE LA LAGUNA*	07/07/2020 15:23:08
	María de las Maravillas Aguiar Aguilar *UNIVERSIDAD DE LA LAGUNA*	08/07/2020 15:55:11

Universidad de La Laguna
Oficina de Sede Electrónica
Entrada
Nº registro: 2020/46124
Nº reg. oficina: OF002/2020/45309
Fecha: 07/07/2020 15:26:22

If elliptical galaxies follow the $R^{1/4}$ law (de Vaucouleurs 1948):

$$\mu(R) = \mu(0)e^{-b(R/R_{\rm s})^{1/4}} \tag{1.1}$$

where R is the radius with respect to the galaxy centre, $\mu(0)$ is the central surface brightness, the scale radius is chosen to be $R_{\rm s} \equiv R_{\rm e}$ (the effective radius) and $b = 7.67$ fixed from the requirement that $R_{\rm e}$ encloses half the total flux of the galaxy[3], then the expectation is that its luminosity profile $\mu(R^{1/4})$ is linear down to the faintest brightness levels. However, de Vaucouleurs showed that the profile of M87 can only be fully described by two components: the spheroidal (a $R^{1/4}$ main body) and an exponential (the corona or halo). This departure from the $R^{1/4}$ law could be suggestive of a different formation scenario for the outer part of the galaxy. Additionally, de Vaucouleurs demonstrated that the $B - V$ colour of the galaxy decreased (i.e. became bluer) with increasing radius.

After these key studies, imaging of several other elliptical galaxies (Arp & Bertola 1971), low and moderately rich clusters as well as isolated galaxies of various morphology (Kormendy & Bahcall 1974) showed further evidence for the existence of faint stellar haloes in galaxy outskirts, including the intra-cluster or intra-group light found within galactic clusters or groups, respectively. While elliptical galaxies generally showed large halo sizes, those in the majority of spirals are somewhat smaller, some with an abrupt cut-off radius (Sect. 1.3.2). More attention was also given to ensure that the haloes observed were not caused by instrumental artifacts. Interestingly, the colour profile of M87 by de Vaucouleurs (1969) was reproduced only ten years ago by Rudick et al. (2010) using extremely deep imaging from the Burrell Schmidt telescope down to $\mu_{lim,B} \sim 29\,{\rm mag/arcsec^2}$. For comparison, de Vaucoulerus limit of $\mu_{lim,B} \sim 27\,{\rm mag/arcsec^2}$ is comparable in depth to the Sloan Digital Sky Survey (York et al. 2000) in the g-band, reaffirming that careful analysis of the imaging even half a century ago allowed to start probing the low surface brightness regime.

1.3.2 Truncations

While an 'edge' for elliptical galaxies was not clearly evident, this did not seem to be the case for spiral, disc galaxies. In contrast to elliptical galaxies, the radial surface brightness profiles of disc galaxies could be decomposed into a bulge component (Eq. 1.1) and an exponentially declining disc (e.g. Patterson 1940; de Vaucouleurs 1959c; Freeman 1970) i.e.,

$$\mu(R) = \mu_0 e^{-R/R_{\rm d}} \tag{1.2}$$

where $R_{\rm d}$ is the disc scale length ($R_{\rm d}$ is the radius where the light profile drops by a factor of e with respect to μ_0). Do such profiles end? Do galaxies have an 'edge'?

Potential answers to these questions emerged when van der Kruit (1979) studied the surface photometry of several highly inclined disc galaxies using the 48-inch Palomar Schmidt telescope (the same instrument used by Arp & Bertola (1969)), going down to a surface brightness limit of $\mu_{lim,J} \sim 27.5$ mag/arcsec^2. He was primarily interested in determining whether edge-on stellar discs showed, at the faintest levels, any indication of the warps that were detected in

[3] *Any* fractional scale radius $R_{\rm s}$ could have been chosen, e.g. the radius enclosing 70%, 80% or 90% of the total galaxy light and b adjusted accordingly. de Vaucouleurs chose $R_{\rm e}$ probably because how galaxies behaved in their outer regions was very poorly understood in the 1940s–50s.

Este documento incorpora firma electrónica, y es copia auténtica de un documento electrónico archivado por la ULL según la Ley 39/2015.
Su autenticidad puede ser contrastada en la siguiente dirección https://sede.ull.es/validacion/

Identificador del documento: 2622200 Código de verificación: mbm0ekWs

Firmado por:	ROSHAN NUSHKIA CHAMBA *UNIVERSIDAD DE LA LAGUNA*	Fecha: 07/07/2020 13:28:26
	IGNACIO TRUJILLO CABRERA *UNIVERSIDAD DE LA LAGUNA*	07/07/2020 13:58:21
	Johan Hendrik Knapen Koelstra *UNIVERSIDAD DE LA LAGUNA*	07/07/2020 15:23:08
	María de las Maravillas Aguiar Aguilar *UNIVERSIDAD DE LA LAGUNA*	08/07/2020 15:55:11

Universidad de La Laguna
Oficina de Sede Electrónica
Entrada
Nº registro: 2020/46124
Nº reg. oficina: OF002/2020/45309
Fecha: 07/07/2020 15:26:22

large amplitudes in HI at that time. While he found that this was indeed the case for edge-on galaxies, he also made another discovery about their outer regions. Van der Kruit noticed that the radial extent of three edge-on disc galaxies in his sample did not grow with deeper exposures:

> *'[A]t the edges of the disc the decrease in apparent surface brightness is exceedingly steep. This sharp drop implies that galaxies do not retain their exponential light distribution to such faint levels. [I]t can be estimated that this behavior starts at face-on brightness levels around $B = 29$ to 30, indeed well below present levels for face-on galaxies. Unless there is no relation between mass and light this implies that in edge-on galaxies we actually observe the outer edges of stellar discs.'*
>
> —van der Kruit (1979)

In other words, at least for edge-on systems where the line-of-sight integration allowed the study of their discs to much larger radii than was possible for face-on galaxies (with photographic plates), van der Kruit detected a feature in their radial profiles which he believed were the edges of their respective stellar discs.

The existence of such edges or cut-offs were later (more comprehensively) confirmed in van der Kruit & Searle (1981a,b). These authors were interested in creating an accurate disc model for edge-on galaxies which was grounded within a physical framework, unlike the two-component (and highly uncertain) disc models used to describe the light distribution of spiral galaxies at that time (Eqs. 1.1 and 1.2). Figure 1.5 shows their results for two galaxies (initially published in van der Kruit 1979), namely, NGC 5907 and NGC 4565, including their disc model (thick line). The location of the cut-off is marked as '$R_{\rm max}$' and was called a truncation. These profiles show that the truncation is a clear deviation from the exponential profile of a disc in its outskirts. If an edge is viewed as 1) the location where a sudden *change* in an object's property occurs such as its colour or brightness and 2) this location encloses the bulk of the main body in question, then truncations are the closest feature compatible with this concept for galaxies.

Following this discovery, many authors investigated the role of truncations in discs, finding that the feature is a key indicator for the many processes that shape the formation and early evolution of discs (see van der Kruit & Freeman 2011, for a review). For instance, it has been suggested that truncations can be associated to a peak in the angular momentum distribution of the disc which, by conservation of angular momentum (Fall & Efstathiou 1980), provides a snapshot of the same distribution in the protogalaxy (van der Kruit 1987). Truncations may also be linked to the location in the disc where there is a threshold in star formation activity (Kennicutt 1989a; Roškar et al. 2008) and even trace past and ongoing star formation in disc galaxies (see Elmegreen & Hunter 2017). In both these scenarios, the presence of stars beyond the truncation can be understood if there is a mechanism of radial migration (e.g. Debattista et al. 2017). Therefore, even if the angular momentum of stars reflects that of the protogalaxy, substantial redistribution of angular momentum is expected to take place due to secular evolution processes such as bar formation (Debattista et al. 2006). Other investigations have related the origin of truncations to the aftermath of an interaction with a companion galaxy (Laurikainen & Salo 2001), warps van der Kruit (2007) or to the heating and stripping of stars by dark matter subhaloes (de Jong et al. 2007). All of these works illustrate that multiple phenomena can lead to a truncation in a galaxy's profile but how such processes interplay is still not well understood.

Este documento incorpora firma electrónica, y es copia auténtica de un documento electrónico archivado por la ULL según la Ley 39/2015.
Su autenticidad puede ser contrastada en la siguiente dirección https://sede.ull.es/validacion/

Identificador del documento: 2622200 Código de verificación: mbm0ekWs

Firmado por:	ROSHAN NUSHKIA CHAMBA *UNIVERSIDAD DE LA LAGUNA*	Fecha: 07/07/2020 13:28:26
	IGNACIO TRUJILLO CABRERA *UNIVERSIDAD DE LA LAGUNA*	07/07/2020 13:58:21
	Johan Hendrik Knapen Koelstra *UNIVERSIDAD DE LA LAGUNA*	07/07/2020 15:23:08
	María de las Maravillas Aguiar Aguilar *UNIVERSIDAD DE LA LAGUNA*	08/07/2020 15:55:11

Universidad de La Laguna
Oficina de Sede Electrónica
Entrada
Nº registro: 2020/46124
Nº reg. oficina: OF002/2020/45309
Fecha: 07/07/2020 15:26:22

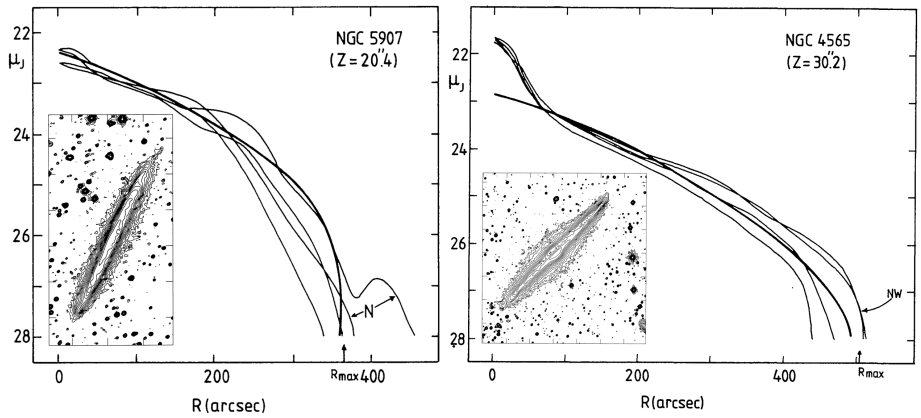

Figure 1.5: Surface brightness profiles of NGC5907 (left) and NGC4565 (right). The truncated exponential disc model for these galaxies are over-plotted (thick line). The embedded panels show surface brightness contours for each galaxy down to 27.5 J-mag/arcsec^2 on the IIIa-J plates taken from the Palomar Schimdt telescope. $R_{\rm max}$ corresponds to the location of the sharp truncation or cut-off. *Adapted from van der Kruit & Searle (1981a).*

1.3.3 Low surface brightness galaxies

Up until the mid-1970s, astronomers could not always comprehensively account for any selection biases in galaxy catalogues or samples when drawing conclusions about the properties or distributions of these objects. Consequences of these limitations arose when Freeman (1970) demonstrated that spiral galaxies have a constant central surface brightness at $\mu(0) = 21.65$ mag/arcsec^2 in the B-band. This result came to be known as Freeman's law.[4] If this 'law' were true, then it would imply that any galaxy formation model aiming to describe discs (its varying mass-to-light ratio, star formation history, angular momentum, etc.) should ultimately reach this central brightness value. It was Disney (1976) who later argued that Freeman's law is not real and is likely due to a selection effect. Disney was suspicious of the sudden drop in the number of galaxies when $\mu(0) \rightarrow \mu_{sky}$:

> *'[S]uppose the Earth were situated near the centre of a giant elliptical galaxy, then the mean surface brightness of the sky would appear some 8–9 mag brighter than is observed from our position in the Galaxy (*~ 23 *mag/arcsec*^{2} *)...Optical astronomers would then find extragalactic space an empty void; spiral and irregular galaxies would be quite invisible and all they would easily detect of galaxies would be the core regions of ellipticals very similar to their own. They would be blinded to much of the Universe by the surface brightness of their parent galaxy. But this blinding is clearly a relative matter and we should ask to what extent we are blinded by the spiral galaxy in which*

[4] Historically, and in this context, a *law* refers to a *physical law* because astronomers believed Freeman's result to be universal for spiral galaxies, much like how de Vaucouleurs $R^{1/4}$ *law* was for elliptical galaxies.

Este documento incorpora firma electrónica, y es copia auténtica de un documento electrónico archivado por la ULL según la Ley 39/2015.
Su autenticidad puede ser contrastada en la siguiente dirección https://sede.ull.es/validacion/

Identificador del documento: 2622200 Código de verificación: mbm0ekWs

Firmado por:	ROSHAN NUSHKIA CHAMBA *UNIVERSIDAD DE LA LAGUNA*	Fecha: 07/07/2020 13:28:26
	IGNACIO TRUJILLO CABRERA *UNIVERSIDAD DE LA LAGUNA*	07/07/2020 13:58:21
	Johan Hendrik Knapen Koelstra *UNIVERSIDAD DE LA LAGUNA*	07/07/2020 15:23:08
	María de las Maravillas Aguiar Aguilar *UNIVERSIDAD DE LA LAGUNA*	08/07/2020 15:55:11

Universidad de La Laguna
Oficina de Sede Electrónica
Entrada
Nº registro: 2020/46124
Nº reg. oficina: OF002/2020/45309
Fecha: 07/07/2020 15:26:22

we exist, faint as it may appear by comparison.'

—Disney (1976)

Disney's main point was that a complete picture of the galaxy population was unattainable due to the inability to observe those galaxies which are even fainter than the intrinsic brightness of the sky. However, his hypothesis that the brightness of the sky is due to the position of Earth in the Galaxy is incorrect — it is due to the recombination of atoms in the atmosphere. In general, being in a position inside our Galaxy or any other galaxy does not preclude us from observing objects much fainter than the average brightness of stars in the neighbourhood. Therefore, the inability to observe galaxies fainter than the night sky in the past was not at all because of our position in the Galaxy as Disney argued, but due to limitations in deep imaging.

Regardless of Disney's reasoning, he presupposed the existence of a population of low surface brightness galaxies that were otherwise missing in observations. This prediction was realised when extended dwarf-like low surface brightness galaxies were observed in the Virgo cluster by Sandage & Binggeli (1984). Figure 1.6 shows that these galaxies were barely visible in the photographic plates of that era as they have central surface brightnesses $\mu(0) > 25\,\mathrm{mag/arcsec^2}$ i.e. more than ten times fainter than the night sky. Owing to their large diameter ($\sim 10\,\mathrm{kpc}$), Sandage & Binggeli (1984) referred to these faint, low-mass galaxies as 'large dwarfs'. A few years later, the accidental discovery of Malin I by Bothun et al. (1987) — the most extended low surface brightness disc known to date (a radius of about $\sim 160\,\mathrm{kpc}$ (Galaz et al. 2015)) — further echoed Disney's revelation on 'iceberg' galaxies:

'Galaxies are like icebergs and what is seen above the sky background may be no reliable measure of what lies underneath.'

—Disney (1976)

Even fainter galaxies then began to be unveiled (e.g. Impey et al. 1988; Bothun et al. 1991; Dalcanton et al. 1997a) which lead to a definite proof that laws such as Freeman's were a consequence of a selection bias (see McGaugh et al. 1995). These results showed convincing evidence that the number density of the low surface brightness galaxy population was much higher than previously thought (e.g. about 5 orders of magnitude higher than predicted by Freeman's law). Could these galaxies be the missing satellites discussed in Sect. 1.2?

Este documento incorpora firma electrónica, y es copia auténtica de un documento electrónico archivado por la ULL según la Ley 39/2015.
Su autenticidad puede ser contrastada en la siguiente dirección https://sede.ull.es/validacion/

Identificador del documento: 2622200 Código de verificación: mbm0ekWs

Firmado por:	ROSHAN NUSHKIA CHAMBA *UNIVERSIDAD DE LA LAGUNA*	Fecha: 07/07/2020 13:28:26
	IGNACIO TRUJILLO CABRERA *UNIVERSIDAD DE LA LAGUNA*	07/07/2020 13:58:21
	Johan Hendrik Knapen Koelstra *UNIVERSIDAD DE LA LAGUNA*	07/07/2020 15:23:08
	María de las Maravillas Aguiar Aguilar *UNIVERSIDAD DE LA LAGUNA*	08/07/2020 15:55:11

Universidad de La Laguna
Oficina de Sede Electrónica
Entrada
Nº registro: 2020/46124
Nº reg. oficina: OF002/2020/45309
Fecha: 07/07/2020 15:26:22

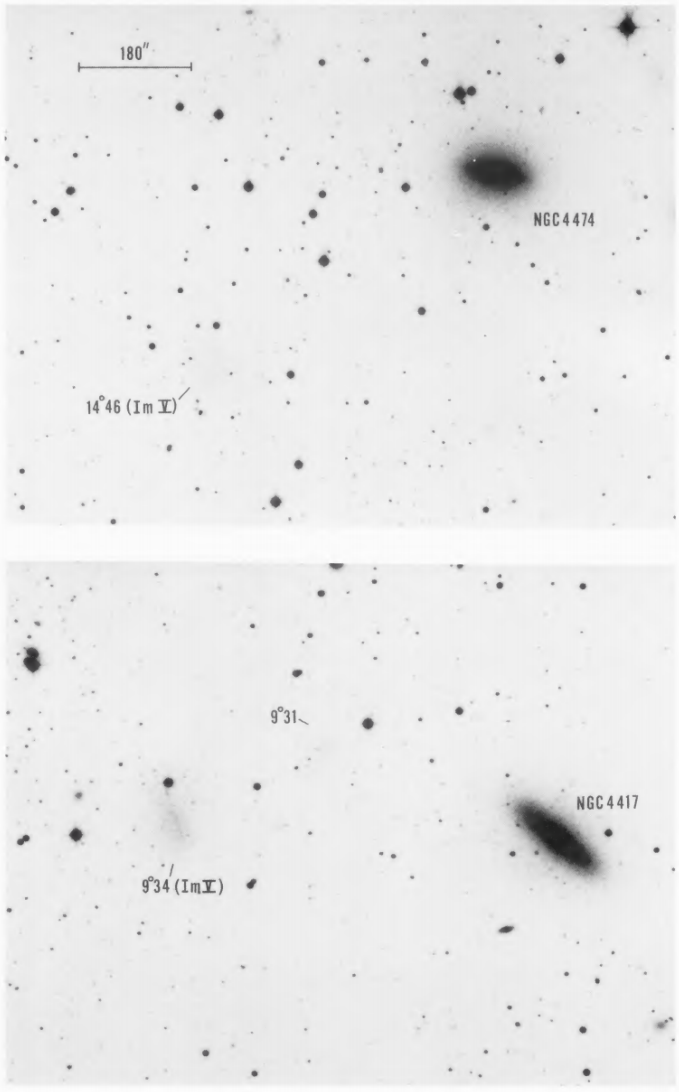

Figure 1.6: Two extended, low surface brightness galaxies ($\mu(0, B) > 25\,\mathrm{mag/arsec}^2$ and diameters in the order of 10 kpc) in the Virgo cluster, 14°46 (upper panel, VCC 1287) and 9°34 (lower panel, MCG+02-32-063), labelled as morphology type Im V due to their lumpiness. The 'normal' bright neighbours of these faint galaxies are included within the frame for contrast. These panels are reproduced using the IIIa-J 1.2 m Palomar Schimdt plate. *Credit: Sandage & Binggeli (1984).*

Este documento incorpora firma electrónica, y es copia auténtica de un documento electrónico archivado por la ULL según la Ley 39/2015.
Su autenticidad puede ser contrastada en la siguiente dirección https://sede.ull.es/validacion/

Identificador del documento: 2622200 Código de verificación: mbm0ekWs

Firmado por:	ROSHAN NUSHKIA CHAMBA *UNIVERSIDAD DE LA LAGUNA*	Fecha: 07/07/2020 13:28:26
	IGNACIO TRUJILLO CABRERA *UNIVERSIDAD DE LA LAGUNA*	07/07/2020 13:58:21
	Johan Hendrik Knapen Koelstra *UNIVERSIDAD DE LA LAGUNA*	07/07/2020 15:23:08
	María de las Maravillas Aguiar Aguilar *UNIVERSIDAD DE LA LAGUNA*	08/07/2020 15:55:11

Universidad de La Laguna
Oficina de Sede Electrónica
Entrada
Nº registro: 2020/46124
Nº reg. oficina: OF002/2020/45309
Fecha: 07/07/2020 15:26:22

1.4 Deep imaging: a frontier for galaxy evolution studies

The discovery of stellar haloes, truncations and low surface brightness galaxies described above all demonstrate that deep imaging has played an important role in the early development of our knowledge on the population of galaxies and their properties. In this section, I provide a brief overview on the technological and observational advancements in astronomical deep imaging. I then discuss two contemporary works, namely Trujillo & Fliri (2016) and van Dokkum et al. (2015a), as highlights on the study of stellar haloes and low surface brightness galaxies, respectively. These particular investigations will be used to motivate the research undertaken in this thesis. In keeping within the scope of this thesis, only surveys and imaging in the optical wavelengths from ground-based telescopes will be treated in this Section. The data reduction/observational procedures and other technicalities such as the careful coaddition of images or background subtraction methods will also not be treated for the same reason. The relevant methods used in this thesis will be left in Chapters 2–4 for the reader.

1.4.1 From deep photographic sky surveys to CCD imaging

In the 1950s, the well-known 1.2 m Schmidt telescope in the Palomar Observatory in California, USA was used to perform one of the first photographic sky surveys in astronomy. The survey was called the Palomar Observatory Sky Survey or POSS-I (Minkowski & Abell 1963). POSS-I consisted of $\sim$ 1000 plates, each with a $6.5^\circ \times 6.5^\circ$ field of view (FOV) in two wavelength ranges (roughly in the blue and red) and was generally limited to objects with redshift $z < 0.1$. This corresponds to a point source depth of 20 mag and 21 mag in the red and blue plates, respectively. In surface brightness depth this is $\mu_{lim,red} \sim 25\,\mathrm{mag/arcsec^2}$. One POSS-I plate could consist of between 10^5–10^6 stars and galaxies. Catalogues created by the visual inspection of these large POSS plates are certainly heroic achievements. Notable examples are Nilson (1973) who catalogued $\sim 13,000$ galaxies called the Uppsala General Catalogue (UGC) and Vorontsov-Vel'Yaminov & Arkhipova (1962) who catalogued 34,000 galaxies between 1962–68 called the Morphological Catalogue of Galaxies (MCG, compiled in Vorontsov-Velyaminov & Krasnogorskaya 1994).[5] It is remarkable that a number of low surface brightness galaxies were also catalogued in MCG (see Sandage & Binggeli 1984, and Fig. 1.6).

While POSS-I imaged the Northern Sky, the 1.2 m UK Schmidt telescope in the Anglo-Australian Observatory (AAO), Australia and the 1.0 m Schmidt telescope of the European Southern Observatory (ESO) in Chile began observations of the Southern skies in the 1970s–90s (see e.g. Reshetnikov 2005; Djorgovski et al. 2013, and references therein). The combined efforts of these observatories (called the ESO/SERC Southern Sky Survey) led to improved versions of the IIIa-J plates for imaging low signal-to-noise sources against the sky background (see Malin & Hadley 1999, for a brief review) and thus deeper imaging than POSS-I (by ~ 1.5 mag). A key player in making the images from the UK Schmidt telescope even deeper was David Malin. He developed techniques to enhance low surface brightness features in the improved

[5] For the reader interested in historical debate, Vorontsov-Velyaminov's catalogue (MCG) seemed to have been discriminated against by several astronomers, including de Vaucouleurs et al. (1964, in the Reference Catalogue of Bright Galaxies) who had access to the relevant published MCG volumes. Drs. de Vaucouleurs call galaxies that were catalogued in the MCG with other names or as 'anonymous' systems. See the thread of correspondences (or what we would now call 'tweets') exchanged in Vorontsov-Velyaminov (1974), de Vaucouleurs & de Vaucouleurs (1975) and Vorontsov-Velyaminov (1975).

Este documento incorpora firma electrónica, y es copia auténtica de un documento electrónico archivado por la ULL según la Ley 39/2015.
Su autenticidad puede ser contrastada en la siguiente dirección https://sede.ull.es/validacion/

Identificador del documento: 2622200 Código de verificación: mbm0ekWs

Firmado por:	ROSHAN NUSHKIA CHAMBA *UNIVERSIDAD DE LA LAGUNA*	Fecha: 07/07/2020 13:28:26
	IGNACIO TRUJILLO CABRERA *UNIVERSIDAD DE LA LAGUNA*	07/07/2020 13:58:21
	Johan Hendrik Knapen Koelstra *UNIVERSIDAD DE LA LAGUNA*	07/07/2020 15:23:08
	María de las Maravillas Aguiar Aguilar *UNIVERSIDAD DE LA LAGUNA*	08/07/2020 15:55:11

Universidad de La Laguna
Oficina de Sede Electrónica
Entrada
Nº registro: 2020/46124
Nº reg. oficina: OF002/2020/45309
Fecha: 07/07/2020 15:26:22

IIIa-J photographic plates from the UK Schimdt (e.g. Malin 1978, 1981). This immediately led to several discoveries such as shell-like features in the outer regions of elliptical galaxies (Malin & Carter 1980) and the famous Malin I (Bothun et al. 1987) mentioned in Sect. 1.3.3. The imaging used in Malin & Carter (1980) for example reached a depth of $\mu_{lim,J} \sim 27\,\mathrm{mag/arcsec^2}$. But Malin's plate stacking technique was later shown to reach $\sim 1\,\mathrm{mag}$ even fainter than a single UK Schmidt plate, i.e. $\mu_{lim,B} \sim 28\,\mathrm{mag/arcsec^2}$ (e.g. Malin 1988; Bland-Hawthorn et al. 1993; Malin & Hadley 1999). An example is shown in Fig. 1.7 on the next page where four UK Schmidt plates were stacked.[6] Thus, Malin and his collaborators demonstrated the possibility of deeper surface photometry than possible with POSS-I plates.

In parallel with the developments in deep photographic plates, there were also efforts to digitise the full plates from ESO/SERC, POSS-I and later the $\sim$ 1–1.5 mag deeper POSS-II (Reid et al. 1991) in the late 1980s. As reviewed by Reshetnikov (2005), the plates from these surveys were effectively read only after various plate digitising machines were developed. It was these efforts which lead to the first digital sky surveys like DSS (Digital Sky Survey; Lasker et al. 1989) and DPOSS (Digital POSS; Djorgovski et al. 1998) in the 1990s.[7] In particular, the first of these surveys, the DSS (Lasker et al. 1989), was an initiative led by the Space Telescope Science Institute to scan/digitise POSS-I (and later POSS-II) photographic plates as a requirement for operations with the *Hubble Space Telescope* (*HST*).[8] The DSS was the first high quality, public digital survey of the full sky in the optical regime. It was used to create the Guide Star Catalogue so that the *HST* can be precisely pointed to a source of interest and guide the *HST* during the observation. Interestingly, the use of the more stable, efficient and relatively low noise charge-coupled devices (CCDs) for astronomical imaging was first championed by researchers preparing for the *HST* mission at the NASA Jet Propulsion Laboratory (JPL) between 1973–1979 (McLean 2002). Once Smith (1976) demonstrated the superiority of astronomical images resulting from a JPL CCD-camera, many observatories began developing CCD arrays for their respective telescopes. As the *HST* was launched in 1990, it can be considered the first deep CCD-camera based observatory in astronomy. Thus began the era when digital sky surveys from photographic plates were replaced by imaging with CCDs.

In the following sections, I will briefly overview the contemporary state-of-the-art surveys using CCD imaging and show examples of investigations that demonstrated the possibility of going even deeper than, for example, the plates enhanced by Malin.

[6] In stacking N photographic plates, the magnitude limit is expected to improve by $2.5\log[\sqrt{N}]$.

[7] Prior to digitisation, physical copies of the plates from surveys like POSS-I (in the form of glass or film) were sold to the astronomical community worldwide (see Morgan 1995).

[8] The *HST* has a rich history, dating back to ideas from the 1920s (Oberth 1923). While an overview on the history of space telescopes is beyond the scope of this thesis, it is interesting to realise that in the early development of a 'Large Space Telescope' concept at NASA in the 1960s, it was hypothesised that physical copies of data in the form of film (or plates) would be retrieved in capsules from the telescope back to Earth. This was because the technology for transmitting data from, for example, weather satellites at that time could not provide data with high enough resolution suitable for astronomy. At least until the technology to fully digitise images (CCDs) and automate data retrieval was perfected in the 1980s–90s, whether space telescopes should be manned or man-tended in orbit* during observations was also considered. I refer the interested reader to Shayler & Harland (2016, Chapter 2 '*The dream*') for a brief history on these early developments.
*`https://twitter.com/NushkiaC/status/1267518698404876297`

Este documento incorpora firma electrónica, y es copia auténtica de un documento electrónico archivado por la ULL según la Ley 39/2015.
Su autenticidad puede ser contrastada en la siguiente dirección https://sede.ull.es/validacion/

Identificador del documento: 2622200 Código de verificación: mbm0ekWs

Firmado por:	ROSHAN NUSHKIA CHAMBA *UNIVERSIDAD DE LA LAGUNA*	Fecha: 07/07/2020 13:28:26
	IGNACIO TRUJILLO CABRERA *UNIVERSIDAD DE LA LAGUNA*	07/07/2020 13:58:21
	Johan Hendrik Knapen Koelstra *UNIVERSIDAD DE LA LAGUNA*	07/07/2020 15:23:08
	María de las Maravillas Aguiar Aguilar *UNIVERSIDAD DE LA LAGUNA*	08/07/2020 15:55:11

Universidad de La Laguna
Oficina de Sede Electrónica
Entrada
Nº registro: 2020/46124
Nº reg. oficina: OF002/2020/45309
Fecha: 07/07/2020 15:26:22

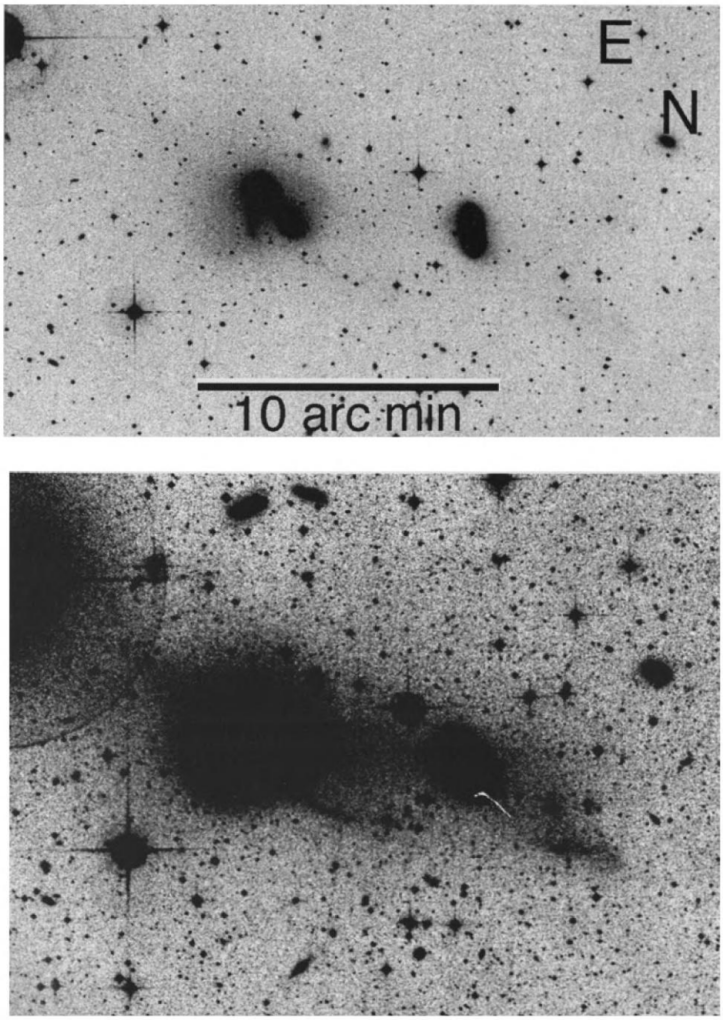

Figure 1.7: The Hickson 90 group of galaxies. Upper image from a single UK Schmidt IIIa-J plate. Lower image, enhanced and combined images from four such plates. Figure and caption taken from Malin & Hadley (1999).

Este documento incorpora firma electrónica, y es copia auténtica de un documento electrónico archivado por la ULL según la Ley 39/2015.
Su autenticidad puede ser contrastada en la siguiente dirección https://sede.ull.es/validacion/

Identificador del documento: 2622200 Código de verificación: mbm0ekWs

Firmado por:	ROSHAN NUSHKIA CHAMBA *UNIVERSIDAD DE LA LAGUNA*	Fecha: 07/07/2020 13:28:26
	IGNACIO TRUJILLO CABRERA *UNIVERSIDAD DE LA LAGUNA*	07/07/2020 13:58:21
	Johan Hendrik Knapen Koelstra *UNIVERSIDAD DE LA LAGUNA*	07/07/2020 15:23:08
	María de las Maravillas Aguiar Aguilar *UNIVERSIDAD DE LA LAGUNA*	08/07/2020 15:55:11

Universidad de La Laguna
Oficina de Sede Electrónica
Entrada
Nº registro: 2020/46124
Nº reg. oficina: OF002/2020/45309
Fecha: 07/07/2020 15:26:22

1.4.2 State-of-the-art surveys

One of the first ambitious wide field surveys from the ground in contemporary extragalactic astronomy is the Sloan Digital Sky Survey[9] (SDSS; York et al. 2000). The Sloan Legacy Survey in the early 2000s (SDSS-I, 2000–2005; SDSS-II, 2005–2008) used a 2.5 m telescope that observed more than one-quarter of the night sky in the u, g, r, i and z-bands. It produced spectra for 930,000 galaxies, 120,000 quasars and 225,000 stars.[10] These products lead to several important studies such as the first statistical analysis on the size distribution of galaxies (Shen et al. 2003), the Galaxy luminosity function (Blanton et al. 2003) as well as large strides in deriving cosmological parameters (e.g. Tegmark et al. 2004) and stellar population synthesis models (e.g. Bruzual & Charlot 2003), to list a few. The latest generation of the SDSS (SDSS-IV, 2014–2020) is extending precision cosmological measurements to a critical early phase of cosmic history (eBOSS), expanding its revolutionary infrared spectroscopic survey of the Galaxy (APOGEE-2), and for the first time using the Sloan spectrographs to make spatially resolved maps of individual galaxies (MaNGA)[11], over one-third of the sky (see also a latest map of the Universe from SDSS in Fig. 1.1). Therefore, the SDSS is enormously increasing our knowledge on the structure, spectral characteristics, and spatial distribution of galaxies in the nearby ($z < 0.2$) Universe than was possible in the era of photographic plates (see Sect. 1.4.1). Before proceeding any further in this short overview, let us introduce a formalism that can be used to quote the limiting surface brightness depth of SDSS or any other survey. This will aid a robust comparison between the depth of different imaging surveys that will be further discussed later in Sect. 1.4.3.

In general, the limiting surface brightness depth of imaging can be computed as the $x\sigma$ fluctuation (where x corresponds to the number of deviations) with respect to the background of the image that is measured over an area A. This is called a metric, i.e. $(x\sigma; A\,\mathrm{arcsec}^2)$. As a rule of thumb, A is optimally chosen according to the apparent size of objects under consideration (using a circle, box etc.). Therefore, in the SDSS g-band, we may write that the limiting surface brightness depth is $\mu_{lim,g} \sim 26.5\,\mathrm{mag/arcsec}^2$ $(3\sigma; R = 12'')$ (Kniazev et al. 2004), where A was chosen to be the area of a circle with radius $R = 12''$. This is a reasonable choice for A because Kniazev et al. (2004) was interested in the search for new dwarf and low surface brightness galaxies in SDSS. Hereafter, it is this formalism and notation that will be used to quote the limiting surface brightness depths of any survey or imaging discussed.

The limiting SDSS depth stated above is similar to that of a single UK Schmidt plate shown in Fig. 1.7. Therefore SDSS alone is not considered a deep survey. Current surveys are now able to observe extragalactic sources about 2–3 magnitudes deeper than SDSS (e.g. Mihos et al. 2005; Martínez-Delgado et al. 2010; Ferrarese et al. 2012; Merritt et al. 2014; Capaccioli et al. 2015; Duc et al. 2015; Koda et al. 2015; Trujillo & Fliri 2016; Mihos et al. 2017). Such deep surveys have opened the possibility of studying the low surface brightness Universe with CCD imaging. This was not immediately straightforward because deep surface photometry generally requires excellent flat fielding at degree scales. Currently used CCD arrays do not have as large a field of view than that of photographic plates, so this demanded clever telescope design (e.g. Mihos

[9] It is interesting that the name 'Sloan Digital Sky Survey' is reminiscent of the early digital sky surveys described in Sect. 1.4.1 like DSS (Lasker et al. 1989). Surveys like DSS were probably named in reference to the digitisation of photographic plates, whereas SDSS in reference to the survey being totally digital as the images were obtained using a CCD-camera.

[10] `http://classic.sdss.org/`

[11] `https://www.sdss.org/surveys/`

Este documento incorpora firma electrónica, y es copia auténtica de un documento electrónico archivado por la ULL según la Ley 39/2015.
Su autenticidad puede ser contrastada en la siguiente dirección https://sede.ull.es/validacion/

Identificador del documento: 2622200 Código de verificación: mbm0ekWs

Firmado por:	ROSHAN NUSHKIA CHAMBA *UNIVERSIDAD DE LA LAGUNA*	Fecha: 07/07/2020 13:28:26
	IGNACIO TRUJILLO CABRERA *UNIVERSIDAD DE LA LAGUNA*	07/07/2020 13:58:21
	Johan Hendrik Knapen Koelstra *UNIVERSIDAD DE LA LAGUNA*	07/07/2020 15:23:08
	María de las Maravillas Aguiar Aguilar *UNIVERSIDAD DE LA LAGUNA*	08/07/2020 15:55:11

Universidad de La Laguna
Oficina de Sede Electrónica
Entrada
Nº registro: 2020/46124
Nº reg. oficina: OF002/2020/45309
Fecha: 07/07/2020 15:26:22

et al. 2005) and observational strategies (e.g. Trujillo & Fliri 2016, who produced the current deepest image from the ground, discussed later in Sect. 1.4.3). As an example to illustrate that CCD imaging can now be as deep or even deeper than the stacked photographic plates, the first two columns in Fig. 1.8 shows deep images from the Stellar Tidal Stream Survey (STSS; Martínez-Delgado et al. 2010) and the last column shows the deep UK Schmidt plates processed by David Malin in the 1980s–90s[12] for two of the galaxies shown. The STSS images have a limiting depth of $\mu_{lim,V} \sim 28.5\,\mathrm{mag/arcsec^2}$ ($5\sigma; R = 1''$), which is 2.5 mag deeper than SDSS and 0.5 mag deeper than the enhanced plates. It is important to point out that the galaxies observed by Martínez-Delgado et al. (2010) were not randomly chosen but pre-selected using enhanced SDSS images because they appeared to have some 'brighter' faint structures.

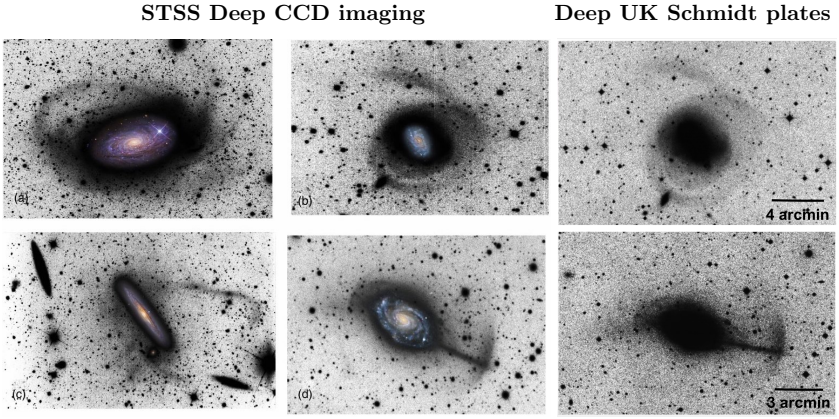

Figure 1.8: Comparison between deep CCD imaging and deep photographic plates. The first two columns show stellar streams detected around spiral galaxies with deep imaging (limiting depth $\mu_{lim,V} \sim 28.5\,\mathrm{mag/arcsec^2}$) from the STSS (Martínez-Delgado et al. 2010). The images are composite RGB-luminance to highlight faint structures detected using data taken from small (0.1–0.5 m) aperture telescopes. The galaxies shown are: (a) M63; (b) NGC 1084; (c) NGC 4216; (d) NGC 4651. The last column shows NGC 1084 (top) and NGC 4651 (bottom) taken from David Malin's archive[10] of stacked UK Schmidt plates ($\mu_{lim,B} \sim 28\,\mathrm{mag/arcsec^2}$, roughly 0.5 mag shallower than STSS).

The detected features shown in Fig. 1.8 in the galaxy outskirts can be compared with those predicted in ΛCDM simulations (Sect. 1.2). Interestingly, different types of faint structures (streams, tails and shells) have also been defined and studied in the context of past major or minor and wet or dry events with the host galaxy (Duc et al. 2015; Mancillas et al. 2019). Systematic searches for unknown tidal features in other deep surveys is an active area of research (e.g. Atkinson et al. 2013; Kado-Fong et al. 2018; Hood et al. 2018; Morales et al. 2018; Mosenkov et al. 2020). Although many of these works adopt different criteria and definitions of tidal features, the general result from these observational studies is that shells and streams from

[12]See David Malin's image archive in `https://images.datacentral.org.au/malin/DEEP/`

Este documento incorpora firma electrónica, y es copia auténtica de un documento electrónico archivado por la ULL según la Ley 39/2015.
Su autenticidad puede ser contrastada en la siguiente dirección https://sede.ull.es/validacion/

Identificador del documento: 2622200 Código de verificación: mbm0ekWs

Firmado por:	ROSHAN NUSHKIA CHAMBA *UNIVERSIDAD DE LA LAGUNA*	Fecha: 07/07/2020 13:28:26
	IGNACIO TRUJILLO CABRERA *UNIVERSIDAD DE LA LAGUNA*	07/07/2020 13:58:21
	Johan Hendrik Knapen Koelstra *UNIVERSIDAD DE LA LAGUNA*	07/07/2020 15:23:08
	María de las Maravillas Aguiar Aguilar *UNIVERSIDAD DE LA LAGUNA*	08/07/2020 15:55:11

Universidad de La Laguna
Oficina de Sede Electrónica
Entrada
Nº registro: 2020/46124
Nº reg. oficina: OF002/2020/45309
Fecha: 07/07/2020 15:26:22

mergers or satellite disruption are the most common types of features in galaxy outskirts.

Similar to the search for tidal structures, many catalogues of a growing number of previously unknown low surface brightness galaxies (e.g. Müller et al. 2017; Venhola et al. 2017; Greco et al. 2018; González et al. 2018; Prole et al. 2018), including the effort to target these objects using deep spectroscopy (Ruiz-Lara et al. 2018; Ferré-Mateu et al. 2018), have been produced. In particular, the re-discovery of dwarf-like low surface brightness galaxies (and called 'ultra-diffuse galaxies') by van Dokkum et al. (2015a), first found in Virgo by Sandage & Binggeli (1984) (Sect. 1.3.3), will be discussed in more detail later in Sect. 1.4.5. However, as previously mentioned in Sect. 1.2, studies on the low surface brightness galaxy population now overlap with those addressing the open question of the 'missing satellite problem' (e.g. Kim et al. 2018; Read & Erkal 2019) and the faint end of galaxy luminosity functions (e.g. Geha et al. 2017; Tanaka et al. 2018; Yue et al. 2018; Bennet et al. 2020). But the studies on these open questions with deep imaging are still in its infancy, the majority of which have only examined the issue for nearby Milky Way-like galaxies.

Another topic of research using deep integrated photometry is that of galactic stellar haloes. One of the first statistical study on stellar haloes used stacked versions of SDSS images for 1000 edge-on disc galaxies, reaching $\mu_{lim,g} \sim 29\,\mathrm{mag/arcsec^2}$ ($1\sigma; 4 \times 4\,\mathrm{arcsec^2}$) in the images (Zibetti et al. 2004). Many other investigations followed this approach of stacked imaging to achieve similar depths for the study of galactic haloes (e.g. de Jong 2008; Jablonka et al. 2010; Tal & van Dokkum 2011; Bakos & Trujillo 2012). In fact, the deep images from the IAC Stripe 82 Legacy Project (hereafter IAC Stripe82 Fliri & Trujillo 2016) that will be used in this thesis was created by carefully stacking images from repeated observations that were performed during the Sloan Supernova Survey (82 runs in the five SDSS filters Frieman et al. 2008). The surface brightness limits of the IAC Stripe 82 images are $\mu_{lim,r} = 28.5\,\mathrm{mag/arcsec^2}$ and $\mu_{lim,g} = 29.1\,\mathrm{mag/arcsec^2}$ ($3\sigma; 10 \times 10\,\mathrm{arcsec^2}$) in the latest public release (Román & Trujillo 2018). The use of the deep IAC Stripe 82 Legacy Project in this thesis is motivated in Chapters 2–4 and will be shown to be sufficiently deep for the research work presented therein. However, for the study of stellar haloes particularly, the best and most robust results have been achieved with direct observations. To illustrate this, the work by Trujillo & Fliri (2016) where the mass of the stellar halo of UGC 00180 was estimated using the deepest optical imaging from the ground with the Gran Telescopio Canarias, will be discussed in more detail in Sect. 1.4.3. In that section, I will demonstrate one of the ways in which results from deep integrated light can be fairly and robustly compared to ΛCDM predictions from simulations.

Ongoing surveys using the Hyper Suprime-Cam (Aihara et al. 2018) or next generation surveys like the Legacy Survey of Space and Time[13] (LSST; LSST Science Collaboration et al. 2009) will certainly allow to explore tidal structures, faint satellite galaxies and stellar haloes for a few thousand galaxies. In particular, the imaging from LSST is expected to be extremely deep, $\mu_{lim} \sim 31.5\,\mathrm{mag/arcsec^2}$ ($3\sigma; 10 \times 10\,\mathrm{arcsec^2}$), and homogeneous. Space-based telescopes are also promising in this avenue, with the current deepest observation using the *HST* reaching depths fainter than $31.5\,\mathrm{mag/arcsec^2}$ (see Borlaff et al. 2019). Of course ultra-deep imaging comes with a lot of challenges like dealing with scattered light from the point spread function (Infante-Sainz et al. 2020), sky subtraction and masking of extended sources (Haigh, Chamba et al., A&A submitted), but these technicalities are beyond the scope of this thesis and will not be

[13]Previously named the Large Synoptic Survey Telescope.

Este documento incorpora firma electrónica, y es copia auténtica de un documento electrónico archivado por la ULL según la Ley 39/2015.
Su autenticidad puede ser contrastada en la siguiente dirección https://sede.ull.es/validacion/

Identificador del documento: 2622200 Código de verificación: mbm0ekWs

Firmado por:	ROSHAN NUSHKIA CHAMBA *UNIVERSIDAD DE LA LAGUNA*	Fecha: 07/07/2020 13:28:26
	IGNACIO TRUJILLO CABRERA *UNIVERSIDAD DE LA LAGUNA*	07/07/2020 13:58:21
	Johan Hendrik Knapen Koelstra *UNIVERSIDAD DE LA LAGUNA*	07/07/2020 15:23:08
	María de las Maravillas Aguiar Aguilar *UNIVERSIDAD DE LA LAGUNA*	08/07/2020 15:55:11

Universidad de La Laguna
Oficina de Sede Electrónica
Entrada
Nº registro: 2020/46124
Nº reg. oficina: OF002/2020/45309
Fecha: 07/07/2020 15:26:22

treated in detail (see Knapen & Trujillo 2017, for a review). However, the relevant deep imaging methods used in this thesis are presented in Chapters 2–4.

1.4.3 Going beyond 31 mag/arsec^2: unveiling galactic stellar haloes

With the goal of exploring how deep one can go into the Universe with integrated surface photometry, Trujillo & Fliri (2016) pointed the 10.4 m Gran Telescopio Canarias (GTC) for 8.1h on UGC 00180, a galaxy analagous to the Andromeda Galaxy but located at a distance of ~ 150 Mpc. These authors were able to reach a surface brightness limit compatible with those achieved from star counting techniques: $\mu_{lim,r} = 31.5$ mag/arcsec^2 ($3\sigma; 10\times10$ arcsec^2). The area of a box 10×10 arcsec^2 was optimally chosen because Trujillo & Fliri (2016) was interested in characterising the stellar halo of the galaxy, and this area corresponds to the average dimensions of stellar halo structures beyond the Local Group. The imaging by these authors is the current deepest image of a galaxy from ground-based telescopes. In general, imaging with depth fainter than 30 mag/arcsec^2 can be referred to as 'ultra-deep'.[14]

Figure 1.9 shows the ultra-deep GTC image and the corresponding surface brightness profile of the object in the r-band (μ_r). The profile using SDSS imaging is also included for comparison.

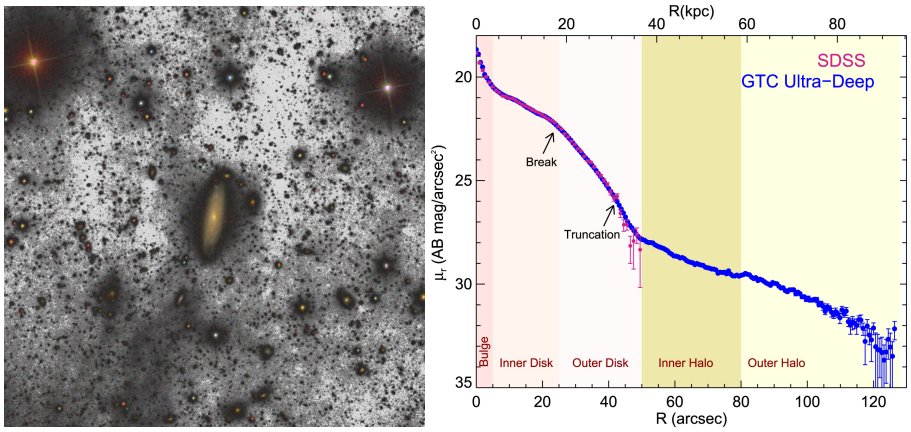

Figure 1.9: Ultra-deep image of UGC 00180, a galaxy analogous to Andromeda, observed with the 10.4m GTC, one of the largest ground-based optical telescopes in the world. *Left:* SDSS *gri*-band colour composite image overlaid on the deep GTC r-band data in grey scale to highlight the low surface brightness structures detected. *Right:* The surface brightness profile of the galaxy in the r-band (μ_r) from GTC (blue) and SDSS (pink) imaging. The location of the break and truncation are also marked. The GTC profile goes down 5 mag deeper compared to the SDSS one. *Credit: GTC, Gabriel Pérez and Trujillo & Fliri (2016).*

[14] Although astronomers have not yet reached a consensus on how to quantify the depth of images, one may find imaging limited to e.g. 28.5 mag/arcsec^2 also called 'ultra-deep'. But I think the term 'ultra-deep' is more meaningful for imaging limits > 30 mag/arcsec^2 ($3\sigma; 10 \times 10$arcsec^2) because this is when the properties of faint stellar haloes can be studied with higher confidence.

Este documento incorpora firma electrónica, y es copia auténtica de un documento electrónico archivado por la ULL según la Ley 39/2015.
Su autenticidad puede ser contrastada en la siguiente dirección https://sede.ull.es/validacion/

Identificador del documento: 2622200 Código de verificación: mbm0ekWs

Firmado por:	ROSHAN NUSHKIA CHAMBA *UNIVERSIDAD DE LA LAGUNA*	Fecha: 07/07/2020 13:28:26
	IGNACIO TRUJILLO CABRERA *UNIVERSIDAD DE LA LAGUNA*	07/07/2020 13:58:21
	Johan Hendrik Knapen Koelstra *UNIVERSIDAD DE LA LAGUNA*	07/07/2020 15:23:08
	María de las Maravillas Aguiar Aguilar *UNIVERSIDAD DE LA LAGUNA*	08/07/2020 15:55:11

Universidad de La Laguna
Oficina de Sede Electrónica
Entrada
Nº registro: 2020/46124
Nº reg. oficina: OF002/2020/45309
Fecha: 07/07/2020 15:26:22

The GTC profile reaches extremely low surface brightness $\mu_r \sim 33\,\mathrm{mag/arcsec^2}$ unveiling UGC 00180's stellar halo. This limit can be compared to that of the SDSS profile in the following way. In general, for two separate observations using telescopes i and j with diameters and exposure times on source given by (D_i, t_i) and (D_j, t_j), respectively, the difference in limiting surface brightness achievable in j with respect to i can be approximated using:

$$\Delta\mu_{i,j} = 2.5 \log \left[\left(\frac{D_j^2 t_j}{D_i^2 t_i} \right)^{0.5} \right]. \tag{1.3}$$

Therefore, using i = SDSS (2.5 m, 53 s) and j = GTC (10.4 m, 8.1 h) , $\Delta\mu_{\mathrm{SDSS,GTC}}$ is approximately 5 mag, which means that the GTC observation is a striking five magnitudes deeper than the SDSS observation. This is indeed the case and is clear from Fig. 1.9, and means that it is a direct combination of telescope diameter, integration time and careful data reduction that leads to very deep imaging.

Using the ultra-deep GTC profile (after accounting for the effect of the point spread function, shown in Chapter 4), Trujillo & Fliri (2016) found that the amount of stellar mass in the halo of UGC 00180 is about 3% that of its total stellar mass, a result consistent with ΛCDM predictions as well as those obtained from star counting techniques for similar nearby galaxies. In fact, this was the first time that deep imaging of integrated light reached a comparable depth as imaging of resolved stellar populations, including a close match in stellar halo fractions for galaxies within the same stellar mass range. These results are shown in the stellar halo mass fraction–total stellar mass plane in Fig. 1.10.

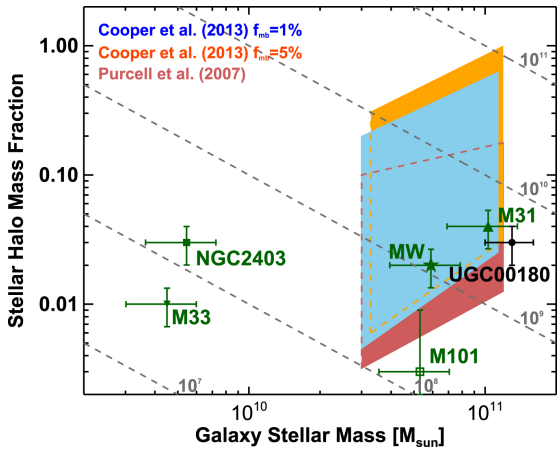

Figure 1.10: Stellar halo mass fraction vs. total galaxy stellar mass. Green points are measurements for nearby galaxies from the literature (see text below). Model predictions from Purcell et al. (2007) (red polygon) and Cooper et al. (2013) (blue and orange) are overplotted for dark matter haloes with $12 < \log M_{200}/M_\odot < 12.5$. The dashed lines correspond to the positions of stellar haloes with the labelled stellar masses fixed. *Credit: Trujillo & Fliri (2016).*

Este documento incorpora firma electrónica, y es copia auténtica de un documento electrónico archivado por la ULL según la Ley 39/2015.
Su autenticidad puede ser contrastada en la siguiente dirección https://sede.ull.es/validacion/

Identificador del documento: 2622200 Código de verificación: mbm0ekWs

Firmado por:	ROSHAN NUSHKIA CHAMBA *UNIVERSIDAD DE LA LAGUNA*	Fecha: 07/07/2020 13:28:26
	IGNACIO TRUJILLO CABRERA *UNIVERSIDAD DE LA LAGUNA*	07/07/2020 13:58:21
	Johan Hendrik Knapen Koelstra *UNIVERSIDAD DE LA LAGUNA*	07/07/2020 15:23:08
	María de las Maravillas Aguiar Aguilar *UNIVERSIDAD DE LA LAGUNA*	08/07/2020 15:55:11

Universidad de La Laguna
Oficina de Sede Electrónica
Entrada
Nº registro: 2020/46124
Nº reg. oficina: OF002/2020/45309
Fecha: 07/07/2020 15:26:22

The stellar halo mass fractions for the Milky Way (MW; Carollo et al. 2010, using SDSS), M31 (Courteau et al. 2011, SDSS; $\mu_{lim,i} \sim 27\,\mathrm{mag/arcsec^2}$), M33 (McConnachie et al. 2010, PAnDAs using the Canada–France–Hawaii Telescope (CFHT); $\mu_{lim,V} \sim 33\,\mathrm{mag/arcsec^2}$) and NGC 2403 (Barker et al. 2012, Subaru Telescope; $\mu_{lim,V} \sim 32\,\mathrm{mag/arcsec^2}$) were derived using star counting techniques and M101 from broad-band imaging (van Dokkum et al. 2014; Merritt et al. 2016, Dragonfly Telephoto Array; $\mu_{lim,r} \sim 29.8$ $(1\sigma; 10 \times 10\,\mathrm{arcsec^2})$). The predictions from the ΛCDM models by Purcell et al. (2007) and Cooper et al. (2013) for galaxies inhabiting dark matter haloes with $12 < \log M_{200}/M_{\odot} < 12.5$ are also over-plotted in the shaded regions for comparison with the data points. Both MW and M31 match the simulations extremely well. M33 and NGC 2403 are outside the shaded regions because, for their stellar mass, they inhabit haloes a factor of 10 smaller than the shaded range shown (see e.g. Seigar 2011, for M33). In the case of UGC 00180, the stellar halo mass computed by Trujillo & Fliri (2016) offsets the theoretical predictions (within uncertainties), which could imply that the dark matter halo of UGC 00180 is potentially $\log M_{200}/M_{\odot} > 12.5$. In contrast, the measurement for M101 by van Dokkum et al. (2014) is lower than expected for its stellar mass and is thus not well described by the predictions from Cooper et al. (2013). However the galaxy is statistically compatible with the models from Purcell et al. (2007).

It is important to emphasise that each of these estimates from the literature are derived from imaging of different telescopes, surface brightness limits and metrics as well as different definitions of the stellar halo. Of course, any metric or definition could in principle be chosen but they become very relevant when one seeks to compare results. For example, it is not uncommon to find 1σ surface brightness limits using different spatial scales in the literature, e.g. $1''$ (Venhola et al. 2017), $13''$ (Mihos et al. 2013) or $12''$ and $60''$ (Merritt et al. 2016). A handy relation to convert the limiting surface brightness (at a given wavelength λ) from metric $(x_1\sigma; A_1)$ to $(x_2\sigma; A_2)$ is:

$$\mu_{lim,\lambda}(x_2\sigma; A_2) = \mu_{lim,\lambda}(x_1\sigma; A_1) - 2.5\log\left[x_2/x_1\right] + 2.5\log\left[(A_2/A_1)^{0.5}\right], \tag{1.4}$$

where x_k is the number of variations σ and A_k is the area used for $k = \{1, 2\}$. For comparison with the limit from imaging with the GTC, using Eq. 1.4, the limit of the Dragonfly imaging used for the M101 result is $\mu_{lim,r} \sim 28.6\,\mathrm{mag/arcsec^2}$ $(3\sigma; 10 \times 10\,\mathrm{arcsec^2})$. If similar imaging was used for UGC 00180, then $\sim 90\%$ of its halo would have gone undetected (from the right panel of Fig. 1.9). This could potentially shed light on the very low stellar mass fraction found for M101 compared to the theoretical prediction, reaffirming that it is necessary to go beyond $30\,\mathrm{mag/arcsec^2}$ in image depth to detect stellar haloes of galaxies like that in UGC 00180 with confidence, prior to making any strict conclusions.

However, the comparison between observations and simulations using the stellar halo mass–total stellar mass parameter space shown here is not statistical. This will only be possible in the future with surveys such as LSST (LSST Science Collaboration et al. 2009). If carefully processed, LSST images will reach a depth similar to the GTC imaging but over half the sky. Therefore, a similar analysis as that performed by Trujillo & Fliri (2016) could be extended to a few thousand galaxies using homogeneous imaging, and the results used to populate the stellar halo mass–total stellar mass plane. Such an undertaking will ultimately provide a uniform and statistically robust test for the stellar halo masses predicted in ΛCDM models, not only for late-type galaxies like UGC 00180, but also for other morphological galaxy types and stellar masses.

Este documento incorpora firma electrónica, y es copia auténtica de un documento electrónico archivado por la ULL según la Ley 39/2015.
Su autenticidad puede ser contrastada en la siguiente dirección https://sede.ull.es/validacion/

Identificador del documento: 2622200 Código de verificación: mbm0ekWs

Firmado por:	ROSHAN NUSHKIA CHAMBA *UNIVERSIDAD DE LA LAGUNA*	Fecha: 07/07/2020 13:28:26
	IGNACIO TRUJILLO CABRERA *UNIVERSIDAD DE LA LAGUNA*	07/07/2020 13:58:21
	Johan Hendrik Knapen Koelstra *UNIVERSIDAD DE LA LAGUNA*	07/07/2020 15:23:08
	María de las Maravillas Aguiar Aguilar *UNIVERSIDAD DE LA LAGUNA*	08/07/2020 15:55:11

Universidad de La Laguna
Oficina de Sede Electrónica
Entrada
Nº registro: 2020/46124
Nº reg. oficina: OF002/2020/45309
Fecha: 07/07/2020 15:26:22

1.4.4 The structure of the outer disc

The deeper GTC profile shown in Fig. 1.9 also unveiled a truncation in the outer disc of UGC 00180 around $\sim 30\,\mathrm{kpc}$, a feature that was otherwise undetected in the shallower SDSS profile. This finding reinforces the need for deep imaging to observe truncations in galaxies which are not only in the edge-on orientation. Some effort has been made in this direction (e.g. Martín-Navarro et al. 2014; Peters et al. 2017) but only for a handful of Milky Way-like galaxies. In particular, Martín-Navarro et al. (2014) has shown that stellar haloes can 'outshine' the truncations of face-on disc galaxies. In other words, that the surface brightness at which truncations occur in face-on galaxies is comparable to the stellar haloes of the galaxies in the outskirts i.e. at $\mu_r \sim 28\,\mathrm{mag/arcsec^2}$. This effect probably occurs for massive galaxies and not for lower mass objects that do not have a significant stellar halo structure. Therefore the results by Martín-Navarro et al. (2014) does not generalise to all face-on galaxies. However, the result justifies why truncations have been predominantly studied in edge-on Milky Way-like galaxies and not their face-on counterparts: the absence of a stronger contrast between the stellar halo and disc in the face-on configuration ($\sim 3\,\mathrm{mag}$ fainter than in the edge-on galaxies).

While Martín-Navarro et al. (2014) demonstrated the potential hindrance to the detection of truncations in face-on galaxies using disc+halo models, Peters et al. (2017) further investigated this finding using a sample of 22 moderately inclined late-type galaxies (Sb–SABm). Peters et al. (2017) used images of the galaxies from the deep IAC Stripe 82 dataset (Fliri & Trujillo 2016) and report the presence of truncations in only three out of those studied. These results will be re-examined in the future using the latest version of the IAC Stripe 82 images (Román & Trujillo 2018) where the background subtraction of the survey has been greatly improved (preliminary results are shown in Chapter 4).

Interestingly, Peters et al. (2017) also demonstrated a linear correlation between the sizes of the galaxies (indicated by the radial location of the isophote at $\mu_r = 25\,\mathrm{mag/arcsec^2}$) and the location of either the identified breaks or truncations of the objects. However, the broader idea that the location of the break in spiral galaxies could be used to investigate the evolution of discs can be traced to the works by Pérez (2004), Trujillo & Pohlen (2005) and Azzollini et al. (2008). In particular, Trujillo & Pohlen (2005) proposed the use of the break as a direct size indicator for discs and studied how the position of the break shifted as a function of redshift (upto $z < 1.1$). Subsequently, Azzollini et al. (2008) conducted a much larger search for breaks using a sample of ~ 500 disc dominated galaxies with $z < 1.1$ and showed that the break radius has increased by a factor of $\sim 1.3 \pm 0.1$. This result is suggestive of a moderate inside-out growth of discs. However, the use of the break location as a size indicator has not been explored much more since these investigations.

For completeness, it is worth pointing out that Pérez (2004), Trujillo & Pohlen (2005) and Azzollini et al. (2008) measure the location of the break (like that labelled in Fig. 1.9) but interchangeably refer to the breaks as truncations. This is related to the confusion in the literature between the original truncations discovered by van der Kruit (1979) for edge-on galaxies and Type II profile breaks. This confusion was first recognised and described by Martín-Navarro et al. (2012). However, it is now accepted that truncations and Type-II breaks are two differentiated features (as marked for UGC 00180 in Fig. 1.9) that are not necessarily mutually exclusive. In this thesis, the term 'truncation' will always be referred to the feature in a galaxy's profile that implies an edge (see Sect. 1.3.2).

Este documento incorpora firma electrónica, y es copia auténtica de un documento electrónico archivado por la ULL según la Ley 39/2015.
Su autenticidad puede ser contrastada en la siguiente dirección https://sede.ull.es/validacion/

Identificador del documento: 2622200 Código de verificación: mbm0ekWs

Firmado por:	ROSHAN NUSHKIA CHAMBA *UNIVERSIDAD DE LA LAGUNA*	Fecha: 07/07/2020 13:28:26
	IGNACIO TRUJILLO CABRERA *UNIVERSIDAD DE LA LAGUNA*	07/07/2020 13:58:21
	Johan Hendrik Knapen Koelstra *UNIVERSIDAD DE LA LAGUNA*	07/07/2020 15:23:08
	María de las Maravillas Aguiar Aguilar *UNIVERSIDAD DE LA LAGUNA*	08/07/2020 15:55:11

Universidad de La Laguna
Oficina de Sede Electrónica
Entrada
Nº registro: 2020/46124
Nº reg. oficina: OF002/2020/45309
Fecha: 07/07/2020 15:26:22

As previously introduced in Sect. 1.3.2, truncations have been shown to be related with the star formation threshold in disc galaxies (Kennicutt 1989a). On this aspect, Martínez-Lombilla et al. (2019) has recently used integrated light images in the near ultra-violet (NUV GALEX; Morrissey et al. 2007), optical (SDSS; York et al. 2000) and near infrared (S^4G; Sheth et al. 2010) and shown that truncations are linked to star formation thresholds in the two edge-on Milky Way-like galaxies studied in van der Kruit (1979) and shown in Fig. 1.5. Martínez-Lombilla et al. (2019) find that the truncations of NGC 5907 and NGC 4565 occur at a surface brightness of about $\mu_r \sim 25.5\,\mathrm{mag/arcsec^2}$, after de-projecting the brightness by the effect of the inclination. This result is compatible with that in van der Kruit (1979). Furthermore, using the $NUV-r$ and $g-r$ colour profiles of these galaxies, Martínez-Lombilla et al. (2019) estimate that the truncated locations have a stellar mass density of $\Sigma_{\star,\mathrm{trunc}} \sim 1\,M_\odot/\mathrm{pc}^2$. Assuming a 30% integrated gas-to-star conversion, this density corresponds to the critical gas density threshold theoretically expected to trigger in-situ star formation in galactic discs, i.e. $\Sigma_c \sim 3\,M_\odot/\mathrm{pc}^2$ in Schaye (2004). Therefore, these results reinforce the idea that truncations truly imply an edge (Sect. 1.3.2), not only in terms of their visual appearance in the radial profiles, but also in terms of the information they hold on the star formation allowed to occur in galaxies.

Building on these results, in Chapter 2 of this thesis (published in Trujillo, Chamba, & Knapen 2020), the location of the expected gas density threshold for star formation in galaxies is proposed as a physically motivated definition for galaxy size. This is intuitively very meaningful: first for being one of the ways in which galaxies grow in extension and second given the fact that star formation thresholds physically imply an edge. While the location at a fixed iso-mass density of $1\,M_\odot/\mathrm{pc}^2$ is used as a proxy for the size definition, called R_1 (motivated by the results in Martínez-Lombilla et al. (2019) described above) in Chapter 2, ongoing work presented in Chapter 4 is an attempt to measure the threshold density at the location of the truncation or 'edge' for individual galaxies (R_{edge}). Consequently, R_{edge} is closer to the size definition proposed in Chapter 2 (Chamba et al. in prep). We prefer to use the general term 'edge' because truncations were specifically defined for edge-on systems (van der Kruit & Searle 1981a,b), while we are locating the same feature in the face-on orientation. In both Chapter 2 and 4, we use a sample of ~ 1000 galaxies with stellar masses between $10^7\,M_\odot < M_\star < 10^{12}\,M_\odot$ (i.e. dwarfs to massive ellipticals) to study the size–stellar mass plane using R_1 (Chapter 2) and R_{edge} (ongoing work in Chapter 4). It will be shown that current deep, multi-band imaging surveys are readily capable of measuring threshold densities like $1\,M_\odot/\mathrm{pc}^2$ for Milky Way-like objects or $0.5\,M_\odot/\mathrm{pc}^2$ for the dwarfs, which thus makes the proposed size definition practical to measure and catalogue for large galaxy samples. I leave the details of the analyses and samples used in those Chapters for the reader. But one of the broader propositions stemming from this work is to explore whether R_{edge} could be used to define the onset of the stellar halo. This may be addressed in more detail in future projects (Chapter 5).

In the next sub-section, I introduce the so-called 'ultra-diffuse galaxies' as an example of the consequences of using the most commonly used size measure for galaxies – the effective or half-life radius (Eq. 1.1) — to motivate the need for a better size definition. This is work that will be presented in Chapter 3 (and has been published in Chamba, Trujillo, & Knapen 2020).

Este documento incorpora firma electrónica, y es copia auténtica de un documento electrónico archivado por la ULL según la Ley 39/2015.
Su autenticidad puede ser contrastada en la siguiente dirección https://sede.ull.es/validacion/

Identificador del documento: 2622200 Código de verificación: mbm0ekWs

Firmado por:	ROSHAN NUSHKIA CHAMBA *UNIVERSIDAD DE LA LAGUNA*	Fecha: 07/07/2020 13:28:26
	IGNACIO TRUJILLO CABRERA *UNIVERSIDAD DE LA LAGUNA*	07/07/2020 13:58:21
	Johan Hendrik Knapen Koelstra *UNIVERSIDAD DE LA LAGUNA*	07/07/2020 15:23:08
	María de las Maravillas Aguiar Aguilar *UNIVERSIDAD DE LA LAGUNA*	08/07/2020 15:55:11

Universidad de La Laguna
Oficina de Sede Electrónica
Entrada
Nº registro: 2020/46124
Nº reg. oficina: OF002/2020/45309
Fecha: 07/07/2020 15:26:22

1.4.5 Ultra-diffuse galaxies

Inspired by the deep images of the Virgo cluster by Mihos et al. (2005), van Dokkum et al. (2015a) sought to observe the Coma Cluster using the Dragonfly Telephoto Array and measure the luminosity and colour of its intra-cluster light. After reducing the acquired images, this team of researchers spotted a total of forty-seven low surface brightness, spatially resolved objects which were not listed in any Coma cluster catalogues. Using data from the CFHT (Head et al. 2014), van Dokkum et al. (2015a) measured the properties of these galaxies: $R_{\rm e}$, $\mu(0)$ in the g-band or $\mu(0,g)$, colours and stellar masses. The CFHT data was used because it is comparable in depth to the Dragonfly images in the same field: $\mu_{lim,g} \sim 27.8\,{\rm mag/arcsec^2}$ ($3\sigma; 10 \times 10\,{\rm arcsec^2}$), but with much better spatial resolution, $0.186''$/pixel, compared to the $2.8''$/pixel in Dragonfly. Figure 1.11 shows three diffuse objects from the Coma cluster as seen in CFHT $g+i$ band images. In contrast to the first images of similar galaxies in Virgo from the Sandage & Binggeli (1984) atlas (Fig. 1.6), the ~ 2 mag deeper CFHT images make the diffuse galaxies more easily visible and therefore more accurate measurements of their properties may be determined.

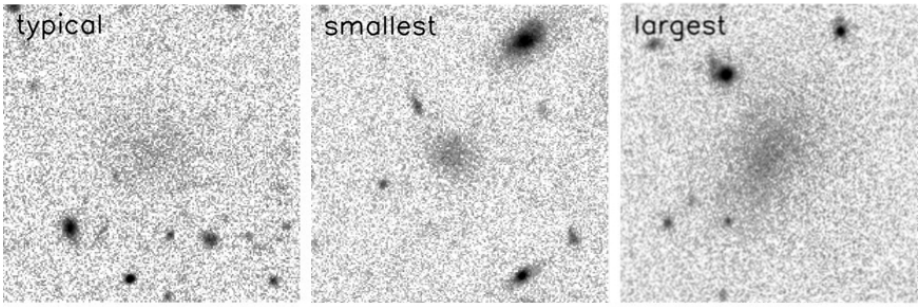

Figure 1.11: Diffuse Coma galaxies in CFHT $g+i$ images. Each panel spans $37'' \times 37''$. The galaxy on the left is close to the median of the sample (named DF1; with $R_{\rm e} = 3.1\,{\rm kpc}$ and $\mu(0,g) = 25.1\,{\rm mag/arcsec^2}$), and the middle and right panels show the galaxy in the sample with the smallest and largest $R_{\rm e}$, (DF43; 1.5 kpc) and (DF44; 4.6 kpc), respectively. *Adapted from van Dokkum et al. (2015a).*

Figure 1.12 shows the $R_{\rm e} - \mu(0,g)$ plane for the Coma objects as well as a collection of galaxies from the literature: a general population from SDSS (Simard et al. 2011), the elliptical dwarfs in Virgo (Gavazzi et al. 2005), and the Milky Way (Bovy & Rix 2013). At a fixed $\mu(0,g)$, the new galaxies have comparatively larger $R_{\rm e}$ than the dwarf galaxies, but average colours $< g-i > \sim 0.8$ consistent with an extrapolation of the red sequence of dwarf galaxies in Coma and with similar stellar masses 10^7–$10^8\,M_\odot$.

Using these results, van Dokkum et al. (2015a) argue that although these faint galaxies are low-mass systems in the dwarf galaxy regime, they have $R_{\rm e}$ typical of $L_\star$ spiral and elliptical galaxies (i.e. they are 'Milky Way-sized'). While similar galaxies were referred to as 'large dwarfs' in the 1980s (i.e. because the objects have large *diameters* ~ 10 kpc. See Sect. 1.3.3), van Dokkum et al. (2015a) believe that 'dwarf' is not an appropriate term for these objects

Este documento incorpora firma electrónica, y es copia auténtica de un documento electrónico archivado por la ULL según la Ley 39/2015.
Su autenticidad puede ser contrastada en la siguiente dirección https://sede.ull.es/validacion/

Identificador del documento: 2622200 Código de verificación: mbm0ekWs

Firmado por:	ROSHAN NUSHKIA CHAMBA *UNIVERSIDAD DE LA LAGUNA*	Fecha: 07/07/2020 13:28:26
	IGNACIO TRUJILLO CABRERA *UNIVERSIDAD DE LA LAGUNA*	07/07/2020 13:58:21
	Johan Hendrik Knapen Koelstra *UNIVERSIDAD DE LA LAGUNA*	07/07/2020 15:23:08
	María de las Maravillas Aguiar Aguilar *UNIVERSIDAD DE LA LAGUNA*	08/07/2020 15:55:11

Universidad de La Laguna
Oficina de Sede Electrónica
Entrada
Nº registro: 2020/46124
Nº reg. oficina: OF002/2020/45309
Fecha: 07/07/2020 15:26:22

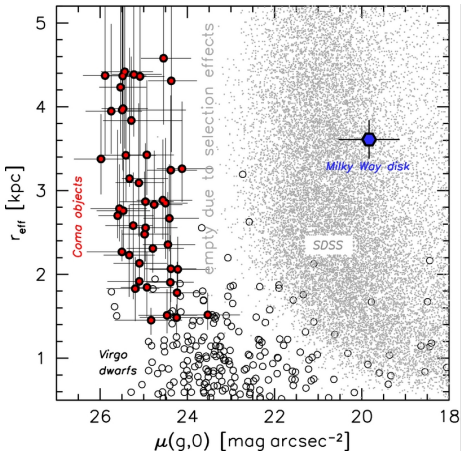

Figure 1.12: Location of the Coma ultra-diffuse galaxies in the effective radius —- central surface brightness plane, compared to galaxies at $0.02 < z < 0.03$ in SDSS (Simard et al. 2011), dwarf early-type galaxies in the Virgo cluster (Gavazzi et al. 2005), and the Milky Way disc (Bovy & Rix 2013). *Credit: van Dokkum et al. (2015a).*

that have larger R_e. Instead, these authors decided to call the newly found Coma objects 'ultra-diffuse galaxies' (UDGs):

> *'We propose the term 'ultra-diffuse galaxies', or UDGs, for galaxies with $R_e \gtrsim 1.5$ kpc and $\mu(0,g) \gtrsim 24$ mag/arcsec^2. We stress that this term does not imply that these objects are distinct from the general galaxy population; these are simply the largest [in R_e] and most diffuse objects in a continuous distribution.'*
>
> —van Dokkum et al. (2015a)

In other words, the choice of parameter restrictions $R_e \gtrsim 1.5$ kpc and $\mu(0,g) \gtrsim 24$ mag/arcsec^2 to define UDGs has no physical preconceptions, but only to operatively select the most diffuse objects among the general galaxy population. In fact, at the distance of Coma (~ 100 Mpc), 1.5 kpc corresponds roughly to $\sim 3''$, which is close to the pixel size of Dragonfly. Additionally, given the last statement in the original definition of UDGs quoted above, it is interesting that the question of whether these galaxies represent a separate population of objects turned into a huge debate.[15] This probably occured because along with this original definition, an intriguing formation mechanism for UDGs was also proposed by these authors:

> *'An intriguing formation scenario is that UDGs are 'failed' $\sim L_\star$ galaxies, which lost their gas after forming their first generation(s) of stars at high redshift (by ram pressure stripping or other effects). If this is the case they may have very high dark*

[15] At the time of writing this Chapter, 239 articles have 'ultra-diffuse galaxies' in their abstracts, only in a span of five years since van Dokkum et al. (2015a) was published.

Este documento incorpora firma electrónica, y es copia auténtica de un documento electrónico archivado por la ULL según la Ley 39/2015.
Su autenticidad puede ser contrastada en la siguiente dirección https://sede.ull.es/validacion/

Identificador del documento: 2622200 Código de verificación: mbm0ekWs

Firmado por:	ROSHAN NUSHKIA CHAMBA *UNIVERSIDAD DE LA LAGUNA*	Fecha: 07/07/2020 13:28:26
	IGNACIO TRUJILLO CABRERA *UNIVERSIDAD DE LA LAGUNA*	07/07/2020 13:58:21
	Johan Hendrik Knapen Koelstra *UNIVERSIDAD DE LA LAGUNA*	07/07/2020 15:23:08
	María de las Maravillas Aguiar Aguilar *UNIVERSIDAD DE LA LAGUNA*	08/07/2020 15:55:11

Universidad de La Laguna
Oficina de Sede Electrónica
Entrada
Nº registro: 2020/46124
Nº reg. oficina: OF002/2020/45309
Fecha: 07/07/2020 15:26:22

matter fractions, which could also help explain their survival in the cluster.'
—van Dokkum et al. (2015a)

In other words, UDGs are 'failed' ($L_\star$) giants or Milky Way-like galaxies because they have similar R_e to these galaxies (i.e. 'Milky Way-sized') but they were unable to form the same quantity of stars as these giant objects in the cluster environment. In particular, the effect of ram pressure stripping at high redshift during the infall of UDGs into the cluster (e.g. Yozin & Bekki 2015) or tidal heating and stripping (Carleton et al. 2019) which can explain the properties of UDGs in clusters.

While many more UDGs in other clusters were indeed found (e.g. Koda et al. 2015; Mihos et al. 2015; van der Burg et al. 2016; Mancera Piña et al. 2018), the likelihood of the 'failed giants' scenario was significantly challenged when UDGs outside clusters (e.g. Román & Trujillo 2017b; Cohen et al. 2018) and in the field (Bellazzini et al. 2017; Prole et al. 2019) were detected. This is because effects such as ram pressure stripping or tidal heating do not occur in very low density environments. Additionally, the UDGs outside clusters have been shown to be blue (Román & Trujillo 2017b) and HI rich (Trujillo et al. 2017; Spekkens & Karunakaran 2018), in stark contrast to what the 'failed high-$L_\star$ galaxy' hypothesis requires.

In fact, the majority of the observational (see also e.g. Beasley & Trujillo 2016; Amorisco 2018) and theoretical studies (e.g. Amorisco & Loeb 2016; Di Cintio et al. 2017; Chan et al. 2018) on UDGs support their dwarf-like origins rather than of Milky Way-like objects. For example, it has been shown that UDGs follow the same large scale distribution in groups and clusters (Román & Trujillo 2017a) and the distribution of their dark matter haloes (Amorisco 2018) as dwarf galaxies. In particular, Amorisco & Loeb (2016) demonstrated that UDGs naturally populate the high-spin tail of the dark matter halo distribution of dwarf galaxies, a result which has long been known for low surface brightness galaxies (see Dalcanton et al. 1997b). Additionally, Di Cintio et al. (2017) proposed that internal processes such as strong feedback outflows can expand regular dwarfs into UDGs and their diffuse nature is retained as they infall into clusters. Despite these evidences, the astronomical community has not reached a consensus on the nature of UDGs.

The debate and continuous interest in UDGs in the literature has mostly been sustained by 1) the study of the dark matter content of iconic UDGs like DF44 which was reported to have an extremely high globular cluster population (~ 100) for its mass and therefore embedded in a $10^{12}\,M_\odot$ dark matter halo (van Dokkum et al. 2016, 2019) and [KKS2000]04, referred to as NGC1052-DF2, reported to be a galaxy lacking dark matter (van Dokkum et al. 2018; Danieli et al. 2019)[16], 2) the ability of current hydrodynamical simulations to resolve faint low-mass galaxies like UDGs and study their formation and evolution (e.g. Tremmel et al. 2019; Di Cintio et al. 2019; Wright et al. 2020, and references therein), 3) the massive hunt for low surface brightness galaxies like UDGs in field surveys (Prole et al. 2019; Barbosa et al. 2020), 4) the effort to target these faint objects spectroscopically (Ferré-Mateu et al. 2018; Ruiz-Lara et al. 2018, 2019) and 5) the study of their HI content (see e.g. Leisman et al. 2017; Spekkens & Karunakaran 2018; Mancera Piña et al. 2019) in more detail. All these studies largely overlap with that of low surface brightness galaxies. However, for what ever the reason, UDGs are not directly identified by a fraction of the astronomical community as the simple faint dwarf galaxies

[16]Although neither of these studies have been confirmed or reproduced by other research groups, finding completely different results (e.g. Trujillo et al. 2019; Ruiz-Lara et al. 2019, Saifollahi et al. (submitted)).

Este documento incorpora firma electrónica, y es copia auténtica de un documento electrónico archivado por la ULL según la Ley 39/2015.
Su autenticidad puede ser contrastada en la siguiente dirección https://sede.ull.es/validacion/

Identificador del documento: 2622200 Código de verificación: mbm0ekWs

Firmado por:	ROSHAN NUSHKIA CHAMBA *UNIVERSIDAD DE LA LAGUNA*	Fecha: 07/07/2020 13:28:26
	IGNACIO TRUJILLO CABRERA *UNIVERSIDAD DE LA LAGUNA*	07/07/2020 13:58:21
	Johan Hendrik Knapen Koelstra *UNIVERSIDAD DE LA LAGUNA*	07/07/2020 15:23:08
	María de las Maravillas Aguiar Aguilar *UNIVERSIDAD DE LA LAGUNA*	08/07/2020 15:55:11

Universidad de La Laguna
Oficina de Sede Electrónica
Entrada
Nº registro: 2020/46124
Nº reg. oficina: OF002/2020/45309
Fecha: 07/07/2020 15:26:22

first detected by Sandage & Binggeli (1984) and Impey et al. (1988), even though the galaxies that are identified in these classical works share similar properties as the UDGs.

Due to the continued interest in the low surface brightness galaxies dubbed UDGs in the astronomical literature, in Chapter 3 of this thesis, I present a study on the nature of these galaxies which was published in Chamba, Trujillo, & Knapen (2020), and provide further support to the dwarf-like characteristics of UDGs. Rather than investigating specific evolutionary scenarios proposed for these galaxies in the literature, the original idea that UDGs are 'Milky way-sized' or that they have extraordinarily large sizes for their stellar mass (van Dokkum et al. 2015a) is re-examined. In Chapter 3, it will be shown that using $R_{\rm e}$ as a size measure for these galaxies is the crux of the issue surrounding the continued interest in the study of UDGs as a 'bewildering'[17] population of galaxies, despite a lot of evidence to their dwarf origins. As a matter of fact, van Dokkum et al. (2015a) was very clear that the term UDG does not imply that they are galaxies radically different from the general dwarf galaxy population (see the discussion on the definition of UDGs 1.4.5 above). However, astronomers have until now gone on to address questions such as, are UDGs a distinct population of galaxies and are they different to dwarfs? that can readily be answered by van Dokkum et al. (2015a): *'We stress that this term [UDG] does not imply that these objects are distinct from the general galaxy population'.*

As I have further described in this sub-section, the failed giant galaxy hypothesis stemmed from the fact that UDGs have large $R_{\rm e}$ – which can be similar to that of Milky Way-like galaxies – compared to regular dwarf galaxies. Additionally, I pointed out that the classical reports on the discovery of low surface brightness galaxies with central surface brightness $< 25\,{\rm mag/arcsec^2}$ (e.g. Sandage & Binggeli 1984; Impey et al. 1988) referred to these galaxies as 'large dwarfs', motivated by the fact that their apparent total diameters in the photographic plates were $\sim 10\,{\rm kpc}$, while their stellar mass is within the dwarf regime. Considering that dwarf galaxies were historically defined primarily using the central surface brightness–absolute magnitude plane ($\mu(0)$–M) (Binggeli 1994)[18], it is more than appropriate to call galaxies with low central surface brightness and low total luminosity as 'large dwarfs', contrary to what van Dokkum et al. (2015a) argue. To illustrate this, I show the $\mu(0)$–M plane discussed in Binggeli (1994) in Fig. 1.13.

From this figure, it is immediately clear that the UDGs will populate the lower end of the labelled dwarfs region. This is because historically, dwarfs have always been referred to those galaxies that have low total luminosity and low central surface brightness in the $\mu(0)$–M plane (see Binggeli 1994, and references therein), independent of how extended they could be. Therefore, using the $R_{\rm e}$–$\mu(0)$ plane shown in Fig. 1.12 to group galaxies is misleading and insensitive to the nomenclature adopted by pioneers like Binngeli and Impey when defining the low surface brightness dwarf galaxies that they discovered in the 1980s. Before proceeding to the next section where I discuss the size–stellar mass plane, I leave the reader with the comment by Binngeli on the definition of dwarf galaxies:

> *'One has to decide on the meaning of the term "dwarf". Does "dwarf" merely mean small and/or faint, or does it additionally mean low surface brightness? Our*

[17] In reference to a Lorentz Centre Workshop on '*The Bewildering Nature of Ultra-diffuse Galaxies*' attended by my collaborators and myself in the summer of 2018 in Leiden.

[18] I encourage the reader interested in historical nomenclature to refer to Binggeli (1994) for a discussion on how to define 'dwarf galaxy'.

Este documento incorpora firma electrónica, y es copia auténtica de un documento electrónico archivado por la ULL según la Ley 39/2015.
Su autenticidad puede ser contrastada en la siguiente dirección https://sede.ull.es/validacion/

Identificador del documento: 2622200 Código de verificación: mbm0ekWs

Firmado por:	ROSHAN NUSHKIA CHAMBA *UNIVERSIDAD DE LA LAGUNA*	Fecha: 07/07/2020 13:28:26
	IGNACIO TRUJILLO CABRERA *UNIVERSIDAD DE LA LAGUNA*	07/07/2020 13:58:21
	Johan Hendrik Knapen Koelstra *UNIVERSIDAD DE LA LAGUNA*	07/07/2020 15:23:08
	María de las Maravillas Aguiar Aguilar *UNIVERSIDAD DE LA LAGUNA*	08/07/2020 15:55:11

Universidad de La Laguna
Oficina de Sede Electrónica
Entrada
Nº registro: 2020/46124
Nº reg. oficina: OF002/2020/45309
Fecha: 07/07/2020 15:26:22

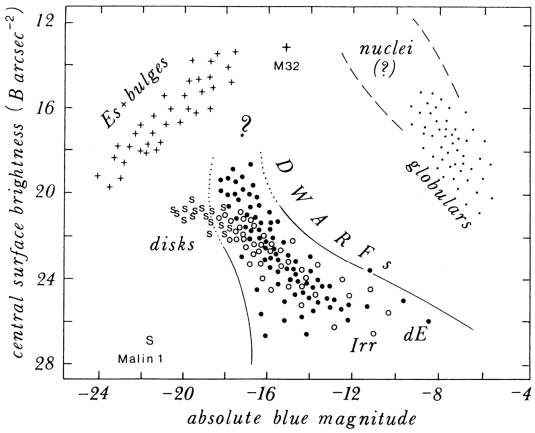

Figure 1.13: The central surface brightness–absolute magnitude plane to define dwarf galaxies and other populations. The galaxies dubbed 'ultra-diffuse galaxies' nowadays will readily populate the lower end of the dwarfs region marked in the diagram. *Credit: Binggeli (1994).*

> *(Sandage & Binggeli 1984) and most other people's convention is to assign the term "dwarf" to the great majority of faint galaxies that have low surface brightness.'*
>
> —Binggeli (1994)

Therefore, there can be no doubt that the UDGs are the same population of faint dwarf galaxies as those studied by Sandage & Binggeli (1984) and Impey et al. (1988) all those decades ago, provided that the dwarfs or any other galaxy type is defined using a *distribution* in certain common properties like luminosity and central brightness in (Binggeli 1994) or total mass in modern astronomy (see also the discussion by Conselice 2018, on the fact that UDGs are the well-known and studied dwarf spheroidal galaxies).

1.4.6 Summary and highlights

In Section 1.4, I have provided an overview on the developments in deep imaging and shown how it has allowed to probe galaxy formation and evolution until the frontier, bounded by current technological limits, via the study of galaxy outskirts and low surface brightness galaxies. In particular, I have shown that current CCD cameras allow to reach depths even fainter than possible with a single photographic plate (Sect. 1.4.1–1.4.3). I also motivated the use of deep imaging to study the edges of galaxies and the potential use of the edge as a physical galaxy size definition (Sect. 1.4.4). These ideas will be expanded in Chapters 2 and 4 of this thesis. I have also introduced ultra-diffuse galaxies, discussed the failed 'Milky Way-sized' hypothesis and argued that these objects are faint dwarfs, sharing similar properties to those low surface brightness galaxies first identified by Sandage & Binggeli (1984) (Sect. 1.4.5). In the next section, I will discuss the size–mass plane in some depth to motivate its use in this thesis to

Este documento incorpora firma electrónica, y es copia auténtica de un documento electrónico archivado por la ULL según la Ley 39/2015.
Su autenticidad puede ser contrastada en la siguiente dirección https://sede.ull.es/validacion/

Identificador del documento: 2622200 Código de verificación: mbm0ekWs

Firmado por:	ROSHAN NUSHKIA CHAMBA *UNIVERSIDAD DE LA LAGUNA*	Fecha: 07/07/2020 13:28:26
	IGNACIO TRUJILLO CABRERA *UNIVERSIDAD DE LA LAGUNA*	07/07/2020 13:58:21
	Johan Hendrik Knapen Koelstra *UNIVERSIDAD DE LA LAGUNA*	07/07/2020 15:23:08
	María de las Maravillas Aguiar Aguilar *UNIVERSIDAD DE LA LAGUNA*	08/07/2020 15:55:11

Universidad de La Laguna
Oficina de Sede Electrónica
Entrada
Nº registro: 2020/46124
Nº reg. oficina: OF002/2020/45309
Fecha: 07/07/2020 15:26:22

1) characterise the new physically motivated size definition (Chapter 2 and ongoing work in Chapter 4) and 2) demonstrate the misleading connotation that the effective radius ($R_{\rm e}$) has as a galaxy size measure, using ultra-diffuse galaxies as an example to address this issue (Chapter 3).

1.5 The size–stellar mass relation

Global trends or correlations among properties of galaxies such as their size, mass, luminosity or velocity are called scaling relations. In general, scaling relations have been shown to provide empirical evidence of the physical laws that govern the growth and evolution of galaxies. Examples of such relations include the fundamental plane of elliptical galaxies in the $\log R_{\rm e}$–$\log \sigma_0$–$< \mu_e >$ space (σ_0 is the central velocity dispersion, and $< \mu_e >$ is the mean surface brightness within $R_{\rm e}$ expressed in mag/arcsec^2; Djorgovski & Davis 1987), the Tully–Fisher relation for spiral galaxies between their luminosity and rotation velocity (Tully & Fisher 1977) and the size–luminosity or size–stellar mass relation (Fish 1963; Sérsic 1968b). For instance, the Tully-Fisher relation has been used to estimate distances for spiral galaxies, and as a relation between dynamical mass (due to stars, gas and dark matter) and luminosity. In this section, I will discuss the origins of the size–mass relation and motivate its use in this thesis to unravel the growth of galactic structure and the nature of ultra-diffuse galaxies.

1.5.1 Motivation for studies on galaxy formation and evolution

Early models for disc galaxies (White & Rees 1978; Fall & Efstathiou 1980), followed by the comprehensive analyses by Mo et al. (1998) and Dutton et al. (2007), showed that scaling relations like Tully–Fisher (Tully & Fisher 1977) can be reproduced using fairly simple arguments. In particular, Mo et al. (1998) showed that the sizes of galaxies (as parameterised by the disc scale length $R_{\rm d} = R_{\rm e}/b_1$ by setting $n = 1$ in Eq. 1.7) are determined by the sizes of their initial rotationally supported gaseous disc, which are fixed by the angular momentum of gas. If the angular momentum of gas is proportional to that of dark matter (J), then this model predicts that galaxy size should scale as $R_{\rm d} \propto \lambda(J) R_{200}$, where $\lambda(J)$ is the global spin parameter of the halo and R_{200} is the virial radius such that $M_{200} = (4\pi/3)200\rho_{\rm crit}R_{200}^3$ and $\rho_{\rm crit}$ is the critical density of the Universe.

These simple models opened a fundamentally important research line in the field of galaxy formation and evolution: the connection between galaxy size, angular momentum and the dark matter halo. With the advent of the SDSS and programmes using the *HST*, the study of galaxy size–stellar mass distributions using hundreds to thousands of galaxies became a possibility, both at low and high redshift (e.g. Shen et al. 2003; Trujillo et al. 2004; McIntosh et al. 2005; Barden et al. 2005; Trujillo et al. 2007; Buitrago et al. 2008; van der Wel et al. 2014). These works captured the growth of galactic structures with cosmic time, the so-called 'inside-out' growth, with the more massive galaxies showing a stronger evolution due to merging and accretion, compared to a milder evolution for disc galaxies. At the same time, several theoretical investigations addressed the question on the distribution of galaxy size, angular momentum and their dark matter haloes (e.g. Somerville et al. 2008; Kim & Lee 2013; Kravtsov 2013; Agertz & Kravtsov 2016; Zoldan et al. 2018). For example, Kravtsov (2013) used the abundance matching ansatz, i.e. galaxies are ranked according to their stellar masses (in descending order) and matched

Este documento incorpora firma electrónica, y es copia auténtica de un documento electrónico archivado por la ULL según la Ley 39/2015.
Su autenticidad puede ser contrastada en la siguiente dirección https://sede.ull.es/validacion/

Identificador del documento: 2622200 Código de verificación: mbm0ekWs

Firmado por:	ROSHAN NUSHKIA CHAMBA *UNIVERSIDAD DE LA LAGUNA*	Fecha: 07/07/2020 13:28:26
	IGNACIO TRUJILLO CABRERA *UNIVERSIDAD DE LA LAGUNA*	07/07/2020 13:58:21
	Johan Hendrik Knapen Koelstra *UNIVERSIDAD DE LA LAGUNA*	07/07/2020 15:23:08
	María de las Maravillas Aguiar Aguilar *UNIVERSIDAD DE LA LAGUNA*	08/07/2020 15:55:11

Universidad de La Laguna
Oficina de Sede Electrónica
Entrada
Nº registro: 2020/46124
Nº reg. oficina: OF002/2020/45309
Fecha: 07/07/2020 15:26:22

to simulated haloes ranked in the same order so the most massive galaxies are assumed to be embedded in the most massive dark matter haloes and etc, to test this prediction. He found that the 3D half-mass radii ($R_{\mathrm{e},M_\star}$) of observed galaxies (estimated using the 2D projected radii from observations) scale linearly with R_{200}, i.e. $R_{\mathrm{e},M_\star} \propto 0.015 R_{200}$. Under the assumption that $R_{\mathrm{e},M_\star} \propto \lambda(J) R_{200}$, Kravtsov (2013) showed that the scatter of galaxy size in this plane (~ 0.5 dex) roughly corresponds to the expected distribution of the halo spin parameter. Therefore, the size–stellar mass plane is a reflection of the size–virial radius plane, if galaxy sizes are controlled by the angular momentum in their underlying dark matter halo. In this regard, the size–stellar mass relation offers an observational probe of the growth of galaxies and their haloes, both at low and high redshift.

Indeed, this is currently a very active area of research, with investigations studying the galaxy size–dark matter halo relations at high redshift (Huang et al. 2017; Somerville et al. 2018) as well as calling for a more precise connection between the angular momentum of galaxies and their dark matter haloes (e.g. Jiang et al. 2019; Zanisi et al. 2020). Many of the predictions from these contemporary studies are still in general agreement with observations. However, as the majority of works use the effective radius to represent galaxy size, the current consensus on the size evolution of galaxies is in reality a consensus on their R_{e} evolution. In a strict sense, R_{e} is a measurement of galaxy light concentration and not necessarily that of galaxy size, even though it has units of length. For this reason, assessing the suitability of R_{e} (and its variants such as $R_{\mathrm{e},M_\star}$) as a size measure for galaxies certainly requires more attention.

In fact, only a few works in the literature have explored the use of other indicators for galaxy size that are completely different in nature to R_{e} or other light concentration measures. These include the break radii for disc galaxies studied at low and moderately high redshift ($z \sim 1$; Trujillo & Pohlen 2005; Azzollini et al. 2008) and various isophotal measures (Saintonge & Spekkens 2011; Hall et al. 2012; Muñoz et al. 2015). However, the reason why R_{e} is currently the preferred size measure for galaxies over other parameters is probably because of the advantage of R_{e} when observational conditions or limitations prevent the outer regions of galaxies to be measured accurately, e.g. at high redshift due to cosmological dimming by a factor $\propto (1+z)^4$. In other words, R_{e} is practically more advantageous than isophotal size measures at very high redshift because R_{e} is independent of absolute intensity values in a galaxy. Regardless of R_{e}'s superiority at redshifts $z > 1$ due to current observational constraints, I will now provide a short review on the historical origins of the classical size measures in the literature, namely, R_{e} and isophotal measures such as D_{25} (Redman 1936) and the Holmberg (1958) radius, to support the necessity of critically regarding the current convention that R_{e} is a measurement of galaxy size.

1.5.2 Historical perspectives on the concept of galaxy size

Prior to the popularisation of the effective radius (R_{e}; de Vaucouleurs 1948) as a galaxy size measurement, it was common to refer to the extensions of galaxies as 'diameter' or 'dimension' in the literature. The apparent diameters of galaxies was initially discussed by Hubble (1926) and in later works 'diameter' was defined using the location of surface brightness isophotes. Redman (1936) was the first to suggest such a definition as a 'conventional' measure for the diameter of elliptical 'nebulae'. He showed that the measurements of the angular diameters for six elliptical galaxies made by Hubble (1926) and Shapley (1934) were dependant on observing conditions (instrumental and atmospheric) under which the photographic plates were subjected.

Este documento incorpora firma electrónica, y es copia auténtica de un documento electrónico archivado por la ULL según la Ley 39/2015.
Su autenticidad puede ser contrastada en la siguiente dirección https://sede.ull.es/validacion/

Identificador del documento: 2622200 Código de verificación: mbm0ekWs

Firmado por:	ROSHAN NUSHKIA CHAMBA *UNIVERSIDAD DE LA LAGUNA*	Fecha: 07/07/2020 13:28:26
	IGNACIO TRUJILLO CABRERA *UNIVERSIDAD DE LA LAGUNA*	07/07/2020 13:58:21
	Johan Hendrik Knapen Koelstra *UNIVERSIDAD DE LA LAGUNA*	07/07/2020 15:23:08
	María de las Maravillas Aguiar Aguilar *UNIVERSIDAD DE LA LAGUNA*	08/07/2020 15:55:11

Universidad de La Laguna
Oficina de Sede Electrónica
Entrada
Nº registro: 2020/46124
Nº reg. oficina: OF002/2020/45309
Fecha: 07/07/2020 15:26:22

Therefore, the measurements from these earlier works were difficult to reproduce, owing to the absence of a clear boundary for the galaxies. For these reasons, he proposed the use of a fixed surface brightness isophote at 25 mag/arcsec^2 as a definition of the diameter for elliptical galaxies (relevant text highlighted here in bold in the following excerpt):

> '*Enough has been said to make it clear how extremely difficult it is to discuss questions relating to the diameters or mean surface brightnesses of these objects...* ***There is in fact no boundary to any of these nebulae; they all shade off imperceptibly into empty space, so that we can only speak of a "diameter" by defining some conventional boundary****, much as we have a conventional definition for the "half-width" of a spectrum line, another entity which is not definitely bounded.*
>
> ...
>
> *The best alternative is to* ***define the boundary as the locus of points at which the surface brightness has a certain value in stellar magnitudes per square second of arc...the mean limit is 25^m.3/square second of arc, which is practically identical with*** *the limit 25^m.2/sec.^{2} found by Hubble (1932) for* ***the faintest surface brightness detectable on certain photographs*** *(70–90 minutes exposure) taken with the 60-inch reflector at Mount Wilson. Hubble concludes that a reasonable limit for prolonged exposures under the best conditions is probably between 26^m.5/sec.^{2} and 27^m.0/sec.^{2} – This applies to Mount Wilson ; the...limit [of photographs from the Solar Physics Observatory in Cambridge] would not be quite so faint.* ***It seems that a conventional boundary at 25^m/square second of arc would have the following advantages: (a) It would allow a definite measure of the "diameter" of the nebula ; (b) it can be attained on photographs made in an indifferent climate ; (3) it would include most of the light of the nebula.***'
>
> —Redman (1936)

In other words, the specific 25 mag/arcsec^2 isophote or 'boundary' chosen by Redman stemmed from two facts: 1) it was approximately the mean limiting depth of photographic plates from Cambridge and 2) it enclosed the bulk of the light distribution of the galaxies he studied. It should be noted, however, that Redman (1936) used photograhs of only five elliptical galaxies (out of the six in the sample considered) to propose this definition of 'diameter of the nebula'. Hereafter, the isophote at 25 mag/arcsec^2 in B-band (parameterised by the major-axis of an ellipse) will be denoted as D_{25}, following the notation in the well-known Second and Third Reference Catalogue of Galaxies (RC2 and RC3; de Vaucouleurs et al. 1976, 1991).[19]

A second isophotal measure for diameter emerged two decades later when Holmberg (1958) heroically extracted microphotometer tracings of three hundred nebulae imaged using 103a photographic plates[20], taken mostly from Mount Wilson between 1947–55. Holmberg sought to

[19] D_{25} is frequently (and incorrectly) referred to as R_{25} in the literature. In RC2 (and RC3), R_{25} is the *ratio* between the major and minor axes at the location of the 25 mag/arcsec^2 isophote in B-band.

[20] The 103a photographic plate series were less sensitive to low signal-to-noise sources compared to the IIIa plates in the 1970s (Sect. 1.4.1).

Este documento incorpora firma electrónica, y es copia auténtica de un documento electrónico archivado por la ULL según la Ley 39/2015.
Su autenticidad puede ser contrastada en la siguiente dirección https://sede.ull.es/validacion/

Identificador del documento: 2622200 Código de verificación: mbm0ekWs

Firmado por:	ROSHAN NUSHKIA CHAMBA *UNIVERSIDAD DE LA LAGUNA*	Fecha: 07/07/2020 13:28:26
	IGNACIO TRUJILLO CABRERA *UNIVERSIDAD DE LA LAGUNA*	07/07/2020 13:58:21
	Johan Hendrik Knapen Koelstra *UNIVERSIDAD DE LA LAGUNA*	07/07/2020 15:23:08
	María de las Maravillas Aguiar Aguilar *UNIVERSIDAD DE LA LAGUNA*	08/07/2020 15:55:11

Universidad de La Laguna
Oficina de Sede Electrónica
Entrada
Nº registro: 2020/46124
Nº reg. oficina: OF002/2020/45309
Fecha: 07/07/2020 15:26:22

measure accurate total magnitudes, colour indices and apparent dimensions of galaxies distributed in the Northern Sky. He defines 'diameter' as the radial location in a galaxy where the photographic density with respect to the background in the plate is 0.5%, noting that:

> '*[A] relative plate density of* 0.5% *corresponds, on an average, to surface magnitudes of* $26^{\rm m}.5$ *(photogr. reg.) and* $26^{\rm m}.0$ *(photogv. reg.), per square second. Since a density of* 0.5% *is close to the practical measuring limit, the two magnitudes mentioned represents the limiting surface magnitudes of the plates.*'
>
> —Holmberg (1958)

Therefore, while the limiting surface brightness magnitudes in the collection of photographic plates (regions) used by Holmberg (1958) was 26.5 mag/arcsec^2, the *definition* of 'diameter' was based on a relative density of 0.5% in the sample of galaxies with respect to the background in the plates. Indeed, such a statistical definition of diameter depends on the sample of galaxies and the limiting depth of images, which would then correspond to different surface brightness isophotes. For operational purposes, however, Holmberg's radius ($R_{\rm H}$) has been measured using the location of the isophote at 26.5 mag/arcsec^2 in the B-band (which is close to the photographic band used by Holmberg 1958).[21] Similarly, in Chapters 2 and 3 of this thesis, we have used a *proxy* for Holmberg's radius, fixing the isophote at 26 mag/arcsec^2 in the SDSS g-band.

From the above discussion, it is clear that both D_{25} and $R_{\rm H}$ were operatively selected by Redman (1936) and Holmberg (1958), respectively, to measure the maximum apparent boundaries of galaxies. While it seems as though de Vaucouleurs advocated the use of $R_{\rm e}$ as a measure of galaxy dimension throughout his career[22], he frequently included the isophotal measures in galaxy catalogues (D_{25} in RC2 and RC3) and in studies where he consistently adopted the terms 'diameter' and 'dimension' interchangably to refer to these parameters (including $R_{\rm e}$, see also e.g. de Vaucouleurs 1959d). However, the use of 'diameter' and 'dimension' interchangably in the literature to describe the concept of galaxy size was evident as early as the 1930s–40s, i.e. before de Vaucouleurs (1948) introduced $R_{\rm e}$. This was a period when long exposures and homogenous plates were increasingly used to quantitatively compare the dimensions of spheroidal and spiral galaxies[23]:

> '*Since galaxies, like planetary atmospheres, probably fade out indefinitely, the extreme* ***diameters*** *are not very important in themselves (if the peripheral masses are negligible); but the* ***dimensions*** *out to a given light or mass density become very significant if evolutionary trends are under consideration and comparative* ***sizes*** *and gradients must be discussed.*
>
> ...

[21] See van der Kruit (2007, Appendix A) for a discussion on the precise definition of Holmberg's radius, as well as a demonstration of the remarkable reproducibility of the measurements by Holmberg (1958) despite the many difficulties he faced in tracing plates. It is also noteworthy that Holmberg (1958) measured the properties of several low surface brightness galaxies (with a mean surface brightness < 26 mag/arcsec^2).

[22] All of his publications in this Chapter but I also refer the reader to the International Astronomical Union Symposium (IAUS) proceedings de Vaucouleurs (1974) and de Vaucouleurs (1987).

[23] This was an interesting issue in that era of extragalactic observations because reflector or refractor plates showed that spiral galaxies were significantly larger (by a factor 5) than ellipticals, and astronomers were interested in looking for 'growth' in dimensions along the Hubble sequence (Shapley (1942) but see also de Vaucouleurs (1959c) and references therein).

Este documento incorpora firma electrónica, y es copia auténtica de un documento electrónico archivado por la ULL según la Ley 39/2015.
Su autenticidad puede ser contrastada en la siguiente dirección https://sede.ull.es/validacion/

Identificador del documento: 2622200 Código de verificación: mbm0ekWs

Firmado por:	ROSHAN NUSHKIA CHAMBA *UNIVERSIDAD DE LA LAGUNA*	Fecha: 07/07/2020 13:28:26
	IGNACIO TRUJILLO CABRERA *UNIVERSIDAD DE LA LAGUNA*	07/07/2020 13:58:21
	Johan Hendrik Knapen Koelstra *UNIVERSIDAD DE LA LAGUNA*	07/07/2020 15:23:08
	María de las Maravillas Aguiar Aguilar *UNIVERSIDAD DE LA LAGUNA*	08/07/2020 15:55:11

Universidad de La Laguna
Oficina de Sede Electrónica
Entrada
Nº registro: 2020/46124
Nº reg. oficina: OF002/2020/45309
Fecha: 07/07/2020 15:26:22

> *A by-product of Miss [Dr] Patterson's photometry [using homogenous, long exposure plates from Havard Observatories] has been the measurement of* ***boundaries****. From this material, the intercomparison of dimensions of spheroidal and spiral galaxies now becomes possible…and is, in fact, about the first to be precisely suited [to address this problem].*'
>
> —Shapley (1942)

From the above excerpt from Shapley (1942), it is quite clear that 'diameters', 'dimensions' and 'boundaries' (highlighted here in bold for emphasis) all refer to the size of galaxies. The fact that many different terms are used to describe the same concept suggests that a clear framework to define exactly what 'size' meant for a galaxy had not yet been realised. This is probably because the outer regions of galaxies were poorly understood in that era (this was recognised) and that observations were highly biased towards the brightest regions of galaxies (also Sect. 1.3.3). Regardless of these issues, even in these early discussions, astronomers were concerned about the right method of comparing the relative diameters or sizes of galaxies to study their growth and evolution. Shapley was well aware that only long-exposure, homogenous datasets (i.e. deep imaging) can be used to compare the sizes of different galaxy populations. Furthermore, he recognised that if sizes of different populations are to be compared in the context of evolutionary scenarios, then the choice of the dimension parameter is extremely relevant.

Given the situation regarding the nomenclature and description of galaxy size in the 1930–40s (and even after de Vaucouleurs introduced $R_{\rm e}$ in the 1950s), it begs the question of when did astronomers start referring to parameters such as $R_{\rm e}$, D_{25} and $R_{\rm H}$ as size? At least in the case of $R_{\rm e}$, this seems to have happened slowly and gradually, starting around the 1960s–70s, after the works by de Vaucouleurs (1959d), Fish (1963) and Sérsic (1968b). The details of how this may have happened will now be described.

After $R_{\rm e}$ was introduced by de Vaucouleurs (1948) in the form of the $R^{1/4}$ model for elliptical galaxies (Eq. 1.1), many astronomers agreed that it was a universal and physical law for these galaxies. A significant number of investigations were thus dedicated to understand what the $R^{1/4}$ law implied about the formation of elliptical galaxies. Fish (1963) was the first to demonstrate a correlation between de Vaucouleurs' $R_{\rm e}$ and absolute luminosity L for elliptical galaxies in the Virgo cluster, $L \sim R_{\rm e}^{3/2}$. He called this the 'Luminosity Concentration Law': probably because $R_{\rm e}$ is a measurement of light concentration in galaxies and a 'law' because he attempted to interpret the correlation in terms of the Hoyle (1953) model for galaxy formation. Fish expanded on these results a year later, by studying the correlation between the mass and potential energy of elliptical galaxies i.e. $R_{\rm e} \propto M^{\alpha}$:

> '*The significance of a relationship between mass and potential energy in elliptical galaxies lies in two facts. First, the relationship describes the* ***degree of concentration*** *of the elliptical galaxies at the time of star formation. Second, it reveals the dependence of the radiation upon total mass during the condensation of the protogalaxy out of the pregalactic medium. The first fact permits drawing conclusions about conditions for star formation. The second allows selection between the physical events that might have occurred during the contraction of the protogalaxy.*
>
> ...

Este documento incorpora firma electrónica, y es copia auténtica de un documento electrónico archivado por la ULL según la Ley 39/2015.
Su autenticidad puede ser contrastada en la siguiente dirección https://sede.ull.es/validacion/

Identificador del documento: 2622200 Código de verificación: mbm0ekWs

Firmado por:	ROSHAN NUSHKIA CHAMBA *UNIVERSIDAD DE LA LAGUNA*	Fecha: 07/07/2020 13:28:26
	IGNACIO TRUJILLO CABRERA *UNIVERSIDAD DE LA LAGUNA*	07/07/2020 13:58:21
	Johan Hendrik Knapen Koelstra *UNIVERSIDAD DE LA LAGUNA*	07/07/2020 15:23:08
	María de las Maravillas Aguiar Aguilar *UNIVERSIDAD DE LA LAGUNA*	08/07/2020 15:55:11

Universidad de La Laguna
Oficina de Sede Electrónica
Entrada
Nº registro: 2020/46124
Nº reg. oficina: OF002/2020/45309
Fecha: 07/07/2020 15:26:22

> *(A relationship between mass and angular momentum in elliptical galaxies would provide further information on the condensation process, but no significant correlation is found to exist between these two parameters.)*'
>
> —Fish (1964)

In other words, while it was possible to make a physical interpretation of $R_{\rm e}$–mass or $R_{\rm e}$–luminosity correlations using galaxy formation ideas in that period, considering $R_{\rm e}$ as a measure of the 'degree of concentration' (highlighted here in bold) for elliptical galaxies, a relationship with angular momentum of the galaxy was still far from being understood. Apart from the above physical interpretations he lays out in the paper, Fish (1964) also notes that de Vaucouleurs' $R_{\rm e}$ is much more reliable to obtain compared to isophotal radii that demanded accurate photometry and knowledge of absolute values of surface brightness. Rewriting de Vaucouleurs law as:

$$\mu(R) = \mu_e e^{-7.76[(R/R_{\rm e})^{1/4}-1]} \tag{1.5}$$

where $\mu_e = \mu(R_{\rm e})$, one can readily show that

$$\log\left(\frac{\mu(R)}{\mu(0)}\right) = -3.37\left(\frac{R}{R_{\rm e}}\right)^{1/4} + C \tag{1.6}$$

with C a constant. Therefore, by simply plotting $\mu(R)$ vs. $R^{1/4}$, it is possible to determine $R_{\rm e}$ from the slope of the relation, provided an accurate linear regression:

> '*This fact reveals an advantage of the de Vaucouleurs definition of radius over an isophotal definition, because an isophotal radius can be no more reliable than the accuracy with which the zero point of the photometry is determined. Good zero points require fairly elaborate procedures in surface photometry, particularly if the technique is completely photographic. It should also be mentioned that the simple form for the potential energy given by equation (8) [$\Omega \propto GM/R_{\rm e}$] is not valid for a radius defined simply as the distance from the nucleus to a given isophote.*'
>
> —Fish (1964)

What this means is that Fish preferred $R_{\rm e}$ because it was more robust compared to measurements of isophotal radii using photographic plates at that time and also because $R_{\rm e}$ generated very simple and elegant equations for physical quantities, like potential energy Ω. Therefore, given the limitations in imaging in the 1960s as well as the difficulty in simulating galaxy formation theories, it is completely justifiable that a lot of astronomers used $R_{\rm e}$ to analyse the formation of elliptical galaxies in these times. However, even in Fish's paper, $R_{\rm e}$ was never perceived (or explicitly associated) as a diameter or size definition for galaxies, but as a measurement of concentration and 'radius' because it has units of length.

Four years later, Sérsic (1968a) made similar efforts in the understanding of the formation of elliptical galaxies by generalising de Vaucouleurs $R^{1/4}$ law using an index 'n':

$$\mu(R) = \mu(0)e^{-b_n(R/R_{\rm e})^{1/n}}. \tag{1.7}$$

This is called the Sérsic law. Setting $n = 4$ and $n = 1$ gives back Eq. 1.1 (the $R^{1/4}$ law for ellipticals) and 1.2 (exponential discs for spirals), respectively: Sérsic was well aware that

Este documento incorpora firma electrónica, y es copia auténtica de un documento electrónico archivado por la ULL según la Ley 39/2015.
Su autenticidad puede ser contrastada en la siguiente dirección https://sede.ull.es/validacion/

Identificador del documento: 2622200 Código de verificación: mbm0ekWs

Firmado por:	ROSHAN NUSHKIA CHAMBA *UNIVERSIDAD DE LA LAGUNA*	Fecha: 07/07/2020 13:28:26
	IGNACIO TRUJILLO CABRERA *UNIVERSIDAD DE LA LAGUNA*	07/07/2020 13:58:21
	Johan Hendrik Knapen Koelstra *UNIVERSIDAD DE LA LAGUNA*	07/07/2020 15:23:08
	María de las Maravillas Aguiar Aguilar *UNIVERSIDAD DE LA LAGUNA*	08/07/2020 15:55:11

Universidad de La Laguna
Oficina de Sede Electrónica
Entrada
Nº registro: 2020/46124
Nº reg. oficina: OF002/2020/45309
Fecha: 07/07/2020 15:26:22

not all elliptical galaxies followed the $R^{1/4}$ law.[24] He subsequently studied the 'mass–radius diagram', i.e. the mass–R_e relationship, for a sample of early and late-type galaxies that same year (Sérsic 1968b). He included late-type spiral galaxies in his sample partly because Fish (1964) associated the elliptical galaxies he characterised with neighbouring spirals to ascertain whether spirals were 'youthful' or not.

Sérsic's diagram is shown in Fig. 1.14. Even though he used a relatively small sample, recognising selection effects and an over-representation of interacting galaxies (which is probably why he did not attempt to quantify the slope or dispersion of the relation), Sérsic's diagram already begins to reflect two distinct sequences: an almost flat region in the R_e–mass plane for late-type galaxies and a separate sequence for the ellipticals. Like those before him, Sérsic was interested in trying to find out whether an evolutionary sequence occurred along these Hubble sequences. For this reason, he interpreted the region around $10^{11}\,M_\odot$ as a 'transition region' between the late and early-types because it was dominated by the interacting galaxies in his sample.

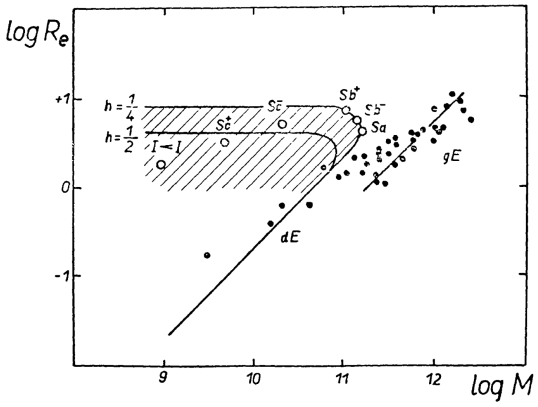

Figure 1.14: The first mass–radius diagram for galaxies. The shaded region suggests the qualitative dispersion of the individual data points. The spiral (open circles), elliptical (black circles) and dwarf elliptical (dE) galaxies are clearly marked, already showing hints of the different sequences that these galaxy types populate in this parameter space. *Credit: Sérsic (1968b).*

It is of importance to point out that the R_e for the spiral galaxies studied by Sérsic (1968b) was computed using de Vaucouleurs (1959d) calibrated, linear relation between R_e and D_{25}, and not by fitting an exponential model to the profiles of spirals. In fact, de Vaucouleurs (1959d) can be considered the first attempt to compare different measures of the parameters we call size today, i.e. R_e and D_{25}. It was also during this time that de Vaucouleurs promoted the 'effective radius' to an 'effective dimension', essentially placing it and the isophotal diameters (or 'brightness dimensions' as he called them) on the same footing. This could be an early source

[24] Some researchers would even tweak the background level in imaging just to force galaxies under study to the $R^{1/4}$ model (pointed out by D'Onofrio et al. 1994).

Este documento incorpora firma electrónica, y es copia auténtica de un documento electrónico archivado por la ULL según la Ley 39/2015.
Su autenticidad puede ser contrastada en la siguiente dirección https://sede.ull.es/validacion/

Identificador del documento: 2622200 Código de verificación: mbm0ekWs

Firmado por:	ROSHAN NUSHKIA CHAMBA *UNIVERSIDAD DE LA LAGUNA*	Fecha: 07/07/2020 13:28:26
	IGNACIO TRUJILLO CABRERA *UNIVERSIDAD DE LA LAGUNA*	07/07/2020 13:58:21
	Johan Hendrik Knapen Koelstra *UNIVERSIDAD DE LA LAGUNA*	07/07/2020 15:23:08
	María de las Maravillas Aguiar Aguilar *UNIVERSIDAD DE LA LAGUNA*	08/07/2020 15:55:11

Universidad de La Laguna
Oficina de Sede Electrónica
Entrada
Nº registro: 2020/46124
Nº reg. oficina: OF002/2020/45309
Fecha: 07/07/2020 15:26:22

for the confusion in the literature between what the original notion of dimension or diameter (as discussed in e.g. Hubble 1926; Redman 1936; Spitzer 1942) meant and what the effective radius was tracing, i.e. light concentration (e.g. in Fish 1963). Subsequent comparisons were conducted by Vorontsov-Vel'Yaminov (1961) and Genkin & Genkina (1970). But although these comparisons have been completely ignored to date, it turns out that they provide further insight on the development towards calling parameters like $R_{\rm e}$, D_{25} or $R_{\rm H}$ as 'size', as well as a base on which the work presented in this thesis can be viewed of fundamental importance. In the light of this, I highlight some of the discussion in the work by Vorontsov-Vel'Yaminov (1961) and Genkin & Genkina (1970) below.

1.5.3 A tale of two citations

Although astronomers had devoted a lot of attention towards the use of de Vaucouleurs law in the early 1960s, there is little evidence to suggest that most of these researchers had considered the negative implications (if any) on the use of $R_{\rm e}$ for the understanding of elliptical galaxies, as well as galaxies of other types. Additionally, although the dimensions or diameters of galaxies had indeed been discussed in the context of $R_{\rm e}$, D_{25} and $R_{\rm H}$, the concept of 'size' itself was not yet explicitly defined in these early works — it seemed as though it was continuously assumed that they all could be used to describe galaxy size and for any galaxy type. On this aspect, Vorontsov-Vel'Yaminov (1961) calls for a more explicit definition of the dimension of galaxies and offers a critical perspective on the use of diameters to compare elliptical and spiral galaxies as performed in the work of de Vaucouleurs:

> '*Different methods of determination of the diameters of spiral galaxies give results which are principally not comparable. It is proposed that diameters of distinctly visible spiral patterns be compared. Their diameters depend only very slightly on exposures, etc. The definition of diameters of elliptical galaxies to be used for comparison is less obvious.* ***At the present stage, the comparison of diameters*** *of spiral and elliptical* ***galaxies has no sense until the physical and practical determination of the boundaries of galaxies has been properly adjusted****.*'
>
> —Vorontsov-Vel'Yaminov (1961)

In other words, the determination of diameters for ellipticals and spirals should be performed separately because of their different internal structure, and for this reason comparisons are difficult if not impossible, unless a more physically meaningful and practical approach is adopted (in bold here for emphasis). However, in the early 1960s, finding such a definition of diameter or size was not possible as the outskirts of galaxies were not known (Vorontsov-Vel'Yaminov (1961) recognised this), at least not until the first detection of stellar haloes (Sect. 1.3.1).

The second of these works, Genkin & Genkina (1970)[25], seems to be the first ever paper to have 'size' in its title, i.e. '*Comparisons of Galaxy Sizes*', referring to the 'effective diameter' and isophotal diameters. Like de Vaucouleurs (1959d) (also in de Vaucouleurs 1959a), these authors were interested in establishing a statistical relationship between the different size definitions for galaxies. However, they also correctly point out that $R_{\rm e}$ is not very well suited for spiral galaxies, while it is more appreciable for elliptical galaxies (highlighted here in bold):

[25] At the time of writing, this is the only paper which cites Vorontsov-Vel'Yaminov (1961).

Este documento incorpora firma electrónica, y es copia auténtica de un documento electrónico archivado por la ULL según la Ley 39/2015.
Su autenticidad puede ser contrastada en la siguiente dirección https://sede.ull.es/validacion/

Identificador del documento: 2622200 Código de verificación: mbm0ekWs

Firmado por:	ROSHAN NUSHKIA CHAMBA *UNIVERSIDAD DE LA LAGUNA*	Fecha: 07/07/2020 13:28:26
	IGNACIO TRUJILLO CABRERA *UNIVERSIDAD DE LA LAGUNA*	07/07/2020 13:58:21
	Johan Hendrik Knapen Koelstra *UNIVERSIDAD DE LA LAGUNA*	07/07/2020 15:23:08
	María de las Maravillas Aguiar Aguilar *UNIVERSIDAD DE LA LAGUNA*	08/07/2020 15:55:11

Universidad de La Laguna
Oficina de Sede Electrónica
Entrada
Nº registro: 2020/46124
Nº reg. oficina: OF002/2020/45309
Fecha: 07/07/2020 15:26:22

> '*In general a determination of effective dimensions does not appear to be of any value at all for spiral galaxies. On the one hand, the* ***effective sizes are not related to any structural features*** *of spiral systems, while on the other, [...]* ***[f]or elliptical galaxies having no structural features, the effective size is a very convenient parameter****, although it remains difficult to determine.*'
>
> —Genkin & Genkina (1970)

In other words, echoing Vorontsov-Vel'Yaminov (1961), R_e is not related to any physical characteristics of galaxies, it is not physically motivated. Additionally, as R_e was primarily introduced via a model to parameterize the light distribution for elliptical galaxies specifically (de Vaucouleurs 1948), R_e is consequently not valuable for spiral galaxies.

Although both the above works recognised the limitations of using R_e very early on, it continues to be the top choice among astronomers for characterising galaxy size, and therefore to study the size–stellar mass relation. As mentioned in the previous section, this could be a consequence of the reliability of R_e for galaxies at high redshift ($z > 1$) where absolute surface brightness values are currently almost impossible to obtain with confidence. But the popularity of R_e began even before high redshift studies emerged, perhaps due to the use of R_e in several classical works on massive elliptical galaxies the 1970s–80s (e.g. Kormendy 1977; Djorgovski & Davis 1987). In these works, R_e was used in various scaling relations that were later shown to produce constraints on galaxy formation models for elliptical galaxies. A closer look at Kormendy (1977), however, is interesting because the author[26] showed that the Hubble (1930), de Vaucouleurs (1948) and King (1962) models for spheroidal galaxies '*all measure essentially the same physics*'— in other words, the physics underlying the galaxy is independant of R_e specifically. And yet, R_e continues to be the preferred size measure, for all galaxy types, possibly due to influence from high redshift studies and because R_e is associated to the most convenient fitting functions for galaxy profiles.

1.6 Thesis scope and overview

In this Chapter, I have motivated the importance of deep imaging in the understanding of galaxy formation and evolution within the ΛCDM paradigm (Sect. 1.1–1.2). In particular, in Sect. 1.3, I summarised key observational discoveries in astronomy that made use of deep images: stellar haloes (Sect. 1.3.1), truncations (Sect. 1.3.2) and low surface brightness galaxies (Sect. 1.3.3). I then placed the work undertaken in this thesis within a broader context of the research lines opened by these discoveries in Sect. 1.4. This includes a brief overview on the development of deep photographic imaging and CCD imaging (Sect. 1.4.1), state-of-the-art deep imaging surveys from current ground-based telescopes (Sect. 1.4.2) and a summary of how the deepest imaging can be used to quantify the mass in the stellar haloes of galaxies (Sect. 1.4.3) as well as to understand the structure of the outer disc (Sect. 1.4.4). I also introduced the definition of 'ultra-diffuse galaxies' and the proposed failed, Milky Way-sized formation mechanism for these objects in Sect. 1.4.5, including a historical anecdote from Binggeli (1994) which suggests that ultra-diffuse galaxies are simply faint dwarfs. Finally in Sect. 1.5, I discussed the motivations

[26] Interestingly, Kormendy pursued this work during his PhD.

Este documento incorpora firma electrónica, y es copia auténtica de un documento electrónico archivado por la ULL según la Ley 39/2015.
Su autenticidad puede ser contrastada en la siguiente dirección https://sede.ull.es/validacion/

Identificador del documento: 2622200 Código de verificación: mbm0ekWs

Firmado por:	ROSHAN NUSHKIA CHAMBA *UNIVERSIDAD DE LA LAGUNA*	Fecha: 07/07/2020 13:28:26
	IGNACIO TRUJILLO CABRERA *UNIVERSIDAD DE LA LAGUNA*	07/07/2020 13:58:21
	Johan Hendrik Knapen Koelstra *UNIVERSIDAD DE LA LAGUNA*	07/07/2020 15:23:08
	María de las Maravillas Aguiar Aguilar *UNIVERSIDAD DE LA LAGUNA*	08/07/2020 15:55:11

Universidad de La Laguna
Oficina de Sede Electrónica
Entrada
Nº registro: 2020/46124
Nº reg. oficina: OF002/2020/45309
Fecha: 07/07/2020 15:26:22

for studying the size distribution of galaxies in the context of galaxy formation and evolution (Sect. 1.5.1) and the historical origins of the popularity of R_e and other classical parameters such as D_{25} as a size measure (Sect. 1.5.2). In particular, I showed that parameters such as R_e and the isophotal radii have always been assumed to represent galaxy size, but never explicitly demonstrated in these terms within a clear physical framework (by physical, I mean a property innately linked to how galaxies grow and evolve in size). R_e was specifically chosen to parameterise the $R^{1/4}$ model for elliptical galaxies. de Vaucouleurs (1948) fixed the scaling radius $R_s \equiv R_e$ in Eq. 1.1 probably because galaxy outskirts were not well observed using photographic plates at that time. However, in principle, *any* R_s (i.e. radii enclosing different fractions of total galaxy light) could have been used for this purpose and therefore this makes R_e an arbitrary parameter that has consequences on the interpretation of scaling relations (for a discussion on this issue see Graham 2019).

As mentioned previously, R_e was preferred among many astronomers in the past primarily because the outskirts of galaxies were not well understood or observed with low enough uncertainty (at least not until the low signal-to-noise IIIa-J plates were improved in the 1970s and stacked to produce deep images (Sect. 1.4.1)). To some extent, this is still especially true for very high redshift galaxies (discussed in Sec. 1.5.1), which has potentially influenced how astronomers view the use of R_e as a size measure for galaxies. But at the same time, in the case of nearby galaxies, even when their outskirts were being observed with much greater accuracy, starting with massive surveys like SDSS (York et al. 2000), the association of R_e to galaxy size had already been so deeply established in the astronomical literature that there seemed to be no room for criticism. In fact, the first statistical exploration of the mass–size relation in the nearby Universe made use of SDSS (Shen et al. 2003) which catalogued R_e for a million galaxies in the late 1990s–early 2000s. Therefore, subsequent studies in the last 15–20 years probing the size evolution of galaxies at higher redshift were probably forced to select R_e to represent galaxy size for consistency, because the work by Shen et al. (2003) was a reference for objects at low redshift. In this regard, it is studies using R_e to represent the sizes of nearby galaxies (since the works by e.g. de Vaucouleurs (1959d), Fish (1963), Sérsic (1968b) and later Shen et al. (2003)) which have influenced studies at high redshift afterwards, eventually leading to a convention that R_e is a measure of galaxy size.

However, investigations attempting to study the mass–size relation have also used radii enclosing other fractions of the total galaxy light, e.g. R_{90} that encloses 90% of the galaxy light (Nair et al. 2011) or R_{80} that encloses 80% (Miller et al. 2019). In addition to the classical D_{25} and Holmberg radius, isophotal measures have also been explored to represent galaxy size for disc galaxies, e.g. $R_{23.5,i}$ which is the radius where $\mu = 23.5\,\mathrm{mag/arcsec^2}$ in the optical SDSS i-band (Hall et al. 2012) as well as the isophote at $25.5\,\mathrm{mag/arcsec^2}$ in the 3.6μ near-infrared imaging from the Spitzer Survery of Stellar Structure in Galaxies (S4G) survey (Sheth et al. 2010; Muñoz-Mateos et al. 2015). All these measures are somewhat arbitrary in the sense that they do not necessarily hold any physical information on the formation of galaxies. However, thus far, it is R_e (or variants such as $r_{1/2}$) that has been used in important theoretical studies on the connection between size, mass and angular momentum of galaxies (Mo et al. 1998; Somerville et al. 2008; Kravtsov 2013; Jiang et al. 2019) and in the calibration of current hydrodynamical simulations, e.g. in EAGLE (Crain et al. 2015) and IllustrisTNG (Pillepich et al. 2018b), among others.

In light of the above situation, in this thesis, I present a physically motivated definition

Este documento incorpora firma electrónica, y es copia auténtica de un documento electrónico archivado por la ULL según la Ley 39/2015.
Su autenticidad puede ser contrastada en la siguiente dirección https://sede.ull.es/validacion/

Identificador del documento: 2622200 Código de verificación: mbm0ekWs

Firmado por:	ROSHAN NUSHKIA CHAMBA *UNIVERSIDAD DE LA LAGUNA*	Fecha: 07/07/2020 13:28:26
	IGNACIO TRUJILLO CABRERA *UNIVERSIDAD DE LA LAGUNA*	07/07/2020 13:58:21
	Johan Hendrik Knapen Koelstra *UNIVERSIDAD DE LA LAGUNA*	07/07/2020 15:23:08
	María de las Maravillas Aguiar Aguilar *UNIVERSIDAD DE LA LAGUNA*	08/07/2020 15:55:11

Universidad de La Laguna
Oficina de Sede Electrónica
Entrada
Nº registro: 2020/46124
Nº reg. oficina: OF002/2020/45309
Fecha: 07/07/2020 15:26:22

for the size of a galaxy using deep imaging, published in Trujillo, Chamba, & Knapen (2020) and Chapter 2 of this thesis. The work is not only timely, given knowledge on the outskirts of galaxies and their formation, but fundamentally necessary as until now, an explicit, more physical and practical definition of the luminous size for galaxies has barely been explored. In fact, to some extent, we are still very much in a similar situation as that pointed out in Vorontsov-Vel'Yaminov (1961) all those decades ago: how can the diameters of different galaxy types be fairly compared within a physical framework? This question is addressed in Chamba, Trujillo, & Knapen (2020) and Chapter 3 of this thesis, which points out that the use of $R_{\rm e}$ to compare the sizes of galaxies is misleading. An example is the statement that ultra-diffuse galaxies are 'Milky Way-sized' (van Dokkum et al. 2015a), an interpretation which has lead to a questionable theory on how these galaxies might have formed: the so-called failed $L_\star$ galaxy hypothesis discussed in Sect. 1.4.5.

This thesis is organised as follows. The size–stellar mass plane is studied using a newly proposed physical size definition in Chapter 2 and compared with other popular size measures like $R_{\rm e}$. A sample of ~ 1000 nearby galaxies ($z < 0.1$), spanning five orders of magnitude in stellar mass ($10^{11} M_\odot < M_\star < 10^{12} M_\odot$) and morphology from dwarfs to giant ellipticals is used for this purpose. In Chapter 3, I demonstrate the implications of the proposed size parameter on the understanding of ultra-diffuse galaxies. Chapter 4 consists of ongoing work related to the results in Chapter 2. And finally, a summary of the main conclusions and possible future research avenues based on the work of this thesis are presented in Chapter 5.

Este documento incorpora firma electrónica, y es copia auténtica de un documento electrónico archivado por la ULL según la Ley 39/2015.
Su autenticidad puede ser contrastada en la siguiente dirección https://sede.ull.es/validacion/

Identificador del documento: 2622200 Código de verificación: mbm0ekWs

Firmado por:	ROSHAN NUSHKIA CHAMBA *UNIVERSIDAD DE LA LAGUNA*	Fecha: 07/07/2020 13:28:26
	IGNACIO TRUJILLO CABRERA *UNIVERSIDAD DE LA LAGUNA*	07/07/2020 13:58:21
	Johan Hendrik Knapen Koelstra *UNIVERSIDAD DE LA LAGUNA*	07/07/2020 15:23:08
	María de las Maravillas Aguiar Aguilar *UNIVERSIDAD DE LA LAGUNA*	08/07/2020 15:55:11

Universidad de La Laguna
Oficina de Sede Electrónica
Entrada
Nº registro: 2020/46124
Nº reg. oficina: OF002/2020/45309
Fecha: 07/07/2020 15:26:22

2

A physically motivated definition for the size of galaxies in an era of ultra-deep imaging

As discussed in Chapter 1 (Sect. 1.4), present-day multi-wavelength deep imaging surveys allow to characterise the outskirts of galaxies with unprecedented precision. Therefore, deep imaging offers a new front to define a physically motivated measurement of size for galaxies (Sect. 1.5–1.6). In this Chapter, I present the article '*A physically motivated definition for the size of galaxies in an era of ultra-deep imaging*' published in MNRAS, 493, 87-105 (2020). The associated erratum is included in Appendix A.1.

2.1 Introduction

The sizes of galaxies play a pivotal role in our understanding of how they form and evolve. While the size of an everyday object is quite an intuitive concept, in the case of galaxies where there are no clear edges, measuring their extent is a non-trivial task. The absence of a clear border leads to two different ways of measuring the size of galaxies in the astronomical literature. The first and today's most popular approach is identifying the size of a galaxy as the radial distance containing half of its light (i.e. its effective radius $R_{\rm e}$). A second and fairly common approach to indicate galaxy size is the location of a fixed surface brightness isophote.

The effective radius has been used to characterise the size of galaxies since at least the publication by de Vaucouleurs (1948). Obviously, using half of the light of a galaxy to indicate its size is an arbitrary definition. Other fractions of light could be and in fact have been used as well for this task, for example the radial distance containing 90% of the light of the galaxy (R_{90}) or the Petrosian and Kron radii (Petrosian 1976; Kron 1980, for a review on how the Petrosian and Kron radii relate to the commonly used surface brightness distribution provided by the Sérsic (1968a) model and how such size definitions are affected by the depth of images see Graham & Driver (2005)).

One of the reasons for the popularity of $R_{\rm e}$ is its robustness against many observational issues. In particular, as the surface brightness profiles of the vast majority of galaxies decline very rapidly (with a steepness equal to or larger than an exponential), the effective radius is barely affected by the depth of the images (Trujillo et al. 2001). This robustness makes $R_{\rm e}$ quite

Este documento incorpora firma electrónica, y es copia auténtica de un documento electrónico archivado por la ULL según la Ley 39/2015.
Su autenticidad puede ser contrastada en la siguiente dirección https://sede.ull.es/validacion/

Identificador del documento: 2622200 Código de verificación: mbm0ekWs

Firmado por:	ROSHAN NUSHKIA CHAMBA *UNIVERSIDAD DE LA LAGUNA*	Fecha: 07/07/2020 13:28:26
	IGNACIO TRUJILLO CABRERA *UNIVERSIDAD DE LA LAGUNA*	07/07/2020 13:58:21
	Johan Hendrik Knapen Koelstra *UNIVERSIDAD DE LA LAGUNA*	07/07/2020 15:23:08
	María de las Maravillas Aguiar Aguilar *UNIVERSIDAD DE LA LAGUNA*	08/07/2020 15:55:11

Universidad de La Laguna
Oficina de Sede Electrónica
Entrada
Nº registro: 2020/46124
Nº reg. oficina: OF002/2020/45309
Fecha: 07/07/2020 15:26:22

appealing as a measurement for galaxy size as different authors using different datasets can reach an agreement on the size. However, despite its undeniable value, $R_{\rm e}$ is incapable of describing the global (luminous) size of galaxies (see an in-depth discussion in Graham 2019). This limits our use of $R_{\rm e}$ as a direct measurement of galaxy size because $R_{\rm e}$ measures light concentration and strongly depends on the shape of the light profile. Consider, for example, two disc galaxies with similar appearance but with bulges of very different brightness. The global $R_{\rm e}$ of the galaxy with a prominent bulge will be significantly smaller than that of the one with a faint bulge. For this reason, and as we will demonstrate in this Chapter, galaxies with the same extension can have very different effective radii. This is not a minor issue and has serious consequences when one wants to address or infer the nature of galaxies (Chapter 3; Chamba, Trujillo, & Knapen 2020). In addition, the $R_{\rm e}$ of a galaxy can vary significantly with wavelength (see e.g. Kennedy et al. 2015).

The second approach for measuring galaxy size is based on the radial location of a given isophote. The two most common size definitions are D_{25} based on the radial location of the isophote at $\mu_B = 25$ mag/arcsec^2 and the Holmberg radius ($R_{\rm H}$) defined as the radial distance of the isophote at $\mu_B = 26.5\,$mag/arcsec^2 (Holmberg 1958). D_{25} was popularised in the famous Second Reference Catalogue of Bright Galaxies by de Vaucouleurs et al. (1976). The authors of the catalogue refer to Redman (1936) as the first to propose D_{25} and to Liller (1960) as the first to adopte it. These two surface brightness values correspond roughly to 10% and 3% (respectively) of the brightness of the (darkest) night sky in the B-band in ground-based observatories. D_{25} and $R_{\rm H}$ were motivated by the typical depth of optical images 60 years ago, and created to measure the maximum extension of galaxies visible at that time (de Vaucouleurs et al. 1976). In this sense, measuring galaxy size using such a definition was not motivated by any particular physical reason and both D_{25} and $R_{\rm H}$ simply reflect the technological limitation in the 1960s. Such isophotal size definitions are not limited to the optical bands only. For example, Muñoz-Mateos et al. (2015) characterised the global extensions of the galaxies in the infrared Spitzer Survery of Stellar Structure in Galaxies (S^{4}G) survey (Sheth et al. 2010) using $\mu_{3.6} = 25.5$ mag/arcsec^2 as a size indicator. In the context of exploring the scaling relations between size, luminosity and velocity of late-type galaxies, Saintonge & Spekkens (2011) and Hall et al. (2012) found that the use of $R_{23.5,{\rm i}}$ (i.e. the radial location of the isophote $\mu_i = 23.5$ mag/arcsec^2) yields the smallest scatter in the size–luminosity relation.

In contrast to $R_{\rm e}$ and the isophotal size measures, there has also been some effort to characterise galaxy size using physically motivated parameters. An example of such a size parameter is the exponential scale length $R_{\rm d}$ which is connected with the angular momentum of dynamically stable discs (see e.g. Mo et al. 1998, 2010). However, in practice, due to the complexity of galactic discs (which include bars, spiral arms, etc) the use of $R_{\rm d}$ has been shown to be complicated to reproduce by different authors. In fact, for the same galaxies, $R_{\rm d}$ has been measured with a scatter of $\sim 25\%$ (see e.g. Knapen & van der Kruit 1991; Möllenhoff 2004).

All the above size measures were introduced using relatively shallow imaging surveys. More recently, however, a revolution in the limiting depth of new astronomical imaging surveys has happened. As we will propose in this Chapter, image depth is no longer the limitation it once was to find a more representative and physically motivated definition for galaxy size. While the most commonly used astronomical survey, the Sloan Digital Sky Survey (SDSS; Abazajian et al. 2003), reaches a comparable depth that obtained in photographic plates (i.e. $\sim 26.5\,$mag/arcsec^2 in the g-band, which is equivalent to a 3σ fluctuation with respect to the background of the image

Este documento incorpora firma electrónica, y es copia auténtica de un documento electrónico archivado por la ULL según la Ley 39/2015.
Su autenticidad puede ser contrastada en la siguiente dirección https://sede.ull.es/validacion/

Identificador del documento: 2622200 Código de verificación: mbm0ekWs

Firmado por:	ROSHAN NUSHKIA CHAMBA *UNIVERSIDAD DE LA LAGUNA*	Fecha: 07/07/2020 13:28:26
	IGNACIO TRUJILLO CABRERA *UNIVERSIDAD DE LA LAGUNA*	07/07/2020 13:58:21
	Johan Hendrik Knapen Koelstra *UNIVERSIDAD DE LA LAGUNA*	07/07/2020 15:23:08
	María de las Maravillas Aguiar Aguilar *UNIVERSIDAD DE LA LAGUNA*	08/07/2020 15:55:11

Universidad de La Laguna
Oficina de Sede Electrónica
Entrada
Nº registro: 2020/46124
Nº reg. oficina: OF002/2020/45309
Fecha: 07/07/2020 15:26:22

measured in an area of 10×10 arcsec^2; Kniazev et al. 2004; Pohlen & Trujillo 2006), surveys conducted a decade later (i.e. Martínez-Delgado et al. 2010; Ferrarese et al. 2012; Merritt et al. 2014; Capaccioli et al. 2015; Duc et al. 2015; Koda et al. 2015; Fliri & Trujillo 2016; Mihos et al. 2017) are regularly observing 2–3 mag deeper than SDSS. The current observational limit taken from ground-based telescopes is 31.5 mag/arcsec^2 in the r-band, (equivalent to a 3σ fluctuation with respect to the background of the image in an area of 10×10 arcsec^2; Trujillo & Fliri 2016) and a similar depth is expected to be achieved with ultra-deep surveys that are currently in operation such as the Hyper Suprime Cam Survey (Aihara et al. 2018) and the future Large Synoptic Survey Telescope (LSST; Ivezic et al. 2008) survey. Going beyond this depth has been only possible with ultra-deep imaging taken from space (see e.g. Borlaff et al. 2019).

In this Chapter, I present the article published by Trujillo, Chamba, & Knapen (2020) where a physically motivated definition to measure the size of galaxies has been proposed. We demonstrate that using the location of the gas density threshold for star formation in galaxies is a natural size indicator, where by *natural* we mean a size indicator that is connected with the intuitive concept of an edge. In other words, a size indicator that can be linked to a sharp contrast or change in the properties of the objects being explored. In practical terms, we will show that using the radial location of the contour at a stellar mass density of 1 $M_{\odot}$/pc^2 (R_1) corresponds roughly to the location of the gas density threshold for star formation. This definition is innately linked to the separation of the majority of stars that were born in-situ from stars that were mostly accreted throughout a galaxy's history, potentially extending its use to define the stellar halo (N. Chamba et al. in prep). In addition, as will be discussed below, R_1 provides a more direct association to what an observer recognises as the total extension of a galaxy than $R_{\rm e}$. While measuring R_1 would have been difficult using past imaging surveys due to the required level ($\mu_r > 26\,$mag/arcsec^2) to identify isophotes with a low mass density around 1 $M_{\odot}$/pc^2, the reader will recognise that current surveys are able to reach such depth without much difficulty.

Finally, using a physically motivated definition for measuring the size of galaxies is not just another way of measuring the extensions of these objects such as $R_{\rm H}$, D_{25} or their variants. This statement cannot be emphasised enough, given the history on galaxy size definitions since Hubble (1926) discussed in the Introduction (Sect. 1.5.2). Furthermore, we will show that the use of R_1 substantially modifies the scaling relations where galaxy size is an important parameter. This is particularly the case compared to $R_{\rm e}$. Firstly, the use of R_1 significantly decreases the scatter of the stellar mass–size relation by a factor of 2.5. Secondly, using R_1, galaxies with stellar masses from $10^7\,M_{\odot}$ to $10^{11}\,M_{\odot}$ share the same stellar mass–size trend. And thirdly, the overall decrease in scatter essentially tightens the observed correlation between galaxy size and stellar mass, thus allowing to gain insight about the size of an object if its stellar mass is known or viceversa. We will discuss whether these findings indicate a more fundamental meaning of the new size estimator R_1 compared to the more arbitrary effective radius. And finally, how R_1 compares with other size indicators such as the radius enclosing half of the stellar mass ($R_{\rm e,M_\star}$), the Holmberg radius and $R_{23.5,\rm i}$ is also explored for completeness.

This Chapter is structured as follows. In Sect. 2.2, the motivation behind a new size definition based on the location of the gas density threshold for star formation in galaxies is presented. In Sect. 2.3 and 2.4, the data and sample used is described. The methodology is described in Sect. 2.5 and the results in Sect. 2.6. Section 2.7 discusses the results obtained and they are summarised in Sect. 2.8. Through out this Chapter, a standard ΛCDM cosmology with Ω_m =

Este documento incorpora firma electrónica, y es copia auténtica de un documento electrónico archivado por la ULL según la Ley 39/2015.
Su autenticidad puede ser contrastada en la siguiente dirección https://sede.ull.es/validacion/

Identificador del documento: 2622200 Código de verificación: mbm0ekWs

Firmado por:	ROSHAN NUSHKIA CHAMBA *UNIVERSIDAD DE LA LAGUNA*	Fecha: 07/07/2020 13:28:26
	IGNACIO TRUJILLO CABRERA *UNIVERSIDAD DE LA LAGUNA*	07/07/2020 13:58:21
	Johan Hendrik Knapen Koelstra *UNIVERSIDAD DE LA LAGUNA*	07/07/2020 15:23:08
	María de las Maravillas Aguiar Aguilar *UNIVERSIDAD DE LA LAGUNA*	08/07/2020 15:55:11

Universidad de La Laguna
Oficina de Sede Electrónica
Entrada
Nº registro: 2020/46124
Nº reg. oficina: OF002/2020/45309
Fecha: 07/07/2020 15:26:22

0.3, $\Omega_\Lambda = 0.7$ and $H_0 = 70$ km s^{-1} Mpc^{-1} is assumed.

2.2 Towards a physically motivated definition for the size of galaxies

When defining a new way to measure the size of galaxies, it is important to select a physical criterion intimately linked to the way galaxies increase in extension. Galaxies are expected to grow both in stellar mass and size by two different phenomena. The first is based on the transformation of gas into stars and the second is due to the accretion of new stars by merging and tidal interactions with other galaxies. While the merging process is stochastic and difficult to model, the transformation of gas into stars is strongly connected with the gas density of these systems.

Above a given gas density threshold, gas is transformed into stars. Consequently, the position of these newborn stars is encircled by the location of such a critical gas density (Spitzer 1968; Quirk 1972; Fall & Efstathiou 1980; Kennicutt 1989b). The radial location of this gas density threshold is thus suggestive of a natural way to define the size of galaxies. This is the expectation for the vast majority of galaxies, i.e. those whose main channel of stellar mass growth is the transformation of gas into stars. This includes almost all the dwarf galaxies and the majority of disc galaxies where growth by merging activity with other minor objects is expected to be small (see e.g. Toth & Ostriker 1992). The critical gas surface density for star formation is theoretically estimated to be $\Sigma_c \sim 3$–$10\,M_\odot/\mathrm{pc}^2$ (see e.g. Schaye 2004). If the integrated effect of transforming gas into stars in a galaxy is not 100%, a reasonable way of defining the size of a galaxy would be to locate a stellar mass isocontour at $\Sigma_\star \sim 1$–$3\,M_\odot/\mathrm{pc}^2$. Such a range in surface density corresponds to an integrated gas-to-star transformation between $\sim$ 10–30%. A way to test whether such a definition is reliable and a better proxy for the global luminous extension of galaxies compared to other size indicators such as R_e is to explore the stellar mass density at which the edges of disc galaxies appear (i.e. the location of their truncations). Such an analysis has not been conducted exhaustively yet, but preliminary results towards this goal are presented in Chapter 4. However, there are some examples in the literature where this has been done in detail. For instance, in UGC00180, a galaxy with similar properties to M31, the truncation is located at $\sim 2.5\,M_\odot/\mathrm{pc}^2$ (this is an upper limit as the projection effect has not been taken into account; Trujillo & Fliri 2016). For another two edge-on nearby galaxies (NGC4565 and NGC5907), the stellar mass density at their truncation radii is between 1–2 $M_\odot/\mathrm{pc}^2$ (Martínez-Lombilla et al. 2019). The fact that the fraction of stars beyond the truncation of NGC4565 and NGC5907 declines to 0.1–0.2% reinforces the idea that such a stellar mass density is a good proxy for defining the luminous size of a galaxy. This number is compatible with a tiny fraction of stars that migrated from a region within the truncation radius to the outskirts. Unlike R_e, an added value to the physically motivated size definition proposed here is that the measurement corresponds to what the human eye identifies as the border of an object.

In what follows, *the radial location of the gas density threshold for star formation is proposed as a physical size definition.* Based on theoretical arguments and observational evidence of Milky Way-like galaxies, an operative way to estimate this density threshold for star formation is by using a stellar mass density isocontour at $\Sigma_\star \sim 1\,M_\odot/\mathrm{pc}^2$. The radial position of such an isomass contour is referred to R_1. Obviously, the choice of $1\,M_\odot/\mathrm{pc}^2$, instead of, for example, 0.5, 2 or $3\,M_\odot/\mathrm{pc}^2$, depends on the exact integrated efficiency of gas accretion and subsequent star formation among different galaxies. Therefore, depending on the galaxies' characteristics, other

Este documento incorpora firma electrónica, y es copia auténtica de un documento electrónico archivado por la ULL según la Ley 39/2015.
Su autenticidad puede ser contrastada en la siguiente dirección https://sede.ull.es/validacion/

Identificador del documento: 2622200 Código de verificación: mbm0ekWs

Firmado por:	ROSHAN NUSHKIA CHAMBA *UNIVERSIDAD DE LA LAGUNA*	Fecha: 07/07/2020 13:28:26
	IGNACIO TRUJILLO CABRERA *UNIVERSIDAD DE LA LAGUNA*	07/07/2020 13:58:21
	Johan Hendrik Knapen Koelstra *UNIVERSIDAD DE LA LAGUNA*	07/07/2020 15:23:08
	María de las Maravillas Aguiar Aguilar *UNIVERSIDAD DE LA LAGUNA*	08/07/2020 15:55:11

Universidad de La Laguna
Oficina de Sede Electrónica
Entrada
Nº registro: 2020/46124
Nº reg. oficina: OF002/2020/45309
Fecha: 07/07/2020 15:26:22

values could perhaps better enclose the location of in-situ star formation. In this Chapter, a relatively low integrated transformation from gas into stars has preferably been adopted because it allows to be as inclusive as possible. In this regard, if anything, the new measure for the size of galaxies could lead to slightly larger sizes where the total conversion from gas to stars is higher than assumed here (see Appendix A.2). On the contrary, if this conversion to stars is even lower (as may well be the case for dwarf galaxies), the new measure of size will be biased towards smaller sizes (see Chapter 3; Chamba, Trujillo, & Knapen 2020). In Appendix A.3, the use of alternative proxies to locate the radial location of the gas density threshold for star formation is discussed.

In the previous paragraphs, we have motivated the use of the radial location of the stellar mass isocontour at $\Sigma_\star \sim 1\,M_\odot/\mathrm{pc}^2$ as an operative method to locate the gas density threshold for star formation and thus characterise a physical size for galaxies. This size measure should work particularly well for galaxies whose main growth channel is the transformation of gas into stars. What would be the plight of such a definition for spheroidal galaxies? Those galaxies are thought to form a significant fraction of their stars in an early-on intense starburst and later on add new stars (mostly to their periphery) through merging with other (satellite) galaxies. Most of this secondary growth is produced by dry minor mergers (see e.g. Trujillo et al. 2011). As a matter of fact, we will demonstrate that the proposed size definition is useful to separate the core of spheroidal galaxies (predominantly formed by an intense star formation burst) from the material that is later on accreted by minor merging. A discussion of the limits of the new size measure is given in Appendix A.4.

2.3 Imaging Data: the IAC Stripe82 Legacy Project

To estimate the location of the density threshold for star formation through the position of the $1\ M_\odot/\mathrm{pc}^2$ isomass contour, a survey with multi-wavelength colour information is necessary. As will be explained in Sect. 2.5, the stellar mass density profiles of the objects can be estimated using different combinations of optical bands. In this work, we used the deep IAC Stripe82 Legacy Project (hereafter IAC Stripe82) data set (Fliri & Trujillo 2016; Román & Trujillo 2018). This data set is a co-addition of the SDSS Stripe82 data (Frieman et al. 2008) with the goal of retaining the faintest surface brightness structures. The average seeing is 1 arcsec and the pixel scale is 0.396 arcsec. The total area of the survey is 275 square degrees. These images are freely available (`http://research.iac.es/proyecto/stripe82/`). In addition to the imaging data, the public release also includes photometric catalogues (Fliri & Trujillo 2018). The mean limiting surface brightness of the survey are $\mu_g = 29.1$, $\mu_r = 28.6$, and $\mu_i = 28.1$ mag arcsec^2 (equivalent to a 3σ fluctuation with respect to the background of the image in an area of 10×10 arcsec^2).

2.4 Target selection

Having introduced a new size definition based on the radial location of the gas density threshold for star formation, we will now explore its use across a galaxy mass range as large as possible and how it performs for different morphological types. This is relevant as the star formation history could be very different depending on the galaxy's characteristics. The cosmological volume

Este documento incorpora firma electrónica, y es copia auténtica de un documento electrónico archivado por la ULL según la Ley 39/2015.
Su autenticidad puede ser contrastada en la siguiente dirección https://sede.ull.es/validacion/

Identificador del documento: 2622200 Código de verificación: mbm0ekWs

Firmado por:	ROSHAN NUSHKIA CHAMBA *UNIVERSIDAD DE LA LAGUNA*	Fecha: 07/07/2020 13:28:26
	IGNACIO TRUJILLO CABRERA *UNIVERSIDAD DE LA LAGUNA*	07/07/2020 13:58:21
	Johan Hendrik Knapen Koelstra *UNIVERSIDAD DE LA LAGUNA*	07/07/2020 15:23:08
	María de las Maravillas Aguiar Aguilar *UNIVERSIDAD DE LA LAGUNA*	08/07/2020 15:55:11

Universidad de La Laguna
Oficina de Sede Electrónica
Entrada
Nº registro: 2020/46124
Nº reg. oficina: OF002/2020/45309
Fecha: 07/07/2020 15:26:22

covered by the Stripe82 data, together with its depth, thus allows a relatively large sample of galaxies with a wide range of stellar masses and morphologies to be collected.

In total, a sample of 1005 galaxies with $z < 0.09$ spanning five orders of magnitude in stellar mass ($10^7\,M_\odot < M_\star < 10^{12}\,M_\odot$) was selected for this work. This collection of galaxies extends from the dwarf galaxies regime up to giant spirals and ellipticals. All the galaxies with $M_\star > 10^9\,M_\odot$ were selected from the Nair & Abraham (2010) catalogue, which includes a detailed visual classification of about 14000 galaxies in the SDSS footprint. Only those galaxies listed in this catalogue that were within the Stripe82 area (i.e. 1010 objects) were selected. Unfortunately, the Nair & Abraham (2010) catalogue lacks objects with stellar masses below $10^9\ M_\odot$. For this reason, less massive galaxies ($10^7\,M_\odot < M_\star < 3 \times 10^9\,M_\odot$), were retrieved from the Maraston et al. (2013) catalogue. However, morphological information in unavailable. To have enough spatial resolution for the size analysis, only nearby dwarf galaxies are selected, i.e. with $0.002 < z < 0.018$. Within such a redshift range and the Stripe82 area, 323 galaxies from the Maraston et al. (2013) catalogue are obtained.

Of the total 1333 initially selected galaxies, 1005 were used for the final analysis, and 328 galaxies removed for multiple reasons. In some cases, the galaxies are located very close to a bright star or galaxy (152 objects), making the retrieval of their surface brightness profile unreliable. In other cases (103 objects) the galaxies are dramatically affected by dust contamination from Galactic cirri or several neighbouring objects that crowd the outskirts of the galaxy. 48 galaxies that have an axis ratio smaller than 0.3 were also removed (See 2.5.2). 22 galaxies for which the TType was classified as 'unknown' in the Nair & Abraham (2010) catalogue were discarded. And finally, 3 galaxies were removed as they appeared at the edge of the Stripe82 footprint and only part of the galaxy was visible in the images.

The sample of massive galaxies was separated into two morphological groups depending on the TType classification by Nair & Abraham (2010). Those galaxies with TType > -1 (in total 464 objects) were called "spiral galaxies" and contain morphologies from S0/a to Im, while those with TType < -1 (in total 279 objects) are dubbed "ellipticals" and contain the morphological classes E0 to S0+. After the cleaning process, the remaining "dwarfs" comprise 262 galaxies in the final sample. For completeness, in Table 2.2, the TType for dwarf galaxies is indicated as -99 (see Sect. 2.6).

2.5 Methodology

As explained in the Introduction, in this Chapter the stellar mass–size relation of galaxies is explored using a new size definition. This mass–size relation will also be compared with those resulting from the use of traditional size measurements such as the effective radius, the half-mass radius and the Holmberg and $\mu_i = 23.5$ mag/arcsec^2 isophotal radii. To estimate the structural parameters necessary for this analysis, number of steps need to be conducted. These are explained in the following subsections. For all galaxies, images in the g and r filters of 600 kpc × 600 kpc in size in the rest-frame of each galaxy and centred on the object of interest are created. The pipeline developed for this work is written using `Python v. 3.6.5`[1].

[1] `https://www.python.org/`

Este documento incorpora firma electrónica, y es copia auténtica de un documento electrónico archivado por la ULL según la Ley 39/2015.
Su autenticidad puede ser contrastada en la siguiente dirección https://sede.ull.es/validacion/

Identificador del documento: 2622200 Código de verificación: mbm0ekWs

Firmado por:	ROSHAN NUSHKIA CHAMBA *UNIVERSIDAD DE LA LAGUNA*	Fecha: 07/07/2020 13:28:26
	IGNACIO TRUJILLO CABRERA *UNIVERSIDAD DE LA LAGUNA*	07/07/2020 13:58:21
	Johan Hendrik Knapen Koelstra *UNIVERSIDAD DE LA LAGUNA*	07/07/2020 15:23:08
	María de las Maravillas Aguiar Aguilar *UNIVERSIDAD DE LA LAGUNA*	08/07/2020 15:55:11

Universidad de La Laguna
Oficina de Sede Electrónica
Entrada
Nº registro: 2020/46124
Nº reg. oficina: OF002/2020/45309
Fecha: 07/07/2020 15:26:22

2.5.1 Removal of scattered light from point sources and masking

The scattered light from bright stars was modelled and subtracted using the procedure of Trujillo & Fliri (2016). This is a key step that is necessary to explore low surface brightness features with confidence (see e.g. Uson et al. 1991; Slater et al. 2009). All stars brighter than 17 mag were identified using the G-band reported in the GAIA DR 1 catalogue (Gaia Collaboration 2016). To produce the scattered light field, the extended (radial size of ~ 8 arcmin) point spread function (PSF) models in all the SDSS bands created by Infante-Sainz et al. (2020) were used. The pipeline to remove the scattered light from point sources in the IAC Stripe82 fields will be fully described in a future publication and applied to the full IAC Stripe82 survey (N. Chamba et al. in prep.).

Once the scattered light is removed from the images, it is necessary to mask all remaining sources that affect the light distribution of the galaxy being explored. To conduct this task, a Python implementation of `MTOBjects` (Teeninga et al. 2016), a tree-based detection scheme which is robust against false positives, especially important for the identification of extended low signal-to-noise structures in deep imaging (C. Haigh et al. submitted), was used. For this work, the algorithm parameter `move_up = 0.3` and the α parameter for statistical testing was set to its default value.

2.5.2 The effect of inclination

The surface brightness of galaxies (particularly those following a disc–like configuration) is strongly affected by the inclination of the object. The larger the inclination of a galaxy, the brighter it appears to an observer as the number of stars along the line of sight increases. As the proposed size definition requires a proper estimation of the flux in the outer regions of galaxies, the brightness of galaxies by the effect of its inclination must be accounted for. This is not straightforward and has been investigated in-depth in multiple papers (see e.g. Holmberg 1958, 1975; Tully & Fouque 1985; Giovanelli et al. 1994). To estimate the correction needed, a 3D disc model assuming an exponential decline for the radial light distribution (de Vaucouleurs 1959b; Freeman 1970) and a sech^2 in the vertical z direction was created. This is expected for an isothermal population in a plane-parallel system (Spitzer 1942; Camm 1950). The luminosity distribution of the model is:

$$L(R,z) = L_0 \exp\left(\frac{-R}{h}\right) sech^2\left(\frac{z}{2z_0}\right) \tag{2.1}$$

where L_0 is the central luminosity density, h is the scale length and z_0 is the scale height. The model was created using `IMFIT` (we used the model `ExponentialDisk3D` with `n = 1`; Erwin 2015). Three different models with $z_0/h = 0.08$, 0.12 and 0.17 are probed. The ratio of these parameters covers the values measured for the thin disc of our own Milky Way and its uncertainties (Bland-Hawthorn & Gerhard 2016). This model is an idealised version of discs. Real discs are much more complex, containing clumps, dust, warps, etc. In addition, possible corrections due to internal dust has not been considered here. Therefore, any dependence of the model on wavelength is neglected (for a detailed analysis of this issue see Kourkchi et al. 2019).

Since the most important aspect for the size analysis in this work with respect to the effect of inclination is on the brightness of the intermediate-outer regions of galaxies, the difference in surface brightness ($\Delta\mu$) at a given inclination i ($\mu_{\rm inc}$) is compared to the face-on orientation

Este documento incorpora firma electrónica, y es copia auténtica de un documento electrónico archivado por la ULL según la Ley 39/2015.
Su autenticidad puede ser contrastada en la siguiente dirección https://sede.ull.es/validacion/

Identificador del documento: 2622200 Código de verificación: mbm0ekWs

Firmado por:	ROSHAN NUSHKIA CHAMBA *UNIVERSIDAD DE LA LAGUNA*	Fecha: 07/07/2020 13:28:26
	IGNACIO TRUJILLO CABRERA *UNIVERSIDAD DE LA LAGUNA*	07/07/2020 13:58:21
	Johan Hendrik Knapen Koelstra *UNIVERSIDAD DE LA LAGUNA*	07/07/2020 15:23:08
	María de las Maravillas Aguiar Aguilar *UNIVERSIDAD DE LA LAGUNA*	08/07/2020 15:55:11

Universidad de La Laguna
Oficina de Sede Electrónica
Entrada
Nº registro: 2020/46124
Nº reg. oficina: OF002/2020/45309
Fecha: 07/07/2020 15:26:22

($\mu_{\rm face-on}$) at a radial distance of $R = 5h$ (i.e. $\Delta\mu = \mu_{\rm face-on} - \mu_{\rm inc}$). The difference $\Delta\mu$ was estimated at all inclinations along the semi-major axis of the model galaxy (see Fig. 2.1).

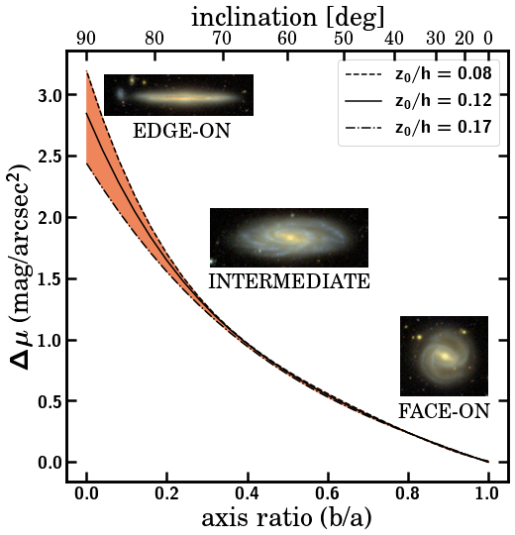

Figure 2.1: Difference in surface brightness $\Delta\mu = \mu_{\rm face-on} - \mu_{\rm inc}$ between the face-on orientation and a given inclination for a disc–like galaxy. The figure shows $\Delta\mu$ along the semi-major axis of a galaxy model at a radial distance $R = 5h$ and is explored for three different disc thicknesses (shown in the legend) parameterized using z_0/h.

Figure 2.1 shows that the difference in brightness $\Delta\mu$ produced by different disc thicknesses (as parameterized by z_0/h) is only noticeable at very large inclinations (i.e. $i > 70$ degrees). For this reason, any galaxy with an axis ratio smaller than 0.3 from the sample (Sec 2.4) was removed. To facilitate the reader with the application of this inclination correction, Table 2.1 lists the values of the coefficients of a polynomial fit to the different models shown in Fig. 2.1:

$$\Delta\mu = \sum_{j=0}^{4} \alpha_j (b/a)^j \tag{2.2}$$

with $b/a = \cos(i)$, the ratio of the semi-minor to the semi-major axis of the isophote used to measured the inclination of galaxies. The polynomial fit provided is very accurate, with an error in $\Delta\mu < 0.01$ mag. How this correction is applied to real data is explained in the next Section. In this work, the correction corresponding to the ratio $z_0/h = 0.12$ was used.

2.5.3 Stellar mass density profiles

After the removal of scattered light and masking the images, the surface brightness profiles of the galaxies in the g and r bands were used to obtain their stellar mass density profiles. The

Este documento incorpora firma electrónica, y es copia auténtica de un documento electrónico archivado por la ULL según la Ley 39/2015.
Su autenticidad puede ser contrastada en la siguiente dirección https://sede.ull.es/validacion/

Identificador del documento: 2622200 Código de verificación: mbm0ekWs

Firmado por:	ROSHAN NUSHKIA CHAMBA *UNIVERSIDAD DE LA LAGUNA*	Fecha: 07/07/2020 13:28:26
	IGNACIO TRUJILLO CABRERA *UNIVERSIDAD DE LA LAGUNA*	07/07/2020 13:58:21
	Johan Hendrik Knapen Koelstra *UNIVERSIDAD DE LA LAGUNA*	07/07/2020 15:23:08
	María de las Maravillas Aguiar Aguilar *UNIVERSIDAD DE LA LAGUNA*	08/07/2020 15:55:11

Universidad de La Laguna
Oficina de Sede Electrónica
Entrada
Nº registro: 2020/46124
Nº reg. oficina: OF002/2020/45309
Fecha: 07/07/2020 15:26:22

Table 2.1: Values of the polynomial coefficients to correct the surface brightness profiles of disc–like galaxies for the inclination effect.

z_0/h	α_0	α_1	α_2	α_3	α_4
0.08	3.195	-10.396	17.584	-16.033	5.657
0.12	2.845	-7.833	10.792	-8.482	2.679
0.17	2.440	-5.273	4.577	-1.932	0.185

Notes. The coefficients have been calculated for three different disc thicknesses which are parameterised by the ratio z_0/h. As the effect of inclination in the intermediate and outer regions of galaxies is what is relevant for this work, this correction has been estimated at a distance $R = 5h$ (see text for details).

surface brightness profiles are obtained using elliptical apertures with a fixed centre, axis ratio q and position angle (PA). As a first guess for the centre of the galaxies, the R.A. and Dec information provided by the SDSS catalogues were adopted.

To determine the axis ratio and PA, for each galaxy those pixels where the surface brightness is between 25 and 26 mag/arcsec^2 in the g-band were first selected. The spatial distribution of these pixels were then fit to an ellipse. The PA (in degrees) is the angle between the semi-major axis and the horizontal axis, measured in the counter clockwise direction from the horizontal axis. The fit parameters (centre, axis ratio and PA) of the ellipses were then visually checked to ensure the outermost parts of the galaxies were characterised properly. If not, they are corrected accordingly. Once fixed, surface brightness profiles of the galaxies are extracted by averaging their flux over annuli parameterised by the fit ellipse. These profiles are extracted up to a radial distance of 200 arcsec which is well beyond the visual extension of the galaxies in the sample. This is crucial in order to retrieve a sensible characterisation of the outer part of galaxies, particularly when the criterion adopted is based on the location of a low stellar mass density contour such as 1 $M_\odot/\mathrm{pc}^2$.

Another important effect that must be accounted for when obtaining surface brightness profiles is defining the level of the background. Although the IAC Stripe82 images used are background subtracted, in some occasions the subtraction was not precise enough to be a reliable representation of the (local) surrounding background value of the galaxies (i.e. a slight under- or overestimation). For this reason, to have the most accurate background subtraction as possible, a similar procedure to that developed by Pohlen & Trujillo (2006) was adopted. The radial distance up to which the profiles have been extracted (i.e. 200 arcsec) is about two times the location of the isophote at 26.5 mag/arcsec^2 (r-band) in the case of ellipticals and three times for the spiral and dwarf galaxies. This allows to determine the background brightness in regions very close to the galaxies by identifying the asymptotic value in the number of counts around the object. This value was fit, subtracted/added to the images and the profile were obtained once more.

We then correct the surface brightness profiles for Galactic extinction. The extinction corrections A_g and A_r are obtained from NED taking into account the location of each galaxy on the sky (`https://ned.ipac.caltech.edu/forms/calculator.html`). Following this, the effect of the inclination (see Sect. 2.5.2) is corrected for spiral and dwarf galaxies as follows. For

Este documento incorpora firma electrónica, y es copia auténtica de un documento electrónico archivado por la ULL según la Ley 39/2015.
Su autenticidad puede ser contrastada en la siguiente dirección https://sede.ull.es/validacion/

Identificador del documento: 2622200 Código de verificación: mbm0ekWs

Firmado por:	ROSHAN NUSHKIA CHAMBA *UNIVERSIDAD DE LA LAGUNA*	Fecha: 07/07/2020 13:28:26
	IGNACIO TRUJILLO CABRERA *UNIVERSIDAD DE LA LAGUNA*	07/07/2020 13:58:21
	Johan Hendrik Knapen Koelstra *UNIVERSIDAD DE LA LAGUNA*	07/07/2020 15:23:08
	María de las Maravillas Aguiar Aguilar *UNIVERSIDAD DE LA LAGUNA*	08/07/2020 15:55:11

Universidad de La Laguna
Oficina de Sede Electrónica
Entrada
Nº registro: 2020/46124
Nº reg. oficina: OF002/2020/45309
Fecha: 07/07/2020 15:26:22

each galaxy, their inclination based on the axis ratio determined previously was measured. The inclination correction, $\Delta\mu$, is then directly applied to the derived surface brightness profiles. The same inclination correction is applied for both g and r profiles, therefore the colour radial profile of galaxies remains unaffected. Due to limited photometric information, any correction for internal dust is not attempted here.

The final step is to obtain the stellar mass-to-light ratio (M/L) profile. Once the M/L is known, the following equation (see e.g. Bakos et al. 2008):

$$\log \Sigma_\star = \log(M/L)_\lambda - 0.4(\mu_\lambda - \mu_{\mathrm{abs},\odot,\lambda}) + 8.629 \tag{2.3}$$

where $\mu_{\mathrm{abs},\odot,\lambda}$ is the absolute magnitude of the Sun at wavelength λ, is used to obtain the stellar mass density (in $M_\odot/\mathrm{pc}^2$) as a function of the surface brightness.

The M/L is computed using the procedure described by Roediger & Courteau (2015). In particular, the parameters provided by these authors that correspond to the Bruzual & Charlot (2003, BC03) models and a Chabrier IMF (Chabrier 2003). As a basis for this estimation, the $g-r$ colour and the surface brightness in the g-band were used.

Despite the obvious advantage of decreasing the effect of galactic dust by using the i-band instead of the bluer g and r bands, the use of the latter filters to estimate the new size indicator is preferred for two main reasons. Firstly, the sky brightness in the i-band is around two magnitudes brighter than in the g-band (see e.g. Fig. 1 in Hall et al. 2012). This effect is not compensated by the brighter emission of the stellar populations towards the red (which is typically between $g-i=0.5$ to 1 mag for spiral galaxies). As a result, the redder SDSS bands are noisier at a given surface brightness because all the SDSS bands have the same integration time. Secondly, as the newly proposed size indicator is estimated through a colour combination, the effect of the PSF on the surface brightness profiles should not be very different from band to band. This applies for g and r, but in the case of the i-band, the SDSS PSF is significantly different for those in g and r, as can be seen in de Jong (2008, Figure 2) and Infante-Sainz et al. (2020, Figure 8).

2.5.4 Estimating the structural parameters of galaxies

Once the stellar mass density profiles of the galaxies are created, it is straightforward to obtain the total stellar mass and the location of R_1, the proxy for the location of the gas density threshold for star formation that is adopted as a measure of size in this work. This procedure has been performed for all the galaxies in the sample. Their mass density profiles were then integrated to get a homogeneous determination of their total stellar masses. The integration takes into account the axis ratio of the galaxy and therefore assumes an elliptical symmetry for the distribution of light, from the central position of the object up to the radial location provided by the 29 mag/arcsec^2 isophote (g-band). This estimate of the total stellar mass is a lower limit to the total mass of the object. However, the limiting isophote adopted here is extremely faint, therefore the amount of stellar mass beyond such an isophote is expected to be very low ($< 3\%$; Trujillo et al. 2001). This approach for estimating the total stellar mass is preferred instead of assuming a shape for the light distribution (i.e. exponential, de Vaucouleurs, etc) and extrapolating the stellar mass density profiles to infinity. In Appendix A.5, the method employed to determine stellar mass here is compared with that of the Portsmouth Spectro-Photometric Stellar Mass computation (Maraston et al. 2013) and the results show that both

Este documento incorpora firma electrónica, y es copia auténtica de un documento electrónico archivado por la ULL según la Ley 39/2015.
Su autenticidad puede ser contrastada en la siguiente dirección https://sede.ull.es/validacion/

Identificador del documento: 2622200 Código de verificación: mbm0ekWs

Firmado por:	ROSHAN NUSHKIA CHAMBA *UNIVERSIDAD DE LA LAGUNA*	Fecha: 07/07/2020 13:28:26
	IGNACIO TRUJILLO CABRERA *UNIVERSIDAD DE LA LAGUNA*	07/07/2020 13:58:21
	Johan Hendrik Knapen Koelstra *UNIVERSIDAD DE LA LAGUNA*	07/07/2020 15:23:08
	María de las Maravillas Aguiar Aguilar *UNIVERSIDAD DE LA LAGUNA*	08/07/2020 15:55:11

Universidad de La Laguna
Oficina de Sede Electrónica
Entrada
Nº registro: 2020/46124
Nº reg. oficina: OF002/2020/45309
Fecha: 07/07/2020 15:26:22

mass determinations are similar. Finally, the location of R_1 is directly ascertained using the stellar mass density profiles. Estimates of the half-mass radii are done using the cumulative mass density profiles.

The effective radii of galaxies are determined from the g-band images (our deepest data).[2]. The growth curve in g was used to obtain the radial location within which half of the total light of the galaxy is contained. Similar to the determination of total stellar mass, the total light of the galaxy is measured as the light enclosed by the observed 29 mag/arcsec^2 isophote (g-band). By definition, $R_{\rm e}$ is not affected by Galactic extinction nor the inclination correction of the profiles except indirectly for the location of the 29 mag/arcsec^2 isophote (g-band). Additionally, the Holmberg Radius ($R_{\rm H}$) is measured for all galaxies in the sample. Lacking the B-band in the survey, the location of the observed isophote at $\mu_g = 26$ mag/arcsec^2 was considered as a proxy for $R_{\rm H}$. Using the i-band profiles, the radial location of the isophote corresponding to 23.5 mag/arcsec^2 (i.e. $R_{23.5,{\rm i}}$) was also determined. Both isophotal sizes were estimated after correcting the profiles for Galactic extinction and cosmological dimming. All these structural parameters for the galaxies in the sample are provided in Table 2.2.

2.6 Results

Figure 2.2 shows a few representative galaxies in the sample to illustrate the difference between the location of their R_1 and $R_{\rm e}$ contours. The size based on the location of the gas density threshold for star formation much better represents the intuitive concept of the size of galaxies, such as its edge or boundary compared to $R_{\rm e}$. Expanding on this point, Fig. 2.3 shows the location of R_1 and $R_{\rm e}$ for two galaxies with clear signatures of on-going stellar accretion. In these examples, the location of R_1 may serve as a marker to separate the stellar material which is in the form of streams (formed *ex-situ*) from those stars which are located in the bulk (*in-situ*) of the main galaxy. An in-depth analysis of the use of R_1 (and its variants) for this purpose will be presented in a future publication (N. Chamba et al. in prep).

2.6.1 The properties of the R_1–mass relation

The main result of this Chapter is shown in Fig. 2.4: the mass–size relation spanning over five orders of magnitude in stellar mass (10^7–10^{12} $M_\odot$). The figure illustrates how the mass–size relation changes when using R_1 instead of $R_{\rm e}$ as a size measurement of galaxies. To extract both the slope and dispersion of the relations, a Huber Regressor (Huber 1964), which is a linear regression model that is robust to outliers, was implemented. A number of enlightening results are as follows:

- R_1 is a factor of 5 to 10 larger than $R_{\rm e}$ in all galaxies.
- The observed scatter of the stellar mass–size relation is significantly lower by a factor of ~ 2 (from $\sigma_{R_{\rm e}} \sim 0.17$ dex to $\sigma_{R_1} \sim 0.09$ dex) compared to the scatter using $R_{\rm e}$ as a size indicator. As we will show in the next section, once the observational and methodological

[2]To check the robustness of the estimation of $R_{\rm e}$ using the g-band, the same quantity using the i-band is also estimated. Indeed, a very tight correlation between both effective radii (Pearson correlation coefficient r = 0.996) is found. As expected, $R_{e,g}$ is slightly larger than $R_{e,i}$: $R_{e,g}/R_{e,i} = 1.030 \pm 0.002$, with a dispersion of 0.083. Both effective radii are thus very similar.

Este documento incorpora firma electrónica, y es copia auténtica de un documento electrónico archivado por la ULL según la Ley 39/2015.
Su autenticidad puede ser contrastada en la siguiente dirección https://sede.ull.es/validacion/

Identificador del documento: 2622200 Código de verificación: mbm0ekWs

Firmado por:	ROSHAN NUSHKIA CHAMBA *UNIVERSIDAD DE LA LAGUNA*	Fecha: 07/07/2020 13:28:26
	IGNACIO TRUJILLO CABRERA *UNIVERSIDAD DE LA LAGUNA*	07/07/2020 13:58:21
	Johan Hendrik Knapen Koelstra *UNIVERSIDAD DE LA LAGUNA*	07/07/2020 15:23:08
	María de las Maravillas Aguiar Aguilar *UNIVERSIDAD DE LA LAGUNA*	08/07/2020 15:55:11

Universidad de La Laguna
Oficina de Sede Electrónica
Entrada
Nº registro: 2020/46124
Nº reg. oficina: OF002/2020/45309
Fecha: 07/07/2020 15:26:22

Table 2.2: Characteristics of the galaxies used in this work.

JID	R.A. (deg)	Dec (deg)	q	PA (deg)	A_g (mag)	A_r (mag)	A_i (mag)	z	TT	R_e (kpc)	$R_{e,M_\star}$ (kpc)	$R_{23.5,i}$ (kpc)	R_H (kpc)	R_1 (kpc)	Log $\left[\frac{M_\star}{M_\odot}\right]$
J010301.72-010639.46	15.75723	-1.11113	0.88	95.0	0.134	0.093	0.069	0.0175	-2	2.45	3.67	7.94	11.67	18.56	10.38
J005753.69-004852.90	14.47382	-0.81479	0.96	120.0	0.094	0.065	0.048	0.0419	-2	2.78	4.47	12.41	17.27	25.08	11.03
J000150.32+010155.24	0.45973	1.03172	0.49	179.0	0.085	0.059	0.044	0.0862	-5	24.99	29.13	46.05	71.98	148.12	11.82
J003934.82+005135.83	9.89529	0.85979	0.71	61.0	0.066	0.046	0.034	0.0146	5	8.64	7.70	16.39	20.87	23.01	10.37
J012223.77-005230.73	20.59913	-0.87523	0.44	42.0	0.169	0.117	0.087	0.0271	4	16.17	9.65	32.27	44.35	44.04	10.96
J021219.69-004841.46	33.08210	-0.81153	0.89	37.0	0.097	0.067	0.050	0.0408	0	9.18	5.90	23.68	32.61	37.17	11.24
J021808.12+004529.8	34.53385	0.75830	0.64	133.0	0.130	0.090	0.067	0.0092	-99	1.00	1.49	1.79	2.86	2.97	8.05
J233646.86+003724.2	354.19526	0.62341	0.86	88.0	0.113	0.078	0.058	0.0088	-99	2.13	2.38	2.58	4.44	5.44	8.65
J010607.19+004633.5	16.52997	0.77599	0.84	48.0	0.084	0.058	0.043	0.0174	-99	5.43	5.21	4.14	10.87	10.91	9.10
J235618.80-001820.17	359.07860	-0.30583	0.71	99.0	0.124	0.086	0.064	0.0241	-3	4.11	5.08	16.70	26.56	48.39	11.15
J024331.30+001824.49	40.88040	0.30676	0.36	108.0	0.124	0.086	0.064	0.0267	3	8.82	5.72	22.89	30.75	29.43	10.57

Notes. Unless explicitly stated otherwise, the quantities provided in this table have been derived in this work. This table includes the name of the galaxies (Abolfathi et al. 2018), their spatial location (Abolfathi et al. 2018), their axis ratio (q) and the position angle of the ellipses (PA) used to extract the surface brightness profiles (measured counter-clockwise starting from the horizontal axis), Galactic extinctions in the g, r and i bands (from NED), spectroscopic redshift (z) (Abolfathi et al. 2018), morphological type (Nair & Abraham 2010, TType = -99 corresponds to dwarf galaxies), effective radius R_e (measured in the g-band), the half-mass radius ($R_{e,M_\star}$), the radius corresponding to the location of the isophote with $\mu_i = 23.5$ mag/arcsec^2 (i.e. $R_{23.5,i}$), the Holmberg Radius (R_H), the radial location R_1 of the isomass contour at 1 $M_\odot$ pc $^{-2}$ and the stellar mass of galaxies (assuming a Chabrier IMF). The quantities are given showing only the significant figures up to which the values can be regarded reliable. The table shows those galaxies in Fig. 2.2 and 2.3, in order of appearance. The complete table is available in the online version of Trujillo, Chamba, & Knapen (2020).

Este documento incorpora firma electrónica, y es copia auténtica de un documento electrónico archivado por la ULL según la Ley 39/2015.
Su autenticidad puede ser contrastada en la siguiente dirección https://sede.ull.es/validacion/

Identificador del documento: 2622200 Código de verificación: mbm0ekWs

Firmado por: ROSHAN NUSHKIA CHAMBA — Fecha: 07/07/2020 13:28:26
UNIVERSIDAD DE LA LAGUNA

IGNACIO TRUJILLO CABRERA — 07/07/2020 13:58:21
UNIVERSIDAD DE LA LAGUNA

Johan Hendrik Knapen Koelstra — 07/07/2020 15:23:08
UNIVERSIDAD DE LA LAGUNA

María de las Maravillas Aguiar Aguilar — 08/07/2020 15:55:11
UNIVERSIDAD DE LA LAGUNA

Universidad de La Laguna
Oficina de Sede Electrónica
Entrada
Nº registro: 2020/46124
Nº reg. oficina: OF002/2020/45309
Fecha: 07/07/2020 15:26:22

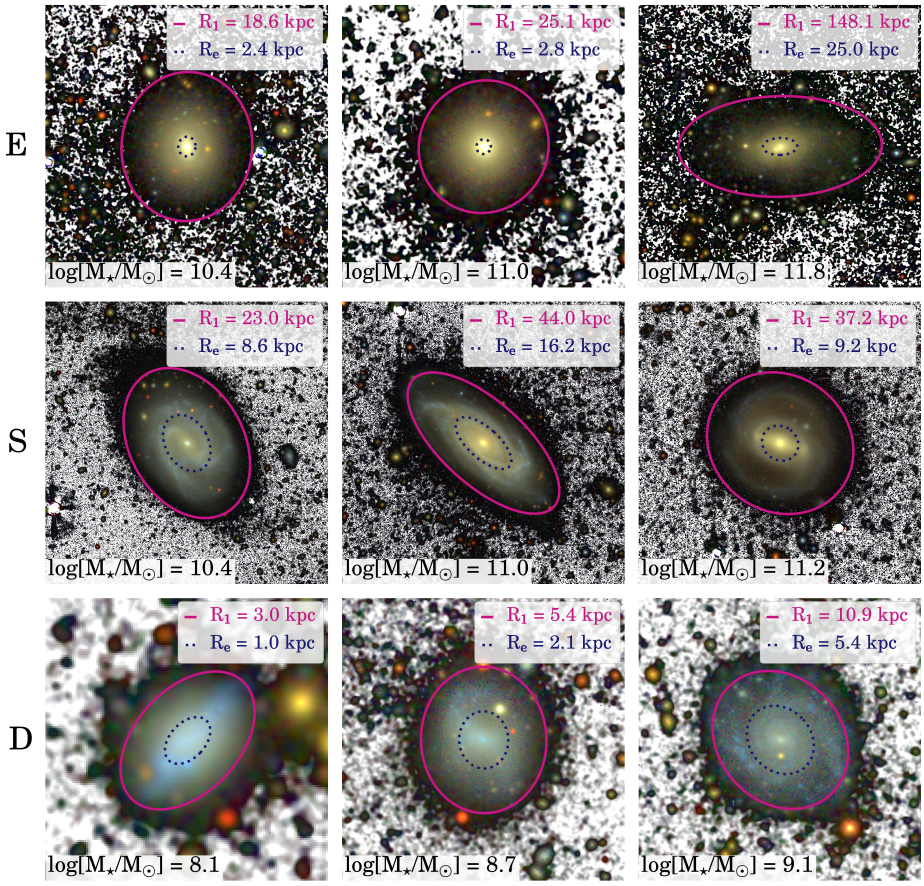

Figure 2.2: Collection of galaxy images showing the location of their R_e and R_1, the isomass contour at 1 $M_\odot/pc^2$. The top row shows galaxies which have been classified as ellipticals (E0–S0+), the middle row shows spiral (S0/a–Sm) galaxies, and the lower row shows dwarf galaxies. The galaxies are displayed with increasing stellar mass from left to right. This figure clearly illustrates how the proxy for the gas density threshold for star formation (R_1) nicely encloses the bulk of the stellar mass of galaxies. The coloured regions of the images are the IAC Stripe82 g, r and i band composite, while the black and white background is the sum of the 3 bands. The background level of these images is ~ 29.1 mag/arcsec^2 (3σ 10×10 arcsec^2; r-band). Table 2.2 lists details of the galaxies shown.

Este documento incorpora firma electrónica, y es copia auténtica de un documento electrónico archivado por la ULL según la Ley 39/2015.
Su autenticidad puede ser contrastada en la siguiente dirección https://sede.ull.es/validacion/

Identificador del documento: 2622200 Código de verificación: mbm0ekWs

Firmado por:	ROSHAN NUSHKIA CHAMBA *UNIVERSIDAD DE LA LAGUNA*	Fecha: 07/07/2020 13:28:26
	IGNACIO TRUJILLO CABRERA *UNIVERSIDAD DE LA LAGUNA*	07/07/2020 13:58:21
	Johan Hendrik Knapen Koelstra *UNIVERSIDAD DE LA LAGUNA*	07/07/2020 15:23:08
	María de las Maravillas Aguiar Aguilar *UNIVERSIDAD DE LA LAGUNA*	08/07/2020 15:55:11

Universidad de La Laguna
Oficina de Sede Electrónica
Entrada
Nº registro: 2020/46124
Nº reg. oficina: OF002/2020/45309
Fecha: 07/07/2020 15:26:22

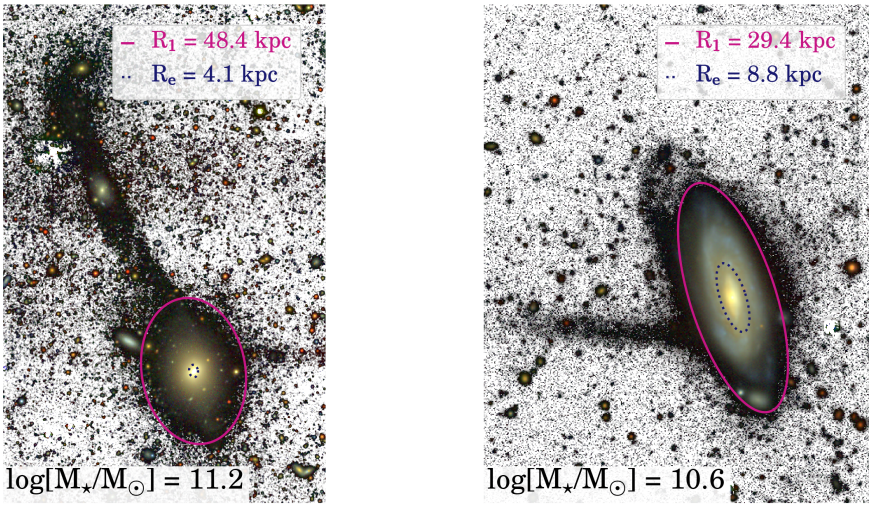

Figure 2.3: Separating *in-situ* star formation from *ex-situ* stellar accretion using R_1, the size measure adopted in this work. The two images show how the isomass contour at 1 $M_\odot/\mathrm{pc}^2$ (i.e. R_1 or the proxy for the location of the gas density threshold for star formation) nicely divides the structure of galaxies into two different parts: the inner region where the bulk of the stars is contained and where *in-situ* star formation is or has been taking place and the external region where streams of on-going accretion are clearly visible. The left panel shows a massive elliptical and the right panel corresponds to a spiral galaxy with similar stellar mass to the Milky Way. More extensive analysis is to be published in N. Chamba et al. in prep. See Table 2.2 for details on the galaxies shown.

uncertainties are accounted for, the scatter of the stellar mass–size relation drops even more to a tiny 0.06 dex (i.e. a factor of ~ 2.5 smaller than the intrinsic scatter using R_e). The observed global scatter of the R_1–mass relation is also lower than the observed one found using other popular size estimators ($\sigma_{R_{e,M_\star}} \sim 0.12$ dex, $\sigma_{R_H} \sim 0.11$ dex and $\sigma_{R_{23.5,i}} \sim 0.11$ dex; see Table 2.3).

- The average 2D stellar density (as measured within R_1) changes from $\sim 10\,M_\odot/\mathrm{pc}^2$ for the less massive galaxies to $\sim 100\,M_\odot/\mathrm{pc}^2$ for the most massive spiral galaxies. Above $10^{11}\,M_\odot$, the average 2D stellar density of the galaxies decreases again.

- From 10^7 to $10^{11}\,M_\odot$ all galaxies are located on the same mass–size relation following a power law, $R_1 \propto M_\star^\beta$, with $\beta = 0.35 \pm 0.01$. This value is compatible with the one found by Hall et al. (2012) who compared the disc scale lengths of spiral galaxies with their luminosities and found $\beta = 0.377 \pm 0.007$. Interestingly, $\beta \sim 1/3$ would correspond to almost the same 3D stellar mass density ($\sim 4.5 \times 10^{-3}\,M_\odot/\mathrm{pc}^3$) if all the stars were

Este documento incorpora firma electrónica, y es copia auténtica de un documento electrónico archivado por la ULL según la Ley 39/2015.
Su autenticidad puede ser contrastada en la siguiente dirección https://sede.ull.es/validacion/

Identificador del documento: 2622200 Código de verificación: mbm0ekWs

Firmado por:	ROSHAN NUSHKIA CHAMBA *UNIVERSIDAD DE LA LAGUNA*	Fecha: 07/07/2020 13:28:26
	IGNACIO TRUJILLO CABRERA *UNIVERSIDAD DE LA LAGUNA*	07/07/2020 13:58:21
	Johan Hendrik Knapen Koelstra *UNIVERSIDAD DE LA LAGUNA*	07/07/2020 15:23:08
	María de las Maravillas Aguiar Aguilar *UNIVERSIDAD DE LA LAGUNA*	08/07/2020 15:55:11

Universidad de La Laguna
Oficina de Sede Electrónica
Entrada
Nº registro: 2020/46124
Nº reg. oficina: OF002/2020/45309
Fecha: 07/07/2020 15:26:22

distributed in a sphere of radius R_1.

- Above 10^{11} $M_\odot$, the slope of the relation rises to $\beta = 0.58 \pm 0.02$. This likely indicates that the most massive galaxies have formed or gained their stars very differently compared to galaxies with lower masses.

Table 2.3 shows the best-fit parameters to a power law of the form $R \propto M_\star^\beta$ using all the galaxies in the size–stellar mass relation as well as separate fits using each subsample (i.e. dwarfs, S0/a—Sm and E0–S0+). This analysis was performed using the new size indicator R_1 as well as other popular size indicators: R_e, $R_{\mathrm{e,M}_\star}$, R_H and $R_{23.5,\mathrm{i}}$. The uncertainties in the best fit slope (β) and dispersion of the observed relations ($\sigma_{\mathrm{R_{obs}}}$) are computed using a simple bootstrap method. One third of the measured points on the relation were randomly selected and fit at each iteration, for 1000 iterations. The spread in the distribution of the fits from this exercise is what is reported as the uncertainty in β and σ. As mentioned above, the observed global scatter of the R_1–mass relation is significantly smaller than the one observed using R_e and lower than the observed scatter with all other size estimators, i.e. $R_{\mathrm{e,M}_\star}$, R_H and $R_{23.5,\mathrm{i}}$. The values of the scatter in the size–mass relations are, however, affected by uncertainties in estimating the stellar mass and the background around the galaxies. To quantify how these uncertainties affect the observed scatter of the different relations and therefore compare the intrinsic scatter of the relation using R_1 with the other size indicators, a number of tests were conducted. These are described in the next subsection.

2.6.2 The intrinsic scatter of the R_1–mass relation

There are two main sources of uncertainty which affect the observed scatter in the size–mass relations. The first is the accuracy in measuring the background level around the galaxies. For some galaxies (particularly the massive ellipticals or those with red stellar populations) the surface brightness at which R_1 is measured is very faint ($\mu_g \sim 28\,\mathrm{mag/arcsec^2}$) and therefore, a slight under- or over- subtraction of the background would bend the surface brightness profiles of these objects and move the location of R_1. To quantify how this can affect the position of R_1 and the rest of the size indicators, all observed surface brightness profiles were randomly subtracted/added by a number of counts compatible with the uncertainty in the background level around each galaxy. This variation of the background allows to measure the variation in size for each galaxy which can then be used to estimate its contribution to the total observed dispersion in the size–mass plane. This contribution ($\sigma_{\mathrm{R_{back}}}$) is shown in Table 2.3. The background determination affects the size determination for massive ellipticals more than for spirals and/or small dwarfs. This is because the latter are mainly star-forming objects and therefore the surface brightness at which R_1 is located is brighter ($\mu_g \sim 26$–27 mag/arcsec^2). This explanation also applies for the isophotal sizes R_H and $R_{23.5,\mathrm{i}}$. However, for R_e and $R_{\mathrm{e,M}_\star}$, the scatter due to the background correction is negligible.

The other significant source of scatter in the size–mass plane is the uncertainty in measuring the total stellar mass of galaxies from the integrated stellar mass density profile of the objects. As explained in Sect. 2.5.4, the total stellar mass is measured by integrating the stellar mass density profile. To quantify how the uncertainty in the total stellar mass affects these results, the following uncertainties in measuring the stellar mass have been assumed: $\delta_{mass} = 0.24 \pm 0.01$ dex (for the entire sample), $\delta_{mass} = 0.19 \pm 0.01$ dex (for the E0–S0+ subsample), $\delta_{mass} = 0.24 \pm$

Este documento incorpora firma electrónica, y es copia auténtica de un documento electrónico archivado por la ULL según la Ley 39/2015.
Su autenticidad puede ser contrastada en la siguiente dirección https://sede.ull.es/validacion/

Identificador del documento: 2622200 Código de verificación: mbm0ekWs

Firmado por:	ROSHAN NUSHKIA CHAMBA *UNIVERSIDAD DE LA LAGUNA*	Fecha: 07/07/2020 13:28:26
	IGNACIO TRUJILLO CABRERA *UNIVERSIDAD DE LA LAGUNA*	07/07/2020 13:58:21
	Johan Hendrik Knapen Koelstra *UNIVERSIDAD DE LA LAGUNA*	07/07/2020 15:23:08
	María de las Maravillas Aguiar Aguilar *UNIVERSIDAD DE LA LAGUNA*	08/07/2020 15:55:11

Universidad de La Laguna
Oficina de Sede Electrónica
Entrada
Nº registro: 2020/46124
Nº reg. oficina: OF002/2020/45309
Fecha: 07/07/2020 15:26:22

Table 2.3: Best fit power law slope β and the observed dispersion of different size–mass relations.

Galaxy Type	β	$\sigma_{R_{obs}}$	r	$\sigma_{R_{back}}$	$\sigma_{R_{mass}}$	$\sigma_{R_{int}}$
			$R_{\rm i}$–stellar mass			
All	0.365 ± 0.005	0.089 ± 0.005	0.971	0.045 ± 0.003	0.047 ± 0.003	0.061 ± 0.005
E0–S0+	0.580 ± 0.022	0.090 ± 0.006	0.936	0.060 ± 0.004	0.054 ± 0.004	0.040 ± 0.006
S0/a–Sm	0.332 ± 0.014	0.089 ± 0.005	0.881	0.045 ± 0.003	0.035 ± 0.002	0.068 ± 0.005
Dwarfs	0.362 ± 0.016	0.088 ± 0.006	0.931	0.020 ± 0.003	0.056 ± 0.006	0.065 ± 0.006
			$R_{\rm e}$–stellar mass			
All	0.247 ± 0.011	0.168 ± 0.009	0.811	$\sim$0.001	0.067 ± 0.005	0.154 ± 0.009
E0–S0+	0.553 ± 0.032	0.108 ± 0.009	0.894	$\sim$0.001	0.092 ± 0.006	0.057 ± 0.009
S0/a–Sm	0.225 ± 0.026	0.162 ± 0.009	0.556	$\sim$0.001	0.047 ± 0.002	0.155 ± 0.009
Dwarfs	0.283 ± 0.040	0.221 ± 0.012	0.621	$\sim$0.001	0.064 ± 0.004	0.212 ± 0.012
			$R_{\rm e,M_\star}$–stellar mass			
All	0.204 ± 0.006	0.117 ± 0.008	0.854	$\sim$0.001	0.052 ± 0.003	0.105 ± 0.008
E0–S0+	0.509 ± 0.021	0.086 ± 0.007	0.918	$\sim$0.001	0.075 ± 0.006	0.042 ± 0.007
S0/a–Sm	0.196 ± 0.022	0.120 ± 0.009	0.595	$\sim$0.001	0.040 ± 0.002	0.113 ± 0.009
Dwarfs	0.175 ± 0.027	0.139 ± 0.008	0.638	$\sim$0.001	0.038 ± 0.003	0.134 ± 0.008
			$R_{\rm H}$–stellar mass			
All	0.304 ± 0.007	0.109 ± 0.005	0.940	0..003 $\pm$ 0.001	0.056 ± 0.004	0.094 ± 0.005
E0–S0+	0.478 ± 0.017	0.065 ± 0.005	0.950	0.004 ± 0.001	0.026 ± 0.003	0.059 ± 0.005
S0/a–Sm	0.266 ± 0.014	0.105 ± 0.005	0.783	0.003 ± 0.001	0.035 ± 0.004	0.099 ± 0.005
Dwarfs	0.307 ± 0.028	0.148 ± 0.008	0.790	0.002 ± 0.001	0.095 ± 0.014	0.113 ± 0.008
			$R_{23.5,\rm i}$–stellar mass			
All	0.330 ± 0.006	0.106 ± 0.006	0.944	0.002 ± 0.001	0.062 ± 0.005	0.086 ± 0.005
E0–S0+	0.443 ± 0.013	0.056 ± 0.005	0.956	0.002 ± 0.001	0.021 ± 0.002	0.052 ± 0.005
S0/a–Sm	0.285 ± 0.016	0.104 ± 0.006	0.804	0.003 ± 0.001	0.052 ± 0.005	0.090 ± 0.006
Dwarfs	0.354 ± 0.026	0.143 ± 0.010	0.836	0.001 ± 0.001	0.097 ± 0.012	0.105 ± 0.010

Notes. The values for the entire sample as well as for the different families of galaxies are provided. The third column corresponds to the Pearson r correlation coefficient. The contribution to the observed scatter produced by the uncertainty in the background of the images ($\sigma_{R_{back}}$) and in stellar mass estimation ($\sigma_{R_{mass}}$) are also computed. The last column shows the intrinsic scatter of the size–mass relation ($\sigma_{R_{int}}$) after accounting for the uncertainty in the background and the stellar mass of the objects.

Este documento incorpora firma electrónica, y es copia auténtica de un documento electrónico archivado por la ULL según la Ley 39/2015.
Su autenticidad puede ser contrastada en la siguiente dirección https://sede.ull.es/validacion/

Identificador del documento: 2622200 Código de verificación: mbm0ekWs

Firmado por: ROSHAN NUSHKIA CHAMBA — Fecha: 07/07/2020 13:28:26
UNIVERSIDAD DE LA LAGUNA

IGNACIO TRUJILLO CABRERA — 07/07/2020 13:58:21
UNIVERSIDAD DE LA LAGUNA

Johan Hendrik Knapen Koelstra — 07/07/2020 15:23:08
UNIVERSIDAD DE LA LAGUNA

María de las Maravillas Aguiar Aguilar — 08/07/2020 15:55:11
UNIVERSIDAD DE LA LAGUNA

Universidad de La Laguna
Oficina de Sede Electrónica
Entrada
Nº registro: 2020/46124
Nº reg. oficina: OF002/2020/45309
Fecha: 07/07/2020 15:26:22

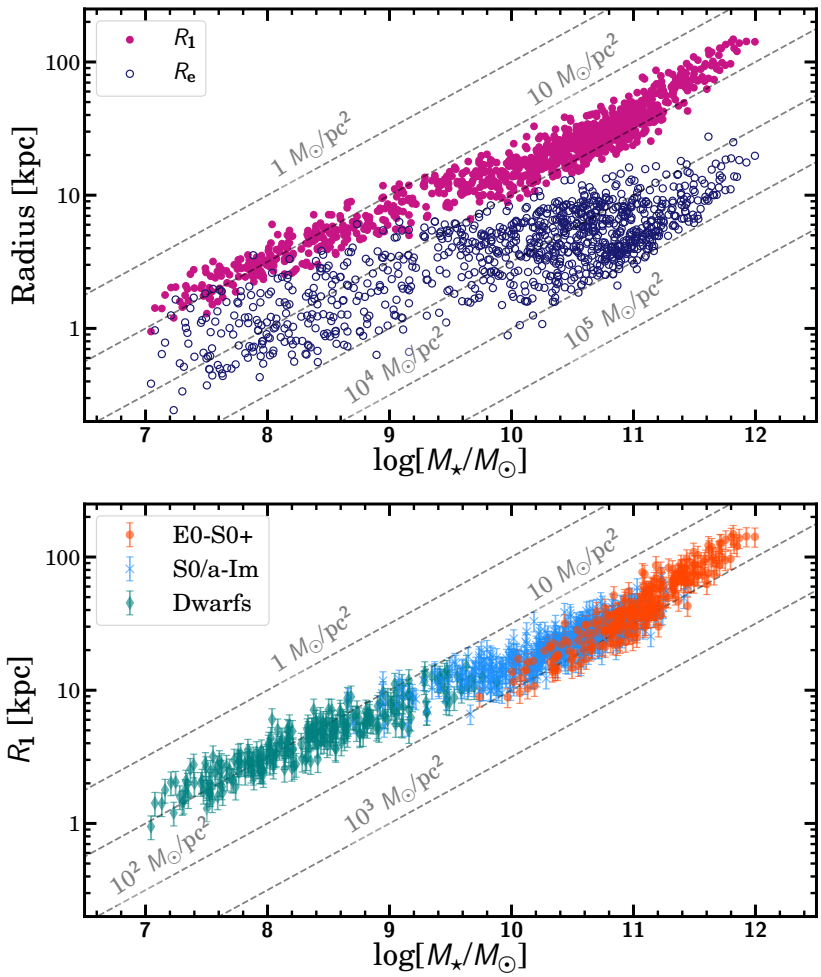

Figure 2.4: Stellar mass–size relation for the galaxy sample used in this work. Upper panel: The observed R_1–mass and R_e–mass relations, where R_e has been measured using the g-band. The scatter of the relation using R_1 is significantly smaller compared to that with R_e. Lower panel: The same R_1–mass relation after splitting the sample into three categories: ellipticals (E0–S0+), spirals (S0/a–Sm) and dwarfs as labelled in the legend. Spiral and dwarf galaxies follow the same trend, while massive ellipticals with $M_\star > 10^{11}\,M_\odot$ show a tilt with respect to less massive galaxies. The grey dashed lines correspond to locations in the plane with constant (projected) stellar mass density.

Este documento incorpora firma electrónica, y es copia auténtica de un documento electrónico archivado por la ULL según la Ley 39/2015.
Su autenticidad puede ser contrastada en la siguiente dirección https://sede.ull.es/validacion/

Identificador del documento: 2622200 Código de verificación: mbm0ekWs

Firmado por:	ROSHAN NUSHKIA CHAMBA *UNIVERSIDAD DE LA LAGUNA*	Fecha: 07/07/2020 13:28:26
	IGNACIO TRUJILLO CABRERA *UNIVERSIDAD DE LA LAGUNA*	07/07/2020 13:58:21
	Johan Hendrik Knapen Koelstra *UNIVERSIDAD DE LA LAGUNA*	07/07/2020 15:23:08
	María de las Maravillas Aguiar Aguilar *UNIVERSIDAD DE LA LAGUNA*	08/07/2020 15:55:11

Universidad de La Laguna
Oficina de Sede Electrónica
Entrada
Nº registro: 2020/46124
Nº reg. oficina: OF002/2020/45309
Fecha: 07/07/2020 15:26:22

0.01 dex (for the S0/a–Sm subsample) and $\delta_{mass} = 0.25 \pm 0.03$ dex (for the Dwarfs subsample). These values were computed by an analysis of the differences between the Portsmouth stellar masses (Maraston et al. 2013) and those measured here using the $g-r$ colour profile (Roediger & Courteau 2015, see Appendix A.5 for further details) for the same galaxies. To model the effect of the mass uncertainty ($\sigma_{\mathrm{R_{mass}}}$) on the scatter of the scaling relationship, all the observed stellar mass profiles were either scaled up or down in mass to place the galaxies on the best fit line through the observed stellar mass plane. This has been performed self-consistently, i.e. taking into account the change in the location of R_1 due to the scaling of the profile. Once all the galaxies are located exactly on top of the best-fit stellar mass–size relation (i.e. with zero scatter), the stellar mass density profiles are randomly scaled up or down again, this time by a quantity compatible with a Gaussian distribution whose standard deviation is given by the above δ_{mass} values. This procedure was repeated 1000 times and on each occasion the scatter of the stellar mass–size plane produced by the uncertainty in measuring the stellar mass is measured. Figure A.6 illustrates the scatter in the stellar mass–size relation caused by the uncertainty in stellar mass. The scatter in the stellar mass–size plane generated by the uncertainty in mass is shown in Table 2.3. Interestingly, for R_1, R_{H} and $R_{23.5,\mathrm{i}}$, the dwarf galaxies are the most affected by the uncertainty in mass determination. This is once again expected as the star formation activity of dwarf galaxies is, on average, more stochastic (Kauffmann 2014) and complicated to model than that of massive spirals and ellipticals. Therefore, a single colour is not a good proxy for the M/L ratio of dwarfs as it is in the case for more gentle star formation histories.

Once the scatter produced by both the uncertainty in the background and the stellar mass determination have been characterised, the intrinsic scatter of the stellar mass–size relations can be calculated. To do this, the two scatters generated by the background level and stellar mass uncertainty have been removed in quadrature from the observed scatter. Obviously, the exact intrinsic scatter of the mass–size relation is difficult to measure as there is some ambiguity in choosing the uncertainty in stellar mass. In this work, the above uncertainty values in stellar mass resulting from the comparison between the Portsmouth stellar masses (Maraston et al. 2013) and the ones retrieved using the *g-r* colour (Roediger & Courteau 2015) have been adopted. Indeed, the intrinsic scatter values are only an approximation, however, as a crude evaluation, the intrinsic scatter of the R_1–mass relation is about a factor of 1.5 smaller than the observed one (i.e. ~ 0.06 dex). This implies that the intrinsic stellar mass–R_1 relation is, indeed, very tight. In future work, this issue can be addressed in much more detail as a result of deeper data and therefore a decrease in the uncertainty in measuring the image background level. In addition, an analysis of the stellar mass–R_1 relation using 3.6μm images from Spitzer is ongoing (S. Díaz-García et al, in prep.), where the uncertainty in measuring the stellar mass should be smaller. This is primarily because in the S^{4}G survey (Sheth et al. 2010), the 3.6μm images have been corrected by the contamination from young stars (Querejeta et al. 2015) and the depth is enough to reach 1 $M_{\odot}/\mathrm{pc}^2$ (Muñoz-Mateos et al. 2015).

Finally, it is worth mentioning how the intrinsic scatter of the new mass–size relation compares with the intrinsic scatter of the other popular size–mass relations. In the case of R_{e} and $R_{\mathrm{e,M_\star}}$, the uncertainty produced by an incorrect background determination is almost negligible. For these cases, $\sigma_{R_{back}} \sim 0.001$ dex. This is because the IAC Stripe82 images are very deep and therefore the effect of the uncertainty in background estimation on the surface brightness profiles barely affects the location of R_{e} and $R_{\mathrm{e,M_\star}}$ which are found at relatively high surface brightness values. Therefore, a large contribution to the observed scatter of these size–mass relations from

Este documento incorpora firma electrónica, y es copia auténtica de un documento electrónico archivado por la ULL según la Ley 39/2015.
Su autenticidad puede ser contrastada en la siguiente dirección https://sede.ull.es/validacion/

Identificador del documento: 2622200 Código de verificación: mbm0ekWs

Firmado por:	ROSHAN NUSHKIA CHAMBA *UNIVERSIDAD DE LA LAGUNA*	Fecha: 07/07/2020 13:28:26
	IGNACIO TRUJILLO CABRERA *UNIVERSIDAD DE LA LAGUNA*	07/07/2020 13:58:21
	Johan Hendrik Knapen Koelstra *UNIVERSIDAD DE LA LAGUNA*	07/07/2020 15:23:08
	María de las Maravillas Aguiar Aguilar *UNIVERSIDAD DE LA LAGUNA*	08/07/2020 15:55:11

Universidad de La Laguna
Oficina de Sede Electrónica
Entrada
Nº registro: 2020/46124
Nº reg. oficina: OF002/2020/45309
Fecha: 07/07/2020 15:26:22

incorrect background level measurements is not expected. In the case of the uncertainty in stellar mass, the first thing to note is given that $R_{\rm e}$ ($R_{\rm e,M_\star}$) is defined as the location where half of the total light (stellar mass) is enclosed, its measurement is not affected by an incorrect mass determination of the object. This is because the only effect any uncertainty in mass could transfer to the shape of the profile is a scaling factor towards higher or lower stellar density. However, although the scatter in the size axis is negligible, the uncertainty in the mass axis will play a role in the total scatter of the size–mass plane. Nonetheless, there are two reasons why such an uncertainty will play a minor role in the observed scatter of these relations. Firstly, the slope of the $R_{\rm e}$ ($R_{\rm e,M_\star}$)–mass relation is rather flat in the region 10^9 to 10^{11} $M_\odot$, therefore the contribution from an uncertainty in the mass to enlarge the scatter of the relationships in this region would be close to zero (for example, in spirals and $R_{\rm e}$, the observed scatter is $\sigma_{\rm R_e} = 0.162$ $\pm$ 0.009 while the intrinsic scatter is almost the same $\sigma_{\rm R_{e,int}} = 0.155 \pm 0.009$). Secondly, as the observed scatters of the $R_{\rm e}$ ($R_{\rm e,M_\star}$)–mass relations are already larger than in the case of R_1 ($\sigma_{\rm R_{obs}}$), the contribution of a similar uncertainty in mass to the intrinsic scatter is very small. In the case of the $R_{\rm e}$–mass relation, as can be seen in Table 2.3, the global observed scatter is only reduced by 9% after accounting for the mass uncertainty, giving an intrinsic scatter of $\sigma_{\rm R_{e,int}}$ = 0.154 $\pm$ 0.009. Therefore, it is reasonable to compare the scatter of the *observed* $R_{\rm e}$–mass relation with the *intrinsic* R_1–mass relation. As shown in Table 2.3, the decrease in scatter from R_1 to $R_{\rm e}$ ranges from a factor of 2.5 (comparing both intrinsic scatters) to 2.75 (comparing the intrinsic scatter using R_1 with the observed scatter using $R_{\rm e}$). Figure 2.5 illustrates how the R_1–mass relation would be observed without the scatter produced by the background level and the stellar mass determination. Finally, for the isophotal sizes $R_{\rm H}$ and $R_{23.5,\rm i}$, the main contributor to the observed scatter is also the uncertainty in measuring the global mass of galaxies. In these cases, the intrinsic scatter for the global size–mass relation decreases by 15-20% compared to the observed values. Compared to the R_1–mass relation, the intrinsic scatter of the global size–mass relations using $R_{\rm H}$ and $R_{23.5,\rm i}$ is a factor of 1.5 and 1.4 larger, respectively. In Sect. 2.7.1, these results are expanded on by comparing the scatter of the size–mass relations as a function of galaxy morphology.

2.7 Discussion

The results of this Chapter show that the use of a physically motivated definition for the size of galaxies based on the location of the gas density threshold for star formation produces a global stellar mass–size relation with a very narrow intrinsic scatter (0.06 dex). In the following subsections, the characteristics of the new size parameter R_1 as well as the R_1–mass relation are compared with those resulting from other popular size measurements.

2.7.1 R_1 compared to other popular size definitions

In this Chapter R_1 was adopted as a proxy for the location of the gas density threshold for star formation in galaxies. Nonetheless, the use of R_1 as a size indicator is reminiscent of definitions based on the B-band isophote at 25 mag/arcsec^2, at 26.5 mag/arcsec^2 (i.e. the Holmberg radius) or in the i-band such as $R_{23.5,\rm i}$. Although the new size definition is not based on the depth of current surveys (as was the case for the size parameters that were defined using photographic plates), it is worth exploring the stellar mass–size plane with popular isophotal size definitions.

Este documento incorpora firma electrónica, y es copia auténtica de un documento electrónico archivado por la ULL según la Ley 39/2015.
Su autenticidad puede ser contrastada en la siguiente dirección https://sede.ull.es/validacion/

Identificador del documento: 2622200 Código de verificación: mbm0ekWs

Firmado por:	ROSHAN NUSHKIA CHAMBA *UNIVERSIDAD DE LA LAGUNA*	Fecha: 07/07/2020 13:28:26
	IGNACIO TRUJILLO CABRERA *UNIVERSIDAD DE LA LAGUNA*	07/07/2020 13:58:21
	Johan Hendrik Knapen Koelstra *UNIVERSIDAD DE LA LAGUNA*	07/07/2020 15:23:08
	María de las Maravillas Aguiar Aguilar *UNIVERSIDAD DE LA LAGUNA*	08/07/2020 15:55:11

Universidad de La Laguna
Oficina de Sede Electrónica
Entrada
Nº registro: 2020/46124
Nº reg. oficina: OF002/2020/45309
Fecha: 07/07/2020 15:26:22

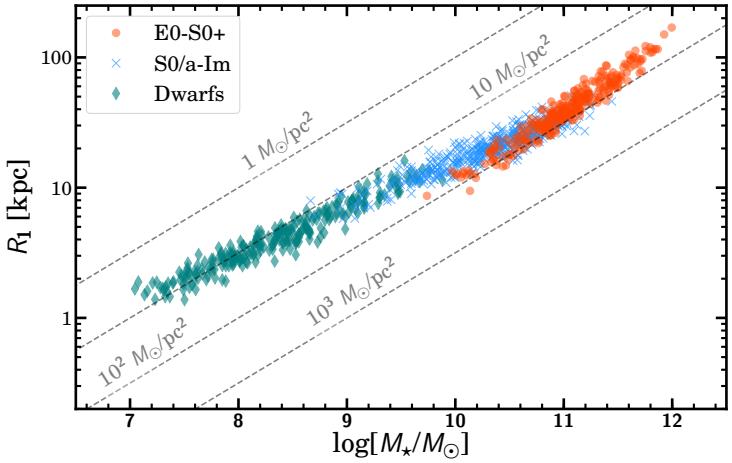

Figure 2.5: Similar to Fig. 2.4 (bottom panel), this figure shows the R_1–stellar mass relation as it would be observed without any uncertainty in measuring the background level of the images and the stellar mass of galaxies. The intrinsic scatter of the relation (0.06 dex) is a factor of 2.5 smaller than the scatter of the R_e–mass relation.

In the absence of the B-band filter in the Stripe82 dataset, as a compromise, the g-band imaging (i.e. the closest filter to the B-band with enough depth) available was used to show the stellar mass–size plane when using the position of the 26 mag/arcsec^2 (g-band) isophote as a size indicator. It is this isophote that is referred to as the Holmberg radius (R_H). A comparison with size based on the location of the i-band isophote 23.5 mag/arcsec^2 ($R_{23.5,i}$) is also included. The results of this exercise are shown in Fig. 2.6.

The observed scatter of the global stellar mass–R_H relation is 0.109 ± 0.005. This value is larger than the one observed for R_1 (0.089 ± 0.005). Interestingly, the scatter is particularly larger for the dwarfs and spirals than for the massive ellipticals. This is understandable as the variability in star formation activity among the less massive galaxies is larger than for the most massive ellipticals. Different star formation levels produce different g-band luminosities for the same stellar mass density, and therefore the scatter is larger when using size indicators based on blue bands (as is the case of R_H). A potential way to decrease the scatter using a single photometric band would be to use a redder band (i.e. one less affected by recent star formation activity). For instance, one would expect the use of the i-band to decrease the scatter of the stellar mass–size relation. This is in fact the case. The observed scatter of the global stellar mass–$R_{23.5,i}$ relation is a bit lower (0.106 ± 0.006 dex) than in the case of R_H using the g-band.

While the observed scatter of the R_1–mass relation is predominantly affected by the uncertainty in background and mass estimation, in the case of the R_H–mass and $R_{23.5,i}$–mass relations, the main contributor to the scatter is the mass uncertainty. This is because the 26 mag/arcsec^2 isophote in the g-band and the 23.5 mag/arcsec^2 in the i-band are brighter than the typical

Este documento incorpora firma electrónica, y es copia auténtica de un documento electrónico archivado por la ULL según la Ley 39/2015.
Su autenticidad puede ser contrastada en la siguiente dirección https://sede.ull.es/validacion/

Identificador del documento: 2622200 Código de verificación: mbm0ekWs

Firmado por:	ROSHAN NUSHKIA CHAMBA *UNIVERSIDAD DE LA LAGUNA*	Fecha: 07/07/2020 13:28:26
	IGNACIO TRUJILLO CABRERA *UNIVERSIDAD DE LA LAGUNA*	07/07/2020 13:58:21
	Johan Hendrik Knapen Koelstra *UNIVERSIDAD DE LA LAGUNA*	07/07/2020 15:23:08
	María de las Maravillas Aguiar Aguilar *UNIVERSIDAD DE LA LAGUNA*	08/07/2020 15:55:11

Universidad de La Laguna
Oficina de Sede Electrónica
Entrada
Nº registro: 2020/46124
Nº reg. oficina: OF002/2020/45309
Fecha: 07/07/2020 15:26:22

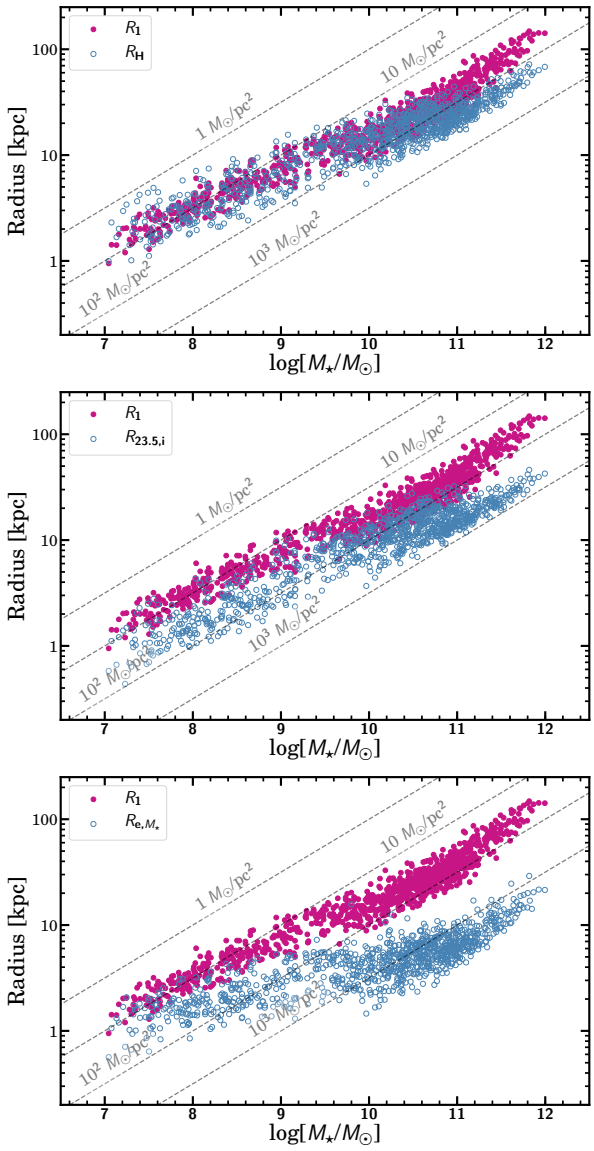

Figure 2.6: Comparing the R_1–mass relation with other size–mass relations using: Holmberg Radius, $R_{\rm H}$ defined in this work as the 26 mag/arcsec^{-2} isophote in SDSS g-band (upper panel), $R_{23.5,\rm i}$, the radial location of the $\mu_i = 23.5$ mag/arcsec^2 isophote (middle panel) and $R_{\rm e,M_\star}$, the half mass radius (lower panel).

Este documento incorpora firma electrónica, y es copia auténtica de un documento electrónico archivado por la ULL según la Ley 39/2015.
Su autenticidad puede ser contrastada en la siguiente dirección https://sede.ull.es/validacion/

Identificador del documento: 2622200 Código de verificación: mbm0ekWs

Firmado por:	ROSHAN NUSHKIA CHAMBA *UNIVERSIDAD DE LA LAGUNA*	Fecha: 07/07/2020 13:28:26
	IGNACIO TRUJILLO CABRERA *UNIVERSIDAD DE LA LAGUNA*	07/07/2020 13:58:21
	Johan Hendrik Knapen Koelstra *UNIVERSIDAD DE LA LAGUNA*	07/07/2020 15:23:08
	María de las Maravillas Aguiar Aguilar *UNIVERSIDAD DE LA LAGUNA*	08/07/2020 15:55:11

Universidad de La Laguna
Oficina de Sede Electrónica
Entrada
Nº registro: 2020/46124
Nº reg. oficina: OF002/2020/45309
Fecha: 07/07/2020 15:26:22

brightness of the isomass contour 1 $M_{\odot}/\mathrm{pc}^2$ (see Sect. 2.6.2). Consequently, the contribution of the uncertainty in the background to the estimation of the location of R_{H} (and $R_{23.5,\mathrm{i}}$) is not very important. Therefore, while the intrinsic scatter of the R_1–mass relation is around 0.06 dex, for R_{H}–mass (and $R_{23.5,\mathrm{i}}$–mass) the global intrinsic scatter decreases to ~ 0.09 dex. The findings shown here are further discussed in the context of the HI–mass relation of galaxies in Appendix A.6.

Although the global size–mass relation using R_1 produces the smallest scatter, it is worth checking whether this is also the case for different galaxy families. The family of galaxies that consistently shows both the lowest observed and intrinsic scatter values in the stellar mass–size plane is the E0–S0+ group. This applies to all the size indicators explored, including the effective and half-mass radii. It is particularly remarkable that the observed scatter using $R_{23.5,\mathrm{i}}$ (0.056 $\pm$ 0.005 dex) is almost comparable to the lowest intrinsic scatter values obtained for this galaxy type using R_1 and the half-mass radius (~ 0.04 dex). The small scatter of the elliptical galaxies is a direct consequence of their low level of internal structure compared to other galaxies. This fact makes the members of this family almost homologous. Therefore, if one is interested in a relative comparison between the size of galaxies within such a family, any size indicator already suggested in the literature is useful.

In the case of the S0/a–Sm family, i.e. those galaxies with very complex internal structure consisting of bars, rings, spiral arms, etc, the difference in scatter among the size indicators is much larger than for the ellipticals. As expected, the size indicators showing the larger scatter for this galaxy type are those which better reflect the light concentration of the objects: i.e. the effective and the half-mass radii. However, those size measurements that are closer to a characterisation of the boundaries of the galaxies (e.g. R_1, R_{H} and $R_{23.5,\mathrm{i}}$) are the ones with lower scatter. A similar result is found for the dwarf galaxies.

In addition to the above results, the scatters found here for spiral galaxies with those measured in the literature are quantitatively compared in the following. Similar to Saintonge & Spekkens (2011) and Hall et al. (2012), the spiral galaxy sample is divded into three categories: Sa–Sab, Sb–Sbc and Sc–Sd. Figure 2.7 shows the stellar mass–size relations for these types using R_1 and $R_{23.5i}$ as size indicators. A similar stratification as the one reported by Saintonge & Spekkens (2011) is seen here, Hall et al. (2012) and Muñoz-Mateos et al. (2015), i.e. at fixed stellar mass (or luminosity), those galaxies having later types are the largest. This is especially manifested at the low mass end. Saintonge & Spekkens (2011) has a sample mostly composed of Sc galaxies. Using $R_{23.5i}$ and the luminosity in the i-band, these authors determined an observed scatter of 0.05 dex. For the same morphological type, in this work (using stellar mass) an observed scatter of 0.101 $\pm$ 0.007 dex is found.

The larger scatter is connected to the fact that stellar mass has been used instead of the luminosity. The observed scatter using R_1 for Sc–Sd galaxies is 0.082 $\pm$ 0.007 dex. As the main source of scatter is the determination of stellar mass, it is worth giving the intrinsic scatter values: 0.096 $\pm$ 0.007 dex ($R_{23.5i}$) and 0.066 $\pm$ 0.007 dex (R_1). Within the common mass range $10^{9.5}$–10^{11} $M_{\odot}$ for all the spiral galaxy types, the observed scatters for the Sc–Sd galaxies are: 0.095 $\pm$ 0.008 dex ($R_{23.5i}$) and 0.077 $\pm$ 0.008 dex (R_1). The scatter reported by Saintonge & Spekkens (2011) is extraordinarily tight. Using a similar sample, Hall et al. (2012) found an observed scatter value for the $R_{23.5i}$–mass relation which ranges from 0.070 dex (for their higher quality sample) to 0.096 dex (their entire sample), which is in closer agreement to the observed value here.

Este documento incorpora firma electrónica, y es copia auténtica de un documento electrónico archivado por la ULL según la Ley 39/2015.
Su autenticidad puede ser contrastada en la siguiente dirección https://sede.ull.es/validacion/

Identificador del documento: 2622200 Código de verificación: mbm0ekWs

Firmado por:	ROSHAN NUSHKIA CHAMBA *UNIVERSIDAD DE LA LAGUNA*	Fecha: 07/07/2020 13:28:26
	IGNACIO TRUJILLO CABRERA *UNIVERSIDAD DE LA LAGUNA*	07/07/2020 13:58:21
	Johan Hendrik Knapen Koelstra *UNIVERSIDAD DE LA LAGUNA*	07/07/2020 15:23:08
	María de las Maravillas Aguiar Aguilar *UNIVERSIDAD DE LA LAGUNA*	08/07/2020 15:55:11

Universidad de La Laguna
Oficina de Sede Electrónica
Entrada
Nº registro: 2020/46124
Nº reg. oficina: OF002/2020/45309
Fecha: 07/07/2020 15:26:22

Another aspect to highlight is the change in the global slope of the stellar mass–size relation as a function of the size indicators explored. Using R_1, the slope is a bit above 1/3 between 10^7 to 10^{11} $M_\odot$. This value is in line with the one found using isophotal radii ($R_{\rm H}$ abd $R_{23.5,\rm i}$) as a size measure. The slopes, however, decrease significantly when using the effective and half-mass radii. The potential meaning of the slope obtained using R_1 is expanded on in subsection 2.7.2.

2.7.2 The slope of the stellar mass–size relation

The slope of the stellar mass–size relation reported here for galaxies within the mass range 10^7 to 10^{11} $M_\odot$ is very close to 1/3. A straightforward calculation shows that if all the stars within R_1 were located within a sphere of such radius, the stellar mass density (in 3D) of all the galaxies in this mass range will be equivalent to $\sim 4.5 \times 10^{-3}\, M_\odot/{\rm pc}^3$. Obviously, the spatial configuration of both dwarf and spiral galaxies is not spherical but disc–like. Nonetheless, it is suggestive to think that the gas that originally formed all these objects was in a spherical-like configuration at an early galaxy phase before its collapse to form the disc configuration. In other words, it is worth speculating whether the currently observed 3D stellar density for all galaxies in the sample is a reflection of a common 3D gas density at an early phase (before collapsing) of the objects. In fact, this constant 3D stellar density could be linked with the expected constant density of dark matter haloes which formed at a given age of the Universe (see e.g. Mo et al. 1998).

It is also worth indicating that while a monotonic increase in the size of galaxies with stellar mass using R_1 (as well as for $R_{\rm H}$ and $R_{23.5,\rm i}$) is visible, the same is not true for $R_{\rm e}$ or $R_{\rm e,M_\star}$. This is particularly manifested in the interval 10^9 to 10^{11} $M_\odot$ in stellar mass where the increase in effective (or in the half-mass) radius of the (mostly) spiral galaxies is very modest. This mass range is where the bulges of spiral galaxies appear. What the reader is witnessing here is the enormous impact of using $R_{\rm e}$ (or $R_{\rm e,M_\star}$) for measuring sizes when a significant amount of the light (or stellar mass) of galaxies can be concentrated in the inner parts of galaxies with a bulge. This small increase in $R_{\rm e}$ (or $R_{\rm e,M_\star}$) between 10^9 to 10^{11} $M_\odot$ is not a minor issue. As the vast majority of works aiming to understand the connection between the galaxy size and the dark matter halo properties use $R_{\rm e}$ as a size indicator (see e.g. Kravtsov 2013; Jiang et al. 2019; Zanisi et al. 2020), the small increase in the effective radius in this mass range can hide a potential connection between the dark and the luminous component of the galaxies. In an ongoing research programme (C. Dalla Vecchia et al. in prep.), it will be shown that the use of R_1 permits the connection of both galaxy components directly, ultimately facilitating our understanding about how these objects form.

2.7.3 The tilt of the stellar mass–size relation at 10^{11} $M_\odot$

A notable feature of the new stellar mass–size relation is the change in slope observed at $\sim 10^{11}\, M_\odot$. The slope changes from $\sim 1/3$ to $\sim 3/5$ (see Table 2.3) for the most massive galaxies. The abrupt change in slope is found in all the size indicators probed in this work. This $\sim 10^{11}\, M_\odot$ stellar mass value marks the shift between objects with disc–like configuration to objects with a spherical symmetry. In addition, this is the stellar mass where the transition from rotationally to pressure-supported systems has been reported (see e.g. Emsellem et al. 2011).

As mentioned in Appendix A.2, this change in slope could be a manifestation of different gas density threshold values for star formation in galaxies that formed at high-z could have had.

Este documento incorpora firma electrónica, y es copia auténtica de un documento electrónico archivado por la ULL según la Ley 39/2015.
Su autenticidad puede ser contrastada en la siguiente dirección https://sede.ull.es/validacion/

Identificador del documento: 2622200 Código de verificación: mbm0ekWs

Firmado por:	ROSHAN NUSHKIA CHAMBA *UNIVERSIDAD DE LA LAGUNA*	Fecha: 07/07/2020 13:28:26
	IGNACIO TRUJILLO CABRERA *UNIVERSIDAD DE LA LAGUNA*	07/07/2020 13:58:21
	Johan Hendrik Knapen Koelstra *UNIVERSIDAD DE LA LAGUNA*	07/07/2020 15:23:08
	María de las Maravillas Aguiar Aguilar *UNIVERSIDAD DE LA LAGUNA*	08/07/2020 15:55:11

Universidad de La Laguna
Oficina de Sede Electrónica
Entrada
Nº registro: 2020/46124
Nº reg. oficina: OF002/2020/45309
Fecha: 07/07/2020 15:26:22

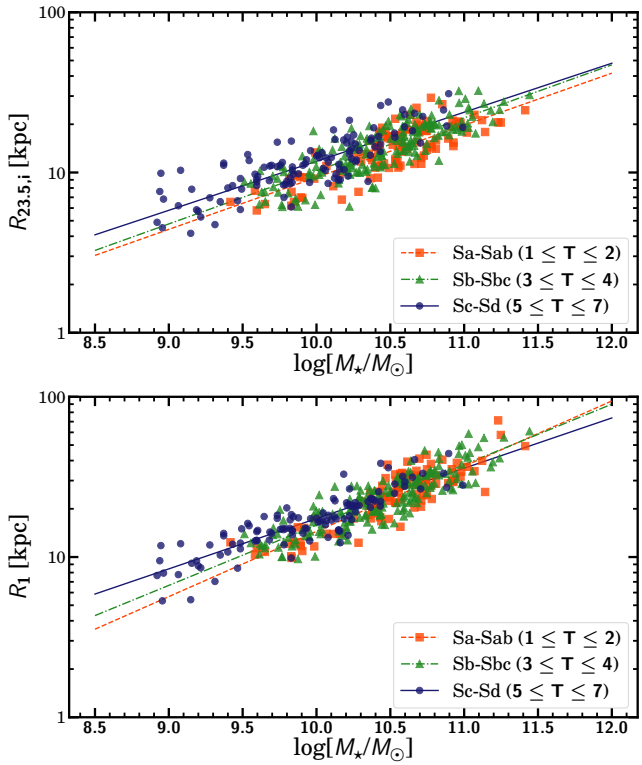

Figure 2.7: Stellar mass–size relation for three morphological groups within the spiral galaxy sample: Sa–Sab (orange squares), Sb–Sbc (green triangles) and Sc–Sd (blue dots). The top panel shows the relation using $R_{23.5,i}$ while the bottom panel shows the same relation using R_1 as the size indicator. Similar to Saintonge & Spekkens (2011), Hall et al. (2012) and Muñoz-Mateos et al. (2015), the spiral galaxies are stratified, with the largest ones (at a fixed stellar mass) belonging to later morphological types.

Este documento incorpora firma electrónica, y es copia auténtica de un documento electrónico archivado por la ULL según la Ley 39/2015.
Su autenticidad puede ser contrastada en la siguiente dirección https://sede.ull.es/validacion/

Identificador del documento: 2622200 Código de verificación: mbm0ekWs

Firmado por:	ROSHAN NUSHKIA CHAMBA *UNIVERSIDAD DE LA LAGUNA*	Fecha: 07/07/2020 13:28:26
	IGNACIO TRUJILLO CABRERA *UNIVERSIDAD DE LA LAGUNA*	07/07/2020 13:58:21
	Johan Hendrik Knapen Koelstra *UNIVERSIDAD DE LA LAGUNA*	07/07/2020 15:23:08
	María de las Maravillas Aguiar Aguilar *UNIVERSIDAD DE LA LAGUNA*	08/07/2020 15:55:11

Universidad de La Laguna
Oficina de Sede Electrónica
Entrada
Nº registro: 2020/46124
Nº reg. oficina: OF002/2020/45309
Fecha: 07/07/2020 15:26:22

Observational evidence has shown that the most massive galaxies underwent a huge burst of star formation at high-z with star formation rates reaching values $\gtrsim$1000 $M_\odot$ yr^{-1} (see e.g. Riechers et al. 2013). The high star formation rates these galaxies have undergone could have injected a lot of energy into the gas, thereby preventing the star formation at low mass densities and consequently increasing the gas density threshold for star formation. A remnant of this huge star formation burst is the core of these massive galaxies that later undergo important merger activity, creating their envelopes (see e.g. Trujillo et al. 2011; Ferreras et al. 2014; Buitrago et al. 2017).

In short, the tilt observed at $\sim 10^{11}\,M_\odot$ in the new stellar mass–size plane may be interpreted as a reflection of a change in the gas density threshold for star formation when the bulk of the most massive galaxies originated.

2.8 Conclusions

In this Chapter, a new approach to define the luminous size of galaxies, aiming to link size with the region where galaxies form stars, has been introduced. Such a physically motivated size definition can be measured using the average radial location of the gas density threshold for star formation. However, in the work presented here, the size definition is made operative by the use of the radial position of a fixed isomass contour at 1 $M_\odot$/pc^2 (here referred to as R_1). This particular value is motivated by both theoretical and observational arguments: it is 1) a proxy for measuring this threshold according to studies on the evolution of stellar discs and 2) the density value found at the location of the truncation in galaxies similar to our own Milky Way.

When using R_1 as a size indicator for galaxies, the global scatter of the stellar mass–size relation explored over five orders of magnitude in stellar mass drops significantly, reaching a value of ~ 0.06 dex. This value is 2.5 times smaller than the scatter measured using the effective radius (~ 0.15 dex) and 1.5 to 1.8 times smaller than those using other traditional sizes indicators such as $R_{23.5,\mathrm{i}}$ (~ 0.09 dex), R_H (~ 0.09 dex) and $R_{\mathrm{e,M}_\star}$ (~ 0.11 dex).

Between 10^7 and $10^{11}\,M_\odot$, the slope of the stellar mass–size relation is very close to 1/3. In a 3D spherical distribution, this corresponds to a constant stellar density of $\sim 4.5\times10^{-3} M_\odot$/pc^3, which could be a reflection of a common gas density when the primordial gas collapsed to form stars. Beyond $10^{11}\,M_\odot$, the stellar mass–size relation gets steeper, reaching a slope of $\sim 3/5$. This drastic increase in size of the most massive galaxies could be linked to its different star formation histories, reflecting that the gas density threshold for star formation was higher at the epoch of their main formation burst.

Este documento incorpora firma electrónica, y es copia auténtica de un documento electrónico archivado por la ULL según la Ley 39/2015.
Su autenticidad puede ser contrastada en la siguiente dirección https://sede.ull.es/validacion/

Identificador del documento: 2622200 Código de verificación: mbm0ekWs

Firmado por:	ROSHAN NUSHKIA CHAMBA *UNIVERSIDAD DE LA LAGUNA*	Fecha: 07/07/2020 13:28:26
	IGNACIO TRUJILLO CABRERA *UNIVERSIDAD DE LA LAGUNA*	07/07/2020 13:58:21
	Johan Hendrik Knapen Koelstra *UNIVERSIDAD DE LA LAGUNA*	07/07/2020 15:23:08
	María de las Maravillas Aguiar Aguilar *UNIVERSIDAD DE LA LAGUNA*	08/07/2020 15:55:11

Universidad de La Laguna
Oficina de Sede Electrónica
Entrada
Nº registro: 2020/46124
Nº reg. oficina: OF002/2020/45309
Fecha: 07/07/2020 15:26:22

3

Are ultra-diffuse galaxies Milky Way-sized?

Now almost 70 years since its introduction, the effective or half-light radius has become a very popular choice for characterising galaxy size (Chapter 1, Sect. 1.5.2). However, the effective radius measures the concentration of light within galaxies and thus does not capture the intuitive definition of size which is related to the edge or boundary of objects (Chapter 2). In this Chapter, I present the article '*Are ultra-diffuse galaxies Milky Way-sized?*' published in A&A, 633, L3 (2020).

3.1 Introduction

Faint galaxies with large effective radii have been known since the 1980s (e.g. Sandage & Binggeli 1984; Impey et al. 1988; Bothun et al. 1991; Dalcanton et al. 1997a), but more recently, the name ultra-diffuse galaxies (UDGs; van Dokkum et al. 2015a) has been coined for galaxies with very similar characteristics. These are galaxies of low stellar density, defined to have low central surface brightness ($\mu_g(0) > 24\,\mathrm{mag/arcsec^2}$) and an effective radius (R_e) of over 1.5 kpc (R_e is the radius which encloses half the total flux from a galaxy; de Vaucouleurs 1948). The question of whether UDGs represent a separate class of galaxies is still under debate. Currently, known UDGs that have been discovered in clusters (Koda et al. 2015; Mihos et al. 2015; Muñoz et al. 2015; van der Burg et al. 2016; Román & Trujillo 2017a; Venhola et al. 2017; Mancera Piña et al. 2018), in groups (Román & Trujillo 2017b; Cohen et al. 2018), and in the field (Bellazzini et al. 2017; Prole et al. 2019) can have R_e as large as 5 kpc which is comparable to that of large (i.e. giant) Milky Way (MW)-like galaxies. As explained in Chapter 1 (Sect. 1.4.5), this fact has been used to suggest that UDGs are 'failed' giants (van Dokkum et al. 2015a). As R_e captures (at most) the central parts of giant galaxies, whether this radius can be used to fairly compare the sizes of UDGs to the more massive galaxies is questionable.

The reason why R_e is incapable of reaching the boundaries of massive galaxies is that according to its definition it depends on how the light is concentrated in these objects. Therefore, if one considers that the sizes of galaxies are indicated by the location of their edges or boundaries (similar to everyday objects), then R_e is undeniably a poor measurement of size. However, the idea of associating the sizes of galaxies to the location of their boundaries (or something very close to them) is not recent. Galaxy size has also been measured using limiting surface

Este documento incorpora firma electrónica, y es copia auténtica de un documento electrónico archivado por la ULL según la Ley 39/2015.
Su autenticidad puede ser contrastada en la siguiente dirección https://sede.ull.es/validacion/

Identificador del documento: 2622200 Código de verificación: mbm0ekWs

Firmado por:	ROSHAN NUSHKIA CHAMBA *UNIVERSIDAD DE LA LAGUNA*	Fecha: 07/07/2020 13:28:26
	IGNACIO TRUJILLO CABRERA *UNIVERSIDAD DE LA LAGUNA*	07/07/2020 13:58:21
	Johan Hendrik Knapen Koelstra *UNIVERSIDAD DE LA LAGUNA*	07/07/2020 15:23:08
	María de las Maravillas Aguiar Aguilar *UNIVERSIDAD DE LA LAGUNA*	08/07/2020 15:55:11

Universidad de La Laguna
Oficina de Sede Electrónica
Entrada
Nº registro: 2020/46124
Nº reg. oficina: OF002/2020/45309
Fecha: 07/07/2020 15:26:22

brightness isophotes, such as for example D_{25} (Redman 1936) or the Holmberg radius (R_H; Holmberg 1958), to characterise the maximum area that galaxies spanned on the photographic plates of that era. However, similar to the effective radius, the isophotal radii were also initially defined for operational purposes and do not directly encompass any physical meaning. In spite of this, isophotal radii (and their variants; see e.g. Hall et al. 2012) as well as sizes based on light concentration, for example $R_{\rm e}$, R_{90} (Nair et al. 2011), and R_{80} (Miller et al. 2019), are being used in important scaling relations such as the fundamental plane (Djorgovski & Davis 1987), size–stellar mass (Fish 1963; Sérsic 1968b), or the size–virial radius relation (Kravtsov 2013), to study the history and formation of galaxies.

In Chapter 2, I presented Trujillo et al. (2020) where a galaxy size parameter based on the location of the gas density threshold for star formation in galaxies is used. We showed that the size–stellar mass relation with this measure for size has an intrinsic dispersion of only ~ 0.06 dex, which is three times smaller than that of the relation with $R_{\rm e}$ as galaxy size (~ 0.18 dex), over five orders of magnitude in stellar mass $10^7\,M_\odot < M_\star < 10^{12}\,M_\odot$. The proposed parameter is also able to capture the boundaries of the stellar distribution of galaxies and can thus represent how large or small these objects are, in contrast to the effective radius. The reader may refer to Chapter 2 for the in-depth discussion on the fundamental meaning of these results and why such a size definition is different from the ones that only measure the extent of galaxies down to a given surface brightness level (e.g. R_H or D_{25}).

To complement the results presented in Chapter 2, in this Chapter, I present Chamba, Trujillo, & Knapen (2020) where we study the implications of using the effective radius as a size measure for UDGs; and how this affects our understanding of these galaxies. We computed the physically motivated size parameter defined in Chapter 2 for a sample of UDGs and compare their sizes to those of dwarfs with stellar masses $10^7\,M_\odot \leq M_\star \leq 10^{8.5}\,M_\odot$ as well as to the sizes of MW-like galaxies ($10^{10}\,M_\odot < M_\star < 10^{11}\,M_\odot$) studied in Chapter 2. Throughout this work a standard ΛCDM cosmology with $\Omega_m = 0.3$, $\Omega_\Lambda = 0.7$ and $H_0 = 70 kms^{-1}$ Mpc^{-1} is assumed.

3.2 Data and sample selection

To have a homogeneous dataset of dwarfs and UDGs both in depth and filter coverage, we use the publicly available background-rectified imaging data in the g and r-bands of the deep IAC Stripe 82 Legacy Project[1] (hereafter IAC Stripe82, Trujillo & Fliri 2016; Román & Trujillo 2018). The UDGs are taken from Román & Trujillo (2017b) and Trujillo et al. (2017). For completeness, two iconic UDGs outside the Stripe 82 footprint were also added to the sample. Imaging data for DF44 (van Dokkum et al. 2015b), a representative example of a UDG with a large $R_{\rm e}$, was obtained from the Gemini archive (GN-2016A-FT-18,PI: P. van Dokkum) and DECaLS data[2] was used for [KKS2000]04 (popularized as NGC1052-DF2)[3]. The control sample analysed consists of 155 dwarf galaxies with stellar masses in the range $10^7\,M_\odot \leq M_\star \leq 10^{8.5}\,M_\odot$ studied in Chapter 2. We focus on this stellar mass regime as it overlaps with the mass range of the selected UDGs for this work. Galaxies with stellar masses in the range of $10^{10}\,M_\odot <$

[1] `http://research.iac.es/proyecto/stripe82/`

[2] `http://portal.nersc.gov/project/cosmo/data/legacysurvey/dr7/coadd/195/1952p270/`

[3] At a distance of 13 Mpc (Trujillo et al. 2019), [KKS2000]04 no longer satisfies the criterion ($R_{\rm e} > 1.5$ kpc) to be defined as a UDG. Nevertheless, due to the popularity of this object after being reported as a 'galaxy lacking dark matter' (van Dokkum et al. 2018), we include it in our sample for analysis.

Este documento incorpora firma electrónica, y es copia auténtica de un documento electrónico archivado por la ULL según la Ley 39/2015.
Su autenticidad puede ser contrastada en la siguiente dirección https://sede.ull.es/validacion/

Identificador del documento: 2622200 Código de verificación: mbm0ekWs

Firmado por:	ROSHAN NUSHKIA CHAMBA *UNIVERSIDAD DE LA LAGUNA*	Fecha: 07/07/2020 13:28:26
	IGNACIO TRUJILLO CABRERA *UNIVERSIDAD DE LA LAGUNA*	07/07/2020 13:58:21
	Johan Hendrik Knapen Koelstra *UNIVERSIDAD DE LA LAGUNA*	07/07/2020 15:23:08
	María de las Maravillas Aguiar Aguilar *UNIVERSIDAD DE LA LAGUNA*	08/07/2020 15:55:11

Universidad de La Laguna
Oficina de Sede Electrónica
Entrada
Nº registro: 2020/46124
Nº reg. oficina: OF002/2020/45309
Fecha: 07/07/2020 15:26:22

$M_\star < 10^{11}\,M_\odot$ from the work in Chapter 2 (449 objects) are also selected to represent MW-like systems.

The IAC Stripe82 and DECaLS images are of similar depth with a limit in surface brightness of $\mu_g = 29.1\,\mathrm{mag/arcsec^2}$ (3σ;$10\times10\,\mathrm{arcsec^2}$). The depth of the Gemini coaddition is $\mu_g \sim 30\,\mathrm{mag/arcsec^2}$ (3σ;$10\times10\,\mathrm{arcsec^2}$). Only the g- and i-band data were available for [KKS2000]04.

Ultra-diffuse galaxies R2 and R3 from Román & Trujillo (2017b) were removed from the UDG sample due to light contamination in the galaxy outskirts produced by surrounding bright sources and/or stars. Therefore, the final sample includes 12 UDGs. None of the dwarf galaxies in our control sample satisfy the criteria for a UDG as in all the cases $\mu_g(0) < 24\,\mathrm{mag/arcsec^2}$.

3.3 Methodology

The same methodology implemented for the work presented in Chapter 2 applies here. However, for completeness, we summarise the main procedures used. The reader may refer to Sect. 2.5 in Chapter 2 for more details.

The entire analysis of this study was carried out on individual image stamps with dimensions of $100\times100\,\mathrm{kpc^2}$ (for the dwarfs and UDGs) and $600\times600\,\mathrm{kpc^2}$ (for the massive galaxies) in the rest frame of each galaxy. The scattered light from point sources was removed from the IAC Stripe82 image stamps using our extended ($\sim 8\,\mathrm{arcmin}$ radius) point spread functions for this telescope[4] (Infante-Sainz et al. 2020). All sources surrounding the galaxy of interest in the image were then masked using `MTObjects` (Teeninga et al. 2016), setting `move_up = 0.3`.

To derive the surface brightness profiles of the galaxies in the sample, the axis-ratio (q) and position angle (PA) of the objects were obtained by fitting an ellipse to an average isophote of 26 mag/arcsec^2 in the g-band images. The centre, q, and PA of each galaxy were then visually verified prior to further analysis. These parameters were fixed and elliptical annuli were used to create the radial profile of each galaxy as well as its growth curve in flux which is needed to determine R_e.

The $g-r$ colour ($g-i$ for DF44) profiles were derived from the surface brightness profiles and converted to mass-to-light ratio (M/L) profiles in g using the relationships from Roediger & Courteau (2015). These M/L and surface brightness profiles in the g-band for all galaxies were then converted to stellar mass density ($\Sigma_\star$) profiles (see Eq. 1 in Bakos et al. 2008) and used to ascertain the size parameter presented in Chapter 2. The profiles were also integrated up to the $\mu_g = 29\,\mathrm{mag/arcsec^2}$ isophote to derive the stellar masses of the galaxies, $M_\star$. Various stellar density thresholds (within the limit in depth of the images used) can easily be determined from such profiles. Here we use R_1, the radius at which $\Sigma_\star = 1\,M_\odot/\mathrm{pc^2}$, as a proxy for the location of the gas density threshold for star formation. For details on the background subtraction of the data, correction of the profiles due to the inclination effect and Galactic extinction, and an estimation of the uncertainties related to our measurements (stellar mass and background), see Chapter 2.

All of the measurements for the UDGs are provided in Appendix B. The measurements for the dwarf sample can be found in the online version of Trujillo et al. (2020). For comparison,we also show the distributions of the UDGs and dwarfs using an isophotal size indicator, the Holmberg

[4] `http://research.iac.es/proyecto/stripe82/pages/advanced-data-products/the-sdss-extended-psfs.php`

Este documento incorpora firma electrónica, y es copia auténtica de un documento electrónico archivado por la ULL según la Ley 39/2015.
Su autenticidad puede ser contrastada en la siguiente dirección https://sede.ull.es/validacion/

Identificador del documento: 2622200 Código de verificación: mbm0ekWs

Firmado por:	ROSHAN NUSHKIA CHAMBA *UNIVERSIDAD DE LA LAGUNA*	Fecha: 07/07/2020 13:28:26
	IGNACIO TRUJILLO CABRERA *UNIVERSIDAD DE LA LAGUNA*	07/07/2020 13:58:21
	Johan Hendrik Knapen Koelstra *UNIVERSIDAD DE LA LAGUNA*	07/07/2020 15:23:08
	María de las Maravillas Aguiar Aguilar *UNIVERSIDAD DE LA LAGUNA*	08/07/2020 15:55:11

Universidad de La Laguna
Oficina de Sede Electrónica
Entrada
Nº registro: 2020/46124
Nº reg. oficina: OF002/2020/45309
Fecha: 07/07/2020 15:26:22

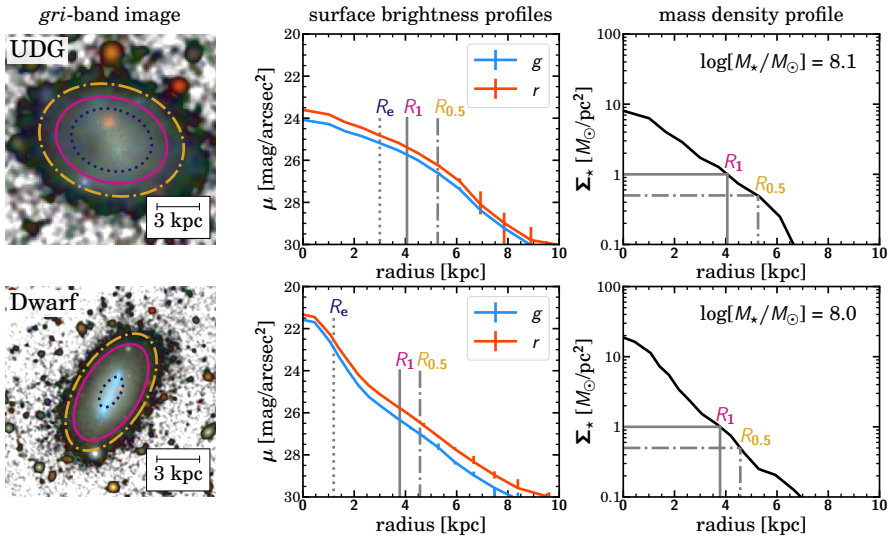

Figure 3.1: Illustration of the consequence of using R_e as galaxy size for UDGs and dwarf galaxies. Here we show two galaxies of similar stellar mass at the same physical scale: UDG-B5 (top) and a representative dwarf galaxy (SDSS J224114.12-003715.0, bottom). The colour image is the *gri*-band composite with a grey-scaled background for contrast and contours showing R_e (dotted), R_1, (solid) and $R_{0.5}$ (dot-dashed). The surface brightness and stellar mass density profiles derived for both galaxies are also shown.

radius (R_H), in Appendix B.2. Lacking the B-band,we used the isophote at 26 mag/arcsec^2 in the g-band as a proxy for R_H.

3.4 Results

Figure 3.1 shows an example of a UDG and a representative dwarf galaxy (i.e. one that lies very close to the centre and best-fit line in both the observed R_e– and R_1–stellar mass relations). Both galaxies have similar stellar mass ($\sim 10^8\,M_\odot$). Their corresponding surface brightness and mass density profiles are shown, and the locations of R_e (dotted), R_1 (solid) and the radius where $\Sigma_\star = 0.5\,M_\odot/\mathrm{pc}^2$ (called $R_{0.5}$; dot-dashed, see Appendix B.3) are marked in the image and profiles. The reason why the effective radius of the UDG is large in comparison to that of the regular dwarf galaxy shown is because the dwarf galaxy has active star forming clumps in its central region. The presence of such clumps in these galaxies means that flux will be more concentrated in the centre which decreases the effective radius and increases their central surface brightness. Consequently, such dwarfs will not be characterised as a UDG. Similar clumps or bright regions are not usually present at the centre of UDGs which makes their effective radii larger compared to the majority of dwarfs.

Este documento incorpora firma electrónica, y es copia auténtica de un documento electrónico archivado por la ULL según la Ley 39/2015.
Su autenticidad puede ser contrastada en la siguiente dirección https://sede.ull.es/validacion/

Identificador del documento: 2622200 Código de verificación: mbm0ekWs

Firmado por:	ROSHAN NUSHKIA CHAMBA *UNIVERSIDAD DE LA LAGUNA*	Fecha: 07/07/2020 13:28:26
	IGNACIO TRUJILLO CABRERA *UNIVERSIDAD DE LA LAGUNA*	07/07/2020 13:58:21
	Johan Hendrik Knapen Koelstra *UNIVERSIDAD DE LA LAGUNA*	07/07/2020 15:23:08
	María de las Maravillas Aguiar Aguilar *UNIVERSIDAD DE LA LAGUNA*	08/07/2020 15:55:11

Universidad de La Laguna
Oficina de Sede Electrónica
Entrada
Nº registro: 2020/46124
Nº reg. oficina: OF002/2020/45309
Fecha: 07/07/2020 15:26:22

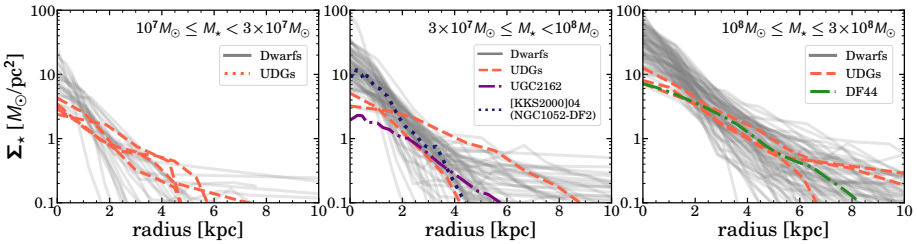

Figure 3.2: Stellar mass density profiles of dwarfs (grey) and UDGs (colours) belonging to three stellar mass bins (left to right).

This last point is further demonstrated in Fig. 3.2 where the $\Sigma_\star$ profiles of dwarf galaxies and UDGs are over-plotted in three panels, corresponding to galaxies in three stellar mass bins: $10^7\,M_\odot \leq M_\star < 3{\times}10^7\,M_\odot$, $3{\times}10^7\,M_\odot \leq M_\star < 10^8\,M_\odot$, and $10^8\,M_\odot \leq M_\star \leq 3\times10^8\,M_\odot$. Ultra-diffuse galaxies tend to be less concentrated than regular dwarfs, with lower central densities by a factor of two to three. However, the global extensions of both types of galaxy are very much alike.

Figure 3.3 shows the R_e–stellar mass and R_1–stellar mass scaling relationships (top panels) and their distributions with respect to the best-fit lines (bottom panels). Three main features are: 1) The dispersion of the observed R_1–stellar mass plane (0.086 ± 0.007 dex) is a factor of 2.5 smaller than that of the observed R_e–stellar mass plane (0.213 ± 0.014 dex) for dwarf galaxies (see also TCK20); 2) UDGs populate the upper portion of the R_e-stellar mass plane. A simple Kolmogrov-Smirnov (KS) test using $R_e/R_{e,fit}$ gives an extremely small p-value of 2.1×10^{-5}. After removing two galaxies that have $R_e < 1.5$ kpc (according to our measurements) in our initial UDG sample, namely [KKS2000]04 (NGC1052-DF2) and UDG-R1 (from Román & Trujillo 2017b), the p-value decreases to 9.3×10^{-6}. Both values indicate that the null hypothesis — that dwarf galaxies and UDGs in this sample arise from the same distribution in size — can be rejected; and 3) UDGs are populated among the dwarf galaxies in the R_1–stellar mass plane, showing no evidence that the distributions in $R_1/R_{1,fit}$ of these galaxies are significantly different (p-value = 0.07). After removing the two galaxies with $R_e < 1.5$ kpc, the p-value increases to 0.09. Therefore, the null hypothesis cannot be rejected. The UDGs shown in this work have extensions that correspond to those of dwarfs. This exercise was repeated using another popular size indicator, the Holmberg radius, and found similar results (see Appendix B.2).

On average, the location of R_1 in surface brightness for galaxies in this mass range is $\mu_g(R_1) \sim 27$ mag/arcsec^2, but can be as faint as 28.5 mag/arcsec^2. Lower stellar mass densities are even more faint (e.g. $R_{0.5}$, see Appendix B.3), reinforcing the importance of high-quality deep images to conduct this work.

Finally, we highlight the main results of this work in Figs. 3.4 and 3.5. Figure 3.4 demonstrates how using a physically motivated size parameter that captures the global extension of galaxies reveals the radical difference between the sizes of UDGs and MW-like galaxies (right panel), in contrast to the effective radius (left panel). While using R_e indicates that UDGs have similar extensions to MW-like galaxies, R_1 shows that the MW-like systems are, on average, ten times larger than the classical dwarfs and UDGs. In fact, the null hypothesis is

Este documento incorpora firma electrónica, y es copia auténtica de un documento electrónico archivado por la ULL según la Ley 39/2015.
Su autenticidad puede ser contrastada en la siguiente dirección https://sede.ull.es/validacion/

Identificador del documento: 2622200 Código de verificación: mbm0ekWs

Firmado por:	ROSHAN NUSHKIA CHAMBA *UNIVERSIDAD DE LA LAGUNA*	Fecha: 07/07/2020 13:28:26
	IGNACIO TRUJILLO CABRERA *UNIVERSIDAD DE LA LAGUNA*	07/07/2020 13:58:21
	Johan Hendrik Knapen Koelstra *UNIVERSIDAD DE LA LAGUNA*	07/07/2020 15:23:08
	María de las Maravillas Aguiar Aguilar *UNIVERSIDAD DE LA LAGUNA*	08/07/2020 15:55:11

Universidad de La Laguna
Oficina de Sede Electrónica
Entrada
Nº registro: 2020/46124
Nº reg. oficina: OF002/2020/45309
Fecha: 07/07/2020 15:26:22

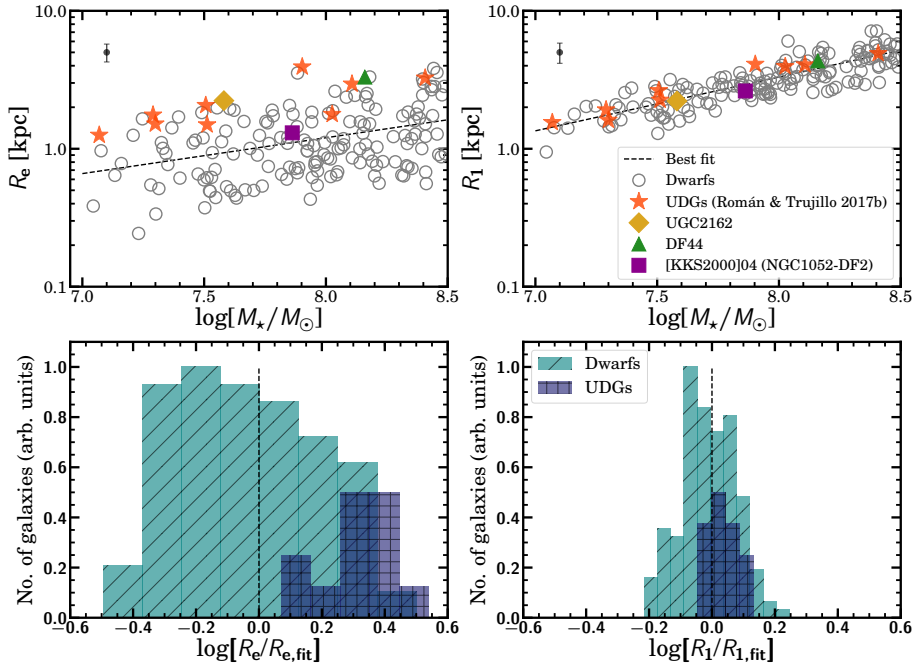

Figure 3.3: Comparison between R_e and the physically motivated size parameter for UDGs and dwarfs. *Top*: R_e–stellar mass relation (left) and the R_1–stellar mass relation (right) for dwarfs (grey) and UDGs (colours). The best-fit line of each relation for the dwarf sample is also over-plotted. The upper left corner of each plot shows the typical uncertainty in our measurements (see TCK20). *Bottom*: Histograms showing the distribution of $R_e/R_{e,fit}$ (left) and $R_1/R_{1,fit}$ (right) where 'fit' refers to the best-fit line of each relation for the dwarf sample.

completely rejected when the R_1 distributions of UDGs and MW-like galaxies are compared (see also Appendix B.3). This result is further illustrated in Fig. 3.5 where an elliptical galaxy (SDSS J223954.96-005918.97) reminiscent of M87, a MW-like spiral galaxy (SDSS J012015.34-002009.00), and the dwarf galaxy and UDG of Fig. 3.1 are shown to the same physical scale. The TType labels for the elliptical and spiral galaxies were taken from Nair & Abraham (2010). From this figure, it is clear that R_1 better represents the edges of galaxies compared to R_e and prevents any misleading notion about the actual extension of galaxies. We emphasise the fact that the galaxies are shown to a similar depth in surface brightness. This is crucial when the sizes of galaxies are compared. Therefore, the strikingly different sizes are *not* a result of the quality of the imaging data.

Este documento incorpora firma electrónica, y es copia auténtica de un documento electrónico archivado por la ULL según la Ley 39/2015.
Su autenticidad puede ser contrastada en la siguiente dirección https://sede.ull.es/validacion/

Identificador del documento: 2622200 Código de verificación: mbm0ekWs

Firmado por:	ROSHAN NUSHKIA CHAMBA *UNIVERSIDAD DE LA LAGUNA*	Fecha: 07/07/2020 13:28:26
	IGNACIO TRUJILLO CABRERA *UNIVERSIDAD DE LA LAGUNA*	07/07/2020 13:58:21
	Johan Hendrik Knapen Koelstra *UNIVERSIDAD DE LA LAGUNA*	07/07/2020 15:23:08
	María de las Maravillas Aguiar Aguilar *UNIVERSIDAD DE LA LAGUNA*	08/07/2020 15:55:11

Universidad de La Laguna
Oficina de Sede Electrónica
Entrada
Nº registro: 2020/46124
Nº reg. oficina: OF002/2020/45309
Fecha: 07/07/2020 15:26:22

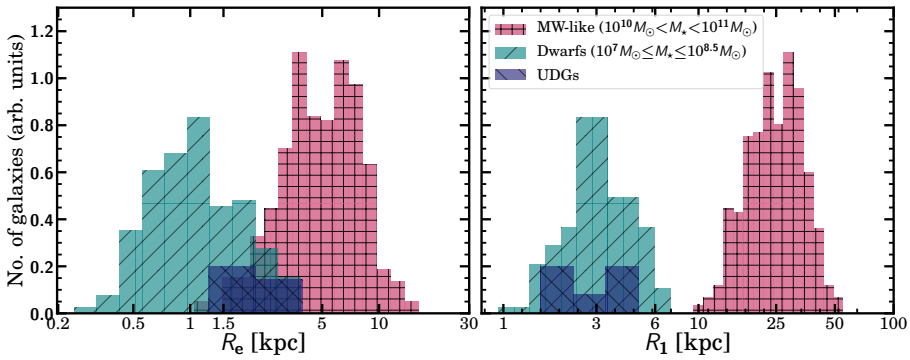

Figure 3.4: Histograms showing the size distribution of UDGs, dwarfs, and MW-like galaxies. In R_e (left), UDGs overlap with the dwarfs and MW-like systems in our sample and in R_1 (right), the UDGs clearly separate from the MW-like galaxies and overlap with the dwarfs. These results show that UDGs have the extensions of dwarfs.

3.5 Discussion

The aim of this study was to investigate how the effective radius, as a size measure for UDGs, affects our understanding of these galaxies. We illustrated that the effective radii of UDGs will generally always be larger compared to that of dwarf galaxies due to the absence of luminous clumps (or substructure like bulges in the case of more massive galaxies) in their central regions. The fact that the large effective radii of UDGs can be compatible with those of MW-like galaxies has led to the interpretation that UDGs are 'Milky Way-sized' (see e.g. van Dokkum et al. 2015a; Koda et al. 2015), when perhaps the more accurate statement is rather that 'UDGs are less concentrated in light than dwarfs and MW-like galaxies'. For this reason, we adopted the physically motivated size measure that was developed in Chapter 1. As this size parameter is also better than the effective radius at representing how large or small galaxies are, it now becomes possible to fairly compare the sizes of UDGs with those of dwarfs and MW-like galaxies. Contrary to previous accounts, we have demonstrated that the sizes of MW-like galaxies and UDGs are actually radically different. As a matter of fact, the sizes of UDGs with the new size definition (as well as with the Holmberg radius) are compatible with those of dwarfs.

However, while the KS test shows no evidence that the size distribution of the UDG and dwarf galaxy populations are different, most of the UDGs lie in the upper half of the R_1–stellar mass relation (Fig. 3.3). This could be related to the incompleteness in our dwarf control sample arising from the spectroscopic target selection criteria of the Sloan Digital Sky Survey (SDSS), requiring that the r-band Petrosian half-light surface brightnesses of targets are at least $\mu_{50} \leq 24.5$ mag/arcsec^2 (Strauss et al. 2002). The lack of faint low-mass galaxies in the dwarf sample can also be seen in the stellar mass density profiles in Fig. 3.2 where there are almost no dwarf galaxies with compatible central densities to UDGs. Any such bias due to spectroscopic incompleteness in the dwarf sample will also equally affect the R_e–stellar mass plane. It is

Este documento incorpora firma electrónica, y es copia auténtica de un documento electrónico archivado por la ULL según la Ley 39/2015.
Su autenticidad puede ser contrastada en la siguiente dirección https://sede.ull.es/validacion/

Identificador del documento: 2622200 Código de verificación: mbm0ekWs

Firmado por:	ROSHAN NUSHKIA CHAMBA *UNIVERSIDAD DE LA LAGUNA*	Fecha: 07/07/2020 13:28:26
	IGNACIO TRUJILLO CABRERA *UNIVERSIDAD DE LA LAGUNA*	07/07/2020 13:58:21
	Johan Hendrik Knapen Koelstra *UNIVERSIDAD DE LA LAGUNA*	07/07/2020 15:23:08
	María de las Maravillas Aguiar Aguilar *UNIVERSIDAD DE LA LAGUNA*	08/07/2020 15:55:11

Universidad de La Laguna
Oficina de Sede Electrónica
Entrada
Nº registro: 2020/46124
Nº reg. oficina: OF002/2020/45309
Fecha: 07/07/2020 15:26:22

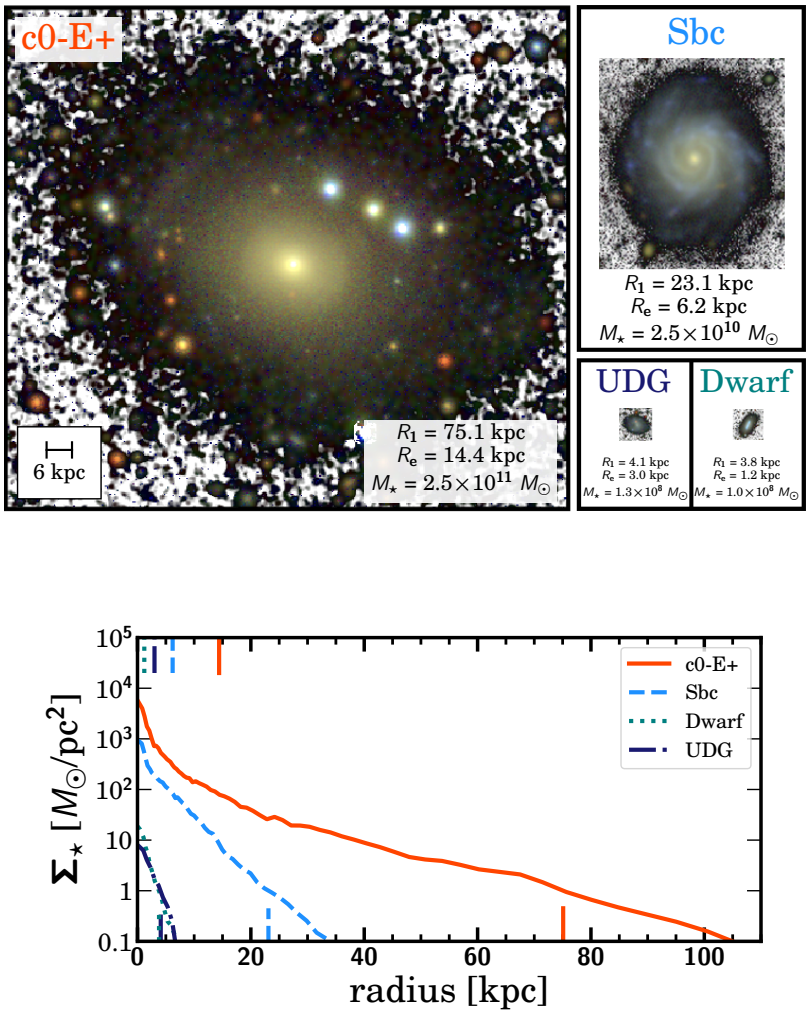

Figure 3.5: *Top:* Representative galaxies of different stellar masses: a giant elliptical ($M_\star \sim 2.5 \times 10^{11}\,M_\odot$), a Milky Way-like galaxy ($M_\star \sim 2.5 \times 10^{10}\,M_\odot$), a UDG and dwarf galaxy ($M_\star \sim 10^8\,M_\odot$). All galaxies are shown to the same physical scale and a similar depth in surface brightness. *Bottom:* The stellar mass density profiles of the same galaxies. The coloured ticks in the upper x-axis mark the location of R_e. Similar ticks in the lower x-axis mark the location of R_1.

Este documento incorpora firma electrónica, y es copia auténtica de un documento electrónico archivado por la ULL según la Ley 39/2015.
Su autenticidad puede ser contrastada en la siguiente dirección https://sede.ull.es/validacion/

Identificador del documento: 2622200 Código de verificación: mbm0ekWs

Firmado por:	ROSHAN NUSHKIA CHAMBA *UNIVERSIDAD DE LA LAGUNA*	Fecha: 07/07/2020 13:28:26
	IGNACIO TRUJILLO CABRERA *UNIVERSIDAD DE LA LAGUNA*	07/07/2020 13:58:21
	Johan Hendrik Knapen Koelstra *UNIVERSIDAD DE LA LAGUNA*	07/07/2020 15:23:08
	María de las Maravillas Aguiar Aguilar *UNIVERSIDAD DE LA LAGUNA*	08/07/2020 15:55:11

Universidad de La Laguna
Oficina de Sede Electrónica
Entrada
Nº registro: 2020/46124
Nº reg. oficina: OF002/2020/45309
Fecha: 07/07/2020 15:26:22

therefore an acceptable exercise to compare these relationships quantitatively. Were the control sample not affected by this potential incompleteness, the similarity between the dwarfs and UDGs in the distribution of their R_1 as well as R_e would be even greater. This should be the case when future deep spectroscopic studies (e.g. Ruiz-Lara et al. 2018; Ferré-Mateu et al. 2018) target more dwarf galaxies with lower central densities and essentially fill the upper portions of both these relations.

The use of the effective radius as a galaxy size measurement has also led to a confusion as to whether UDGs are associated to the dark matter haloes of MW-like (high-luminosity) or dwarf galaxies. Several analyses using simulations (e.g. Di Cintio et al. 2017; Chan et al. 2018) and observations (e.g. Beasley et al. 2016; Beasley & Trujillo 2016; Amorisco et al. 2018) already support the idea that UDGs reside in haloes comparable to those of dwarfs. The results shown in the chapter lend further support to this idea. As the size of a galaxy is believed to be proportional to the virial radius of its halo (Kravtsov 2013), the fact that the UDG sizes agree with those of dwarfs strongly suggest that both types of galaxy occupy the same dark matter haloes.

3.6 Conclusions

In this chapter, we used a proxy for the gas density threshold for star formation as a size indicator for UDGs and dwarf galaxies. We compared the size distribution of these galaxies in a physically important parameter space — the size–stellar mass plane — and showed that there is no evidence that the size distributions of UDGs and dwarfs are different. The UDGs have sizes that are within the size range of dwarfs. The same result holds using the Holmberg radius as a size indicator. If low-mass, extremely diffuse Milky Way-sized galaxies exist, then in the new definition of size adopted in this work, they need to have a radius of about 25 kpc. Such galaxies have not been found in present-day imaging surveys. These results reinforce the importance of using physically meaningful properties in order to fairly compare classes of galaxies and draw conclusions about their nature.

Este documento incorpora firma electrónica, y es copia auténtica de un documento electrónico archivado por la ULL según la Ley 39/2015.
Su autenticidad puede ser contrastada en la siguiente dirección https://sede.ull.es/validacion/

Identificador del documento: 2622200 Código de verificación: mbm0ekWs

Firmado por:	ROSHAN NUSHKIA CHAMBA *UNIVERSIDAD DE LA LAGUNA*	Fecha: 07/07/2020 13:28:26
	IGNACIO TRUJILLO CABRERA *UNIVERSIDAD DE LA LAGUNA*	07/07/2020 13:58:21
	Johan Hendrik Knapen Koelstra *UNIVERSIDAD DE LA LAGUNA*	07/07/2020 15:23:08
	María de las Maravillas Aguiar Aguilar *UNIVERSIDAD DE LA LAGUNA*	08/07/2020 15:55:11

Universidad de La Laguna
Oficina de Sede Electrónica
Entrada
Nº registro: 2020/46124
Nº reg. oficina: OF002/2020/45309
Fecha: 07/07/2020 15:26:22

4

The edges of galaxies: from dwarfs to giants

4.1 Introduction

Unlike everyday objects around us, galaxies do not have clear edges. In general, an edge of an object is defined where a sharp contrast or change in its properties (e.g. colour, shape or texture) occur. As discussed in Chapter 1 (Sec. 1.3.2), the closest feature in galaxies to this concept emerged when truncations in the outskirts of edge-on galaxies were discovered in the late 1970s (van der Kruit 1979). A truncation is a sharp feature in the radial profiles of disc galaxies, beyond which the steepness of the profiles increase. However, until now, truncations have only been studied in Milky Way-like, spiral galaxies. For these galaxies, truncations appear up to four or five times their exponential scale length (van der Kruit & Searle 1982; Fry et al. 1999; Kregel et al. 2002). Observationally, they are about 2 to 3 magnitudes brighter in edge-on galaxies than in face-on ones ($\sim$ 25–26 mag/arcsec^2 in face-on, see e.g. Martínez-Lombilla et al. 2019). This is simply due to the line-of-sight integration through the disc (e.g. Martín-Navarro et al. 2012), but they can also be hidden beneath stellar haloes (Martín-Navarro et al. 2014; Peters et al. 2017) and scattered light caused by the point spread function (de Jong 2008; Sandin 2014).

Interestingly, the truncation has been shown to encode important information on the formation and evolution of galactic discs (van der Kruit & Freeman 2011). However, the origin of truncations is still not completely understood. For instance, it has been shown that truncations can be associated to a peak in the angular momentum distribution of the disc (van der Kruit 1987), linked to thresholds in star formation activity (Kennicutt 1989a; Roškar et al. 2008; Martínez-Lombilla et al. 2019) and trace past and ongoing star formation in disc galaxies (see Elmegreen & Hunter 2017). Other investigations have related the origin of truncations to warps (van der Kruit 2007) which could imply a link between truncations and tidal effects in galaxy outskirts, to the redistribtuion of angular momentum during bar formation (Debattista et al. 2006, 2017), the aftermath of an interaction with a companion galaxy (Laurikainen & Salo 2001), or to the heating and stripping of stars by dark matter subhaloes (de Jong et al. 2007). All these works demonstrate the importance of truncations in the understanding of galaxy formation and evolution. However, considering that truncations are linked to thresholds in star formation further reinforces the physical motivation behind our method of defining the sizes of galaxies (Chapter 2).

Este documento incorpora firma electrónica, y es copia auténtica de un documento electrónico archivado por la ULL según la Ley 39/2015.
Su autenticidad puede ser contrastada en la siguiente dirección https://sede.ull.es/validacion/

Identificador del documento: 2622200 Código de verificación: mbm0ekWs

Firmado por:	ROSHAN NUSHKIA CHAMBA *UNIVERSIDAD DE LA LAGUNA*	Fecha: 07/07/2020 13:28:26
	IGNACIO TRUJILLO CABRERA *UNIVERSIDAD DE LA LAGUNA*	07/07/2020 13:58:21
	Johan Hendrik Knapen Koelstra *UNIVERSIDAD DE LA LAGUNA*	07/07/2020 15:23:08
	María de las Maravillas Aguiar Aguilar *UNIVERSIDAD DE LA LAGUNA*	08/07/2020 15:55:11

Universidad de La Laguna
Oficina de Sede Electrónica
Entrada
Nº registro: 2020/46124
Nº reg. oficina: OF002/2020/45309
Fecha: 07/07/2020 15:26:22

In the current Chapter, I present preliminary material in an ongoing study to define the 'edges' of galaxies, belonging to a wide morphological type and stellar mass range (Chamba, Trujillo & Knapen in prep.). We prefer to adopt the term 'edge' rather than truncation because truncations were specifically defined for edge-on Milky Way-like galaxies in the original work by van der Kruit (1979) and van der Kruit & Searle (1981a,b), while we seek to locate the same feature as viewed in low-inclined and face-on galaxies. We pursue this goal to shed light on the origins of discs and the varied star formation activity among different types of galaxies, as much work has only been conducted on edge-on Milky Way-like galaxies. This is directly related to the work presented in Chapter 2 (and published in Trujillo, Chamba, & Knapen 2020) where the location of the gas density threshold for star formation in galaxies was proposed as a physically motivated definition for galaxy size. In that Chapter, the $1\,M_{\odot}/\mathrm{pc}^2$ isomass contour was specifically chosen as a size measure for two main reasons: 1) to make the size definition operative and 2) because the truncation of Milky Way-like galaxies occurs at this density (see Martínez-Lombilla et al. 2019). Here the isomass contour is not fixed to any particular value. Instead, a feature compatible with an edge was visually identified using surface brightness profiles in the the g and r-band, $g-r$ colour as well as the stellar mass density profiles of galaxies. The same sample of galaxies studied in Chapter 2 (1005 objects) was used for this task. Additionally, galaxies from Bakos & Trujillo (2012) and Peters et al. (2017) were also included for comparison (24 objects). Collectively, the galaxies have stellar masses between $10^7\,M_{\odot} < M_{\star} < 10^{12}\,M_{\odot}$ and morphologies ranging from regular dwarfs to massive ellipticals.

This Chapter is organised as follows. The definition of the edge is described in Sect. 4.2. The imaging data and sample selection used is summarised in Sect. 4.3. The methods used can be found in Sect. 4.4 and preliminary results of this ongoing research project are shown in Sect. 4.5. A standard ΛCDM cosmology with Ω_m=0.3, Ω_{Λ}=0.7 and H_0=70 km s^{-1} Mpc^{-1} is assumed.

4.2 Defining the edge of a galaxy

In face-on galaxies, the truncation in the radial profile of the galaxy is much less prominent compared to edge-on systems. To illustrate this, consider Fig. 4.1 where a comparison between the truncation of a face-on and edge-on Milky Way-like disc galaxy is shown. The upper panels show the *gri*-band composite images of the galaxies, overlaid on the background of the image in grey scale for contrast. The lower panels show a figure taken from Martín-Navarro et al. (2014) where the radial surface brightness profiles in the r-band (μ_r) were derived using the IAC Stripe 82 dataset (Fliri & Trujillo 2016). For each profile, Martín-Navarro et al. (2014) modelled the bulge, disc and stellar halo components of the galaxies that are also overplotted in the figure. For both galaxies, the location of the break can be considered the first change in slope in a galaxy's profile, occurring in the innermost region of the disc, while the truncation is the second change in slope, occurring in the outer disc. As mentioned in Chapter 1 (Sect. 1.4.4), the break and the truncation are two differentiated features and in this thesis, we are only interested in the truncation.

For UGC 00929, the location of the truncation in the disc corresponds to the soft bump in the face-on model for the galaxy whereas the truncation in UGC 00507 corresponds to a much sharper change in slope in its edge-on profile. This large difference between the face-on and edge-on systems arises due to 1) the line-of-sight (LOS) integration through the disc in edge-on

Este documento incorpora firma electrónica, y es copia auténtica de un documento electrónico archivado por la ULL según la Ley 39/2015.
Su autenticidad puede ser contrastada en la siguiente dirección https://sede.ull.es/validacion/

Identificador del documento: 2622200 Código de verificación: mbm0ekWs

Firmado por:	ROSHAN NUSHKIA CHAMBA *UNIVERSIDAD DE LA LAGUNA*	Fecha: 07/07/2020 13:28:26
	IGNACIO TRUJILLO CABRERA *UNIVERSIDAD DE LA LAGUNA*	07/07/2020 13:58:21
	Johan Hendrik Knapen Koelstra *UNIVERSIDAD DE LA LAGUNA*	07/07/2020 15:23:08
	María de las Maravillas Aguiar Aguilar *UNIVERSIDAD DE LA LAGUNA*	08/07/2020 15:55:11

Universidad de La Laguna
Oficina de Sede Electrónica
Entrada
Nº registro: 2020/46124
Nº reg. oficina: OF002/2020/45309
Fecha: 07/07/2020 15:26:22

configurations and 2) the proportion by which the light of the stellar halo matches that of the truncation. For the galaxies shown in Fig. 4.1, the LOS integration results in the truncation being ~ 2 mag brighter for the edge-on galaxy UGC 00507 compared to the face-on UGC 00929. Furthermore, the higher brightness in the edge-on view consequently makes the feature much sharper than in the face-on orientation, thanks to a stronger contrast against the fainter halo.

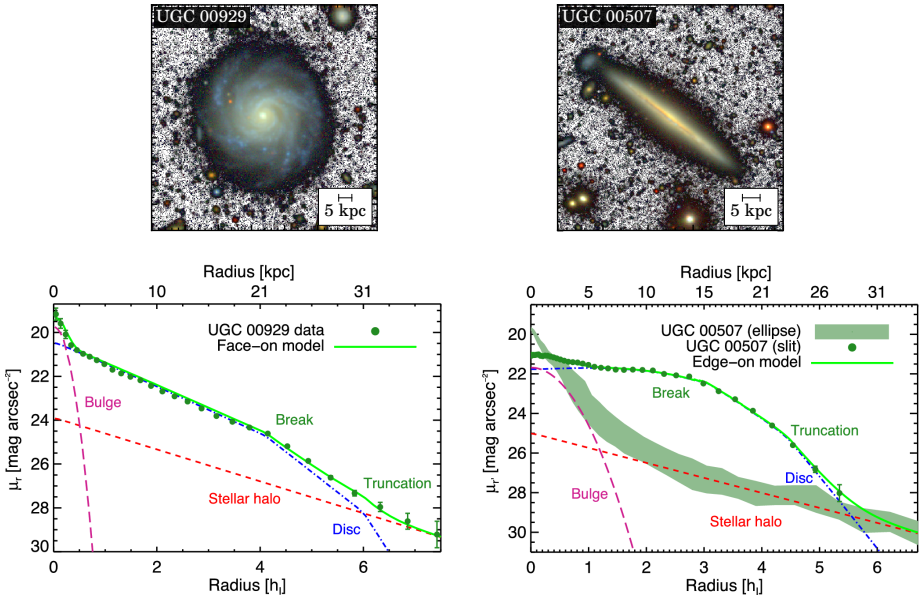

Figure 4.1: Comparison between the truncations in a face-on and edge-on galaxy. *Top*: IAC Stripe 82 *gri*-band composite images of UGC 00929 (left) and UGC 00507 (right). *Bottom*: Figure showing the surface brightness profiles in the r-band (μ_r) of UGC 00929 and UGC 00507, taken from Martín-Navarro et al. (2014). The model fits for each component are also overplotted: the total surface brightness distribution (green solid lines), the disc (blue dashed line), stellar halo (red dashed line) and the bulge (purple dashed line).

To complement the results from Martín-Navarro et al. (2014) for UGC 00929, here we derive the surface brightness profiles μ_g and μ_r, $g-r$ colour and stellar mass density ($\Sigma_\star$) profile for the galaxy using the latest, background rectified version of the deep IAC Stripe 82 images (Román & Trujillo 2018). These radial profiles were obtained in the same manner as that described in Chapter 2 (Sect. 2.5) and are shown in Fig. 4.2. $R_{\rm trunc}$ corresponds to the location of the truncation visually identified in this work, and appears as a bump in the outer most part of the surface brightness profiles. This is marked using a vertical dotted line at $R_{\rm trunc} = 25.5$ kpc[1]. A change in slope in the $g-r$ colour profile at $R_{\rm trunc}$ is also noticeable, beyond which the

[1]Notice that the kpc axis in the figure from Martín-Navarro et al. (2014) (here Fig. 4.1 bottom) is incorrect for UGC 00929. The truncation in that figure is marked at 31 kpc.

Este documento incorpora firma electrónica, y es copia auténtica de un documento electrónico archivado por la ULL según la Ley 39/2015.
Su autenticidad puede ser contrastada en la siguiente dirección https://sede.ull.es/validacion/

Identificador del documento: 2622200 Código de verificación: mbm0ekWs

Firmado por:	ROSHAN NUSHKIA CHAMBA *UNIVERSIDAD DE LA LAGUNA*	Fecha: 07/07/2020 13:28:26
	IGNACIO TRUJILLO CABRERA *UNIVERSIDAD DE LA LAGUNA*	07/07/2020 13:58:21
	Johan Hendrik Knapen Koelstra *UNIVERSIDAD DE LA LAGUNA*	07/07/2020 15:23:08
	María de las Maravillas Aguiar Aguilar *UNIVERSIDAD DE LA LAGUNA*	08/07/2020 15:55:11

Universidad de La Laguna
Oficina de Sede Electrónica
Entrada
Nº registro: 2020/46124
Nº reg. oficina: OF002/2020/45309
Fecha: 07/07/2020 15:26:22

increase towards redder colours continues. This demonstrates that the surface brightness profiles combined with the $g-r$ profiles can aid in the visual identification of truncations in low-inclined and face-on galaxies.

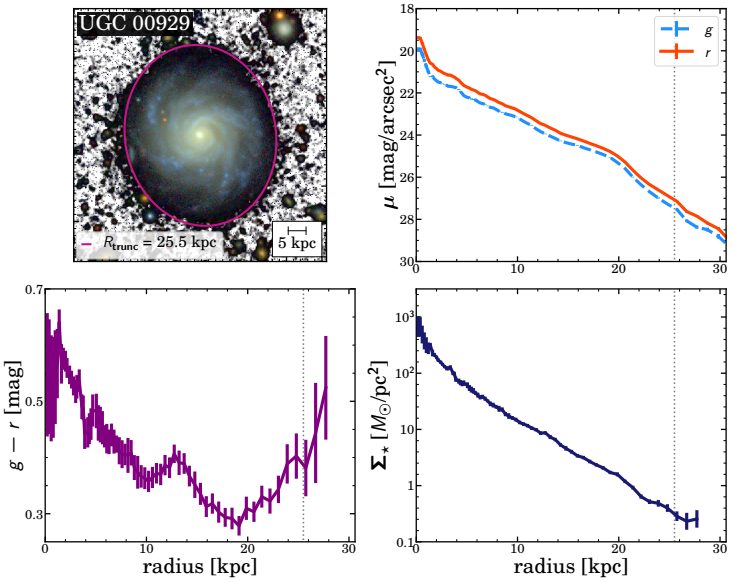

Figure 4.2: Radial profiles for UGC 00929 derived in this work. *Top:* To complement Fig. 4.1, $R_{\rm trunc}$ is overplotted on the galaxy image using a pink isophote (left) and the observed surface brightness profiles both in the g- and r-band are shown (right). *Bottom:* The $g-r$ colour (left) and the stellar mass density $\Sigma_\star$ profile (right) of the galaxy. $R_{\rm trunc}$ is marked using a vertical line in all radial profile panels. Martín-Navarro et al. (2014) marked the truncation at 31 kpc, however, their kpc axis is incorrect (footnote 1 in the previous page.).

In addition to the effect of the stellar halo, Trujillo & Fliri (2016) demonstrated the effect of the point spread function (PSF) on the radial profile of a low-inclined spiral galaxy, UGC 00180, using deep observations from the Gran Telescopio Canarias. This particular work was discussed previously in Chapter 1 within the context of the deepest imaging from the ground to date and how it has been used to estimate the fraction of light in the stellar halo of UGC 00180 (Sect. 1.4.3). In this Chapter, I reproduce two more figures from Trujillo & Fliri (2016) which shows the GTC image after PSF deconvolution (Fig. 4.3) and the resulting profile of UGC 00180 (Fig. 4.4). For clarity, in Fig. 4.4 I have marked the location of the truncation reported in Trujillo & Fliri (2016) using a vertical grey line and used pink vectors to highlight the change in slope at this location in the original profile (blue). The change in slope is greater (by 36.5%) at that location in the profile after accounting for the PSF (black) and thus increases the visibility of the truncation. However, the location of the truncation itself does not change. This justifies

Este documento incorpora firma electrónica, y es copia auténtica de un documento electrónico archivado por la ULL según la Ley 39/2015.
Su autenticidad puede ser contrastada en la siguiente dirección https://sede.ull.es/validacion/

Identificador del documento: 2622200 Código de verificación: mbm0ekWs

Firmado por:	ROSHAN NUSHKIA CHAMBA *UNIVERSIDAD DE LA LAGUNA*	Fecha: 07/07/2020 13:28:26
	IGNACIO TRUJILLO CABRERA *UNIVERSIDAD DE LA LAGUNA*	07/07/2020 13:58:21
	Johan Hendrik Knapen Koelstra *UNIVERSIDAD DE LA LAGUNA*	07/07/2020 15:23:08
	María de las Maravillas Aguiar Aguilar *UNIVERSIDAD DE LA LAGUNA*	08/07/2020 15:55:11

Universidad de La Laguna
Oficina de Sede Electrónica
Entrada
Nº registro: 2020/46124
Nº reg. oficina: OF002/2020/45309
Fecha: 07/07/2020 15:26:22

that here we present results without removing the PSF.

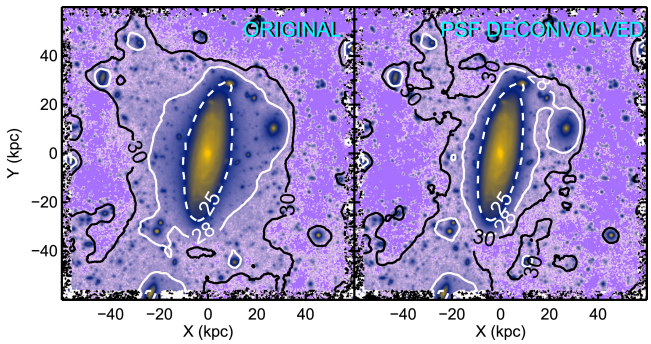

Figure 4.3: Effect of the PSF on the surface brightness distribution of UGC 00180. Isophotal contours at 25, 28, and 30 mag/arcsec^2 around the galaxy in the original (left) and PSF deconvolved image (right) are labelled. The effect of the PSF is particularly relevant when reaching surface brightnesses fainter than 25 mag/arcsec^2 (r-band). *Credit: Trujillo & Fliri (2016).*

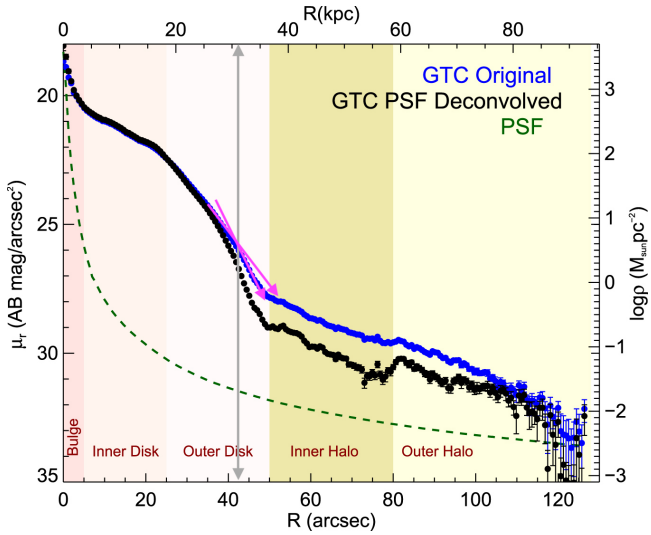

Figure 4.4: Effect of the PSF on the μ_r profile of UGC 00180 from Trujillo & Fliri (2016). For clarity, I have marked $R_{\rm trunc} = 43$ arcsec using a vertical grey line and used pink vectors to highlight the change in slope at this location in the original profile (blue). The result after removing the PSF (black) and profile of the GTC PSF (green) are also plotted.

Este documento incorpora firma electrónica, y es copia auténtica de un documento electrónico archivado por la ULL según la Ley 39/2015.
Su autenticidad puede ser contrastada en la siguiente dirección https://sede.ull.es/validacion/

Identificador del documento: 2622200 Código de verificación: mbm0ekWs

Firmado por:	ROSHAN NUSHKIA CHAMBA *UNIVERSIDAD DE LA LAGUNA*	Fecha: 07/07/2020 13:28:26
	IGNACIO TRUJILLO CABRERA *UNIVERSIDAD DE LA LAGUNA*	07/07/2020 13:58:21
	Johan Hendrik Knapen Koelstra *UNIVERSIDAD DE LA LAGUNA*	07/07/2020 15:23:08
	María de las Maravillas Aguiar Aguilar *UNIVERSIDAD DE LA LAGUNA*	08/07/2020 15:55:11

Universidad de La Laguna
Oficina de Sede Electrónica
Entrada
Nº registro: 2020/46124
Nº reg. oficina: OF002/2020/45309
Fecha: 07/07/2020 15:26:22

From the above two examples discussed, it is already clear that the truncation of a galaxy does not always manifest itself in the same way: for UGC 00929, the truncation appeared as a soft bump in the surface brightness profile and a change in slope in the $g-r$ colour profile (Fig. 4.2) while for UGC 00180, the truncation occurs at the location of a clearer change in slope (Fig. 4.4). In light of this, we prefer to adopt the term 'edge' rather than truncation because truncations were specifically defined for edge-on Milky Way-like galaxies in the original work by van der Kruit (1979) and van der Kruit & Searle (1981a,b), while we seek to locate the same feature as viewed in low-inclined and face-on galaxies. Therefore, the term 'edge' refers to the truncations in galaxies, however it is a generalisation of this feature to cases where differences in shape, orientation or fraction of stellar halo light in galaxies could result in very different manifestations of the truncation in the radial profiles of these galaxies. It is also for this reason that as a first step towards locating the edges of galaxies, from dwarfs to giant ellipticals, over a large stellar mass range $10^7\,M_\odot < M_\star < 10^{12}\,M_\odot$, we have decided to carefully inspect all galaxy profiles visually on a case-by-case basis. Several other examples will be shown in Sect. 4.5 to further demonstrate how the edge has been visually located in this work.

Using the visually identified edges of galaxies, in this Chapter, we show a preliminary version of: 1) the size–stellar mass plane, with size parametrised by the location of the edge which is closer to the physical size definition proposed in Chapter 2 and 2) the distribution of the stellar mass density inferred at the edge location as a function of galaxy stellar mass.

4.3 Data and sample selection

Measuring the stellar mass density at the edge for a large sample of galaxies requires a multi-band survey that is both adequately deep and wide. With this in mind, the deep g- and r-band images of the IAC Stripe 82 Legacy Project[2] is a suitable choice (Trujillo & Fliri 2016; Román & Trujillo 2018). The limiting depth in surface brightness of these images are $\mu_g = 29.1\,(3\sigma; 10\times10\,\mathrm{arcsec}^2)$ and $\mu_r = 28.5\,(3\sigma; 10\times10\,\mathrm{arcsec}^2)$. Extended ($\sim 8$ arcmin) point spread functions (PSF) of the survey (Infante-Sainz et al. 2020) are publicly available.

The same sample of galaxies studied in Chapter 2, namely, elliptical (E0–S0+) and spiral (S0/a–Im) galaxies from Nair & Abraham (2010) and a sample of low-mass dwarf galaxies from Maraston et al. (2013), within the Stripe 82 footprint are used in this work. This can be considered the parent sample in our analysis. The galaxies in this sample have redshift $0.01 < z < 0.1$. Any galaxy with contaminated outskirts due to very bright stars, Galactic cirrus structures or nearby companion/interacting galaxies were removed from the initially selected sample. The final parent sample consists of 1005 galaxies with stellar masses between $10^7 M_\odot < M_\star < 10^{12} M_\odot$ and redshift $z < 0.1$. See Chapter 2 for more details. Additionally, the sample of late-type galaxies studied in Bakos & Trujillo (2012, hereafter B12) and Peters et al. (2017, hereafter P17) is also included in this work (24 galaxies) to complement our investigation in three ways: 1) the galaxies from B12 are located at lower distances and are therefore at a higher spatial resolution. This implies that the edge (if any) should be more prominent for these galaxies, 2) the sample from P17 is interesting because we can study galaxies with larger inclinations and 3) the results reported in B12 and P17 can be compared with those produced here. Upon examination, three galaxies from the P17 sample, namely UGC 2319, UGC 2418

[2] http://research.iac.es/proyecto/stripe82/

Este documento incorpora firma electrónica, y es copia auténtica de un documento electrónico archivado por la ULL según la Ley 39/2015.
Su autenticidad puede ser contrastada en la siguiente dirección https://sede.ull.es/validacion/

Identificador del documento: 2622200 Código de verificación: mbm0ekWs

Firmado por:	ROSHAN NUSHKIA CHAMBA *UNIVERSIDAD DE LA LAGUNA*	Fecha: 07/07/2020 13:28:26
	IGNACIO TRUJILLO CABRERA *UNIVERSIDAD DE LA LAGUNA*	07/07/2020 13:58:21
	Johan Hendrik Knapen Koelstra *UNIVERSIDAD DE LA LAGUNA*	07/07/2020 15:23:08
	María de las Maravillas Aguiar Aguilar *UNIVERSIDAD DE LA LAGUNA*	08/07/2020 15:55:11

Universidad de La Laguna
Oficina de Sede Electrónica
Entrada
Nº registro: 2020/46124
Nº reg. oficina: OF002/2020/45309
Fecha: 07/07/2020 15:26:22

and NGC 7716 were removed due to heavy contamination from bright stars. Therefore, a total of 1026 galaxies were analysed in this work.

To study the stellar population properties (i.e. colour, age and metalicity) at the location of the edge of these galaxies, the extended MILES library in the SDSS bands assuming the Kroupa Universal IMF[3] was used (Vazdekis et al. 2012).

4.4 Methodology

As the goal of this work is to measure the edges of galaxies in their outskirts, accurate surface brightness profiles are a necessity. We thus determine the elliptical parameters (centre, axis-ratio and position angle) that best describe the galaxy outskirts and accurate estimates of the background in the images following an approach similar to that described in Pohlen & Trujillo (2006). However, there are two main obstacles that make these procedures challenging. The first is the masking of all sources in the vicinity of the galaxy in the image and the second is the difficulty in accounting for contamination in the images from scattered light. The image processing techniques used to deal with these challenges have been previously presented in Chapters 2 and 3. These same methods are adopted here so I refer the reader to those Chapters for details. However, some improvements have been made in the pipeline used for this work. In particular, the masking of surrounding sources was increased and the region used to compute the background was chosen to be an elliptical annulus (parameterised by the same elliptical parameters used to describe the shape of the galaxy) between two and three times the total size of the galaxy. The average variation in the background of the images is now 0.82 times smaller than the variation obtained for the analysis presented in Chapters 2 and 3. This means that the surface brightness limit of the profiles has improved by 0.21 mag. These improvements were visually verified for each galaxy.

Once the g and r-band surface brightness profiles of the galaxies are derived, the stellar mass density profile is computed using the mass-to-light ratio (M/L) versus colour relation prescribed by Roediger & Courteau (2015). Explicitly, for a given wavelength λ, the relevant equations are:

$$\log \Sigma_{\star,\lambda} = 0.4(m_{abs,\odot,\lambda} - \mu_\lambda) + \log (M/L)_\lambda + 8.629 \tag{4.1}$$

$$\log (M/L)_\lambda = m_\lambda \times (\text{colour}) + b_\lambda \tag{4.2}$$

In this work, we computed the stellar mass density in the g-band because it is the deepest imaging in our dataset and the $g-r$ colour is used to calculate $(M/L)_g$, using $m_g = 2.029$ and $b_g = -0.984$ (see Table A1. in Roediger & Courteau 2015).

Traditionally, truncations have been identified using the surface brightness profiles of their host galaxies. Here all three profiles for each galaxy, namely, its surface brightness, $g-r$ colour and stellar mass density profile, were visually examined for an edge-like feature. This was performed to account for cases where the edge of a galaxy may not be evident or noticeable in its g or r-band surface brightness profile but in either its colour or mass density profile or both. Examples of the features identified in this work as an edge for each morphological type will be

[3] http://research.iac.es/proyecto/miles/pages/photometric-predictions-based-on-e-miles-seds.php

Este documento incorpora firma electrónica, y es copia auténtica de un documento electrónico archivado por la ULL según la Ley 39/2015.
Su autenticidad puede ser contrastada en la siguiente dirección https://sede.ull.es/validacion/

Identificador del documento: 2622200 Código de verificación: mbm0ekWs

Firmado por:	ROSHAN NUSHKIA CHAMBA *UNIVERSIDAD DE LA LAGUNA*	Fecha: 07/07/2020 13:28:26
	IGNACIO TRUJILLO CABRERA *UNIVERSIDAD DE LA LAGUNA*	07/07/2020 13:58:21
	Johan Hendrik Knapen Koelstra *UNIVERSIDAD DE LA LAGUNA*	07/07/2020 15:23:08
	María de las Maravillas Aguiar Aguilar *UNIVERSIDAD DE LA LAGUNA*	08/07/2020 15:55:11

Universidad de La Laguna
Oficina de Sede Electrónica
Entrada
Nº registro: 2020/46124
Nº reg. oficina: OF002/2020/45309
Fecha: 07/07/2020 15:26:22

shown in the next section. With this careful examination, the radial position, $g-r$ colour and stellar mass density at the edge were also determined. These measurements will be called $R_{\rm edge}$, $(g-r)_{\rm edge}$ and $\Sigma_\star(R_{\rm edge})$ respectively. Additionally, using $(g-r)_{\rm edge}$, a proxy for the age of the stellar population at $R_{\rm edge}$ was ascertained using the MILES predictions, fixing the metallicity at $[M/H] = 0$ and $[M/H] = -0.71$, both of which are acceptable values to probe the stellar populations in dwarfs and giants (see Vazdekis et al. 2012; Radburn-Smith et al. 2014).

4.5 Results

A feature compatible with an edge was found in 741 galaxies out of the 1005 galaxies in the parent sample. Edges were also identified for the 21 galaxies taken from B12 and P17. However, the significant improvements in image masking and background estimation have only been completed (at the moment of writing this Chapter) for the full spiral galaxy sample in this work (330 objects) and only for a handful of elliptical and dwarf galaxies for demonstration in this thesis. Nevertheless, in this section I present preliminary results from this ongoing analysis.

Figure 4.5 shows the μ_g, $g-r$ colour and $\Sigma_\star$ profiles derived in this work for the 741 galaxies with an identified edge (grey) and the average profile (coloured) for each morphological type. The profiles are plotted as a function of $R/R_{\rm edge}$ where R is the distance from the centre of the galaxy and $R_{\rm edge}$ is the location of the edge that has been visually identified. We now focus on the profiles of the spiral galaxies (middle panels) as at the current stage of this research programme, this sub-sample has been reviewed.

One would expect to see a clear edge-like feature at $R/R_{\rm edge} = 1$ in all the averaged radial profiles. However, a change in slope at this location is only clear to the eye in the averaged $g-r$ colour profile of the late-type galaxy groups, Sa–Sab, Sb–Sbc and Sc–Scd. The reason why a clear feature is not as prominent in the averaged μ_g and $\Sigma_\star$ profiles is very likely a consequence of the imprecision in our visual identification of the edge in these galaxies. The typical dispersion in our measurement of $R_{\rm edge}$ is $\sigma_{\rm vis} = 0.04 \pm 0.005$ dex, which was computed using the visual inspections by Chamba and Trujillo for a sub-sample of galaxies that have been repeated (200 objects). While this dispersion is small, it could transfer into an error of $< 5\%$ in the absolute value of a given $R_{\rm edge}$. Additionally, as mentioned in Sect. 4.2, the edge may not appear in the same radial profile in all the galaxies, e.g. the edge could appear in the $g-r$ colour profile and $\Sigma_\star$ but not in the μ_g profile. Therefore, as each profile is weighted equally when computing the average, it is possible that the presence of the feature in, for example, the μ_g profile of galaxy G1 is softened by the absence of the feature in the μ_g profile of galaxy G2. If this description is accurate, and all these issues affect the μ_g, $g-r$ colour and $\Sigma_\star$ profiles equally, then our results imply that the $g-r$ profiles can provide better constraints as to where the edge of a galaxy is located than the μ_g and $\Sigma_\star$ profiles.

In addition to the change in slope at $R/R_{\rm edge} = 1$ in the average $g-r$ colour profiles, we also find a clear stratification of the late-type galaxies: the $g-r$ colour profiles of Sa–Sab galaxies are systematically redder than those of the Sc–Scd ones. Consequently, the $(g-r)_{\rm edge}$ of the Sc–Scd galaxies are bluer than that of the Sa–Sab galaxies. This result is reminiscent of the stratification in the size–stellar mass plane discussed in Chapter 2 (Sect. 2.7) where the Sc–Scd galaxies were found to populate the upper portion of the size–mass plane, the Sb–Sbc the intermediate region and Sa–Sab galaxies populated the lower portion of the relation.

This stratification of the late-types is further illustrated in Fig. 4.6 using individual examples

Este documento incorpora firma electrónica, y es copia auténtica de un documento electrónico archivado por la ULL según la Ley 39/2015.
Su autenticidad puede ser contrastada en la siguiente dirección https://sede.ull.es/validacion/

Identificador del documento: 2622200 Código de verificación: mbm0ekWs

Firmado por:	ROSHAN NUSHKIA CHAMBA *UNIVERSIDAD DE LA LAGUNA*	Fecha: 07/07/2020 13:28:26
	IGNACIO TRUJILLO CABRERA *UNIVERSIDAD DE LA LAGUNA*	07/07/2020 13:58:21
	Johan Hendrik Knapen Koelstra *UNIVERSIDAD DE LA LAGUNA*	07/07/2020 15:23:08
	María de las Maravillas Aguiar Aguilar *UNIVERSIDAD DE LA LAGUNA*	08/07/2020 15:55:11

Universidad de La Laguna
Oficina de Sede Electrónica
Entrada
Nº registro: 2020/46124
Nº reg. oficina: OF002/2020/45309
Fecha: 07/07/2020 15:26:22

of Sa/Sab and Sc/Scd galaxies from the parent sample with stellar masses $10^{10} M_{\odot}, 3 \times 10^{10} M_{\odot}$ and $10^{11} M_{\odot}$, which represents the full mass range of spiral galaxies in our sample in three bins.

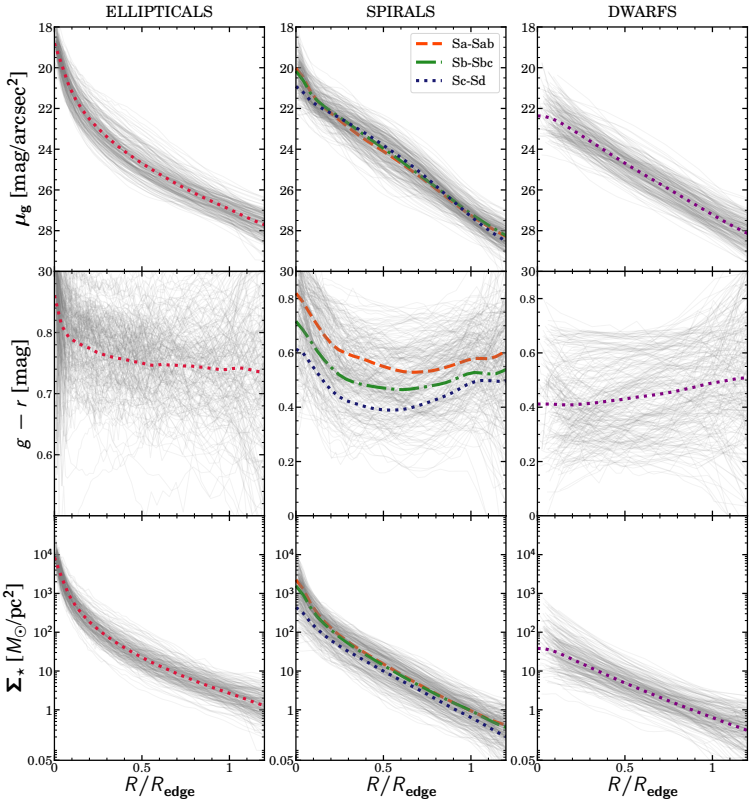

Figure 4.5: Preliminary μ_g, $g-r$ and $\Sigma_\star$ profiles of galaxies in the sample. *Left to right*: The profiles for elliptical, spiral and dwarf galaxies. *Top to bottom*: Panels showing the μ_g (top), $g-r$ colour (middle) and $\Sigma_\star$ (bottom) profiles of galaxies in grey. The average profile for each morphological type is over-plotted and labelled in colour. The x-axes of the profiles are scaled using the measured $R_{\rm edge}$ locations.

The top panels of the figures show *gri*-band composite images of the galaxies, overlaid on the $g+r+i$ image in grey scale, and the bottom panels show their μ_g, $g-r$ colour and $\Sigma_\star$ profiles in the g-band. $R_{\rm edge}$ is marked and labelled using a pink contour on the galaxy images and vertical dotted lines in the profile panels. The SDSS J2000 identifier for each galaxy is also included for reference. All the profiles are shown up to which they can be confidently trusted. This is roughly down to $\mu_r \sim 28\,\mathrm{mag/arcsec^2}$.

Este documento incorpora firma electrónica, y es copia auténtica de un documento electrónico archivado por la ULL según la Ley 39/2015.
Su autenticidad puede ser contrastada en la siguiente dirección https://sede.ull.es/validacion/

Identificador del documento: 2622200 Código de verificación: mbm0ekWs

Firmado por:	ROSHAN NUSHKIA CHAMBA *UNIVERSIDAD DE LA LAGUNA*	Fecha: 07/07/2020 13:28:26
	IGNACIO TRUJILLO CABRERA *UNIVERSIDAD DE LA LAGUNA*	07/07/2020 13:58:21
	Johan Hendrik Knapen Koelstra *UNIVERSIDAD DE LA LAGUNA*	07/07/2020 15:23:08
	María de las Maravillas Aguiar Aguilar *UNIVERSIDAD DE LA LAGUNA*	08/07/2020 15:55:11

Universidad de La Laguna
Oficina de Sede Electrónica
Entrada
Nº registro: 2020/46124
Nº reg. oficina: OF002/2020/45309
Fecha: 07/07/2020 15:26:22

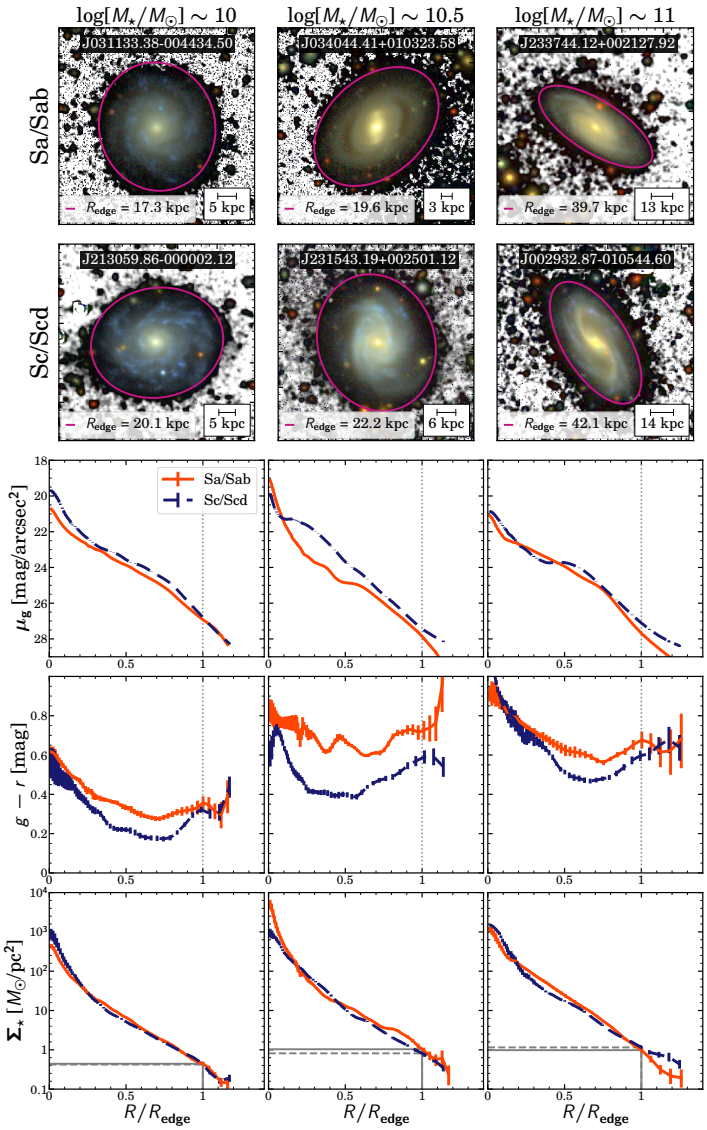

Figure 4.6: Individual examples of Sa/Sab and Sc/Scd galaxies from the parent sample. *Left to right*: The first two rows show *gri*-band colour composite images, overlaid on the background $(g + r + i)$ in grey scale, of a galaxy belonging to each morphological type at a fixed stellar mass: $10^{10}M_\odot$, $3 \times 10^{10}M_\odot$ and $10^{11}M_\odot$. SDSS J2000 identifiers are included for reference. Subsequent rows show the μ_g, $g - r$ and $\Sigma_\star$ profiles for these objects. $R_{\rm edge}$ of the objects are clearly labelled using a pink isophote in the images and vertical grey dotted lines in the profile panels. The stellar mass density at $R_{\rm edge}$ is also marked as a horizontal line for each galaxy in the $\Sigma_\star$ profile panels at the bottom.

Este documento incorpora firma electrónica, y es copia auténtica de un documento electrónico archivado por la ULL según la Ley 39/2015.
Su autenticidad puede ser contrastada en la siguiente dirección https://sede.ull.es/validacion/

Identificador del documento: 2622200 Código de verificación: mbm0ekWs

Firmado por:	ROSHAN NUSHKIA CHAMBA *UNIVERSIDAD DE LA LAGUNA*	Fecha: 07/07/2020 13:28:26
	IGNACIO TRUJILLO CABRERA *UNIVERSIDAD DE LA LAGUNA*	07/07/2020 13:58:21
	Johan Hendrik Knapen Koelstra *UNIVERSIDAD DE LA LAGUNA*	07/07/2020 15:23:08
	María de las Maravillas Aguiar Aguilar *UNIVERSIDAD DE LA LAGUNA*	08/07/2020 15:55:11

Universidad de La Laguna
Oficina de Sede Electrónica
Entrada
Nº registro: 2020/46124
Nº reg. oficina: OF002/2020/45309
Fecha: 07/07/2020 15:26:22

In Fig. 4.6, notice that $\Sigma_\star(R_{\rm edge}) \sim 1 M_\odot/{\rm pc}^2$ for the Milky Way-mass galaxies ($\sim 3 \times 10^{10} M_\odot$) while $\Sigma_\star(R_{\rm edge})$ is slightly lower for galaxies with stellar masses of $\sim 10^{10} M_\odot$. The figure also provides a first order picture as to how the profiles of the galaxies change with increasing stellar mass. As the stellar mass increases from $10^{10} M_\odot$ to $10^{11} M_\odot$, the global colour of the galaxy becomes redder. For example, for the Sc/Scd galaxies shown, the global $g-r$ colour appears to increase from ~ 0.3 to ~ 0.6. These results will be further supported in the next section.

Similarly, individual examples of massive ellipticals ($M_\star \sim 10^{11.5} M_\odot$) are shown in Fig. 4.7 below.

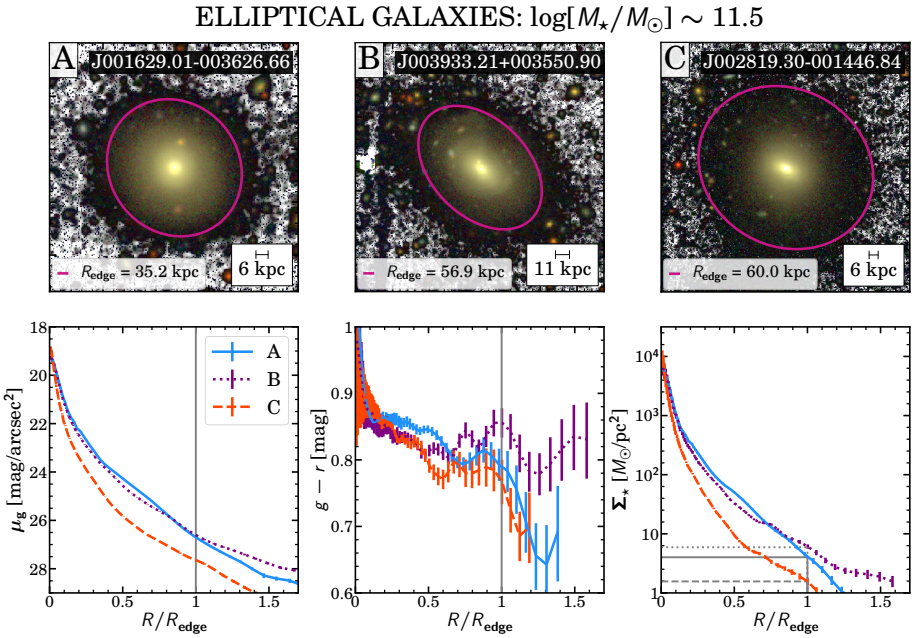

Figure 4.7: Three examples of elliptical galaxies from the parent sample with stellar mass $\log[M_\star/M_\odot] \sim 10^{11}$. *Top: gri*-band colour composite images, overlaid on the background ($g+r+i$) in grey scale, of the galaxies denoted as A (left), B (middle) and C (right). The SDSS J2000 identifier and $R_{\rm edge}$ are labelled for these galaxies as in Fig. 4.6. *Bottom, left to right*: The μ_g, $g-r$ and $\Sigma_\star$ profiles of the objects. The edges for these galaxies are most clearly visible in their colour profiles, in combination with their stellar mass density profiles. The location of this edge feature occurs at mass densities $\Sigma_\star(R_{\rm edge}) > 1\, M_\odot/{\rm pc}^2$.

For these elliptical galaxies, features compatible with the traditional truncations of spiral galaxies are most clearly visible in their colour profiles. From the centre of the galaxy, the $g-r$ colour remains red on average and at the labelled $R_{\rm edge}$ location, a rapid drop towards bluer

Este documento incorpora firma electrónica, y es copia auténtica de un documento electrónico archivado por la ULL según la Ley 39/2015.
Su autenticidad puede ser contrastada en la siguiente dirección https://sede.ull.es/validacion/

Identificador del documento: 2622200 Código de verificación: mbm0ekWs

Firmado por:	ROSHAN NUSHKIA CHAMBA *UNIVERSIDAD DE LA LAGUNA*	Fecha: 07/07/2020 13:28:26
	IGNACIO TRUJILLO CABRERA *UNIVERSIDAD DE LA LAGUNA*	07/07/2020 13:58:21
	Johan Hendrik Knapen Koelstra *UNIVERSIDAD DE LA LAGUNA*	07/07/2020 15:23:08
	María de las Maravillas Aguiar Aguilar *UNIVERSIDAD DE LA LAGUNA*	08/07/2020 15:55:11

Universidad de La Laguna
Oficina de Sede Electrónica
Entrada
Nº registro: 2020/46124
Nº reg. oficina: OF002/2020/45309
Fecha: 07/07/2020 15:26:22

colours occurs. As discussed in Chapter 2, the stellar mass density at the location of the edge is expected to be higher for massive galaxies than that in Milky Way-mass objects, due to their enhanced star formation in the past. In this figure, we find that $\Sigma_\star(R_{\rm edge}) \sim 2$–$10\,M_\odot/{\rm pc}^2$, i.e. $> 1\,M_\odot/{\rm pc}^2$, for the galaxies shown which is a result consistent with this expectation.

The opposite argument holds for the dwarf galaxies. In Fig. 4.8 below, we show three examples of dwarf galaxies with a stellar mass of $\sim 10^8 M_\odot$. These examples were specifically chosen to highlight the diversity in the shape of the colour profiles of dwarf galaxies at this stellar mass.

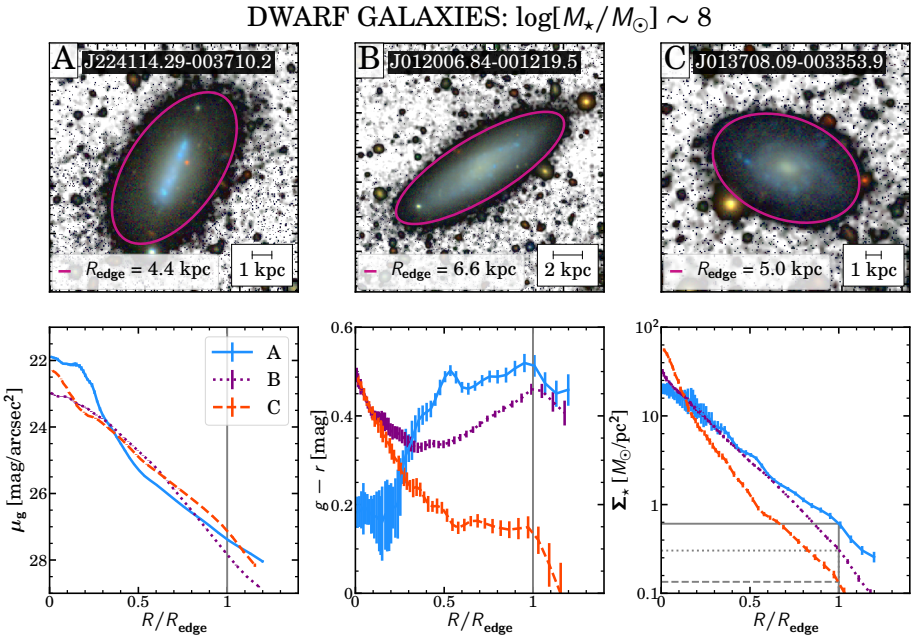

Figure 4.8: As in Fig. 4.7, now for three dwarf galaxies with stellar mass $\log[M_\star/M_\odot] \sim 10^8$. These examples were specifically chosen to illustrate the diversity in the colour profiles of this galaxy population. The location of the edge occurs at mass densities $\Sigma_\star(R_{\rm edge}) < 1\,M_\odot/{\rm pc}^2$.

For these dwarfs, $R_{\rm edge}$ is also clearly visible in their $g-r$ profiles, at much bluer colours compared to the elliptical galaxies. Consequently, $\Sigma_\star(R_{\rm edge}) < 1\,M_\odot/{\rm pc}^2$ for these galaxies. As the integrated gas to star conversion in dwarfs is expected to be much more inefficient compared to the massive galaxies, the results shown here is also consistent with this expectation. We expand on these results for the dwarfs and ellipticals in the next section.

It should be noted that in the cases where hints of an edge appear in the μ (or $\Sigma_\star$) and $g-r$ profiles, we made a compromise and selected $R_{\rm edge}$ based on the average location of the features in both profiles. For this reason, there can be an offset in the location of the change in slope in

Este documento incorpora firma electrónica, y es copia auténtica de un documento electrónico archivado por la ULL según la Ley 39/2015.
Su autenticidad puede ser contrastada en la siguiente dirección https://sede.ull.es/validacion/

Identificador del documento: 2622200 Código de verificación: mbm0ekWs

Firmado por:	ROSHAN NUSHKIA CHAMBA *UNIVERSIDAD DE LA LAGUNA*	Fecha: 07/07/2020 13:28:26
	IGNACIO TRUJILLO CABRERA *UNIVERSIDAD DE LA LAGUNA*	07/07/2020 13:58:21
	Johan Hendrik Knapen Koelstra *UNIVERSIDAD DE LA LAGUNA*	07/07/2020 15:23:08
	María de las Maravillas Aguiar Aguilar *UNIVERSIDAD DE LA LAGUNA*	08/07/2020 15:55:11

Universidad de La Laguna
Oficina de Sede Electrónica
Entrada
Nº registro: 2020/46124
Nº reg. oficina: OF002/2020/45309
Fecha: 07/07/2020 15:26:22

the $g-r$ profile and the marked $R_{\rm edge}$ (middle and right panels in Fig. 4.6 and middle panel in Fig. 4.7). We are in the process of quantifying this further.

For completeness, the profiles created in this work for three galaxies with $z < 0.01$, namely, M77 studied in B12, NGC 493 and NGC 1090 in P17 are shown in Fig. 4.9 on the next page. Similar to the cases described above in Figs. 4.6–4.8, the edge is most clearly visible in the $g-r$ colour profile. A very strong change in colour at the edge is particularly prominent in NGC 1090 (middle), while a more softer change in slope occurs at the edge in that of NGC 493 and M77. In all three cases, the radial colour of the galaxy becomes redder beyond the location of the edge. The presence of edges are not reported for these galaxies in B12 (M77) or P17 (NGC 493 and NGC 1090). The μ_g profiles shown here for these galaxies have been extracted down to $\sim 32\,{\rm mag/arcsec^2}$ because the objects are relatively nearby: 23.1 (for NGC 493; Sorce et al. 2014), 28.6 (NGC 1090; Tully et al. 2016) and 10.1 Mpc (M77; Tully et al. 2009). Consequently, a larger number of pixels are available to average over the elliptical annuli when extracting the profiles, which means that the signal-to-noise ratio in the outskirts is higher. However, the $g-r$ and $\Sigma_\star$ profiles can still only be confidently trusted down to $\mu_g \sim 30\,{\rm mag/arcsec^2}$.

Until now in this Section, we have shown the profiles of only a handful of examples in the galaxy sample to demonstrate how the edge of a galaxy has been visually identified in this work. In most, if not all, of the cases shown, the edge was most evident in the $g-r$ colour profile. Additionally, in all the galaxies shown, the location of the edge marked in this work (called $R_{\rm edge}$) encloses the bulk of the light distribution in the galaxies and is thus closer to a concept of size related to the boundary of objects. However, it is clear that the way in which the edge manifests itself in the profiles is not the same for each galaxy and thus the galaxies must be evaluated on a case-by-case basis. We have undertaken such a programme here for 1026 galaxies (Sect. 4.3) and report the presence of edges in 762 of these objects: 741 in the parent sample and 21 in the combined B12 and P17 sample. These results are shown in Figs. 4.10 and 4.11.

Figure 4.10 shows the observed $R_{\rm edge}$–stellar mass plane (left panels) and the $\Sigma_\star(R_{\rm edge})$–stellar mass plane (right panels). From top to bottom, each row shows the data points in both planes labelled according to each galaxy's morphology, $(g-r)_{\rm edge}$ and age of the stellar population at the edge location. The age at $R_{\rm edge}$ shown was computed using a fixed metallicity of $[M/H] = -0.71$ and the distribution does not change with $[M/H] = 0$. For clarity, the measurements in this work for the additional galaxies taken from B12 and P17 are shown in the $R_{\rm edge}$– and $\Sigma_\star(R_{\rm edge})$–stellar mass planes in Fig. 4.11.

Este documento incorpora firma electrónica, y es copia auténtica de un documento electrónico archivado por la ULL según la Ley 39/2015.
Su autenticidad puede ser contrastada en la siguiente dirección https://sede.ull.es/validacion/

Identificador del documento: 2622200 Código de verificación: mbm0ekWs

Firmado por:	ROSHAN NUSHKIA CHAMBA *UNIVERSIDAD DE LA LAGUNA*	Fecha: 07/07/2020 13:28:26
	IGNACIO TRUJILLO CABRERA *UNIVERSIDAD DE LA LAGUNA*	07/07/2020 13:58:21
	Johan Hendrik Knapen Koelstra *UNIVERSIDAD DE LA LAGUNA*	07/07/2020 15:23:08
	María de las Maravillas Aguiar Aguilar *UNIVERSIDAD DE LA LAGUNA*	08/07/2020 15:55:11

Universidad de La Laguna
Oficina de Sede Electrónica
Entrada
Nº registro: 2020/46124
Nº reg. oficina: OF002/2020/45309
Fecha: 07/07/2020 15:26:22

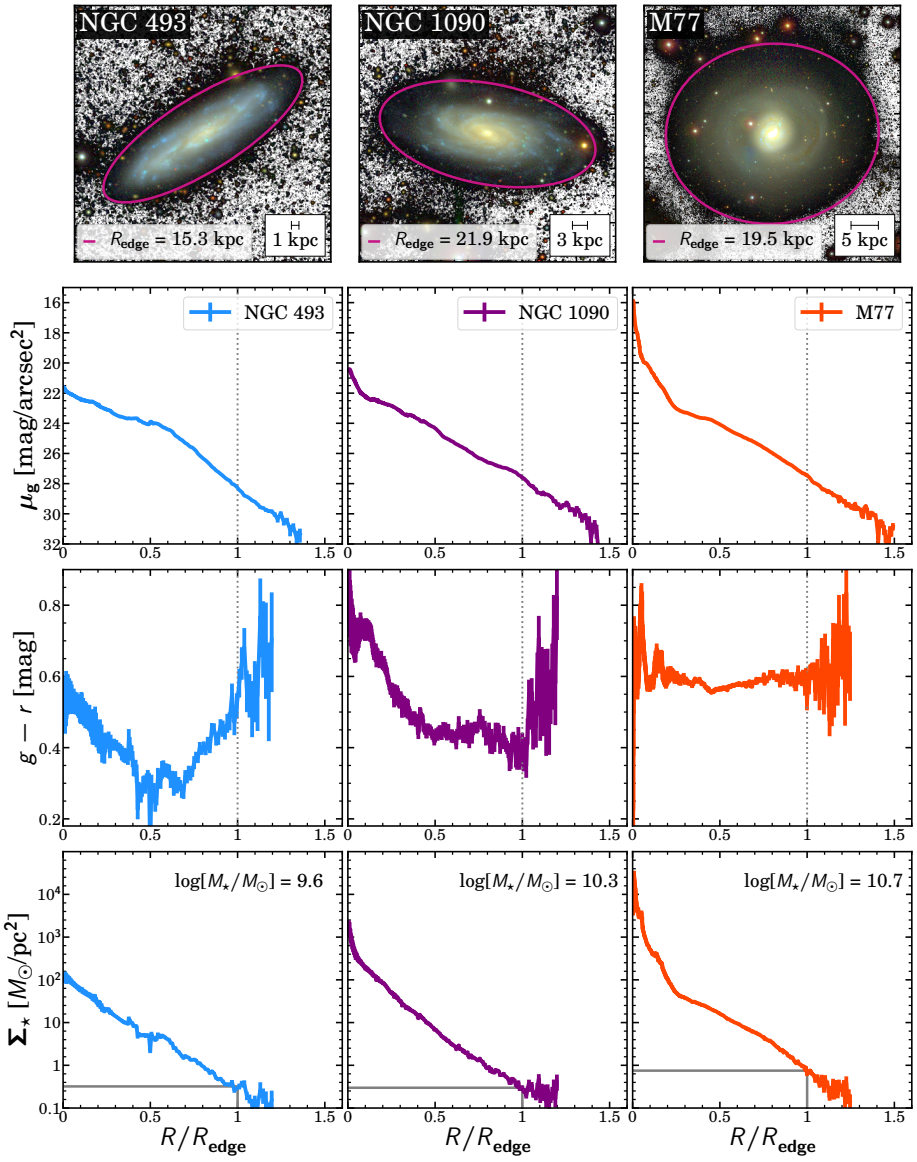

Figure 4.9: As in Fig. 4.6, now for NGC 493 (left), NGC 1090 (middle) and M77 (right). The distances to the objects were taken from Sorce et al. (2014), Tully et al. (2016) and Tully et al. (2009) respectively. The μ_g profiles of these objects can be extracted down to ~ 32 mag/arcsec^2 as they are relatively nearby compared to other galaxies in the sample. However, the $g-r$ and $\Sigma_\star$ profiles can only be trusted down to $\mu_g \sim 30$ mag/arcsec^2.

Este documento incorpora firma electrónica, y es copia auténtica de un documento electrónico archivado por la ULL según la Ley 39/2015.
Su autenticidad puede ser contrastada en la siguiente dirección https://sede.ull.es/validacion/

Identificador del documento: 2622200 Código de verificación: mbm0ekWs

Firmado por:	ROSHAN NUSHKIA CHAMBA *UNIVERSIDAD DE LA LAGUNA*	Fecha: 07/07/2020 13:28:26
	IGNACIO TRUJILLO CABRERA *UNIVERSIDAD DE LA LAGUNA*	07/07/2020 13:58:21
	Johan Hendrik Knapen Koelstra *UNIVERSIDAD DE LA LAGUNA*	07/07/2020 15:23:08
	María de las Maravillas Aguiar Aguilar *UNIVERSIDAD DE LA LAGUNA*	08/07/2020 15:55:11

Universidad de La Laguna
Oficina de Sede Electrónica
Entrada
Nº registro: 2020/46124
Nº reg. oficina: OF002/2020/45309
Fecha: 07/07/2020 15:26:22

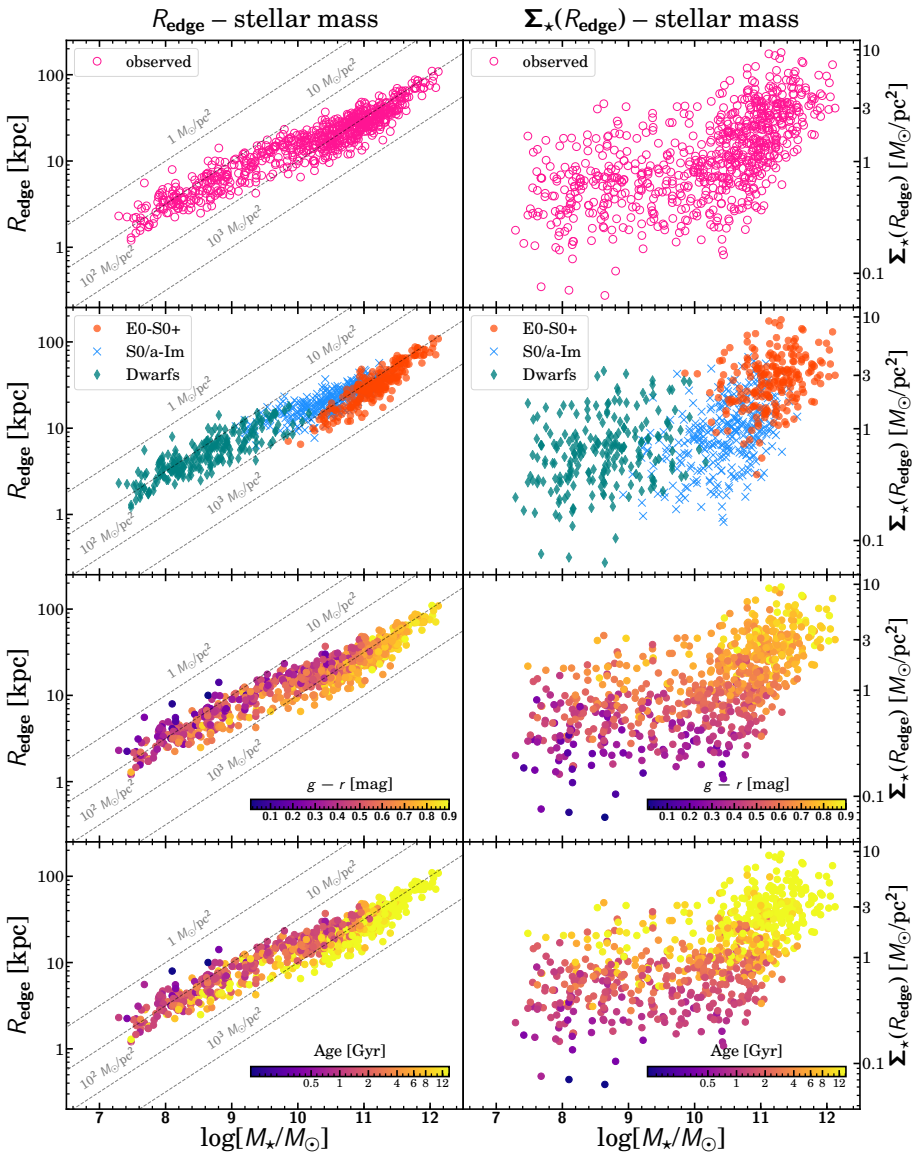

Figure 4.10: $R_{\rm edge}$–stellar mass (left) and $\Sigma_\star(R_{\rm edge})$–stellar mass (right) relations derived in this work for the parent sample. Only those galaxies where an edge was identified are plotted (741 objects). The grey lines in the $R_{\rm edge}$–stellar mass planes are lines of constant stellar mass density within the size of the object. *Top to bottom:* Each row shows the same observed relations (top), colour coded according to the morphology of the galaxies, $(g-r)_{\rm edge}$ and a proxy for the age at $R_{\rm edge}$, for a fixed metallicity $[M/H] = -0.71$. The observed $R_{\rm edge}$–stellar mass relation has a similar structure to the R_1–stellar mass relation in Chapter 2

Este documento incorpora firma electrónica, y es copia auténtica de un documento electrónico archivado por la ULL según la Ley 39/2015.
Su autenticidad puede ser contrastada en la siguiente dirección https://sede.ull.es/validacion/

Identificador del documento: 2622200 Código de verificación: mbm0ekWs

Firmado por:	ROSHAN NUSHKIA CHAMBA *UNIVERSIDAD DE LA LAGUNA*	Fecha: 07/07/2020 13:28:26
	IGNACIO TRUJILLO CABRERA *UNIVERSIDAD DE LA LAGUNA*	07/07/2020 13:58:21
	Johan Hendrik Knapen Koelstra *UNIVERSIDAD DE LA LAGUNA*	07/07/2020 15:23:08
	María de las Maravillas Aguiar Aguilar *UNIVERSIDAD DE LA LAGUNA*	08/07/2020 15:55:11

Universidad de La Laguna
Oficina de Sede Electrónica
Entrada
Nº registro: 2020/46124
Nº reg. oficina: OF002/2020/45309
Fecha: 07/07/2020 15:26:22

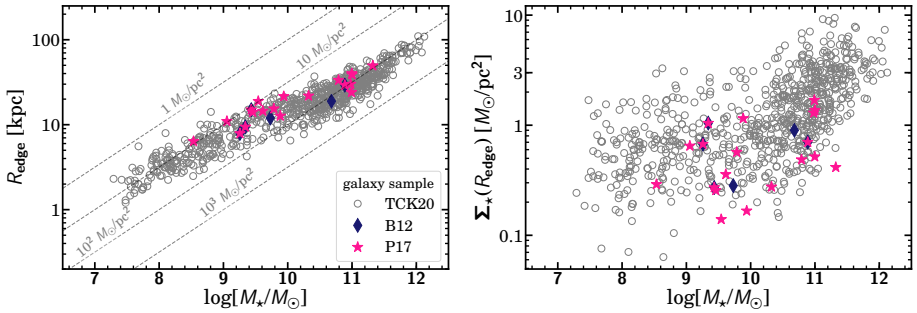

Figure 4.11: Observed $R_{\rm edge}$–stellar mass (left) and $\Sigma_\star(R_{\rm edge})$–stellar mass (right) relations, now including the measurements in this work for the sample of galaxies studied in B12 and P17. The grey circles are the measurements for the parent sample.

The main characteristics of these results are:

- As $R_{\rm edge}$ increases with stellar mass, the corresponding $\Sigma_\star(R_{\rm edge})$ also increases, but non-linearly with a change in slope at $M_\star \sim 2.5 \times 10^{10}\,M_\odot$.
- At a fixed stellar mass in the spiral galaxy regime $10^{10}\,M_\odot < M_\star < 10^{11}\,M_\odot$ in the $R_{\rm edge}$–stellar mass plane, as $R_{\rm edge}$ increases, the observed $(g-r)_{\rm edge}$ changes from ~ 0.7 to ~ 0.35. A similar gradient is visible for the low-mass galaxies ($M_\star < 10^{10} M_\odot$). These trends are also evident in the $\Sigma_\star(R_{\rm edge})$–stellar mass relation. The result is consistent with the observed stratification of the Sa–Sab and Sc–Scd spiral galaxies in Fig. 4.5 and the size–mass plane reported in Chapter 2.
- Using a fixed metallicity of $[M/H] = -0.71$ (e.g. Radburn-Smith et al. 2014), the observed colour gradients in the $R_{\rm edge}$– and $\Sigma_\star(R_{\rm edge})$–stellar mass planes also reflect a gradient in the age of the stellar population at the edges of galaxies. At a fixed stellar mass, the age for the spiral galaxy population increases from ~ 2 Gyr to ~ 12 Gyr as the size of the galaxy decreases. These results are also consistent with a fixed metallicity of $[M/H] = 0$.
- In Fig. 4.11, the galaxies from B12 and P17 lie in the lower portion of the $\Sigma_\star(R_{\rm edge})$–stellar mass relation and, consequently, the upper half of the $R_{\rm edge}$–stellar mass plane. This is because the samples from B12 and P17 comprise of Sb, Sc and galaxies of later types. Therefore, this result is also consistent with the observed stratification of late-type galaxies.

4.6 Analysis

To analyse the results presented in the previous Section, we show the best fit lines to the observed $R_{\rm edge}$– and $\Sigma_\star(R_{\rm edge})$–stellar mass planes in Fig. 4.12 below. The global $R_{\rm edge}$–stellar mass plane follows a power law of the form $R_{\rm edge} \propto M_\star^\beta$ where $\beta = 0.33 \pm 0.006$ (purple line) and the relation has a dispersion of $\sigma_{R_{\rm edge}} = 0.10 \pm 0.009$ dex. This value is slightly lower

Este documento incorpora firma electrónica, y es copia auténtica de un documento electrónico archivado por la ULL según la Ley 39/2015.
Su autenticidad puede ser contrastada en la siguiente dirección https://sede.ull.es/validacion/

Identificador del documento: 2622200 Código de verificación: mbm0ekWs

Firmado por:	ROSHAN NUSHKIA CHAMBA *UNIVERSIDAD DE LA LAGUNA*	Fecha: 07/07/2020 13:28:26
	IGNACIO TRUJILLO CABRERA *UNIVERSIDAD DE LA LAGUNA*	07/07/2020 13:58:21
	Johan Hendrik Knapen Koelstra *UNIVERSIDAD DE LA LAGUNA*	07/07/2020 15:23:08
	María de las Maravillas Aguiar Aguilar *UNIVERSIDAD DE LA LAGUNA*	08/07/2020 15:55:11

Universidad de La Laguna
Oficina de Sede Electrónica
Entrada
Nº registro: 2020/46124
Nº reg. oficina: OF002/2020/45309
Fecha: 07/07/2020 15:26:22

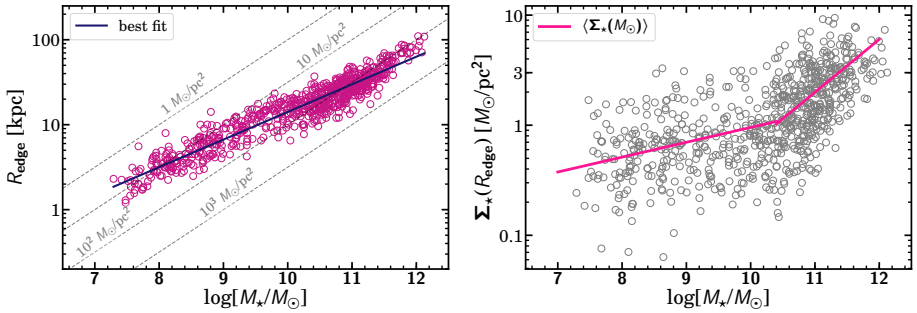

Figure 4.12: Best fit lines for the observed $R_{\rm edge}$–stellar mass plane (left) and the $\Sigma_\star(R_{\rm edge})$–stellar mass plane (right) for the galaxies in the parent sample.

than the global slope of the R_1–stellar mass relation discussed in Chapter 2 (Sec. 2.6). But the dispersion of the relation is slightly higher $\sigma_{R_{\rm edge}} = 0.10 \pm 0.009$ dex. This is because there is an extra uncertainty stemming from the visual identification of $R_{\rm edge}$ ($\sigma_{\rm vis} \sim 0.04$ dex) that was not present in measuring R_1. Naively removing $\sigma_{\rm vis}$ from $\sigma_{R_{\rm edge}}$ in quadrature gives $\bar{\sigma}_{R_{\rm edge}} = 0.092 \pm 0.007$ dex, which is compatible with the observed dispersion in the R_1–stellar mass relation $\sigma_{R_1} = 0.089 \pm 0.005$ dex.

For the individual galaxy populations, β is 0.53 ± 0.02 for the elliptical galaxies (E0–S0+), 0.28 ± 0.02 for spirals (S0/a–Im) and 0.345 ± 0.03 for the dwarfs. All these values are slightly lower compared to the results from the R_1–stellar mass relation. However, the global structure of these size–mass relations are similar: galaxies follow the power law with $\beta = 0.33$ below $M_\star < 10^{11} M_\odot$ and $\beta = 0.53$ above $M_\star > 10^{11} M_\odot$.

In the case of the the $\Sigma_\star(R_{\rm edge})$–stellar mass plane, at the time of writing this thesis we obtained two linear fits to describe the data by separating the sample in two intervals at $M_\star \sim 2.5 \times 10^{10} M_\odot$, i.e. $M_\star < 2.5 \times 10^{10} M_\odot$ (I_1) and $M_\star \geq 2.5 \times 10^{10} M_\odot$ (I_2). We did this because 1) a single polynomial fit to the data performed very poorly and 2) spiral galaxies are over represented in our sample (309 objects out of the 741 galaxies with clear edges). Therefore, by splitting the sample at a stellar mass of $\sim 2.5 \times 10^{10}$, the two intervals I_1 and I_2 are more comparable in terms of sample size (403 and 338 galaxies, respectively) and it is also the location where the slope of the $\Sigma_\star(R_{\rm edge})$–stellar mass relation increases. We have used these two linear fits to determine the average location of the edge (in mass density) $\langle \Sigma_{\rm edge}(M_\star) \rangle$, as a function of galaxy stellar mass, given by:

$$\log[\langle \Sigma_{\rm edge}(M_\star) \rangle] = 0.13 \log[M_\star/M_\odot] - 1.32 \qquad M_\star < 2.5 \times 10^{10} M_\odot (I_1) \tag{4.3}$$

$$\log[\langle \Sigma_{\rm edge}(M_\star) \rangle] = 0.46 \log[M_\star/M_\odot] - 4.74 \qquad M_\star \geq 2.5 \times 10^{10} M_\odot (I_2) \tag{4.4}$$

The above $\langle \Sigma_{\rm edge}(M_\star) \rangle$ relations are plotted as the pink lines in the right panel of Fig. 4.12. The uncertainties in the slopes are $\beta_{I_1} = 0.13 \pm 0.03$ and $\beta_{I_2} = 0.46 \pm 0.05$ and the dispersion in both the relations are similar: $\sigma_{I_1} = 0.29 \pm 0.02$ dex and $\sigma_{I_2} = 0.28 \pm 0.02$ dex.

Este documento incorpora firma electrónica, y es copia auténtica de un documento electrónico archivado por la ULL según la Ley 39/2015.
Su autenticidad puede ser contrastada en la siguiente dirección https://sede.ull.es/validacion/

Identificador del documento: 2622200 Código de verificación: mbm0ekWs

Firmado por:	ROSHAN NUSHKIA CHAMBA *UNIVERSIDAD DE LA LAGUNA*	Fecha: 07/07/2020 13:28:26
	IGNACIO TRUJILLO CABRERA *UNIVERSIDAD DE LA LAGUNA*	07/07/2020 13:58:21
	Johan Hendrik Knapen Koelstra *UNIVERSIDAD DE LA LAGUNA*	07/07/2020 15:23:08
	María de las Maravillas Aguiar Aguilar *UNIVERSIDAD DE LA LAGUNA*	08/07/2020 15:55:11

Universidad de La Laguna
Oficina de Sede Electrónica
Entrada
Nº registro: 2020/46124
Nº reg. oficina: OF002/2020/45309
Fecha: 07/07/2020 15:26:22

We use the linear fits to the $R_{\rm edge}$– and $\Sigma_\star(R_{\rm edge})$–stellar mass planes to illustrate the distribution of the parent sample studied in this work in their measured $R_{\rm edge}$, $\Sigma_\star(R_{\rm edge})$ and $(g-r)_{\rm edge}$ as histograms in Fig. 4.13. For clarity, we have re-scaled these histograms because our sample size is not equal for each morphological type and colour. The top right panel shows that, on average, $\Sigma_\star(R_{\rm edge}) \sim 0.5\,M_\odot/{\rm pc}^2$ for the dwarfs, $\sim 1\,M_\odot/{\rm pc}^2$ for the spirals and $\sim 3\,M_\odot/{\rm pc}^2$ for the elliptical galaxies in the sample. In the bottom panels, on average, galaxies located in the upper half of both, the $R_{\rm edge}$– and $\Sigma_\star(R_{\rm edge})$–stellar mass relations, have bluer edges compared to the lower half. All these results are nicely consistent with the idea that more massive galaxies are expected to have a higher threshold for star formation than low-mass galaxies (also discussed in Chapter 2).

As an exercise, we also use the $\langle\Sigma_{\rm edge}(M_\star)\rangle$ relations (Eqs. 4.3) to ascertain a proxy for location of the edge of each galaxy, $\langle R_{\rm edge}\rangle$. For each galaxy with stellar mass $M_\star$ we locate the position of $\langle\Sigma_{\rm edge}(M_\star)\rangle$ using the stellar mass density profile of the object, i.e. $\Sigma_\star(\langle R_{\rm edge}\rangle) = \langle\Sigma_{\rm edge}(M_\star)\rangle$. The resulting $\langle R_{\rm edge}\rangle$–stellar mass relation for the parent sample is shown in Fig. 4.14. The $\langle R_{\rm edge}\rangle$–stellar mass plane also follows a power law of the form $\langle R_{\rm edge}\rangle \propto M_\star^{\langle\beta\rangle}$. The dispersion of this plane is less than that of the observed $R_{\rm edge}$–stellar mass plane (Fig. 4.12): $\sigma_{\langle R_{\rm edge}\rangle} = 0.082 \pm 0.008$ dex, while the slope is compatible $\langle\beta\rangle = 0.32 \pm 0.005$.

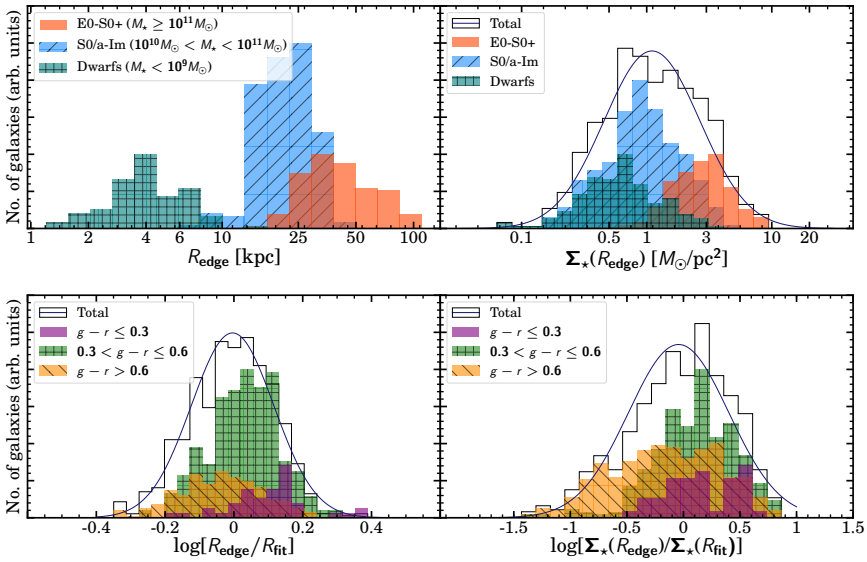

Figure 4.13: Representation of the results shown in Fig. 4.10 as histograms. *Top*: The distribution of $R_{\rm edge}$ (left) and $\Sigma_\star(R_{\rm edge})$. *Bottom*: The distribution of $(g-r)_{\rm edge}$ in the $R_{\rm edge}$–stellar mass (left) and $\Sigma_\star(R_{\rm edge})$–stellar mass (right) relations. The subscript 'fit' refers to the best fit line of each plane (Fig. 4.12).

Este documento incorpora firma electrónica, y es copia auténtica de un documento electrónico archivado por la ULL según la Ley 39/2015.
Su autenticidad puede ser contrastada en la siguiente dirección https://sede.ull.es/validacion/

Identificador del documento: 2622200 Código de verificación: mbm0ekWs

Firmado por:	ROSHAN NUSHKIA CHAMBA *UNIVERSIDAD DE LA LAGUNA*	Fecha: 07/07/2020 13:28:26
	IGNACIO TRUJILLO CABRERA *UNIVERSIDAD DE LA LAGUNA*	07/07/2020 13:58:21
	Johan Hendrik Knapen Koelstra *UNIVERSIDAD DE LA LAGUNA*	07/07/2020 15:23:08
	María de las Maravillas Aguiar Aguilar *UNIVERSIDAD DE LA LAGUNA*	08/07/2020 15:55:11

Universidad de La Laguna
Oficina de Sede Electrónica
Entrada
Nº registro: 2020/46124
Nº reg. oficina: OF002/2020/45309
Fecha: 07/07/2020 15:26:22

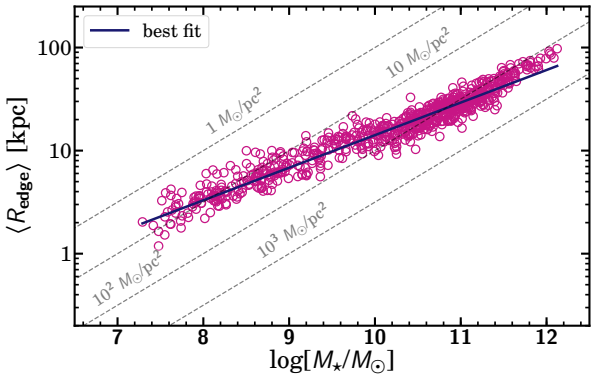

Figure 4.14: $\langle R_{\rm edge} \rangle$–stellar mass relation for the sample.

This result suggests that Eqs. 4.3 and 4.4 could potentially be used to obtain $\langle R_{\rm edge} \rangle$ and thus a proxy for the size of any galaxy, provided its stellar mass is known. This can be useful for larger galaxy samples and automated cataloguing in future multi-band surveys such as LSST. Providing $\langle R_{\rm edge} \rangle$ and $\langle \Sigma_{\rm edge}(M_\star) \rangle$ is also advantageous for cases where the edge is unclear and thus serves as a prediction of where the edge should be for a given galaxy. Strong deviations from this prediction could then provide insights about the stellar population properties in the outskirts of the galaxy in comparison with the parent population.

4.7 Summary and future improvements

In this Chapter, we have measured the location of the edge for a sample of ~ 1000 low-inclined and face-on galaxies, from dwarfs to giant ellipticals, using the deep IAC Stripe 82 imaging. We find that the edge of a galaxy is most evident as a feature in their $g-r$ colour profiles. Additionally, the location of the edge marked in this work (called $R_{\rm edge}$) was shown to enclose the bulk of the light distribution in galaxies and is thus closer to a concept of size related to the boundary of objects. To study the stellar population properties at $R_{\rm edge}$, we have measured the $g-r$ colour and the stellar mass density at this location and studied their distribution in the $R_{\rm edge}$– and $\Sigma_\star(R_{\rm edge})$–stellar mass planes. Several characteristics of the results shown in this Chapter are summarised below:

- The slope of the global $R_{\rm edge}$–stellar mass relation is 1/3 and the dispersion, after accounting for errors in the visual inspection, is $\bar{\sigma}_{R_{\rm edge}} \sim 0.09$ dex. These results are consistent with those shown in Chapter 2 (Sec. 2.6).
- For galaxies with $M_\star < 10^{11}$, those located in the upper half of the $R_{\rm edge}$–stellar mass plane have bluer edges compared to the lower half. These trends are also evident in the $\Sigma_\star(R_{\rm edge})$–stellar mass relation. The result is consistent with the observed stratification of the Sa–Sab and Sc–Scd spiral galaxies in the size–mass plane reported in Chapter 2.

Este documento incorpora firma electrónica, y es copia auténtica de un documento electrónico archivado por la ULL según la Ley 39/2015.
Su autenticidad puede ser contrastada en la siguiente dirección https://sede.ull.es/validacion/

Identificador del documento: 2622200 Código de verificación: mbm0ekWs

Firmado por:	ROSHAN NUSHKIA CHAMBA *UNIVERSIDAD DE LA LAGUNA*	Fecha: 07/07/2020 13:28:26
	IGNACIO TRUJILLO CABRERA *UNIVERSIDAD DE LA LAGUNA*	07/07/2020 13:58:21
	Johan Hendrik Knapen Koelstra *UNIVERSIDAD DE LA LAGUNA*	07/07/2020 15:23:08
	María de las Maravillas Aguiar Aguilar *UNIVERSIDAD DE LA LAGUNA*	08/07/2020 15:55:11

Universidad de La Laguna
Oficina de Sede Electrónica
Entrada
Nº registro: 2020/46124
Nº reg. oficina: OF002/2020/45309
Fecha: 07/07/2020 15:26:22

The measurements for the B12 and P17 galaxy samples are also consistent with these distributions.

- At a fixed stellar mass, the age for the spiral galaxy population increases from $\sim 2\,\mathrm{Gyr}$ to $\sim 12\,\mathrm{Gyr}$ as the size of the galaxy decreases.
- The slope of the $\Sigma_\star(R_{\rm edge})$–stellar mass plane changes from 0.13 to 0.46 at $M_\star \sim 2.5 \times 10^{10} M_\odot$.
- The stellar mass density at $R_{\rm edge}$ varies with morphology: $\Sigma_\star(R_{\rm edge}) \sim 0.5\,M_\odot/\mathrm{pc}^2$ for the dwarfs, $\sim 1\,M_\odot/\mathrm{pc}^2$ for the spirals and $\sim 3\,M_\odot/\mathrm{pc}^2$ for the elliptical galaxies in the sample. These results reaffirm the idea that more massive galaxies are expected to have a higher threshold for star formation than low-mass galaxies, previously discussed in Chapter 2.
- We propose that $\langle R_{\rm edge} \rangle$ can be interpreted as a proxy for the size of a galaxy, provided its stellar mass is knonwn. This is useful for larger galaxy samples and automated cataloguing in future multi-band imaging surveys such as LSST.

A number of improvements can be made on the results presented in this Chapter. As mentioned earlier, only the spiral galaxies have been reviewed at the time of writing this thesis. The dwarf and elliptical galaxy samples also need to be re-examined and verified. The issues related to the uncertainties in our measurements have also not been studied in depth. We plan to perform a detailed analysis on the components contributing to the dispersion in our results such as the error in our visual inspection and uncertainties in background and stellar mass estimation (similar to that presented in Chapter 2, Sect. 2.6.2 for the size–mass relation).

Additionally, we have not yet quantified to what extent there can be an offset between the location of the edge feature in the μ, $g-r$ and $\Sigma_\star$ profiles, in the cases where the feature appears in more than one of these profiles. We have decided to take an average for such cases in our analysis thus far, however, we plan to explore this in more detail in the future.

We also need to improve our fitting procedure in the $\Sigma_\star(R_{\rm edge})$–stellar mass plane. We split the sample in two intervals I_1 and I_2 at a stellar mass of $2.5 \times 10^{10}\,M_\odot$ and performed two separate linear fits for each internal. While this choice is pragmatic, in the future we will explore a different criteria to improve the fitting procedure, for example, by fitting the data after splitting the sample according to morphological type.

We leave the discussion on future work beyond the results shown here for the reader in the next Chapter.

Este documento incorpora firma electrónica, y es copia auténtica de un documento electrónico archivado por la ULL según la Ley 39/2015.
Su autenticidad puede ser contrastada en la siguiente dirección https://sede.ull.es/validacion/

Identificador del documento: 2622200 Código de verificación: mbm0ekWs

Firmado por:	ROSHAN NUSHKIA CHAMBA *UNIVERSIDAD DE LA LAGUNA*	Fecha: 07/07/2020 13:28:26
	IGNACIO TRUJILLO CABRERA *UNIVERSIDAD DE LA LAGUNA*	07/07/2020 13:58:21
	Johan Hendrik Knapen Koelstra *UNIVERSIDAD DE LA LAGUNA*	07/07/2020 15:23:08
	María de las Maravillas Aguiar Aguilar *UNIVERSIDAD DE LA LAGUNA*	08/07/2020 15:55:11

Universidad de La Laguna
Oficina de Sede Electrónica
Entrada
Nº registro: 2020/46124
Nº reg. oficina: OF002/2020/45309
Fecha: 07/07/2020 15:26:22

5

Conclusions and future work

In this final Chapter of my thesis, I summarise the main results and conclusions from Chapters 2–4. I then discuss several future prospects based on the work presented therein.

5.1 Summary of results

5.1.1 A physically motivated definition for the size of galaxies

In Chapter 2, I presented the article '*A physically motivated definition for the size of galaxies in an era of ultra-deep imaging*' published in Trujillo, Chamba, & Knapen (2020) where we introduced a physically motivated definition for galaxy size, based on the location of the gas density threshold for star formation in galaxies. In this particular study, we made our definition operative by using the radial position of a fixed isomass contour at 1 $M_{\odot}/\mathrm{pc}^2$ (called R_1) as a size measure. This particular value was motivated by both theoretical and observational arguments: it is 1) a proxy for measuring this threshold according to studies on the evolution of stellar discs and 2) the density value found at the location of the truncation (Chapter 1, Sect. 1.3.2) in galaxies similar to our own Milky Way.

We showed that when R_1 is used as a size measure for galaxies, the global scatter of the stellar mass–size relation explored over five orders of magnitude in stellar mass reaches a value of ~ 0.06 dex. This value is 2.5 times smaller than the scatter measured using the effective radius (~ 0.15 dex) and 1.5 to 1.8 times smaller than those using other traditional sizes indicators such as $R_{23.5,\mathrm{i}}$ (~ 0.09 dex), R_{H} (~ 0.09 dex) and $R_{\mathrm{e,M}_\star}$ (~ 0.11 dex). A smaller scatter in the size–stellar mass plane necessarily implies a tighter correlation between these two parameters and thus changes the structure of the relationship.

Between a stellar mass of $10^7 M_{\odot} < M_{\star} < 10^{11} M_{\odot}$, we found that the slope of the stellar mass–size relation is very close to 1/3. In a 3D spherical distribution, this corresponds to a constant stellar density of $\sim 4.5 \times 10^{-3}$ $M_{\odot}/\mathrm{pc}^3$, which could be a reflection of a common gas density when the primordial gas collapsed to form stars. However, beyond $M_{\star} > 10^{11} M_{\odot}$, the stellar mass–size relation gets steeper, reaching a slope of $\sim 3/5$. This drastic increase in size of the most massive galaxies could be linked to its different star formation histories, reflecting a higher gas density threshold for star formation in these galaxies at the epoch of their main formation burst.

Este documento incorpora firma electrónica, y es copia auténtica de un documento electrónico archivado por la ULL según la Ley 39/2015.
Su autenticidad puede ser contrastada en la siguiente dirección https://sede.ull.es/validacion/

Identificador del documento: 2622200 Código de verificación: mbm0ekWs

Firmado por:	ROSHAN NUSHKIA CHAMBA *UNIVERSIDAD DE LA LAGUNA*	Fecha: 07/07/2020 13:28:26
	IGNACIO TRUJILLO CABRERA *UNIVERSIDAD DE LA LAGUNA*	07/07/2020 13:58:21
	Johan Hendrik Knapen Koelstra *UNIVERSIDAD DE LA LAGUNA*	07/07/2020 15:23:08
	María de las Maravillas Aguiar Aguilar *UNIVERSIDAD DE LA LAGUNA*	08/07/2020 15:55:11

Universidad de La Laguna
Oficina de Sede Electrónica
Entrada
Nº registro: 2020/46124
Nº reg. oficina: OF002/2020/45309
Fecha: 07/07/2020 15:26:22

5.1.2 The nature of ultra-diffuse galaxies

In Chapter 3, I presented the article '*Are ultra-diffuse galaxies Milky Way-sized?*' published in Chamba, Trujillo, & Knapen (2020) where we used the physically motivated size measure (Chapter 2) to compare the sizes of ultra-diffuse galaxies (UDGs) with dwarfs and Milky Way-like galaxies. We showed that unlike dwarf or Milky Way-like galaxies, UDGs do not have bright clumps or substructure like bulges in their central regions. Therefore, the large effective radiii of UDGs ($R_{\rm e} > 1.5\,$kpc) are directly a consequence of the dependence of $R_{\rm e}$ on how their flux is distributed and not a result of the UDGs being 'Milky Way-sized' as postulated by van Dokkum et al. (2015a).

In fact, our results show that UDGs are actually ten times smaller in extension than Milky Way-like galaxies. Consequently, they are similar in size to dwarf galaxies. This result lends further support to the dwarf-like nature of UDGs (Chapter 1, Sect. 1.4.5). We propose that if Milky Way-sized UDGs exist, then they need to have a total extension of $\sim 25\,$kpc. Until now, such objects have not been discovered in deep imaging surveys. Our results thus show that $R_{\rm e}$ could provide a misleading perception on the sizes of galaxies and reinforces the importance of using physically meaningful properties in order to fairly compare classes of galaxies and draw conclusions about their nature.

5.1.3 Revealing the edges of galaxies with deep imaging

In Chapter 4, I presented first results on the visual identification of the location of the edge (called $R_{\rm edge}$) in low-inclined and face-on galaxies, from dwarfs to giant ellipticals. We have conducted this exercise for ~ 1000 galaxies using their surface brightness profiles μ_g and μ_r, the $g-r$ colour and stellar mass density $\Sigma_\star$ profiles. We defined the edge as a change in slope in the outermost region of the radial profiles of galaxies. Upon initial examination of the profiles, we located edges in 762 galaxies out of the 1026 galaxies studied. We found that the edge is most evident in $g-r$ colour profile of the galaxies where a sharp change from blue to red colours occur beyond $R_{\rm edge}$. The distribution of $R_{\rm edge}$ and the stellar mass density at $R_{\rm edge}$, $\Sigma_\star(R_{\rm edge})$, of the galaxies as a function of their stellar mass is consistent with the interpretation of the results shown in Chapter 2 using R_1. We find that the Sc–Scd galaxies populate the upper portion of the plane because they have bluer edges, while the Sa–Sab galaxies populate the lower portion of the size–mass plane as they have redder edges. Additionally, we found that, on average, $\Sigma_\star(R_{\rm edge}) \sim 0.5\,M_\odot/{\rm pc}^2$ for the dwarfs, $\sim 1\,M_\odot/{\rm pc}^2$ for the spirals and $\sim 3\,M_\odot/{\rm pc}^2$ for the elliptical galaxies in the sample. These results reaffirm the idea that more massive galaxies are expected to have a higher threshold for star formation than low-mass galaxies, previously discussed in Chapter 2.

5.2 Future research questions

This thesis forms part of a long-term project which aims to study the evolution of galaxy structure in the low surface brightness regime, from dwarfs to giants, at low and high redshift. These topics are broad and not fully understood, providing many unresolved questions for further study. Several potential research questions that we wish to address in the future based on the work presented in this thesis are:

Este documento incorpora firma electrónica, y es copia auténtica de un documento electrónico archivado por la ULL según la Ley 39/2015.
Su autenticidad puede ser contrastada en la siguiente dirección https://sede.ull.es/validacion/

Identificador del documento: 2622200 Código de verificación: mbm0ekWs

Firmado por:	ROSHAN NUSHKIA CHAMBA *UNIVERSIDAD DE LA LAGUNA*	Fecha: 07/07/2020 13:28:26
	IGNACIO TRUJILLO CABRERA *UNIVERSIDAD DE LA LAGUNA*	07/07/2020 13:58:21
	Johan Hendrik Knapen Koelstra *UNIVERSIDAD DE LA LAGUNA*	07/07/2020 15:23:08
	María de las Maravillas Aguiar Aguilar *UNIVERSIDAD DE LA LAGUNA*	08/07/2020 15:55:11

Universidad de La Laguna
Oficina de Sede Electrónica
Entrada
Nº registro: 2020/46124
Nº reg. oficina: OF002/2020/45309
Fecha: 07/07/2020 15:26:22

- ***How does the PSF and the inclination of a galaxy affect our view of the edge?***
  In this thesis, we have not explored the effect of the PSF or the inclination in our galaxy size measurements. As our work was focused on low-inclined and face-on galaxies, the effect of the PSF is expected to be less than in edge-on galaxies. However, if we are to extend our analysis to edge-on configurations, then the PSF becomes extremely important to characterise the properties of the edge. We plan to explore these issues for edge-on galaxies using extremely deep imaging from the OSIRIS/GTC in the SDSS g and r-band (proposal ID: 80-GTC61/18B, 8.4 hr; PI: Alejandro Serrano Borlaff).

- ***What is the link between our size definition and the HI distribution in galaxies?***
  In Chapter 2, we have used a stellar mass density threshold as a proxy for the gas density threshold that is theoretically expected for insitu star formation in galactic discs (Schaye 2004). However, a more precise measurement of this threshold may be obtained using HI data. The HI Nearby Galaxies Survey (THINGS; Walter et al. 2008) is suitable for this task and we plan to combine this dataset with deep optical images to explore the connection between the edges of galaxies and the warps detected in HI.

- ***How are the edges of galaxies affected by their environment?***
  All the galaxies studied in this thesis are located in low density environments. Therefore, a natural extension of the work presented here is to study galaxies in higher density environments such as in clusters, and examine how this shapes the size–stellar mass plane. This would be similar to the analysis by Pranger et al. (2017) who studied the effect of the environment in breaks. However, here we propose to study the location of the edge as a function of environment. To address this research question, we plan to use ultra-deep imaging of the Coma and Perseus cluster, observed using the Rich 0.7 m and T80 0.8 m telescopes respectively. The data has already been reduced by our team and is thus ready for analysis.

- ***What is the origin of the size–stellar mass plane?***
  As discussed in Chapter 1 (Sect. 1.5.1), one of the main motivations behind the study of the size distribution of galaxies is its connection with the distribution of angular momentum in the underlying dark matter halo. While this connection has been extensively studied using the effective radius, it would be interesting to explore this topic using our new size measure with hydrodynamical simulations. Such a study could be complemented by an observational analysis of extended HI rotation curves for disc galaxies and the globular cluster population for the elliptical and dwarf galaxies studied in this thesis. Of particular interest is to understand the origins of the stratification of the late-type galaxies in the size–stellar mass plane (Chapters 2 and 4) within this context.

- ***How do the edges of galaxies evolve with cosmic time?***
  While the current consensus on the inside-out size evolution of galaxies is based on the effective radius (Chapter 1, Sect. 1.5.1), it would be worth to revisit this size evolution by tracing the edges of galaxies as a function of redshift ($z < 1.5$). The ongoing work presented in Chapter 4 of this thesis will serve as the reference for the distribution of the edges in the nearby Universe. Therefore, we plan to extend size evolution studies for galaxies in the high- and low-mass end. This would be possible with the combination of

Este documento incorpora firma electrónica, y es copia auténtica de un documento electrónico archivado por la ULL según la Ley 39/2015.
Su autenticidad puede ser contrastada en la siguiente dirección https://sede.ull.es/validacion/

Identificador del documento: 2622200 Código de verificación: mbm0ekWs

Firmado por:	ROSHAN NUSHKIA CHAMBA *UNIVERSIDAD DE LA LAGUNA*	Fecha: 07/07/2020 13:28:26
	IGNACIO TRUJILLO CABRERA *UNIVERSIDAD DE LA LAGUNA*	07/07/2020 13:58:21
	Johan Hendrik Knapen Koelstra *UNIVERSIDAD DE LA LAGUNA*	07/07/2020 15:23:08
	María de las Maravillas Aguiar Aguilar *UNIVERSIDAD DE LA LAGUNA*	08/07/2020 15:55:11

Universidad de La Laguna
Oficina de Sede Electrónica
Entrada
Nº registro: 2020/46124
Nº reg. oficina: OF002/2020/45309
Fecha: 07/07/2020 15:26:22

current *HST* imaging and future research programmes using the *JWST* (Gardner et al. 2006).

- ***Can the new physically motivated size measure be used to define the onset of the stellar halo?***
  As mentioned in Chapter 1 (Sect. 1.4.3), different definitions of the onset of the stellar halo are adopted in the literature. For example, a stellar halo model or a cut-off radius (x times R_e) to mark the bulk of the insitu stellar population in the galaxy. Therefore, it would be interesting to explore whether our new size measure offers a more physically supported formalism to separate the intrinsic galactic disc component from the surrounding tidal structures. As described in Sect. 1.4.3, this can be performed for a few 1000 galaxies using upcoming deep surveys like the LSST (LSST Science Collaboration et al. 2009), provided that effects due to PSF and background estimation can be controlled. The results from such a study could be homogeneously compared with the predictions from ΛCDM simulations, ultimately facilitating our understanding on the assembly history of galaxies.

- ***What is the number density of low surface brightness galaxies in the Universe?***
  As discussed in Chapter 1 (Sect. 1.4.2), deep imaging has also opened the possibility of detecting a very large number (in the order of 1000s) of low surface brightness (LSB) galaxies. These objects can be used to probe the 'missing satellites problem' (Moore et al. 1999; Klypin et al. 1999) beyond the Local Group and study their large scale distribution (Sect. 1.2 and 1.4.2). As a first step towards these long-term goals, all the images used in the analysis presented in Chapters 2–4 of this thesis were masked using `MTObjects` (Teeninga et al. 2013, 2016), which is a software specifically designed to segment faint sources in images. The software (now called `Sourcerer`) is still under development by our SUNDIAL ITN colleagues and we have been involved in a study to compare the performance of `MTObjects` and several other source detection algorithms in the literature (`SExtractor` (Bertin & Arnouts 1996), `NoiseChisel` (Akhlaghi & Ichikawa 2015), `ProFound` (Robotham et al. 2018)) for faint object detection (Haigh, Chamba et al. submitted). We are also involved in an upcoming zooniverse citizen science project called 'Space Fluff' to hunt for LSB galaxies in the Fornax Cluster.[1] I invite the reader to participate in our citizen science project if he/she is interested.

The research questions outlined above show that it is the combination of current and future, ground and space-based facilities for ultra-deep imaging such as the HSC, GTC, *HST*, LSST, Euclid, *JWST* and the Roman Space Telescope (Spergel et al. 2015), that will be of paramount importance for our understanding of galaxy formation and evolution. Eventually, the collective analysis of these datasets would provide answers to the fundamental questions about the Universe introduced in Chapter 1: What is the nature of dark matter and dark energy? How do they trigger star formation and thereafter form structures like the galaxies we can observe today? What are the origins of the shapes of galaxies, their morphology and light distribution? Are low surface brightness galaxies the missing satellites in simulations? And how do the answers to all these questions depend on cosmic time?

[1] `https://www.zooniverse.org/projects/hwiks/space-fluff/about/research`

Este documento incorpora firma electrónica, y es copia auténtica de un documento electrónico archivado por la ULL según la Ley 39/2015.
Su autenticidad puede ser contrastada en la siguiente dirección https://sede.ull.es/validacion/

Identificador del documento: 2622200 Código de verificación: mbm0ekWs

Firmado por:	ROSHAN NUSHKIA CHAMBA *UNIVERSIDAD DE LA LAGUNA*	Fecha: 07/07/2020 13:28:26
	IGNACIO TRUJILLO CABRERA *UNIVERSIDAD DE LA LAGUNA*	07/07/2020 13:58:21
	Johan Hendrik Knapen Koelstra *UNIVERSIDAD DE LA LAGUNA*	07/07/2020 15:23:08
	María de las Maravillas Aguiar Aguilar *UNIVERSIDAD DE LA LAGUNA*	08/07/2020 15:55:11

Universidad de La Laguna
Oficina de Sede Electrónica
Entrada
Nº registro: 2020/46124
Nº reg. oficina: OF002/2020/45309
Fecha: 07/07/2020 15:26:22

Bibliography

Abazajian, K., Adelman-McCarthy, J. K., Agüeros, M. A., et al. 2003, AJ, 126, 2081

Abolfathi, B., Aguado, D. S., Aguilar, G., et al. 2018, ApJS, 235, 42

Agertz, O., & Kravtsov, A. V. 2016, ApJ, 824, 79

Aihara, H., Arimoto, N., Armstrong, R., et al. 2018, PASJ, 70, S4

Akhlaghi, M., & Ichikawa, T. 2015, ApJS, 220, 1

Alonso Asensio, I., Dalla Vecchia, C., Bahé, Y. M., Barnes, D. J., & Kay, S. T. 2020, arXiv e-prints, arXiv:2003.04662

Alpher, R. A., Bethe, H., & Gamow, G. 1948, Physical Review, 73, 803

Alpher, R. A., & Herman, R. 1948, Nature, 162, 774

Amorisco, N. C. 2018, MNRAS, 475, L116

Amorisco, N. C., & Loeb, A. 2016, MNRAS, 459, L51

Amorisco, N. C., Monachesi, A., Agnello, A., & White, S. D. M. 2018, MNRAS, 475, 4235

Arp, H., & Bertola, F. 1969, Astrophys. Lett., 4, 23

—. 1971, ApJ, 163, 195

Atkinson, A. M., Abraham, R. G., & Ferguson, A. M. N. 2013, ApJ, 765, 28

Azzollini, R., Trujillo, I., & Beckman, J. E. 2008, ApJ, 684, 1026

Bakos, J., & Trujillo, I. 2012, arXiv e-prints, arXiv:1204.3082

Bakos, J., Trujillo, I., & Pohlen, M. 2008, ApJ, 683, L103

Barbosa, C. E., Zaritsky, D., Donnerstein, R., et al. 2020, ApJS, 247, 46

Bardeen, J. M., Steinhardt, P. J., & Turner, M. S. 1983, Phys. Rev. D, 28, 679

Barden, M., Rix, H.-W., Somerville, R. S., et al. 2005, ApJ, 635, 959

Este documento incorpora firma electrónica, y es copia auténtica de un documento electrónico archivado por la ULL según la Ley 39/2015.
Su autenticidad puede ser contrastada en la siguiente dirección https://sede.ull.es/validacion/

Identificador del documento: 2622200 Código de verificación: mbm0ekWs

Firmado por:	ROSHAN NUSHKIA CHAMBA *UNIVERSIDAD DE LA LAGUNA*	Fecha: 07/07/2020 13:28:26
	IGNACIO TRUJILLO CABRERA *UNIVERSIDAD DE LA LAGUNA*	07/07/2020 13:58:21
	Johan Hendrik Knapen Koelstra *UNIVERSIDAD DE LA LAGUNA*	07/07/2020 15:23:08
	María de las Maravillas Aguiar Aguilar *UNIVERSIDAD DE LA LAGUNA*	08/07/2020 15:55:11

Universidad de La Laguna
Oficina de Sede Electrónica
Entrada
Nº registro: 2020/46124
Nº reg. oficina: OF002/2020/45309
Fecha: 07/07/2020 15:26:22

Barker, M. K., Ferguson, A. M. N., Irwin, M. J., Arimoto, N., & Jablonka, P. 2012, MNRAS, 419, 1489

Beasley, M. A., Romanowsky, A. J., Pota, V., et al. 2016, ApJ, 819, L20

Beasley, M. A., & Trujillo, I. 2016, ApJ, 830, 23

Bellazzini, M., Belokurov, V., Magrini, L., et al. 2017, MNRAS, 467, 3751

Belokurov, V., Zucker, D. B., Evans, N. W., et al. 2006, ApJ, 642, L137

Bennet, P., Sand, D. J., Crnojević, D., et al. 2020, ApJ, 893, L9

Bertin, E., & Arnouts, S. 1996, A&AS, 117, 393

Bigiel, F., Leroy, A., Walter, F., et al. 2008, AJ, 136, 2846

Binggeli, B. 1994, in European Southern Observatory Conference and Workshop Proceedings, Vol. 49, European Southern Observatory Conference and Workshop Proceedings, 13

Bland-Hawthorn, J., & Gerhard, O. 2016, ARA&A, 54, 529

Bland-Hawthorn, J., Shopbell, P. L., & Malin, D. F. 1993, AJ, 106, 2154

Blanton, M. R., Hogg, D. W., Bahcall, N. A., et al. 2003, ApJ, 592, 819

Blumenthal, G. R., Faber, S. M., Primack, J. R., & Rees, M. J. 1984, Nature, 311, 517

Bonnor, W. B. 1957, MNRAS, 117, 104

Borlaff, A., Trujillo, I., Román, J., et al. 2019, A&A, 621, A133

Bothun, G. D., Impey, C. D., & Malin, D. F. 1991, ApJ, 376, 404

Bothun, G. D., Impey, C. D., Malin, D. F., & Mould, J. R. 1987, AJ, 94, 23

Bovy, J., & Rix, H.-W. 2013, ApJ, 779, 115

Broeils, A. H., & Rhee, M. H. 1997, A&A, 324, 877

Bruzual, G., & Charlot, S. 2003, MNRAS, 344, 1000

Buitrago, F., Trujillo, I., Conselice, C. J., et al. 2008, ApJ, 687, L61

Buitrago, F., Trujillo, I., Curtis-Lake, E., et al. 2017, MNRAS, 466, 4888

Bullock, J. S., & Johnston, K. V. 2005, ApJ, 635, 931

Bullock, J. S., Kravtsov, A. V., & Weinberg, D. H. 2001, ApJ, 548, 33

Camm, G. L. 1950, MNRAS, 110, 305

Capaccioli, M., Spavone, M., Grado, A., et al. 2015, A&A, 581, A10

Este documento incorpora firma electrónica, y es copia auténtica de un documento electrónico archivado por la ULL según la Ley 39/2015.
Su autenticidad puede ser contrastada en la siguiente dirección https://sede.ull.es/validacion/

Identificador del documento: 2622200 Código de verificación: mbm0ekWs

Firmado por:	ROSHAN NUSHKIA CHAMBA *UNIVERSIDAD DE LA LAGUNA*	Fecha: 07/07/2020 13:28:26
	IGNACIO TRUJILLO CABRERA *UNIVERSIDAD DE LA LAGUNA*	07/07/2020 13:58:21
	Johan Hendrik Knapen Koelstra *UNIVERSIDAD DE LA LAGUNA*	07/07/2020 15:23:08
	María de las Maravillas Aguiar Aguilar *UNIVERSIDAD DE LA LAGUNA*	08/07/2020 15:55:11

Universidad de La Laguna
Oficina de Sede Electrónica
Entrada
Nº registro: 2020/46124
Nº reg. oficina: OF002/2020/45309
Fecha: 07/07/2020 15:26:22

Carleton, T., Errani, R., Cooper, M., et al. 2019, MNRAS, 485, 382

Carollo, D., Beers, T. C., Chiba, M., et al. 2010, ApJ, 712, 692

Chabrier, G. 2003, PASP, 115, 763

Chamba, N., Trujillo, I., & Knapen, J. H. 2020, A&A, 633, L3

Chan, T. K., Kereš, D., Wetzel, A., et al. 2018, MNRAS, 478, 906

Christlein, D., Zaritsky, D., & Bland-Hawthorn, J. 2010, MNRAS, 405, 2549

Cohen, Y., van Dokkum, P., Danieli, S., et al. 2018, ApJ, 868, 96

Conselice, C. J. 2018, Research Notes of the American Astronomical Society, 2, 43

Contini, E., De Lucia, G., Villalobos, Á., & Borgani, S. 2014, MNRAS, 437, 3787

Cooper, A. P., D'Souza, R., Kauffmann, G., et al. 2013, MNRAS, 434, 3348

Cooper, A. P., Cole, S., Frenk, C. S., et al. 2010, MNRAS, 406, 744

Courteau, S., Widrow, L. M., McDonald, M., et al. 2011, ApJ, 739, 20

Crain, R. A., Schaye, J., Bower, R. G., et al. 2015, MNRAS, 450, 1937

Dalcanton, J. J., Spergel, D. N., Gunn, J. E., Schmidt, M., & Schneider, D. P. 1997a, AJ, 114, 635

Dalcanton, J. J., Spergel, D. N., & Summers, F. J. 1997b, ApJ, 482, 659

Danieli, S., van Dokkum, P., Abraham, R., et al. 2019, arXiv e-prints, arXiv:1910.07529

de Jong, R. S. 2008, MNRAS, 388, 1521

de Jong, R. S., Seth, A. C., Radburn-Smith, D. J., et al. 2007, ApJ, 667, L49

de Vaucouleurs, A., & de Vaucouleurs, G. 1975, The Observatory, 95, 148

de Vaucouleurs, G. 1948, Annales d'Astrophysique, 11, 247

—. 1959a, Annales de l'Observatoire du Houga, Annales de l'Observatoire du Houga No. v. 2, pt. 2 (Observatoire)

—. 1959b, Handbuch der Physik, 53, 275

—. 1959c, ApJ, 130, 728

—. 1959d, AJ, 64, 397

—. 1969, Astrophys. Lett., 4, 17

de Vaucouleurs, G. 1974, in IAU Symposium, Vol. 58, The Formation and Dynamics of Galaxies, ed. J. R. Shakeshaft, 1

Este documento incorpora firma electrónica, y es copia auténtica de un documento electrónico archivado por la ULL según la Ley 39/2015.
Su autenticidad puede ser contrastada en la siguiente dirección https://sede.ull.es/validacion/

Identificador del documento: 2622200 Código de verificación: mbm0ekWs

Firmado por:	ROSHAN NUSHKIA CHAMBA *UNIVERSIDAD DE LA LAGUNA*	Fecha: 07/07/2020 13:28:26
	IGNACIO TRUJILLO CABRERA *UNIVERSIDAD DE LA LAGUNA*	07/07/2020 13:58:21
	Johan Hendrik Knapen Koelstra *UNIVERSIDAD DE LA LAGUNA*	07/07/2020 15:23:08
	María de las Maravillas Aguiar Aguilar *UNIVERSIDAD DE LA LAGUNA*	08/07/2020 15:55:11

Universidad de La Laguna
Oficina de Sede Electrónica
Entrada
Nº registro: 2020/46124
Nº reg. oficina: OF002/2020/45309
Fecha: 07/07/2020 15:26:22

de Vaucouleurs, G. 1987, in IAU Symposium, Vol. 127, Structure and Dynamics of Elliptical Galaxies, ed. P. T. de Zeeuw, 3

de Vaucouleurs, G., de Vaucouleurs, A., Corwin, Herold G., J., et al. 1991, Third Reference Catalogue of Bright Galaxies

de Vaucouleurs, G., de Vaucouleurs, A., & Corwin, J. R. 1976, in Second reference catalogue of bright galaxies, Vol. 1976, p. Austin: University of Texas Press., Vol. 1976

de Vaucouleurs, G. H., de Vaucouleurs, A., & Shapley, H. 1964, Reference catalogue of bright galaxies

Debattista, V. P., Mayer, L., Carollo, C. M., et al. 2006, ApJ, 645, 209

Debattista, V. P., Roškar, R., & Loebman, S. R. 2017, in Astrophysics and Space Science Library, Vol. 434, Outskirts of Galaxies, ed. J. H. Knapen, J. C. Lee, & A. Gil de Paz, 77

Di Cintio, A., Brook, C. B., Dutton, A. A., et al. 2017, MNRAS, 466, L1

Di Cintio, A., Brook, C. B., Macciò, A. V., Dutton, A. A., & Cardona-Barrero, S. 2019, MNRAS, 486, 2535

Dicke, R. H., Peebles, P. J. E., Roll, P. G., & Wilkinson, D. T. 1965, ApJ, 142, 414

Disney, M. J. 1976, Nature, 263, 573

Djorgovski, S., & Davis, M. 1987, ApJ, 313, 59

Djorgovski, S. G., Gal, R. R., Odewahn, S. C., et al. 1998, in Wide Field Surveys in Cosmology, ed. S. Colombi, Y. Mellier, & B. Raban, Vol. 14, 89

Djorgovski, S. G., Mahabal, A., Drake, A., Graham, M., & Donalek, C. 2013, Sky Surveys, ed. T. D. Oswalt & H. E. Bond, 223

D'Onofrio, M., Capaccioli, M., & Caon, N. 1994, MNRAS, 271, 523

Duc, P.-A., Cuillandre, J.-C., Karabal, E., et al. 2015, MNRAS, 446, 120

Dutton, A. A., van den Bosch, F. C., Dekel, A., & Courteau, S. 2007, ApJ, 654, 27

Efstathiou, G., & Silk, J. 1983, Fund. Cosmic Phys., 9, 1

Eggen, O. J., Lynden-Bell, D., & Sandage, A. R. 1962, ApJ, 136, 748

Einasto, J., Kaasik, A., & Saar, E. 1974, Nature, 250, 309

Einstein, A. 1916, Annalen der Physik, 354, 769

Elmegreen, B. G., & Hunter, D. A. 2017, in Astrophysics and Space Science Library, Vol. 434, Outskirts of Galaxies, ed. J. H. Knapen, J. C. Lee, & A. Gil de Paz, 115

Emsellem, E., Cappellari, M., Krajnović, D., et al. 2011, MNRAS, 414, 888

Este documento incorpora firma electrónica, y es copia auténtica de un documento electrónico archivado por la ULL según la Ley 39/2015.
Su autenticidad puede ser contrastada en la siguiente dirección https://sede.ull.es/validacion/

Identificador del documento: 2622200 Código de verificación: mbm0ekWs

Firmado por:	ROSHAN NUSHKIA CHAMBA *UNIVERSIDAD DE LA LAGUNA*	Fecha: 07/07/2020 13:28:26
	IGNACIO TRUJILLO CABRERA *UNIVERSIDAD DE LA LAGUNA*	07/07/2020 13:58:21
	Johan Hendrik Knapen Koelstra *UNIVERSIDAD DE LA LAGUNA*	07/07/2020 15:23:08
	María de las Maravillas Aguiar Aguilar *UNIVERSIDAD DE LA LAGUNA*	08/07/2020 15:55:11

Universidad de La Laguna
Oficina de Sede Electrónica
Entrada
Nº registro: 2020/46124
Nº reg. oficina: OF002/2020/45309
Fecha: 07/07/2020 15:26:22

Emsellem, E., van der Burg, R. F. J., Fensch, J., et al. 2019, A&A, 625, A76

Erwin, P. 2015, ApJ, 799, 226

Fall, S. M., & Efstathiou, G. 1980, MNRAS, 193, 189

Ferrarese, L., Côté, P., Cuillandre, J.-C., et al. 2012, ApJS, 200, 4

Ferré-Mateu, A., Alabi, A., Forbes, D. A., et al. 2018, MNRAS, 479, 4891

Ferreras, I., Trujillo, I., Mármol-Queraltó, E., et al. 2014, MNRAS, 444, 906

Fish, R. A. 1963, AJ, 68, 72

—. 1964, ApJ, 139, 284

Fliri, J., & Trujillo, I. 2016, MNRAS, 456, 1359

—. 2018, VizieR Online Data Catalog, 745

Freeman, K. C. 1970, ApJ, 160, 811

Friedmann, A. 1922, Zeitschrift fur Physik, 10, 377

Frieman, J. A., Bassett, B., Becker, A., et al. 2008, AJ, 135, 338

Fry, A. M., Morrison, H. L., Harding, P., & Boroson, T. A. 1999, AJ, 118, 1209

Gaia Collaboration. 2016, VizieR Online Data Catalog, 1337

Galaz, G., Milovic, C., Suc, V., et al. 2015, ApJ, 815, L29

Gamow, G. 1948, Nature, 162, 680

Gardner, J. P., Mather, J. C., Clampin, M., et al. 2006, Space Sci. Rev., 123, 485

Gavazzi, G., Donati, A., Cucciati, O., et al. 2005, A&A, 430, 411

Geha, M., Wechsler, R. H., Mao, Y.-Y., et al. 2017, ApJ, 847, 4

Genkin, I. L., & Genkina, L. M. 1970, Soviet Ast., 14, 353

Giovanelli, R., Haynes, M. P., Salzer, J. J., et al. 1994, AJ, 107, 2036

González, N. M., Smith Castelli, A. V., Faifer, F. R., Escudero, C. G., & Cellone, S. A. 2018, A&A, 620, A166

Graham, A. W. 2019, Publ. Astron. Soc. Australia, 36, e035

Graham, A. W., & Driver, S. P. 2005, Publ. Astron. Soc. Australia, 22, 118

Greco, J. P., Greene, J. E., Strauss, M. A., et al. 2018, ApJ, 857, 104

Guth, A. H. 1981, Phys. Rev. D, 23, 347

Este documento incorpora firma electrónica, y es copia auténtica de un documento electrónico archivado por la ULL según la Ley 39/2015.
Su autenticidad puede ser contrastada en la siguiente dirección https://sede.ull.es/validacion/

Identificador del documento: 2622200 Código de verificación: mbm0ekWs

Firmado por:	ROSHAN NUSHKIA CHAMBA *UNIVERSIDAD DE LA LAGUNA*	Fecha: 07/07/2020 13:28:26
	IGNACIO TRUJILLO CABRERA *UNIVERSIDAD DE LA LAGUNA*	07/07/2020 13:58:21
	Johan Hendrik Knapen Koelstra *UNIVERSIDAD DE LA LAGUNA*	07/07/2020 15:23:08
	María de las Maravillas Aguiar Aguilar *UNIVERSIDAD DE LA LAGUNA*	08/07/2020 15:55:11

Universidad de La Laguna
Oficina de Sede Electrónica
Entrada
Nº registro: 2020/46124
Nº reg. oficina: OF002/2020/45309
Fecha: 07/07/2020 15:26:22

Guth, A. H., & Pi, S. Y. 1982, Phys. Rev. Lett., 49, 1110

Hall, M., Courteau, S., Dutton, A. A., McDonald, M., & Zhu, Y. 2012, MNRAS, 425, 2741

Hawking, S. W. 1982, Physics Letters B, 115, 295

Head, J. T. C. G., Lucey, J. R., Hudson, M. J., & Smith, R. J. 2014, MNRAS, 440, 1690

Henden, N. A., Puchwein, E., & Sijacki, D. 2019, arXiv e-prints, arXiv:1911.12367

Holmberg, E. 1958, Meddelanden fran Lunds Astronomiska Observatorium Serie II, 136, 1

—. 1975, Magnitudes, Colors, Surface Brightness, Intensity Distributions Absolute Luminosities, and Diameters of Galaxies, ed. A. Sandage, M. Sandage, & J. Kristian, 123

Hood, C. E., Kannappan, S. J., Stark, D. V., et al. 2018, ApJ, 857, 144

Hoyle, F. 1953, ApJ, 118, 513

Huang, K.-H., Fall, S. M., Ferguson, H. C., et al. 2017, ApJ, 838, 6

Huang, S., Haynes, M. P., Giovanelli, R., & Brinchmann, J. 2012, ApJ, 756, 113

Hubble, E. 1929, Proceedings of the National Academy of Science, 15, 168

—. 1932, ApJ, 76, 106

Hubble, E., & Humason, M. L. 1931, ApJ, 74, 43

Hubble, E. P. 1926, ApJ, 64, 321

—. 1930, ApJ, 71, 231

Huber, P. J. 1964, Ann. Math. Statist., 35, 73

Impey, C., Bothun, G., & Malin, D. 1988, ApJ, 330, 634

Infante-Sainz, R., Trujillo, I., & Román, J. 2020, MNRAS, 491, 5317

Ivezic, Z., Axelrod, T., Brandt, W. N., et al. 2008, Serbian Astronomical Journal, 176, 1

Jablonka, P., Tafelmeyer, M., Courbin, F., & Ferguson, A. M. N. 2010, A&A, 513, A78

Jaskot, A. E., Oey, M. S., Salzer, J. J., et al. 2015, ApJ, 808, 66

Jeans, J. H. 1902, Philosophical Transactions of the Royal Society of London Series A, 199, 1

Jiang, F., Dekel, A., Kneller, O., et al. 2019, MNRAS, 1977

Jiménez-Teja, Y., Dupke, R., Benítez, N., et al. 2018, ApJ, 857, 79

Johnston, K. V., Bullock, J. S., Sharma, S., et al. 2008, ApJ, 689, 936

Kado-Fong, E., Greene, J. E., Hendel, D., et al. 2018, ApJ, 866, 103

Este documento incorpora firma electrónica, y es copia auténtica de un documento electrónico archivado por la ULL según la Ley 39/2015.
Su autenticidad puede ser contrastada en la siguiente dirección https://sede.ull.es/validacion/

Identificador del documento: 2622200 Código de verificación: mbm0ekWs

Firmado por:	ROSHAN NUSHKIA CHAMBA *UNIVERSIDAD DE LA LAGUNA*	Fecha: 07/07/2020 13:28:26
	IGNACIO TRUJILLO CABRERA *UNIVERSIDAD DE LA LAGUNA*	07/07/2020 13:58:21
	Johan Hendrik Knapen Koelstra *UNIVERSIDAD DE LA LAGUNA*	07/07/2020 15:23:08
	María de las Maravillas Aguiar Aguilar *UNIVERSIDAD DE LA LAGUNA*	08/07/2020 15:55:11

Universidad de La Laguna
Oficina de Sede Electrónica
Entrada
Nº registro: 2020/46124
Nº reg. oficina: OF002/2020/45309
Fecha: 07/07/2020 15:26:22

Kauffmann, G. 2014, MNRAS, 441, 2717

Kennedy, R., Bamford, S. P., Baldry, I., et al. 2015, MNRAS, 454, 806

Kennicutt, Robert C., J. 1989a, ApJ, 344, 685

Kennicutt, Jr., R. C. 1989b, ApJ, 344, 685

Kim, J.-h., & Lee, J. 2013, MNRAS, 432, 1701

Kim, S. Y., Peter, A. H. G., & Hargis, J. R. 2018, Phys. Rev. Lett., 121, 211302

King, I. 1962, AJ, 67, 471

Klypin, A., Kravtsov, A. V., Valenzuela, O., & Prada, F. 1999, ApJ, 522, 82

Knapen, J. H., & Trujillo, I. 2017, Astrophysics and Space Science Library, Vol. 434, Ultra-Deep Imaging: Structure of Disks and Haloes, ed. J. H. Knapen, J. C. Lee, & A. Gil de Paz, 255

Knapen, J. H., & van der Kruit, P. C. 1991, A&A, 248, 57

Kniazev, A. Y., Grebel, E. K., Pustilnik, S. A., et al. 2004, AJ, 127, 704

Koda, J., Yagi, M., Yamanoi, H., & Komiyama, Y. 2015, ApJ, 807, L2

Koopmann, R. A., Haynes, M. P., & Catinella, B. 2006, AJ, 131, 716

Kormendy, J. 1977, ApJ, 218, 333

Kormendy, J., & Bahcall, J. N. 1974, AJ, 79, 671

Kourkchi, E., Tully, R. B., Neill, J. D., et al. 2019, arXiv e-prints, arXiv:1909.01572

Kravtsov, A. V. 2013, ApJ, 764, L31

Kregel, M., van der Kruit, P. C., & de Grijs, R. 2002, MNRAS, 334, 646

Krick, J. E., & Bernstein, R. A. 2007, AJ, 134, 466

Kron, R. G. 1980, ApJS, 43, 305

Krumholz, M. R., Leroy, A. K., & McKee, C. F. 2011, ApJ, 731, 25

Lagos, C. D. P., Baugh, C. M., Lacey, C. G., et al. 2011, MNRAS, 418, 1649

Lasker, B. M., McLean, B. J., Shara, M. M., et al. 1989, Bulletin d'Information du Centre de Donnees Stellaires, 37, 15

Laurikainen, E., & Salo, H. 2001, MNRAS, 324, 685

Leisman, L., Haynes, M. P., Janowiecki, S., et al. 2017, ApJ, 842, 133

Lemaître, G. 1927, Annales de la Société Scientifique de Bruxelles, 47, 49

Este documento incorpora firma electrónica, y es copia auténtica de un documento electrónico archivado por la ULL según la Ley 39/2015.
Su autenticidad puede ser contrastada en la siguiente dirección https://sede.ull.es/validacion/

Identificador del documento: 2622200 Código de verificación: mbm0ekWs

Firmado por:	ROSHAN NUSHKIA CHAMBA *UNIVERSIDAD DE LA LAGUNA*	Fecha: 07/07/2020 13:28:26
	IGNACIO TRUJILLO CABRERA *UNIVERSIDAD DE LA LAGUNA*	07/07/2020 13:58:21
	Johan Hendrik Knapen Koelstra *UNIVERSIDAD DE LA LAGUNA*	07/07/2020 15:23:08
	María de las Maravillas Aguiar Aguilar *UNIVERSIDAD DE LA LAGUNA*	08/07/2020 15:55:11

Universidad de La Laguna
Oficina de Sede Electrónica
Entrada
Nº registro: 2020/46124
Nº reg. oficina: OF002/2020/45309
Fecha: 07/07/2020 15:26:22

—. 1931, MNRAS, 91, 483

Leroy, A. K., Walter, F., Brinks, E., et al. 2008, AJ, 136, 2782

Lifshitz, E. M. 1946, Zhurnal Eksperimentalnoi i Teoreticheskoi Fiziki, 16, 587

Liller, M. H. 1960, ApJ, 132, 306

LSST Science Collaboration, Abell, P. A., Allison, J., et al. 2009, arXiv e-prints, arXiv:0912.0201

Malin, D. 1988, in Astrophotography, ed. S. Marx, 125

Malin, D., & Hadley, B. 1999, in Looking Deep in the Southern Sky, ed. R. Morganti & W. J. Couch, 78

Malin, D. F. 1978, Nature, 276, 591

—. 1981, AAS Photo Bulletin, 27, 4

Malin, D. F., & Carter, D. 1980, Nature, 285, 643

Mancera Piña, P. E., Peletier, R. F., Aguerri, J. A. L., et al. 2018, MNRAS, 481, 4381

Mancera Piña, P. E., Fraternali, F., Adams, E. A. K., et al. 2019, ApJ, 883, L33

Mancillas, B., Duc, P.-A., Combes, F., et al. 2019, A&A, 632, A122

Maraston, C., Pforr, J., Henriques, B. M., et al. 2013, MNRAS, 435, 2764

Martell, S. L., & Grebel, E. K. 2010, A&A, 519, A14

Martin, C. L., & Kennicutt, Robert C., J. 2001, ApJ, 555, 301

Martín-Navarro, I., Trujillo, I., Knapen, J. H., Bakos, J., & Fliri, J. 2014, MNRAS, 441, 2809

Martín-Navarro, I., Bakos, J., Trujillo, I., et al. 2012, MNRAS, 427, 1102

Martínez-Delgado, D., Gabany, R. J., Crawford, K., et al. 2010, AJ, 140, 962

Martínez-Lombilla, C., Trujillo, I., & Knapen, J. H. 2019, MNRAS, 483, 664

McConnachie, A. W. 2012, AJ, 144, 4

McConnachie, A. W., Ferguson, A. M. N., Irwin, M. J., et al. 2010, ApJ, 723, 1038

McGaugh, S. S., Bothun, G. D., & Schombert, J. M. 1995, AJ, 110, 573

McIntosh, D. H., Bell, E. F., Rix, H.-W., et al. 2005, ApJ, 632, 191

McLean, I. S. 2002, Experimental Astronomy, 14, 25

Merritt, A., van Dokkum, P., & Abraham, R. 2014, ApJ, 787, L37

Merritt, A., van Dokkum, P., Abraham, R., & Zhang, J. 2016, ApJ, 830, 62

Este documento incorpora firma electrónica, y es copia auténtica de un documento electrónico archivado por la ULL según la Ley 39/2015.
Su autenticidad puede ser contrastada en la siguiente dirección https://sede.ull.es/validacion/

Identificador del documento: 2622200 Código de verificación: mbm0ekWs

Firmado por:	ROSHAN NUSHKIA CHAMBA *UNIVERSIDAD DE LA LAGUNA*	Fecha: 07/07/2020 13:28:26
	IGNACIO TRUJILLO CABRERA *UNIVERSIDAD DE LA LAGUNA*	07/07/2020 13:58:21
	Johan Hendrik Knapen Koelstra *UNIVERSIDAD DE LA LAGUNA*	07/07/2020 15:23:08
	María de las Maravillas Aguiar Aguilar *UNIVERSIDAD DE LA LAGUNA*	08/07/2020 15:55:11

Universidad de La Laguna
Oficina de Sede Electrónica
Entrada
Nº registro: 2020/46124
Nº reg. oficina: OF002/2020/45309
Fecha: 07/07/2020 15:26:22

Mihos, J. C., Harding, P., Feldmeier, J., & Morrison, H. 2005, ApJ, 631, L41

Mihos, J. C., Harding, P., Feldmeier, J. J., et al. 2017, ApJ, 834, 16

Mihos, J. C., Harding, P., Spengler, C. E., Rudick, C. S., & Feldmeier, J. J. 2013, ApJ, 762, 82

Mihos, J. C., Durrell, P. R., Ferrarese, L., et al. 2015, ApJ, 809, L21

Miller, T. B., van Dokkum, P., Mowla, L., & van der Wel, A. 2019, ApJ, 872, L14

Minkowski, R. L., & Abell, G. O. 1963, The National Geographic Society-Palomar Observatory Sky Survey, ed. K. A. Strand, 481

Mo, H., van den Bosch, F. C., & White, S. 2010, Galaxy Formation and Evolution

Mo, H. J., Mao, S., & White, S. D. M. 1998, MNRAS, 295, 319

Möllenhoff, C. 2004, A&A, 415, 63

Montes, M. 2019, arXiv e-prints, arXiv:1912.01616

Montes, M., & Trujillo, I. 2018, MNRAS, 474, 917

—. 2019, MNRAS, 482, 2838

Moore, B., Ghigna, S., Governato, F., et al. 1999, ApJ, 524, L19

Morales, G., Martínez-Delgado, D., Grebel, E. K., et al. 2018, A&A, 614, A143

Morgan, D. H. 1995, in Astronomical Society of the Pacific Conference Series, Vol. 84, IAU Colloq. 148: The Future Utilisation of Schmidt Telescopes, ed. J. Chapman, R. Cannon, S. Harrison, & B. Hidayat, 137

Morrissey, P., Conrow, T., Barlow, T. A., et al. 2007, ApJS, 173, 682

Mosenkov, A., Rich, R. M., Koch, A., et al. 2020, MNRAS, arXiv:2003.03392

Muñoz, R. P., Eigenthaler, P., Puzia, T. H., et al. 2015, ApJ, 813, L15

Muñoz-Mateos, J. C., Sheth, K., Regan, M., et al. 2015, ApJS, 219, 3

Müller, O., Jerjen, H., & Binggeli, B. 2017, A&A, 597, A7

Nair, P., van den Bergh, S., & Abraham, R. G. 2011, ApJ, 734, L31

Nair, P. B., & Abraham, R. G. 2010, ApJS, 186, 427

Navarro, J. F., Frenk, C. S., & White, S. D. M. 1996, ApJ, 462, 563

Nilson, P. 1973, Uppsala general catalogue of galaxies

Oberth, H. 1923, Die Rakete zu den Planetenräumen, Pp. 92 + 2 Tafeln. (München und Berlin: R. Oldenbourg.), 1s. 6d.

Este documento incorpora firma electrónica, y es copia auténtica de un documento electrónico archivado por la ULL según la Ley 39/2015.
Su autenticidad puede ser contrastada en la siguiente dirección https://sede.ull.es/validacion/

Identificador del documento: 2622200 Código de verificación: mbm0ekWs

Firmado por:	ROSHAN NUSHKIA CHAMBA *UNIVERSIDAD DE LA LAGUNA*	Fecha: 07/07/2020 13:28:26
	IGNACIO TRUJILLO CABRERA *UNIVERSIDAD DE LA LAGUNA*	07/07/2020 13:58:21
	Johan Hendrik Knapen Koelstra *UNIVERSIDAD DE LA LAGUNA*	07/07/2020 15:23:08
	María de las Maravillas Aguiar Aguilar *UNIVERSIDAD DE LA LAGUNA*	08/07/2020 15:55:11

Universidad de La Laguna
Oficina de Sede Electrónica
Entrada
Nº registro: 2020/46124
Nº reg. oficina: OF002/2020/45309
Fecha: 07/07/2020 15:26:22

Okamoto, T., Frenk, C. S., Jenkins, A., & Theuns, T. 2010, MNRAS, 406, 208

Ostriker, J. P., Peebles, P. J. E., & Yahil, A. 1974, ApJ, 193, L1

Patterson, F. S. 1940, Harvard College Observatory Bulletin, 914, 9

Peebles, P. J., & Ratra, B. 2003, Reviews of Modern Physics, 75, 559

Peebles, P. J. E. 1969, ApJ, 155, 393

Penzias, A. A., & Wilson, R. W. 1965, ApJ, 142, 419

Pérez, I. 2004, A&A, 427, L17

Perlmutter, S., Aldering, G., Goldhaber, G., et al. 1999, ApJ, 517, 565

Peters, S. P. C., van der Kruit, P. C., Knapen, J. H., et al. 2017, MNRAS, 470, 427

Petrosian, V. 1976, ApJ, 209, L1

Pillepich, A., Madau, P., & Mayer, L. 2015, ApJ, 799, 184

Pillepich, A., Nelson, D., Hernquist, L., et al. 2018a, MNRAS, 475, 648

Pillepich, A., Springel, V., Nelson, D., et al. 2018b, MNRAS, 473, 4077

Planck Collaboration, Aghanim, N., Akrami, Y., et al. 2018, arXiv e-prints, arXiv:1807.06209

Pohlen, M., & Trujillo, I. 2006, A&A, 454, 759

Pranger, F., Trujillo, I., Kelvin, L. S., & Cebrián, M. 2017, MNRAS, 467, 2127

Prole, D. J., Davies, J. I., Keenan, O. C., & Davies, L. J. M. 2018, MNRAS, 478, 667

Prole, D. J., van der Burg, R. F. J., Hilker, M., & Davies, J. I. 2019, MNRAS, 488, 2143

Purcell, C. W., Bullock, J. S., & Zentner, A. R. 2007, ApJ, 666, 20

Querejeta, M., Meidt, S. E., Schinnerer, E., et al. 2015, ApJS, 219, 5

Quirk, W. J. 1972, ApJ, 176, L9

Radburn-Smith, D. J., de Jong, R. S., Streich, D., et al. 2014, ApJ, 780, 105

Read, J. I., & Erkal, D. 2019, MNRAS, 487, 5799

Redman, R. O. 1936, MNRAS, 96, 588

Reid, I. N., Brewer, C., Brucato, R. J., et al. 1991, PASP, 103, 661

Reshetnikov, V. P. 2005, Physics Uspekhi, 48, 1109

Riechers, D. A., Bradford, C. M., Clements, D. L., et al. 2013, Nature, 496, 329

Riess, A. G., Filippenko, A. V., Challis, P., et al. 1998, AJ, 116, 1009

Este documento incorpora firma electrónica, y es copia auténtica de un documento electrónico archivado por la ULL según la Ley 39/2015.
Su autenticidad puede ser contrastada en la siguiente dirección https://sede.ull.es/validacion/

Identificador del documento: 2622200 Código de verificación: mbm0ekWs

Firmado por:	ROSHAN NUSHKIA CHAMBA *UNIVERSIDAD DE LA LAGUNA*	Fecha: 07/07/2020 13:28:26
	IGNACIO TRUJILLO CABRERA *UNIVERSIDAD DE LA LAGUNA*	07/07/2020 13:58:21
	Johan Hendrik Knapen Koelstra *UNIVERSIDAD DE LA LAGUNA*	07/07/2020 15:23:08
	María de las Maravillas Aguiar Aguilar *UNIVERSIDAD DE LA LAGUNA*	08/07/2020 15:55:11

Universidad de La Laguna
Oficina de Sede Electrónica
Entrada
Nº registro: 2020/46124
Nº reg. oficina: OF002/2020/45309
Fecha: 07/07/2020 15:26:22

Roberts, M. S. 1976, Comments on Astrophysics, 6, 105

Robotham, A. S. G., Davies, L. J. M., Driver, S. P., et al. 2018, MNRAS, 476, 3137

Roediger, J. C., & Courteau, S. 2015, MNRAS, 452, 3209

Román, J., & Trujillo, I. 2017a, MNRAS, 468, 703

—. 2017b, MNRAS, 468, 4039

—. 2018, Research Notes of the American Astronomical Society, 2, 144

Roškar, R., Debattista, V. P., Stinson, G. S., et al. 2008, ApJ, 675, L65

Rubin, V. C., Ford, W. K., J., & Thonnard, N. 1978, ApJ, 225, L107

Rudick, C. S., Mihos, J. C., Harding, P., et al. 2010, ApJ, 720, 569

Rudick, C. S., Mihos, J. C., & McBride, C. K. 2011, ApJ, 732, 48

Ruiz-Lara, T., Beasley, M. A., Falcón-Barroso, J., et al. 2018, MNRAS, 478, 2034

Ruiz-Lara, T., Trujillo, I., Beasley, M. A., et al. 2019, MNRAS, 486, 5670

Saintonge, A., & Spekkens, K. 2011, ApJ, 726, 77

Sandage, A., & Binggeli, B. 1984, AJ, 89, 919

Sandin, C. 2014, A&A, 567, A97

Sawala, T., Frenk, C. S., Fattahi, A., et al. 2016, MNRAS, 457, 1931

Schaye, J. 2004, ApJ, 609, 667

Seigar, M. S. 2011, ISRN Astronomy and Astrophysics, 2011, 725697

Sérsic, J. L. 1968a, Atlas de Galaxias Australes (Observatorio Astronomico, Universidad Nacional de Cordoba, 1968)

—. 1968b, Bulletin of the Astronomical Institutes of Czechoslovakia, 19, 105

Shapley, H. 1934, Annals of Harvard College Observatory, 88, 91

—. 1942, Proceedings of the National Academy of Science, 28, 186

Shayler, D., & Harland, D. 2016, The dream. In: The Hubble Space Telescope (Praxis, New York, NY: Springer Praxis Books)

Shen, S., Mo, H. J., White, S. D. M., et al. 2003, MNRAS, 343, 978

Sheth, K., Regan, M., Hinz, J. L., et al. 2010, PASP, 122, 1397

Silk, J. 1968, ApJ, 151, 459

Este documento incorpora firma electrónica, y es copia auténtica de un documento electrónico archivado por la ULL según la Ley 39/2015.
Su autenticidad puede ser contrastada en la siguiente dirección https://sede.ull.es/validacion/

Identificador del documento: 2622200 Código de verificación: mbm0ekWs

Firmado por:	ROSHAN NUSHKIA CHAMBA *UNIVERSIDAD DE LA LAGUNA*	Fecha: 07/07/2020 13:28:26
	IGNACIO TRUJILLO CABRERA *UNIVERSIDAD DE LA LAGUNA*	07/07/2020 13:58:21
	Johan Hendrik Knapen Koelstra *UNIVERSIDAD DE LA LAGUNA*	07/07/2020 15:23:08
	María de las Maravillas Aguiar Aguilar *UNIVERSIDAD DE LA LAGUNA*	08/07/2020 15:55:11

Universidad de La Laguna
Oficina de Sede Electrónica
Entrada
Nº registro: 2020/46124
Nº reg. oficina: OF002/2020/45309
Fecha: 07/07/2020 15:26:22

Simard, L., Mendel, J. T., Patton, D. R., Ellison, S. L., & McConnachie, A. W. 2011, ApJS, 196, 11

Slater, C. T., Harding, P., & Mihos, J. C. 2009, PASP, 121, 1267

Smith, B. A. 1976, in Charge-Coupled Device Technology and Applications, 135–138

Smoot, G. F., Bennett, C. L., Kogut, A., et al. 1992, ApJ, 396, L1

Somerville, R. S., & Davé, R. 2015, ARA&A, 53, 51

Somerville, R. S., Barden, M., Rix, H.-W., et al. 2008, ApJ, 672, 776

Somerville, R. S., Behroozi, P., Pandya, V., et al. 2018, MNRAS, 473, 2714

Sorce, J. G., Tully, R. B., Courtois, H. M., et al. 2014, MNRAS, 444, 527

Spekkens, K., & Karunakaran, A. 2018, ApJ, 855, 28

Spergel, D., Gehrels, N., Baltay, C., et al. 2015, arXiv e-prints, arXiv:1503.03757

Spitzer, L. 1968, Diffuse matter in space (Interscience Publication, 1968)

Spitzer, Jr., L. 1942, ApJ, 95, 329

Starobinsky, A. A. 1982, Physics Letters B, 117, 175

Strauss, M. A., Weinberg, D. H., Lupton, R. H., et al. 2002, AJ, 124, 1810

Tal, T., & van Dokkum, P. G. 2011, ApJ, 731, 89

Tanaka, M., Chiba, M., Hayashi, K., et al. 2018, ApJ, 865, 125

Teeninga, P., Moschini, U., C. Trager, S., & Wilkinson, M. 2016, 1

Teeninga, P., Moschini, U., Trager, S. C., & Wilkinson, M. H. F. 2013, in 11th International Conference "Pattern Recognition and Image Analysis: New Information Technologies" (PRIA-11-2013), IPSI RAS, 746–749

Tegmark, M., Strauss, M. A., Blanton, M. R., et al. 2004, Phys. Rev. D, 69, 103501

Toomre, A., & Toomre, J. 1972, ApJ, 178, 623

Toth, G., & Ostriker, J. P. 1992, ApJ, 389, 5

Tremmel, M., Wright, A. C., Brooks, A. M., et al. 2019, arXiv e-prints, arXiv:1908.05684

Trujillo, I., Chamba, N., & Knapen, J. H. 2020, MNRAS, 493, 87

Trujillo, I., Conselice, C. J., Bundy, K., et al. 2007, MNRAS, 382, 109

Trujillo, I., Ferreras, I., & de La Rosa, I. G. 2011, MNRAS, 415, 3903

Trujillo, I., & Fliri, J. 2016, ApJ, 823, 123

Este documento incorpora firma electrónica, y es copia auténtica de un documento electrónico archivado por la ULL según la Ley 39/2015.
Su autenticidad puede ser contrastada en la siguiente dirección https://sede.ull.es/validacion/

Identificador del documento: 2622200 Código de verificación: mbm0ekWs

Firmado por:	ROSHAN NUSHKIA CHAMBA *UNIVERSIDAD DE LA LAGUNA*	Fecha: 07/07/2020 13:28:26
	IGNACIO TRUJILLO CABRERA *UNIVERSIDAD DE LA LAGUNA*	07/07/2020 13:58:21
	Johan Hendrik Knapen Koelstra *UNIVERSIDAD DE LA LAGUNA*	07/07/2020 15:23:08
	María de las Maravillas Aguiar Aguilar *UNIVERSIDAD DE LA LAGUNA*	08/07/2020 15:55:11

Universidad de La Laguna
Oficina de Sede Electrónica
Entrada
Nº registro: 2020/46124
Nº reg. oficina: OF002/2020/45309
Fecha: 07/07/2020 15:26:22

Trujillo, I., Graham, A. W., & Caon, N. 2001, MNRAS, 326, 869

Trujillo, I., & Pohlen, M. 2005, ApJ, 630, L17

Trujillo, I., Roman, J., Filho, M., & Sánchez Almeida, J. 2017, ApJ, 836, 191

Trujillo, I., Rudnick, G., Rix, H.-W., et al. 2004, ApJ, 604, 521

Trujillo, I., Beasley, M. A., Borlaff, A., et al. 2019, MNRAS, 486, 1192

Tully, R. B., Courtois, H. M., & Sorce, J. G. 2016, AJ, 152, 50

Tully, R. B., & Fisher, J. R. 1977, A&A, 500, 105

Tully, R. B., & Fouque, P. 1985, ApJS, 58, 67

Tully, R. B., Rizzi, L., Shaya, E. J., et al. 2009, AJ, 138, 323

Uson, J. M., Boughn, S. P., & Kuhn, J. R. 1991, ApJ, 369, 46

van der Burg, R. F. J., Muzzin, A., & Hoekstra, H. 2016, A&A, 590, A20

van der Kruit, P. C. 1979, A&AS, 38, 15

—. 1987, A&A, 173, 59

—. 2007, A&A, 466, 883

van der Kruit, P. C., & Freeman, K. C. 2011, ARA&A, 49, 301

van der Kruit, P. C., & Searle, L. 1981a, A&A, 95, 105

—. 1981b, A&A, 95, 116

—. 1982, A&A, 110, 61

van der Wel, A., Franx, M., van Dokkum, P. G., et al. 2014, ApJ, 788, 28

van Dokkum, P., Abraham, R., Brodie, J., et al. 2016, ApJ, 828, L6

van Dokkum, P., Danieli, S., Cohen, Y., et al. 2018, Nature, 555, 629

van Dokkum, P., Wasserman, A., Danieli, S., et al. 2019, ApJ, 880, 91

van Dokkum, P. G., Abraham, R., & Merritt, A. 2014, ApJ, 782, L24

van Dokkum, P. G., Abraham, R., Merritt, A., et al. 2015a, ApJ, 798, L45

van Dokkum, P. G., Romanowsky, A. J., Abraham, R., et al. 2015b, ApJ, 804, L26

Vazdekis, A., Ricciardelli, E., Cenarro, A. J., et al. 2012, MNRAS, 424, 157

Venhola, A., Peletier, R., Laurikainen, E., et al. 2017, A&A, 608, A142

Vorontsov-Velyaminov, B. 1974, The Observatory, 94, 319

Este documento incorpora firma electrónica, y es copia auténtica de un documento electrónico archivado por la ULL según la Ley 39/2015.
Su autenticidad puede ser contrastada en la siguiente dirección https://sede.ull.es/validacion/

Identificador del documento: 2622200 Código de verificación: mbm0ekWs

Firmado por:	ROSHAN NUSHKIA CHAMBA *UNIVERSIDAD DE LA LAGUNA*	Fecha: 07/07/2020 13:28:26
	IGNACIO TRUJILLO CABRERA *UNIVERSIDAD DE LA LAGUNA*	07/07/2020 13:58:21
	Johan Hendrik Knapen Koelstra *UNIVERSIDAD DE LA LAGUNA*	07/07/2020 15:23:08
	María de las Maravillas Aguiar Aguilar *UNIVERSIDAD DE LA LAGUNA*	08/07/2020 15:55:11

Universidad de La Laguna
Oficina de Sede Electrónica
Entrada
Nº registro: 2020/46124
Nº reg. oficina: OF002/2020/45309
Fecha: 07/07/2020 15:26:22

—. 1975, The Observatory, 95, 214

Vorontsov-Vel'Yaminov, B. A. 1961, Soviet Ast., 4, 735

Vorontsov-Vel'Yaminov, B. A., & Arkhipova, V. P. 1962, Morphological catalogue of galaxies, C01, 0

Vorontsov-Velyaminov, B. A., & Krasnogorskaya, A. A. 1994, VizieR Online Data Catalog, VII/62A

Walter, F., Brinks, E., de Blok, W. J. G., et al. 2008, AJ, 136, 2563

Wang, J., Koribalski, B. S., Serra, P., et al. 2016, MNRAS, 460, 2143

White, S. D. M., & Rees, M. J. 1978, MNRAS, 183, 341

Willman, B., Blanton, M. R., West, A. A., et al. 2005, AJ, 129, 2692

Wright, A. C., Tremmel, M., Brooks, A. M., et al. 2020, arXiv e-prints, arXiv:2005.07634

York, D. G., Adelman, J., Anderson, John E., J., et al. 2000, AJ, 120, 1579

Yozin, C., & Bekki, K. 2015, MNRAS, 452, 937

Yue, B., Castellano, M., Ferrara, A., et al. 2018, ApJ, 868, 115

Zanisi, L., Shankar, F., Lapi, A., et al. 2020, MNRAS, 492, 1671

Zel'Dovich, Y. B. 1970, A&A, 500, 13

Zibetti, S., White, S. D. M., & Brinkmann, J. 2004, MNRAS, 347, 556

Zoldan, A., De Lucia, G., Xie, L., Fontanot, F., & Hirschmann, M. 2018, MNRAS, 481, 1376

Zucker, D. B., Belokurov, V., Evans, N. W., et al. 2006, ApJ, 643, L103

Zwicky, F. 1937, ApJ, 86, 217

Este documento incorpora firma electrónica, y es copia auténtica de un documento electrónico archivado por la ULL según la Ley 39/2015.
Su autenticidad puede ser contrastada en la siguiente dirección https://sede.ull.es/validacion/

Identificador del documento: 2622200 Código de verificación: mbm0ekWs

Firmado por:	ROSHAN NUSHKIA CHAMBA *UNIVERSIDAD DE LA LAGUNA*	Fecha: 07/07/2020 13:28:26
	IGNACIO TRUJILLO CABRERA *UNIVERSIDAD DE LA LAGUNA*	07/07/2020 13:58:21
	Johan Hendrik Knapen Koelstra *UNIVERSIDAD DE LA LAGUNA*	07/07/2020 15:23:08
	María de las Maravillas Aguiar Aguilar *UNIVERSIDAD DE LA LAGUNA*	08/07/2020 15:55:11

Universidad de La Laguna
Oficina de Sede Electrónica
Entrada
Nº registro: 2020/46124
Nº reg. oficina: OF002/2020/45309
Fecha: 07/07/2020 15:26:22

A

Appendix: The sizes of galaxies

A.1 Erratum (Trujillo et al., MNRAS, 495, 3777–3779, 2020)

The paper '*A physically motivated definition for the size of galaxies in an era of ultra-deep imaging*' was published in MNRAS, 493, 87-105 (2020), here Chapter 2. After publication of the paper, we discovered that the stellar masses provided in Table 2 (here Table 2.2) were incorrectly multiplied by the axis ratio q that is provided in the same table. The rest of the parameters (sizes, stellar mass density profiles, etc) were not affected by this error. To correct the masses in Table 2.2, the following transformation needs to be applied:

$$\log(M_\star/M_\odot)_{corrected} = \log(M_\star/M_\odot) - \log q \tag{A.1}$$

After the correction of this error the main results of the paper remains unchanged. In fact, the size–mass relations get even tighter as this error was effectively adding extra noise to the relations. Another byproduct of the mass correction is a slight displacement of the entire size-mass relation in the mass axis by around $+0.2$ dex. In what follows we include the corrected version of Figures 4, 6 and 7 (here 2.4, 2.6 and 2.7) that were published in the original paper. We also include the corrected version of the observed values provided in Table 2.3.

Este documento incorpora firma electrónica, y es copia auténtica de un documento electrónico archivado por la ULL según la Ley 39/2015.
Su autenticidad puede ser contrastada en la siguiente dirección https://sede.ull.es/validacion/

Identificador del documento: 2622200 Código de verificación: mbm0ekWs

Firmado por:	ROSHAN NUSHKIA CHAMBA *UNIVERSIDAD DE LA LAGUNA*	Fecha: 07/07/2020 13:28:26
	IGNACIO TRUJILLO CABRERA *UNIVERSIDAD DE LA LAGUNA*	07/07/2020 13:58:21
	Johan Hendrik Knapen Koelstra *UNIVERSIDAD DE LA LAGUNA*	07/07/2020 15:23:08
	María de las Maravillas Aguiar Aguilar *UNIVERSIDAD DE LA LAGUNA*	08/07/2020 15:55:11

Universidad de La Laguna
Oficina de Sede Electrónica
Entrada
Nº registro: 2020/46124
Nº reg. oficina: OF002/2020/45309
Fecha: 07/07/2020 15:26:22

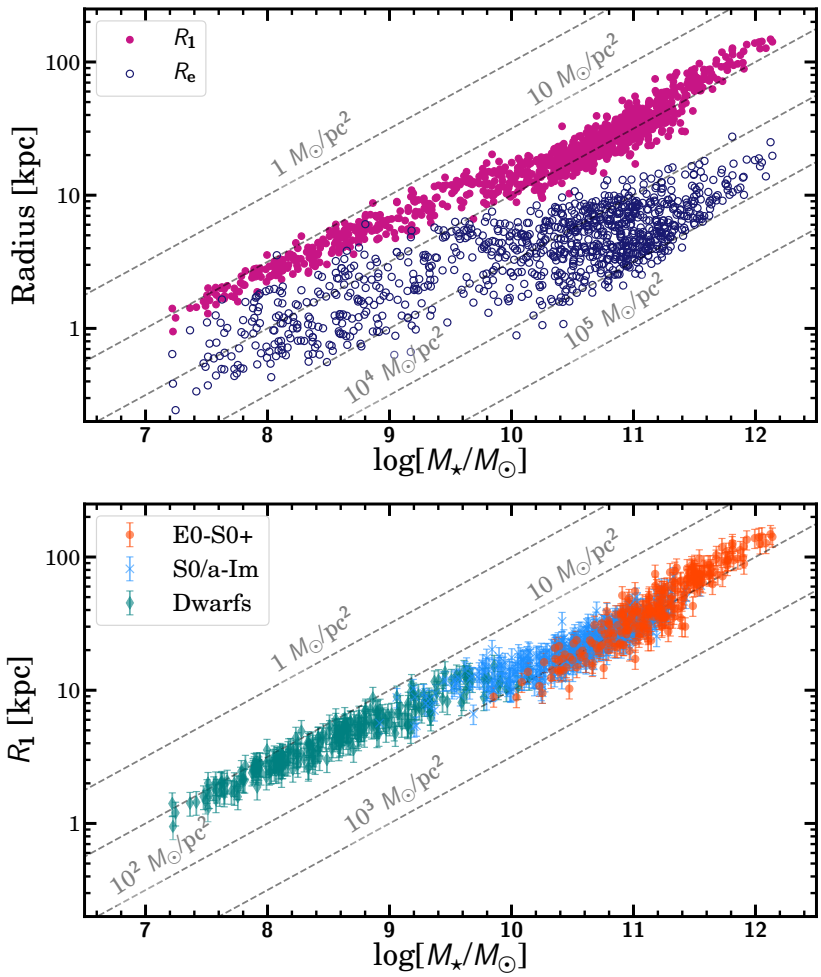

Figure A.1: Stellar mass–size relation for the galaxies in our sample. Upper panel: The observed R_1–mass and R_e–mass relations, where R_e has been measured using the g-band. The scatter of the relation using R_1 is significantly smaller compared to that with R_e. Lower panel: The same R_1–mass relation after splitting our sample into three categories: ellipticals (E0–S0+), spirals (S0/a–Sm) and dwarfs as labelled in the legend. Spiral and dwarf galaxies follow the same trend, while massive ellipticals with $M_\star > 2 \times 10^{11}\, M_\odot$ show a tilt with respect to less massive galaxies. The grey dashed lines correspond to locations in the plane with constant (projected) stellar mass density. This figure replaces Fig. 4 in the original paper (here Fig. 2.4).

Este documento incorpora firma electrónica, y es copia auténtica de un documento electrónico archivado por la ULL según la Ley 39/2015.
Su autenticidad puede ser contrastada en la siguiente dirección https://sede.ull.es/validacion/

Identificador del documento: 2622200 Código de verificación: mbm0ekWs

Firmado por:	ROSHAN NUSHKIA CHAMBA *UNIVERSIDAD DE LA LAGUNA*	Fecha: 07/07/2020 13:28:26
	IGNACIO TRUJILLO CABRERA *UNIVERSIDAD DE LA LAGUNA*	07/07/2020 13:58:21
	Johan Hendrik Knapen Koelstra *UNIVERSIDAD DE LA LAGUNA*	07/07/2020 15:23:08
	María de las Maravillas Aguiar Aguilar *UNIVERSIDAD DE LA LAGUNA*	08/07/2020 15:55:11

Universidad de La Laguna
Oficina de Sede Electrónica
Entrada
Nº registro: 2020/46124
Nº reg. oficina: OF002/2020/45309
Fecha: 07/07/2020 15:26:22

Table A.1: Best fit power law slope β and the observed dispersion of different size–mass relations. We provide the values for the entire sample as well as for the different families of galaxies. The third column corresponds to the Pearson r correlation coefficient. This table replaces the first four columns of Table 3 in the original paper (here Table 2.3).

Galaxy Type	β	$\sigma_{R_{obs}}$	r
	R_1–stellar mass		
All	0.365±0.005	0.082±0.006	0.975
E0–S0+	0.580±0.018	0.094±0.008	0.927
S0/a–Sm	0.353±0.015	0.080±0.005	0.905
Dwarfs	0.384±0.013	0.069±0.005	0.959
	R_e–stellar mass		
All	0.258±0.010	0.159±0.010	0.827
E0–S0+	0.567±0.030	0.109±0.010	0.902
S0/a–Sm	0.250±0.025	0.155±0.009	0.590
Dwarfs	0.317±0.039	0.206±0.012	0.682
	$R_{e,M_\star}$–stellar mass		
All	0.208±0.006	0.116±0.008	0.861
E0–S0+	0.507±0.022	0.090±0.009	0.910
S0/a–Sm	0.203±0.022	0.121±0.008	0.599
Dwarfs	0.198±0.027	0.130±0.008	0.690
	R_H–stellar mass		
All	0.316±0.005	0.094±0.005	0.953
E0–S0+	0.482±0.015	0.061±0.005	0.955
S0/a–Sm	0.291±0.013	0.092±0.005	0.833
Dwarfs	0.339±0.026	0.126±0.007	0.857
	$R_{23.5,i}$–stellar mass		
All	0.342±0.005	0.085±0.005	0.960
E0–S0+	0.453±0.011	0.042±0.004	0.974
S0/a–Sm	0.318±0.014	0.087±0.005	0.866
Dwarfs	0.384±0.021	0.112±0.007	0.905

Este documento incorpora firma electrónica, y es copia auténtica de un documento electrónico archivado por la ULL según la Ley 39/2015.
Su autenticidad puede ser contrastada en la siguiente dirección https://sede.ull.es/validacion/

Identificador del documento: 2622200 Código de verificación: mbm0ekWs

Firmado por: ROSHAN NUSHKIA CHAMBA
UNIVERSIDAD DE LA LAGUNA Fecha: 07/07/2020 13:28:26

IGNACIO TRUJILLO CABRERA
UNIVERSIDAD DE LA LAGUNA 07/07/2020 13:58:21

Johan Hendrik Knapen Koelstra
UNIVERSIDAD DE LA LAGUNA 07/07/2020 15:23:08

María de las Maravillas Aguiar Aguilar
UNIVERSIDAD DE LA LAGUNA 08/07/2020 15:55:11

Universidad de La Laguna
Oficina de Sede Electrónica
Entrada
Nº registro: 2020/46124
Nº reg. oficina: OF002/2020/45309
Fecha: 07/07/2020 15:26:22

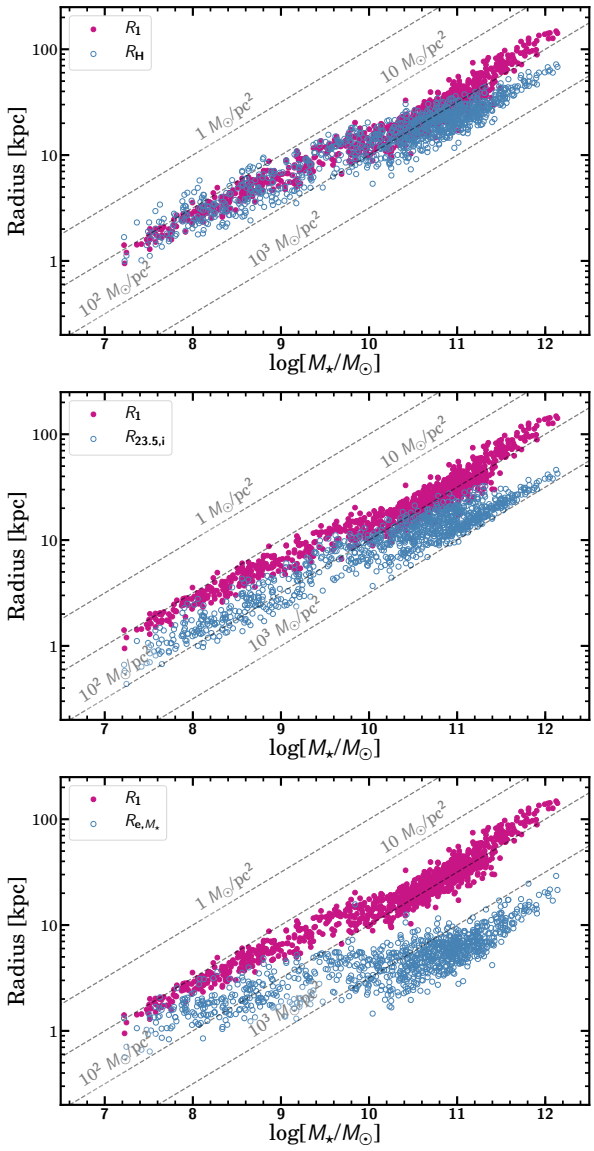

Figure A.2: Comparing the R_1–mass relation with other size–mass relations using: Holmberg Radius, $R_{\rm H}$ defined in this work as the 26 mag/arcsec^{-2} isophote in SDSS g-band (upper panel), $R_{23.5,\rm i}$, the radial location of the $\mu_i = 23.5\,$mag/arcsec^2 isophote (middle panel) and $R_{\rm e,M_\star}$, the half mass radius (lower panel). This figure replaces Fig. 6 in the original paper (here Fig. 2.6).

Este documento incorpora firma electrónica, y es copia auténtica de un documento electrónico archivado por la ULL según la Ley 39/2015.
Su autenticidad puede ser contrastada en la siguiente dirección https://sede.ull.es/validacion/

Identificador del documento: 2622200 Código de verificación: mbm0ekWs

Firmado por:	ROSHAN NUSHKIA CHAMBA *UNIVERSIDAD DE LA LAGUNA*	Fecha: 07/07/2020 13:28:26
	IGNACIO TRUJILLO CABRERA *UNIVERSIDAD DE LA LAGUNA*	07/07/2020 13:58:21
	Johan Hendrik Knapen Koelstra *UNIVERSIDAD DE LA LAGUNA*	07/07/2020 15:23:08
	María de las Maravillas Aguiar Aguilar *UNIVERSIDAD DE LA LAGUNA*	08/07/2020 15:55:11

Universidad de La Laguna
Oficina de Sede Electrónica
Entrada
Nº registro: 2020/46124
Nº reg. oficina: OF002/2020/45309
Fecha: 07/07/2020 15:26:22

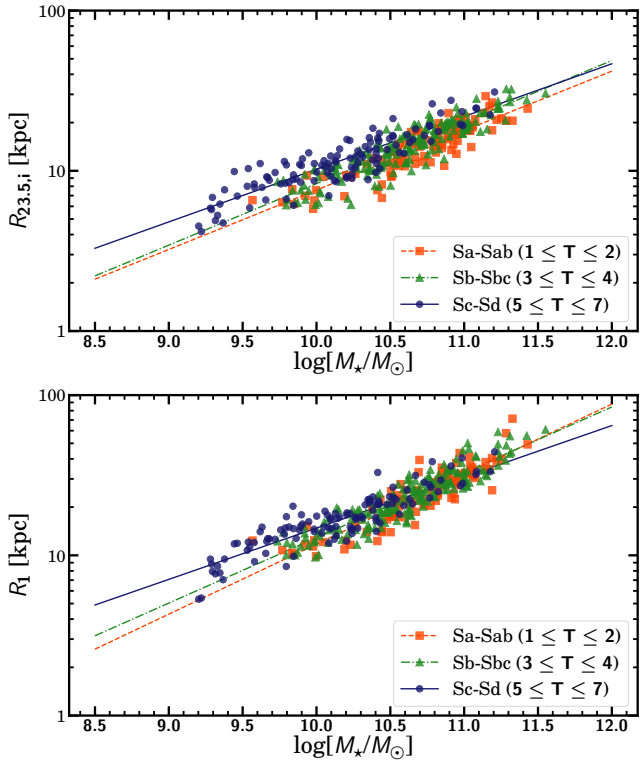

Figure A.3: Stellar mass–size relation for three morphological groups within our spiral galaxy sample: Sa–Sab (orange squares), Sb–Sbc (green triangles) and Sc–Sd (blue dots). The top panel shows the relation using $R_{23.5,i}$ while the bottom panel shows the same relation using R_1 as the size indicator. This figure replaces Fig. 7 in the original paper (here Fig. 2.7).

Este documento incorpora firma electrónica, y es copia auténtica de un documento electrónico archivado por la ULL según la Ley 39/2015.
Su autenticidad puede ser contrastada en la siguiente dirección https://sede.ull.es/validacion/

Identificador del documento: 2622200 Código de verificación: mbm0ekWs

Firmado por:	ROSHAN NUSHKIA CHAMBA *UNIVERSIDAD DE LA LAGUNA*	Fecha: 07/07/2020 13:28:26
	IGNACIO TRUJILLO CABRERA *UNIVERSIDAD DE LA LAGUNA*	07/07/2020 13:58:21
	Johan Hendrik Knapen Koelstra *UNIVERSIDAD DE LA LAGUNA*	07/07/2020 15:23:08
	María de las Maravillas Aguiar Aguilar *UNIVERSIDAD DE LA LAGUNA*	08/07/2020 15:55:11

Universidad de La Laguna
Oficina de Sede Electrónica
Entrada
Nº registro: 2020/46124
Nº reg. oficina: OF002/2020/45309
Fecha: 07/07/2020 15:26:22

A.2 Is 1 $M_\odot/\mathrm{pc}^2$ a good proxy for the location of the gas density threshold for star formation along the 10^7 to 10^{12} $M_\odot$ mass range?

In Chapter 2, the radial position of the isomass contour at 1 $M_\odot/\mathrm{pc}^2$ is porposed as a size indicator motivated by its proximity to the location of the gas density threshold for star formation in galaxies found theoretically (see e.g. Schaye 2004) and because this value is representative of the location of the disc truncation in galaxies similar to the Milky Way (Martínez-Lombilla et al. 2019). However, this value is not guaranteed to be representative of the gas density threshold for star formation in galaxies with very different stellar mass (like dwarfs) or those who were formed during an enormous burst of star formation at high-z (as is the case of the most massive ellipticals). In fact, there are some hints in the results shown here indicating that a running gas density threshold for star formation could be more representative of the size of galaxies. Looking at Fig. 2.2, the reader may appreciate that while 1 $M_\odot/\mathrm{pc}^2$ very well represents the size of spiral galaxies, the use of this value does not fully enclose the extension of dwarf galaxies. A potential explanation for this is that in the case of dwarf galaxies the gas density threshold for star formation is lower than in the case of more massive spirals, and therefore using, for instance, 0.3–0.5 $M_\odot/\mathrm{pc}^2$ instead of 1 $M_\odot/\mathrm{pc}^2$ could be a better proxy for measuring the size of these small systems. This idea of a lower gas density threshold for star formation for dwarf galaxies is observationally supported as on average their amount of H_2 compared to HI (and therefore their star-forming efficiency) is lower than for larger mass systems (see e.g. Leroy et al. 2008; Huang et al. 2012).

On the other hand, the situation would be reversed in the case of massive elliptical galaxies where R_1 is a bit larger than the visual extent of these galaxies. The gas density threshold for star formation during its high-z formation could be larger than whatit is currently for the spiral galaxies. In the local Universe, for instance, it has been found that starburst galaxies have significantly enhanced star formation (Jaskot et al. 2015). In this case, using an isomass contour with a larger density value (i.e. $> 1\,M_\odot/\mathrm{pc}^2$) as size could be a better option for these very massive galaxies. In fact, one of the most notable features of the new stellar mass–size relation is the change in slope of the relation for galaxies above 10^{11} $M_\odot$ in stellar mass (Sec 2.7.3). This could be an indication that the proxy for the location of the gas density threshold for star formation for galaxies (i.e. the isomass contour at 1 $M_\odot/\mathrm{pc}^2$) can be slightly different for galaxies where the bulk of star formation occurred at high-z. For this reason, the changes in the relation using an isomass contour at 3 $M_\odot/\mathrm{pc}^2$ for the size of the most massive objects is explored here. The result of doing such an exercise is shown in Fig. A.4.

Using R_3 instead of R_1 for the most massive galaxies decreases the size of these objects and thus follows the trend observed in R_1 for the less massive galaxies ($M_\star < 10^{11}\,M_\odot$) as marked by the best fit dashed line in Fig. A.4. Beyond $10^{11.4}$ $M_\odot$, however, even with R_3 the galaxies are above this trend in R_1. This is suggestive of an even larger gas density threshold for star formation in these ultra massive objects. The opposite exercise using the dwarf galaxies is explored in Chamba et al. (2020).

Este documento incorpora firma electrónica, y es copia auténtica de un documento electrónico archivado por la ULL según la Ley 39/2015.
Su autenticidad puede ser contrastada en la siguiente dirección https://sede.ull.es/validacion/

Identificador del documento: 2622200 Código de verificación: mbm0ekWs

Firmado por:	ROSHAN NUSHKIA CHAMBA *UNIVERSIDAD DE LA LAGUNA*	Fecha: 07/07/2020 13:28:26
	IGNACIO TRUJILLO CABRERA *UNIVERSIDAD DE LA LAGUNA*	07/07/2020 13:58:21
	Johan Hendrik Knapen Koelstra *UNIVERSIDAD DE LA LAGUNA*	07/07/2020 15:23:08
	María de las Maravillas Aguiar Aguilar *UNIVERSIDAD DE LA LAGUNA*	08/07/2020 15:55:11

Universidad de La Laguna
Oficina de Sede Electrónica
Entrada
Nº registro: 2020/46124
Nº reg. oficina: OF002/2020/45309
Fecha: 07/07/2020 15:26:22

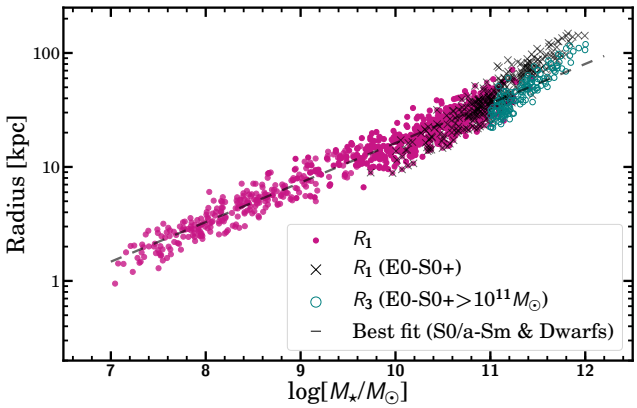

Figure A.4: Stellar mass–size relation using different stellar mass densities as proxies for indicating the size of the most massive galaxies: R_1 and R_3. As can be seen, the size of the most massive objects changes depending on the isomass contour used to measure its size. The figure shows that most of the galaxies from 10^7 to 10^{12} could be allocated in the same stellar mass–size relation (i.e. with a similar slope) if R_3 were used for measuring the size of the galaxies for objects with stellar mass larger than 10^{11} $M_\odot$.

A.3 Other potential size indicators based on the location of the gas density threshold for star formation

Intimately linked to the gas density threshold for star formation is the drop-off of galaxy profiles, both in the optical and in Hα. The position of a sharp decline in the optical profile, often referred to in the literature as breaks or truncations (see a discussion about this in Martín-Navarro et al. 2012), has been used to explore the cosmic size evolution of galaxies (Trujillo & Pohlen 2005; Azzollini et al. 2008). Unfortunately, not all galaxies show a clear deviation from the exponential decline in their profiles that can be used to trace their sizes (Pohlen & Trujillo 2006). While the fact that for Milky Way-like galaxies the truncation is found near a stellar mass density of $\sim 1 M_\odot/\mathrm{pc}^2$ has been used in Chapter 2, it is not known whether this result also holds for galaxies of different stellar mass (see Appendix A.2). In future work (Chapter 4), the issue of identifying the location of truncations in the profiles of the same sample of galaxies analysed here and determining the values of the stellar mass densities at those positions will be explored.

In addition to the drop-off in the optical profile, many disc galaxies show a sharp decline in their Hα profiles. The location of this truncation in Hα is also considered a good indicator of the radial position of the gas density threshold for star formation in actively star forming galaxies (see e.g. Martin & Kennicutt 2001). The Hα emission is directly linked to the presence of massive O stars and therefore the presence of recent star formation. In this sense, the location of the truncation radius in Hα could be a direct indicator of the position of the gas density threshold for star formation and consequently, a very good proxy for galaxy size.

Despite the obvious advantages of using Hα profiles to derive the size of galaxies, there are a

Este documento incorpora firma electrónica, y es copia auténtica de un documento electrónico archivado por la ULL según la Ley 39/2015.
Su autenticidad puede ser contrastada en la siguiente dirección https://sede.ull.es/validacion/

Identificador del documento: 2622200 Código de verificación: mbm0ekWs

Firmado por:	ROSHAN NUSHKIA CHAMBA *UNIVERSIDAD DE LA LAGUNA*	Fecha: 07/07/2020 13:28:26
	IGNACIO TRUJILLO CABRERA *UNIVERSIDAD DE LA LAGUNA*	07/07/2020 13:58:21
	Johan Hendrik Knapen Koelstra *UNIVERSIDAD DE LA LAGUNA*	07/07/2020 15:23:08
	María de las Maravillas Aguiar Aguilar *UNIVERSIDAD DE LA LAGUNA*	08/07/2020 15:55:11

Universidad de La Laguna
Oficina de Sede Electrónica
Entrada
Nº registro: 2020/46124
Nº reg. oficina: OF002/2020/45309
Fecha: 07/07/2020 15:26:22

number of practical limitations to a massive use of this technique. First, there currently appears to be no deep Hα surveys covering a large area of the sky that allow this analysis on all kinds of galaxies. Second, contrary to the use of a stellar mass isocontour, the use of Hα will be restricted to only those galaxies that are currently forming stars. In addition, as is also the case in the optical, not all the disc galaxies show a clear feature in their profiles that can be associated to a sharp decline in on-going star formation (see e.g. Koopmann et al. 2006). Nonetheless, in those cases where the break radii of Hα surface brightness profiles have been measured, a bimodal distribution has been found, with the majority of the galaxies showing breaks at 0.7 or 1.1 R_{25} (Christlein et al. 2010). It remains to be explored whether the breaks in Hα are at the same location as that of the truncations in the optical for large samples of galaxies.

Finally, though the presence of Hα is a clear indication of recent star formation, the Hα line is connected with the presence of stars massive enough to generate a Stroemgren sphere. However, it is easy to imagine (particularly in the outer parts of galaxies where the density is very low) star formation occurring at low levels without the formation of very massive stars. In such a case, where Hα is no longer present, the UV emission could be used as an indicator of recent star formation. As mentioned before, it would be necessary to search for a clear feature that can be associated to a gas density threshold for star formation in a large number of galaxies and thus approach the issue of galaxy size and star formation activity from multiple perspectives.

A.4 The limits of the new size definition

Our size definition is motivated by the location of the gas density threshold for star formation in galaxies. This definition is rather general and there is no reason why this could not be applied to any galaxy where *in-situ* star formation is present. However, in order to make the new size definition operative, the position of the stellar mass density contour at 1 $M_{\odot}/\mathrm{pc}^2$ was adopted. But fixing a specific value means that only the characterisation of the size of objects whose maximum stellar mass density is $\gtrsim 1\,M_{\odot}/\mathrm{pc}^2$ can be probed. For this reason, the brightness of objects that can not be characterised with such a specific prescription is quantified in the following.

Some old and metal-poor galaxies with central surface brightness $\mu_g(0) > 27\,\mathrm{mag/arcsec}^2$ would have a maximum stellar mass density $< 1\,M_{\odot}/\mathrm{pc}^2$ and therefore, they would be unable to have a size estimation based on the 1 $M_{\odot}$ isomass contour adopted here. As the surface brightness of galaxies is not usually reported by their central value but as the brightness averaged within their effective radius (i.e. $\langle\mu\rangle_e$), the $\langle\mu\rangle_e$ that limits the size measure R_1 is computed. This is done by using the relation between central surface brightness and the average surface brightness according to a Sérsic profile:

$$\langle\mu\rangle_e = \mu(0) - 2.5\log\frac{n\Gamma(2n)}{b_n^{2n}} \tag{A.2}$$

where n is the Sérsic index of the model. For $0.5 < n < 2$ (a typical range of variation of the Sérsic index for galaxies with very low surface brightness; see e.g. Román & Trujillo 2017a), this would imply that the use of R_1 is limited to galaxies with $\langle\mu\rangle_e \lesssim 28$–$29\,\mathrm{mag/arcsec}^2$. This surface brightness is extremely low, nonetheless the current faintest galaxies detected in our Local Group (see e.g. Fig. 7 in McConnachie 2012) have such extreme brightness. This again reinforces the idea mentioned in Appendix A.2 that low mass systems have very low

Este documento incorpora firma electrónica, y es copia auténtica de un documento electrónico archivado por la ULL según la Ley 39/2015.
Su autenticidad puede ser contrastada en la siguiente dirección https://sede.ull.es/validacion/

Identificador del documento: 2622200 Código de verificación: mbm0ekWs

Firmado por:	ROSHAN NUSHKIA CHAMBA *UNIVERSIDAD DE LA LAGUNA*	Fecha: 07/07/2020 13:28:26
	IGNACIO TRUJILLO CABRERA *UNIVERSIDAD DE LA LAGUNA*	07/07/2020 13:58:21
	Johan Hendrik Knapen Koelstra *UNIVERSIDAD DE LA LAGUNA*	07/07/2020 15:23:08
	María de las Maravillas Aguiar Aguilar *UNIVERSIDAD DE LA LAGUNA*	08/07/2020 15:55:11

Universidad de La Laguna
Oficina de Sede Electrónica
Entrada
Nº registro: 2020/46124
Nº reg. oficina: OF002/2020/45309
Fecha: 07/07/2020 15:26:22

star formation efficiency and therefore a lower gas density threshold for star formation. Future ultra-deep imaging surveys would allow better calibration of the gas density threshold for star formation values for low dense systems. Nevertheless, the size definition proposed in Chapter 2 could be readily adjusted to these extreme objects by using a lower mass density contour for characterising their sizes.

A.5 Stellar mass determination

As explained in the main body of Chapter 2, stellar masses of all galaxies were calculated using their stellar mass density profiles which were derived using the $g-r$ colour profiles (Roediger & Courteau 2015). These mass estimates are compared with those obtained by the Portsmouth group (Maraston et al. 2013) to evaluate the reliability of the methods adopted here. The 'control' stellar masses were retrieved from the Portsmouth Spectro-Photometric Model Fitting catalogue available on the SDSS webpage.[1] The Portsmouth stellar masses are calculated using the BOSS spectroscopic redshift, $Z_{\rm NOQSO}$ and u, g, r, i, z photometry by means of broad-band SED fitting of stellar population models. Two separate stellar mass calculations were conducted: one assuming a passive template and the other a star-forming template. The version used here is the star-forming template with a Kroupa IMF.

Figure A.5 shows the comparison between the stellar masses estimated in this work and those obtained by the Portsmouth group (when available). The ratio of these two mass estimates is approximately described by a Gaussian distribution. However, there is a systematic offset in the mass estimates by a factor of 1.6 with respect to the Portsmouth masses. This offset could be due to multiple reasons – the IMF nor the aperture used to estimate the total flux of the objects are the same. However, for the work presented in Chapter 2, the most relevant aspect is not the offset but the scatter in the difference between the two mass measurements. By measuring the r.m.s. of the ratio between the two masses, an estimate of this scatter can be made. For the total sample, the r.m.s. of this distribution is 0.24 dex. In addition to showing the distribution of the ratio between the two masses of the entire sample, the distribution of the same ratio for the different galaxy subsamples defined in this work is also overplotted. The r.m.s. of these subsample distributions are: 0.19 dex (E0–S0+), 0.24 dex (S0/a–Sm) and 0.25 dex (Dwarfs).

The above r.m.s. of the subsample distributions is used as a way of estimating the uncertainty in the stellar mass–size relation. Figure A.6 illustrates how the R_1–mass relation with an intrinsic scatter equal to zero would look with only the uncertainty contribution from the stellar mass estimate. In other words, this plot shows the contribution of the mass uncertainty to the observed scatter of the mass–size relation. The scatter of the R_1-mass size relation plotted in Fig. A.6, which is the scatter simply produced by the uncertainty in measuring the stellar mass, is $\sigma_{R_{1,mass}} = 0.047$ dex. That is the contribution of the mass uncertainty to the total observed scatter of the R_1-mass size relation (i.e. $\sigma_{R_1} = 0.089$ dex).

A.6 Comparing the R_1–stellar mass and HI size–mass relations

An extremely tight scaling relation for galaxies is the one which links their total HI mass with the diameter of their HI discs defined by the location of the gas surface density at 1 $M_\odot/{\rm pc}^2$ (Broeils

[1] https://data.sdss.org/datamodel/files/BOSS_GALAXY_REDUX/GALAXY_VERSION/portsmouth_stellarmass.html

Este documento incorpora firma electrónica, y es copia auténtica de un documento electrónico archivado por la ULL según la Ley 39/2015.
Su autenticidad puede ser contrastada en la siguiente dirección https://sede.ull.es/validacion/

Identificador del documento: 2622200 Código de verificación: mbm0ekWs

Firmado por:	ROSHAN NUSHKIA CHAMBA *UNIVERSIDAD DE LA LAGUNA*	Fecha: 07/07/2020 13:28:26
	IGNACIO TRUJILLO CABRERA *UNIVERSIDAD DE LA LAGUNA*	07/07/2020 13:58:21
	Johan Hendrik Knapen Koelstra *UNIVERSIDAD DE LA LAGUNA*	07/07/2020 15:23:08
	María de las Maravillas Aguiar Aguilar *UNIVERSIDAD DE LA LAGUNA*	08/07/2020 15:55:11

Universidad de La Laguna
Oficina de Sede Electrónica
Entrada
Nº registro: 2020/46124
Nº reg. oficina: OF002/2020/45309
Fecha: 07/07/2020 15:26:22

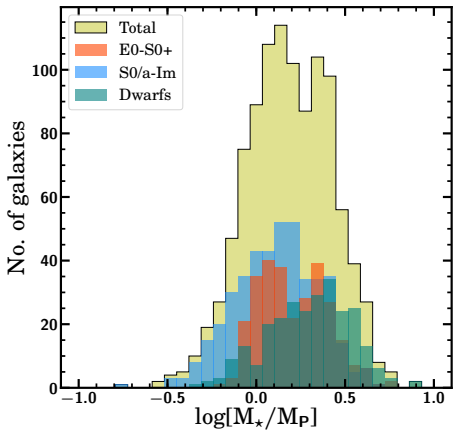

Figure A.5: Uncertainty in measuring the stellar masses of galaxies used in this work. $M_{\rm P}$ corresponds to the stellar mass of the objects reported by the Portsmouth group (Maraston et al. 2013) and $M_\star$ is the mass estimated in this work using the $g-r$ colour profile (Roediger & Courteau 2015). The ratio of these two estimates for the full sample (yellow) and the different galaxy subsamples are labelled in the legend.

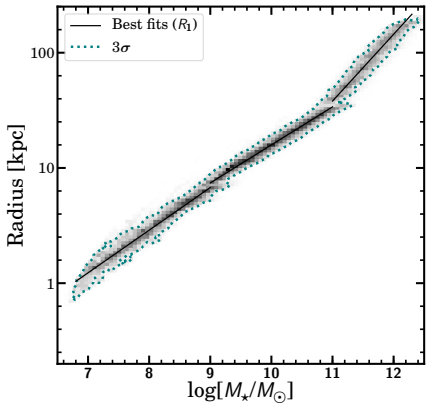

Figure A.6: Scatter in the R_1-mass relation produced by the uncertainty in stellar mass. The figure shows how galaxies spread over the size–mass plane simply due to effect of the uncertainty in measuring the stellar mass of each galaxy. To build this plot, it is assumed that the intrinsic scatter of the size–mass relation is exactly zero and how the uncertainty in measuring the mass will spread around the best fit lines to the observed measurements is followed. The contour shows the 3 σ distribution of the final sample.

Este documento incorpora firma electrónica, y es copia auténtica de un documento electrónico archivado por la ULL según la Ley 39/2015.
Su autenticidad puede ser contrastada en la siguiente dirección https://sede.ull.es/validacion/

Identificador del documento: 2622200 Código de verificación: mbm0ekWs

Firmado por:	ROSHAN NUSHKIA CHAMBA *UNIVERSIDAD DE LA LAGUNA*	Fecha: 07/07/2020 13:28:26
	IGNACIO TRUJILLO CABRERA *UNIVERSIDAD DE LA LAGUNA*	07/07/2020 13:58:21
	Johan Hendrik Knapen Koelstra *UNIVERSIDAD DE LA LAGUNA*	07/07/2020 15:23:08
	María de las Maravillas Aguiar Aguilar *UNIVERSIDAD DE LA LAGUNA*	08/07/2020 15:55:11

Universidad de La Laguna
Oficina de Sede Electrónica
Entrada
Nº registro: 2020/46124
Nº reg. oficina: OF002/2020/45309
Fecha: 07/07/2020 15:26:22

& Rhee 1997). This relation spans over five orders of magnitude in HI mass. A subsequent analysis of this relation has shown that its scatter is extremely low: 0.06 dex and the slope almost exactly 1/2, i.e. 0.506 ± 0.003 (Wang et al. 2016). These values are suggestive of a uniform characteristic HI surface density of $\sim 5\,M_{\odot}/\mathrm{pc}^2$.

In the case of the HI size–mass relation of galaxies, the use of 1 $M_{\odot}/\mathrm{pc}^2$ is a subjective choice and, contrary to the present work, there is no a priory physical motivation to select this value. Interestingly, the scatter of the HI size–mass relation is minimised when the HI size is measured at surface densities between 1 to 2 $M_{\odot}/\mathrm{pc}^2$.

The reason this relation is cited here is because of its potential connection to the size–mass relation presented in Chapter 2. In galaxy formation models (see e.g. Lagos et al. 2011), the HI surface density is regulated by the conversion process from atomic to molecular hydrogen, i.e. HI-to-H_2. Observationally, it is found that the HI surface density saturates at $\sim 9\,M_{\odot}/\mathrm{pc}^2$, and gas at higher surface densities are converted to molecular gas (Bigiel et al. 2008). As H_2 and star formation are closely linked (Krumholz et al. 2011), the HI-to-H_2 process should be reflected in the star formation activity and, therefore, in the location of the gas density threshold for star formation in galaxies. As galaxies observationally have a very similar average HI surface density of $\sim 5M_{\odot}/\mathrm{pc}^2$ (as reflected by the tight HI size–mass relation of galaxies), it seems reasonable to assume that the gas density threshold for star formation is also similar among very different galaxies. It is therefore reasonable to speculate that the small intrinsic scatter of the stellar mass–size relation (based on the location of the gas density threshold for star formation) could be connected with or be a reflection of the tight HI size–mass relation of galaxies.

Este documento incorpora firma electrónica, y es copia auténtica de un documento electrónico archivado por la ULL según la Ley 39/2015.
Su autenticidad puede ser contrastada en la siguiente dirección https://sede.ull.es/validacion/

Identificador del documento: 2622200 Código de verificación: mbm0ekWs

Firmado por:	ROSHAN NUSHKIA CHAMBA *UNIVERSIDAD DE LA LAGUNA*	Fecha: 07/07/2020 13:28:26
	IGNACIO TRUJILLO CABRERA *UNIVERSIDAD DE LA LAGUNA*	07/07/2020 13:58:21
	Johan Hendrik Knapen Koelstra *UNIVERSIDAD DE LA LAGUNA*	07/07/2020 15:23:08
	María de las Maravillas Aguiar Aguilar *UNIVERSIDAD DE LA LAGUNA*	08/07/2020 15:55:11

Universidad de La Laguna
Oficina de Sede Electrónica
Entrada
Nº registro: 2020/46124
Nº reg. oficina: OF002/2020/45309
Fecha: 07/07/2020 15:26:22

B

Appendix: Ultra-diffuse galaxies

B.1 Table of measurements

B.2 Comparison with an isophotal size indicator: The Holmberg radius

Similar to Figs. 3.3 and 3.4, Fig. B.1 shows the distribution of UDGs, dwarfs, and MW-like galaxies using the Holmberg radius. Here the Holmberg radius is defined using the isophote at 26 mag/arcsec^2 in the g-band. The middle panel clearly demonstrates that UDGs have sizes that are within the size range of dwarf galaxies. The KS test using $R_{\rm H}/R_{\rm H,fit}$ gives a p-value of 0.54. Finally, the lower panel shows that the sizes of UDGs are not compatible with those of MW-like galaxies. Therefore, the main conclusions of this study are further reinforced by taking a widely used isophotal size indicator. In other words, the conclusions regarding the sizes of UDGs are *not* related with a specific size definition to describe the extensions of galaxies.

B.3 Other stellar mass density proxies to measure the size of dwarfs and UDGs

In Chapter 2, a size indicator based on the location of the gas density threshold for star formation in galaxies was proposed. On both theoretical and observational grounds, the location of an isomass contour at 1 $M_{\odot}$/pc^2 as a proxy for such a value was chosen. While this value is motivated by the location of the disc truncation in MW-like galaxies (see Martínez-Lombilla et al. 2019), for galaxies such as dwarfs where the level of star formation is lower, a better proxy for their gas density threshold could be given by a lower isomass contour (Leroy et al. 2008; Huang et al. 2012). Therefore, the analysis of this study was repeated using an isomass contour at 0.5 $M_{\odot}$/pc^2 instead of 1 $M_{\odot}$/pc^2 as a galaxy size indicator for UDGs and dwarfs (see Fig. 3.1 for two examples). Lets call this size parameter $R_{0.5}$.

Figure B.2 shows the size distribution of UDGs and dwarfs using $R_{0.5}$ and that of MW-like systems using R_1. Although $R_{0.5}$ increases the sizes of the UDGs and dwarf galaxies as expected, their extensions never reach those of MW-like galaxies. Similar to the results shown in Fig. 3.4 (right panel), the null hypothesis is completely rejected upon comparing the size distributions of UDGs and MW-like galaxies.

Este documento incorpora firma electrónica, y es copia auténtica de un documento electrónico archivado por la ULL según la Ley 39/2015.
Su autenticidad puede ser contrastada en la siguiente dirección https://sede.ull.es/validacion/

Identificador del documento: 2622200 Código de verificación: mbm0ekWs

Firmado por:	ROSHAN NUSHKIA CHAMBA *UNIVERSIDAD DE LA LAGUNA*	Fecha: 07/07/2020 13:28:26
	IGNACIO TRUJILLO CABRERA *UNIVERSIDAD DE LA LAGUNA*	07/07/2020 13:58:21
	Johan Hendrik Knapen Koelstra *UNIVERSIDAD DE LA LAGUNA*	07/07/2020 15:23:08
	María de las Maravillas Aguiar Aguilar *UNIVERSIDAD DE LA LAGUNA*	08/07/2020 15:55:11

Universidad de La Laguna
Oficina de Sede Electrónica
Entrada
Nº registro: 2020/46124
Nº reg. oficina: OF002/2020/45309
Fecha: 07/07/2020 15:26:22

Table B.1: Measured parameters for the sample of UDGs.

Name	R.A. (deg)	Dec (deg)	q	PA (deg)	z	A_g (mag)	A_r (mag)	R_e (kpc)	R_1 (kpc)	R_H (kpc)	Log($M_\star/M_\odot$)
DF44	195.24167	26.97638	0.69	60.0	0.0231	0.034	0.024	3.31	4.34	3.33	8.16
[KKS2000]04	40.44500	−8.40258	0.87	40.0	0.0060	0.081	0.056	1.30	2.62	1.69	7.86
UGC2162	40.09625	1.22917	0.77	25.0	0.0039	0.117	0.081	2.23	2.22	2.91	7.58
UDG-B1	50.08800	−1.17000	0.46	95.0	0.0212	0.213	0.148	3.93	4.11	6.94	7.90
UDG-B3	49.96000	−0.85500	0.86	41.0	0.0212	0.195	0.135	3.26	4.91	5.17	8.41
UDG-B2	9.60000	1.10600	0.50	7.0	0.0141	0.060	0.041	1.76	1.92	3.28	7.29
UDG-B4	9.88900	1.11500	0.67	107.0	0.0141	0.064	0.044	1.49	2.25	2.57	7.51
UDG-B5	9.96900	0.38300	0.75	15.0	0.0141	0.058	0.040	2.95	4.06	4.64	8.11
UDG-R1	9.97400	0.80800	0.64	167.0	0.0141	0.065	0.045	1.26	1.55	0.61	7.07
UDG-R4	9.76900	1.09900	0.63	10.0	0.0141	0.059	0.041	1.52	1.61	1.22	7.30
UDG-R5	358.61600	0.32200	0.59	120.0	0.0266	0.135	0.094	2.07	2.65	1.96	7.51
UDG-R6	358.49700	0.45400	0.73	30.0	0.0266	0.135	0.093	1.78	3.95	2.55	8.03

Notes. The table includes the common name, position, axis ratio (q), and the position angle (PA) of the ellipses used to extract the surface brightness profiles (measured counter clockwise starting from the horizontal axis), the spectroscopic redshifts z (if available) of the galaxies (Román & Trujillo 2017b; Trujillo et al. 2017; van Dokkum et al. 2015b; Emsellem et al. 2019). Galactic extinctions both in the g and r bands (from NED), effective radius R_e (measured in the g-band), the radial location R_1 of the isomass contour at $1\,M_\odot/\mathrm{pc}^2$, the Holmberg Radius (R_H; defined here using the isophote at $26\,\mathrm{mag/arcsec}^2$ in the g-band) and the stellar mass of galaxies (assuming a Chabrier IMF). The quantities are given showing only the significant figures up to which the values can be regarded reliable. The table for the dwarf galaxies is available in the online version of Trujillo et al. (2020).

Este documento incorpora firma electrónica, y es copia auténtica de un documento electrónico archivado por la ULL según la Ley 39/2015.
Su autenticidad puede ser contrastada en la siguiente dirección https://sede.ull.es/validacion/

Identificador del documento: 2622200 Código de verificación: mbm0ekWs

Firmado por: ROSHAN NUSHKIA CHAMBA — *UNIVERSIDAD DE LA LAGUNA* — Fecha: 07/07/2020 13:28:26
IGNACIO TRUJILLO CABRERA — *UNIVERSIDAD DE LA LAGUNA* — 07/07/2020 13:58:21
Johan Hendrik Knapen Koelstra — *UNIVERSIDAD DE LA LAGUNA* — 07/07/2020 15:23:08
María de las Maravillas Aguiar Aguilar — *UNIVERSIDAD DE LA LAGUNA* — 08/07/2020 15:55:11

Universidad de La Laguna
Oficina de Sede Electrónica
Entrada
Nº registro: 2020/46124
Nº reg. oficina: OF002/2020/45309
Fecha: 07/07/2020 15:26:22

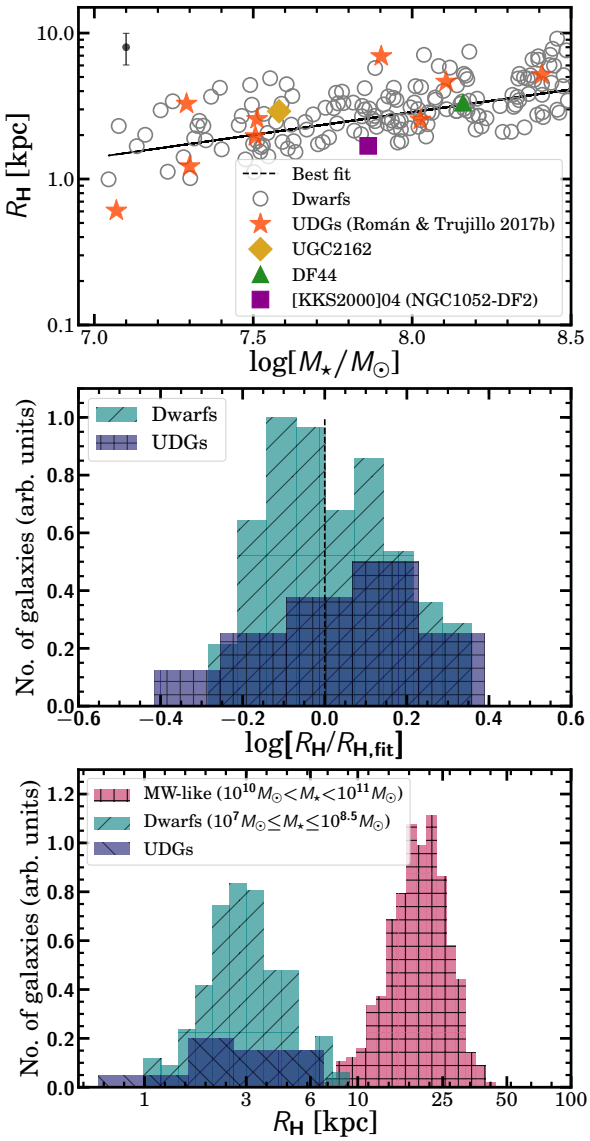

Figure B.1: Distribution of UDGs and dwarf galaxies using the Holmberg radius. *Top*: Holmberg radius ($R_{\rm H}$)–stellar mass plane for dwarfs (grey) and UDGs (colours). The best fit line of the relation for the dwarf sample is also over-plotted. The upper left corner of the plot shows the typical uncertainty in our measurements (see TCK20). *Middle*: Histogram showing the distribution of $R_{\rm H}/R_{\rm H,fit}$ where 'fit' refers to the best-fit line of each relation for the dwarf sample. *Bottom*: Histogram showing the $R_{\rm H}$ distribution of UDGs, dwarfs, and MW-like galaxies.

Este documento incorpora firma electrónica, y es copia auténtica de un documento electrónico archivado por la ULL según la Ley 39/2015.
Su autenticidad puede ser contrastada en la siguiente dirección https://sede.ull.es/validacion/

Identificador del documento: 2622200 Código de verificación: mbm0ekWs

Firmado por:	ROSHAN NUSHKIA CHAMBA *UNIVERSIDAD DE LA LAGUNA*	Fecha: 07/07/2020 13:28:26
	IGNACIO TRUJILLO CABRERA *UNIVERSIDAD DE LA LAGUNA*	07/07/2020 13:58:21
	Johan Hendrik Knapen Koelstra *UNIVERSIDAD DE LA LAGUNA*	07/07/2020 15:23:08
	María de las Maravillas Aguiar Aguilar *UNIVERSIDAD DE LA LAGUNA*	08/07/2020 15:55:11

Universidad de La Laguna
Oficina de Sede Electrónica
Entrada
Nº registro: 2020/46124
Nº reg. oficina: OF002/2020/45309
Fecha: 07/07/2020 15:26:22

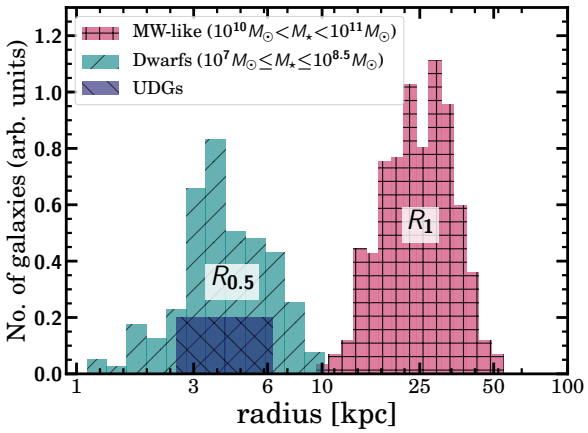

Figure B.2: Histograms showing the size distribution of UDGs ($R_{0.5}$), dwarfs ($R_{0.5}$) and MW-like galaxies (R_1).

Therefore, once again, the conclusion that UDGs do not have sizes comparable to MW-like galaxies remains unchanged even with the use of another gas density threshold for size.

Este documento incorpora firma electrónica, y es copia auténtica de un documento electrónico archivado por la ULL según la Ley 39/2015.
Su autenticidad puede ser contrastada en la siguiente dirección https://sede.ull.es/validacion/

Identificador del documento: 2622200 Código de verificación: mbm0ekWs

Firmado por:	ROSHAN NUSHKIA CHAMBA *UNIVERSIDAD DE LA LAGUNA*	Fecha: 07/07/2020 13:28:26
	IGNACIO TRUJILLO CABRERA *UNIVERSIDAD DE LA LAGUNA*	07/07/2020 13:58:21
	Johan Hendrik Knapen Koelstra *UNIVERSIDAD DE LA LAGUNA*	07/07/2020 15:23:08
	María de las Maravillas Aguiar Aguilar *UNIVERSIDAD DE LA LAGUNA*	08/07/2020 15:55:11

Universidad de La Laguna
Oficina de Sede Electrónica
Entrada
Nº registro: 2020/46124
Nº reg. oficina: OF002/2020/45309
Fecha: 07/07/2020 15:26:22

Este documento incorpora firma electrónica, y es copia auténtica de un documento electrónico archivado por la ULL según la Ley 39/2015.
Su autenticidad puede ser contrastada en la siguiente dirección https://sede.ull.es/validacion/

Identificador del documento: 2622200 Código de verificación: mbm0ekWs

Firmado por:	ROSHAN NUSHKIA CHAMBA *UNIVERSIDAD DE LA LAGUNA*	Fecha: 07/07/2020 13:28:26
	IGNACIO TRUJILLO CABRERA *UNIVERSIDAD DE LA LAGUNA*	07/07/2020 13:58:21
	Johan Hendrik Knapen Koelstra *UNIVERSIDAD DE LA LAGUNA*	07/07/2020 15:23:08
	María de las Maravillas Aguiar Aguilar *UNIVERSIDAD DE LA LAGUNA*	08/07/2020 15:55:11

Universidad de La Laguna
Oficina de Sede Electrónica
Entrada
Nº registro: 2020/46124
Nº reg. oficina: OF002/2020/45309
Fecha: 07/07/2020 15:26:22

Acknowledgements

This thesis would not have been possible without the continuous support and encouragement from my supervisors Nacho Trujillo and Johan Knapen. I can not express my sincere gratitude enough for all the countless hours you devoted to my work and for being patient in the moments I was too stubborn to listen. I consider myself lucky to end up with advisors who have opened my mind to very different opinions and practices within academia. Thank you for everything. I will never forget what you did.

I would also like to thank my IAC big brothers who taught me how to fight with deep data: Javier Román and Raúl Infante-Sainz. You were vital for my PhD as I had never before seen or processed an image of a real galaxy. Thank you very much for all your help and I know you will do great things.

Thank you to Mike Beasley for always leaving your office door open to me and the rest of the TRACES team for interesting conversations whenever I attended your group meetings. To all the staff, secretaries Lourdes, Eva, Carmen, Irene and Yaiza and security members at the IAC – thank you for making me comfortable and safe throughout my PhD, especially when I needed to work late hours. Special thanks to Monique from the IAC Library who helped me gather some of the historical material I needed for Chapter 1 and Jesús Burgos who ensured I could collect my computer screen amidst the COVID-19 lockdown, which greatly improved my efficiency in writing this thesis at home.

To my SUNDIAL colleagues, I will always remember that: 'This project has received funding from the European Union's Horizon 2020 research and innovation programme under the Marie Sklodowska-Curie grant agreement No. 721463'. Thank you so much for all the annual meetings, training schools and secondment visits (thanks Michael Wilkinson, Marlies van der Weijgart (Groningen) and Hugues Talbot (Paris)!). A special thanks to Reynier Peletier for an amazing job in leading the collaboration and winning a grant which allowed me to travel to the conferences I desired. It has been a pleasure to be part of SUNDIAL and the ESR group – you are all fantastic individuals and friends. I wish you only great things.

Mi experiencia durante el doctorado habría sido extremadamente aburrida sin mis queridos Doctorandos. Un millón de gracias por todos los lugares de encuentro espontáneos para juegos, playa, aventuras en toda España durante las Navidades de 2018–19, comidas y más comidas: Efşan, Elham, Alex y Elena, Ale y Tito, Borlaff y Ro, Gonzalo y Elena, David, Javi y Nastia, Pablo, Patri y Ray. Gracias a Cristina, Paula, Núria y Núria por ayudarme a empezar en Canarias, Francesca, Carlos, Awe, Carina, Noelia, María, Jorge y Juan Luis por ser buenos compañeros de oficina, Paz y Maitane por ser unas excelentes 'Journal Clubbers', tan entregadas como yo en la organización de eventos, Isaac por ayudarme a resumir el Universo en tres páginas (Sect. 1.1) y Pedro por recordando los procedimientos ULL en detalle, ¡guau! A mi madre canaria Lales y a sus amigas, Loli, Juana, Lucre, Gloria, Nieves, Conchi y Suso, Elena, Mercedes, África y todos para fiestas con aún más comida. Ustedes crearon para mí un hogar en España y me gustaría que mi próximo hogar fuera la mitad de cálido de lo que ha sido este.

To the Memetastic group, for all the laughter you bring into my life when thesising has proved difficult. And finally to my family, to whom this thesis is dedicated, thank you for all your support – especially your sincere effort to read my first scientific publications (here Chapters 2 and 3). My friends, those with me now and in the past, in Sri Lanka and around the world. You are all wonderful. Here is to more exciting adventures ahead!

Este documento incorpora firma electrónica, y es copia auténtica de un documento electrónico archivado por la ULL según la Ley 39/2015.
Su autenticidad puede ser contrastada en la siguiente dirección https://sede.ull.es/validacion/

Identificador del documento: 2622200 Código de verificación: mbm0ekWs

Firmado por:	ROSHAN NUSHKIA CHAMBA *UNIVERSIDAD DE LA LAGUNA*	Fecha: 07/07/2020 13:28:26
	IGNACIO TRUJILLO CABRERA *UNIVERSIDAD DE LA LAGUNA*	07/07/2020 13:58:21
	Johan Hendrik Knapen Koelstra *UNIVERSIDAD DE LA LAGUNA*	07/07/2020 15:23:08
	María de las Maravillas Aguiar Aguilar *UNIVERSIDAD DE LA LAGUNA*	08/07/2020 15:55:11

Universidad de La Laguna
Oficina de Sede Electrónica
Entrada
Nº registro: 2020/46124
Nº reg. oficina: OF002/2020/45309
Fecha: 07/07/2020 15:26:22

Este documento incorpora firma electrónica, y es copia auténtica de un documento electrónico archivado por la ULL según la Ley 39/2015.
Su autenticidad puede ser contrastada en la siguiente dirección https://sede.ull.es/validacion/

Identificador del documento: 2622200 Código de verificación: mbm0ekWs

Firmado por:	ROSHAN NUSHKIA CHAMBA *UNIVERSIDAD DE LA LAGUNA*	Fecha: 07/07/2020 13:28:26
	IGNACIO TRUJILLO CABRERA *UNIVERSIDAD DE LA LAGUNA*	07/07/2020 13:58:21
	Johan Hendrik Knapen Koelstra *UNIVERSIDAD DE LA LAGUNA*	07/07/2020 15:23:08
	María de las Maravillas Aguiar Aguilar *UNIVERSIDAD DE LA LAGUNA*	08/07/2020 15:55:11